

---

# Estimates of Early Containment Loads from Core Melt Accidents

Draft Report for Comment

---

**U.S. Nuclear Regulatory  
Commission**

Office of Nuclear Reactor Regulation

Containment Loads Working Group



8601070488 851231  
PDR NUREG  
1079 R PDR

## NOTICE

### Availability of Reference Materials Cited in NRC Publications

Most documents cited in NRC publications will be available from one of the following sources:

1. The NRC Public Document Room, 1717 H Street, N.W.  
Washington, DC 20555
2. The Superintendent of Documents, U.S. Government Printing Office, Post Office Box 37082,  
Washington, DC 20013-7082
3. The National Technical Information Service, Springfield, VA 22161

Although the listing that follows represents the majority of documents cited in NRC publications, it is not intended to be exhaustive.

Referenced documents available for inspection and copying for a fee from the NRC Public Document Room include NRC correspondence and internal NRC memoranda; NRC Office of Inspection and Enforcement bulletins, circulars, information notices, inspection and investigation notices; Licensee Event Reports; vendor reports and correspondence; Commission papers; and applicant and licensee documents and correspondence.

The following documents in the NUREG series are available for purchase from the GPO Sales Program: formal NRC staff and contractor reports, NRC-sponsored conference proceedings, and NRC booklets and brochures. Also available are Regulatory Guides, NRC regulations in the *Code of Federal Regulations*, and *Nuclear Regulatory Commission Issuances*.

Documents available from the National Technical Information Service include NUREG series reports and technical reports prepared by other federal agencies and reports prepared by the Atomic Energy Commission, forerunner agency to the Nuclear Regulatory Commission.

Documents available from public and special technical libraries include all open literature items, such as books, journal and periodical articles, and transactions. *Federal Register* notices, federal and state legislation, and congressional reports can usually be obtained from these libraries.

Documents such as theses, dissertations, foreign reports and translations, and non-NRC conference proceedings are available for purchase from the organization sponsoring the publication cited.

Single copies of NRC draft reports are available free, to the extent of supply, upon written request to the Division of Technical Information and Document Control, U.S. Nuclear Regulatory Commission, Washington, DC 20555.

Copies of industry codes and standards used in a substantive manner in the NRC regulatory process are maintained at the NRC Library, 7920 Norfolk Avenue, Bethesda, Maryland, and are available there for reference use by the public. Codes and standards are usually copyrighted and may be purchased from the originating organization or, if they are American National Standards, from the American National Standards Institute, 1430 Broadway, New York, NY 10018.

---

# Estimates of Early Containment Loads from Core Melt Accidents

Draft Report for Comment

---

Manuscript Completed: November 1985  
Date Published: December 1985

Containment Loads Working Group

Office of Nuclear Reactor Regulation  
U.S. Nuclear Regulatory Commission  
Washington, D.C. 20555



## ABSTRACT

The thermal-hydraulic processes and corium debris-material interactions that can result from core melting in a severe accident have been studied to evaluate the potential effect of such phenomena on containment integrity. Pressure and temperature loads associated with representative accident sequences have been estimated for the six various LWR containment types used within the United States. Summaries distilling the analyses are presented and an interpretation of the results provided.

## PREFACE

The potential for containment failure from core melt accidents has been under review within the Commission for some time. The possibility of early failure with the potential for a large release of radioactivity (aerosol concentration is higher early in the accident) is the principle reason for this attention. Containment loads that might lead to such failure can result from loss of primary system integrity and from the thermal-hydraulic material interaction processes following release of the corium melt debris into the containment space.

These issues are described in a joint memorandum dated July 5, 1985, from Themis P. Speis (Director, Division of Safety Technology), Roger J. Mattson (Director, Division of Systems Interaction), and Richard Vollmer (Director, Division of Engineering) to Denwood F. Ross (Deputy Director of the Office of Nuclear Regulatory Research). In this memorandum the authors proposed the development of a program to address the issue of containment loading in severe accident sequences. The proposal was accented by the Senior Review Group for the Severe Accident Research Plan (SARP). The program was implemented through the formulation of a Containment Loads Working Group (CLWG). The Group is composed of expert analysts from Battelle Columbus Laboratories (BCL), Brookhaven National Laboratory (BNL), Los Alamos National Laboratory (LANL), Oak Ridge National Laboratory (ORNL), Sandia National Laboratory (SNL), Purdue University, University of Wisconsin, Factory Mutual Research Corporation (FMRC) and includes staff from the NRC's offices of Research and Regulation. The objective of the Group was to develop an updated evaluation of containment loads (temperature and pressure history) and the associated challenges to containment integrity. These evaluations, together with results from the Containment Performance Working Group (CPWG), provide a basis for assessing the modes and likelihood of containment failure. These results have been used in the Severe Accident Risk Rebaselining Program (SARRP) to help define containment trees which were combined with new estimates of fission product release to develop improved severe accident source terms. These improved source terms are described in NUREG-0956. Executive summaries describing the results from the CLWG and CPWG programs were included as appendices to NUREG-0956.

The CLWG was organized under the direction of Dr. Themis P. Speis, Director of the Division of Safety Technology (DST), in the Office of Nuclear Reactor Regulation (NRR). The overall approach was based on a standard problem methodology. The CLWG management team selected a specific reactor to represent each of the six containment designs deployed in the U.S. These were chosen to overlap with previous assessments, e.g., the Reactor Safety Study (WASH 1400) and the Zion-Indian Point Study (NUREG-0850), etc. and thus afford a basis for evaluating progress in understanding severe accident phenomena.

It was not practical to calculate all possible accident sequences in the detail needed for this study. Therefore, in general, two standard problem sequences were chosen to encompass the major thermal-hydraulic phenomena relevant to containment loading. The problems include accidents involving high primary system pressure at vessel failure (typical of a station blackout accident sequence) and an accident with low primary system pressure at vessel failure (typical of a large loss-of-coolant accident).

The plant-specific approach allowed the definition of each standard problem in the required detail. This forced a sense of realism not only in the narrow parameter sense but also in the overall attitude of addressing phenomena, sequences and issues. Furthermore, together with a common definition of initial conditions and primary system inventory released into the containment at vessel failure, the specification was sufficiently complete to allow reasonably unambiguous comparisons among the results obtained by the CLWG members. On this basis efforts were made to understand differences and, whenever possible, to arrive at consensus conclusions as well as qualitative results. Prior to its complete definition and issuance each standard problem was introduced by a member of the NRC management team to the whole CLWG for review and discussion.

It is left to future studies to determine the extent of variability in response due to sequence definition and individual design variations within each type of containment. It is hoped that the insights developed through the CLWG effort and the results recorded in this report will facilitate the task of assessing this variability. On the other hand, by considering all six types of containment, the coverage is believed to be reasonably broad.

A detailed summary of the results and the conclusions the staff has drawn from those results is provided in the Executive Summary. Based on results from the various studies, several areas are indicated in which reduction of uncertainties would appear beneficial. Perhaps the most important one, as it may affect all reactor types and containments, is that associated with melt release at high pressure (direct heating problems). Since initial evaluations indicate that primary system failure, and hence depressurization, could be possible prior to core melt, a high priority in this area is to address whether a high pressure scenario persisting to core melt is physically realizable. The second important topic, affecting principally the ice-condenser plants, is the issue of hydrogen. This is a rather complex topic and it may be resolved in a number of contributing subproblems including: hydrogen generation, release to containment, ignition, burning, and possibly transition to detonation. Finally, some residual uncertainties in corium-concrete interactions should be mentioned. They concern the long-term temperature evolution of the melt and affect not so much the development of pressure loads as they do the so-called "vaporization release" (source term) and the containment temperature (seal integrity). This problem is of principal interest to Mark I containments.

The principal contents of this report are found in the chapters 2 through 8 corresponding to the six standard problems plus one on potential direct heating effects. All are presented in a similar format that includes: description of relevant geometry, specifications of the standard problem, method of analyses utilized, numerical results and sensitivity studies, likelihood considerations of the various loads, and conclusions and recommendations. Each one of these chapters was written on the basis of the information developed during the CLWG meeting and associated documentation (i.e., presentation viewgraphs, informal reports by individual investigators, etc). The chapters describing the various standard problems have, in fact, been extracted from the consensus summaries provided by each team assigned to that particular standard problem. The group assigned to that problem and the principle authors of the summary are given at the beginning of each chapter. The editor of this report has exercised some judgment in modifying the format of the material provided in the consensus summaries to maintain a consistent structure for this report.

The approach in writing these summaries was not to fully document all the results obtained, and certainly not their bases; but rather to convey a distillation of the understanding and conclusions as they developed during this effort. Three special studies smaller in scope and effort were also completed and they are summarized in appendices to the report.

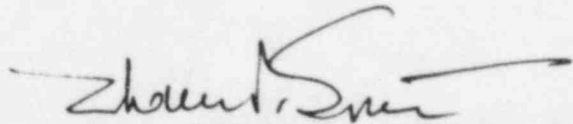
In parallel with the CLWG effort a joint NRC/IDCOR program also came into being. The purpose of this program was to provide a basis of communication for recent developments in the area of severe accidents by the NRC and the U.S. Utility. Much of the information developed by the CLWG was presented in the NRC/IDCOR meetings and was extremely helpful in forming the basis for NRC personnel and contractors to more meaningfully interact with the IDCOR group. A brief summary of the results of these interactions is given in Chapter 9. An international program comparing the analyses of various analysts on two standard problems has also been in progress since the Spring of 1984. The status of this effort is also described in Chapter 9. This Chapter also includes further discussions of the interfacing of the CLWG program with NRC's source term reassessment effort.

The report concludes with Chapter 10 providing the conclusions from an overall perspective of this effort and recommendations for future work.

The technical editor of this report is Cardis L. Allen who received considered help from Randy Newton. We acknowledge the very important contributions from the following NRC contractors who are the real analysts and authors of this work: K. Bergeron, D. Williams, E. Haskins, A. Camp, D. Powers, M. Berman, V. Behr, R. Gasser, C. Shaffer, L. Smith, W. Von Rieseemann, J. Shepherd, J. Cummings, C. Hickox (all of SNL); P. Cybulskis, E. Wootan (BCL); Y. Pratt, T. Ginsberg, G. Greene, K. Perkins, J. Yang, M. Khatib-Rahbar (all of BNL); S. Hodge (ORNL); M. Corradini (University of Wisconsin) T. Theofanous (University of California), G. Travis (LANL) and T. Zalosh, E. Ural (FMRC). Other NRC contributors include T. P. Speis, M. Silberberg, J. Telford, J. Rosenthal, R. Barrett P. Niyogi, R. Curtis, R. Wright, and M. Cunningham.

This draft report provides a summary of the results from the CLWG studies and also includes a number of conclusions with regard to the application of these results. These results and conclusions are being presented for peer review and comment by interested parties. Comments should be addressed in writing within 60 days to:

Mr. Cardis L. Allen  
Division of Safety Technology, NRR  
U. S. Nuclear Regulatory Commission  
Washington, D. C. 20555



Themis P. Speis, Director  
Division of Safety Technology  
Office of Nuclear Reactor Regulation



## TABLE OF CONTENTS

	<u>Page</u>
ABSTRACT	iii
PREFACE	v
TABLE OF CONTENTS	ix
LIST OF TABLES	xiii
LIST OF FIGURES	xv
EXECUTIVE SUMMARY	xix
Chapter 1      INTRODUCTION	1-1
1.1    Origin and Objectives of CLWG	1-1
1.2    The CLWG Standard Problem Approach	1-2
1.3    Factors not Considered by CLWG	1-5
1.4    Structure of this Report	1-6
Chapter 2      PWR LARGE DRY CONTAINMENT (SP-1)	2-1
2.1    Description of Reference Plant Geometry (Zion)	2-1
2.2    Description of Standard Problem and Objectives	2-1
2.3    Discussion of Major Phenomenology	2-2
2.4    Methods of Analysis	2-4
2.5    Numerical Results and Sensitivity Studies	2-4
2.6    Considerations of Loads and Likelihood of Containment Failure	2-5
2.7    Conclusions and Recommendations	2-5
Chapter 3      PWR SUBATMOSPHERIC CONTAINMENT (SP-2)	3-1
3.1    Description of Reference Plant Geometry (Surry)	3-1
3.2    Description of Standard Problem and Objectives	3-1
3.3    Discussion of Major Phenomenology	3-2
3.4    Methods of Analysis	3-2
3.5    Numerical Results and Sensitivity Studies	3-2
3.6    Considerations of Loads and Likelihood of Containment Failure	3-6
3.7    Conclusions and Recommendations	3-6

		<u>Page</u>
Chapter 4	PWR ICE-CONDENSER CONTAINMENT (SP-3)	4-1
	4.1 Description of Reference Plant Geometry (Sequoyah)	4-1
	4.2 Description of Standard Problem and Objectives	4-1
	4.3 Discussion of Major Phenomenology	4-2
	4.4 Methods of Analysis	4-2
	4.5 Numerical Results and Sensitivity Studies	4-5
	4.6 Considerations of Loads and Likelihood of Containment Failure	4-10
	4.7 Conclusions and Recommendations	4-11
Chapter 5	BWR MARK I CONTAINMENT (SP-4)	5-1
	5.1 Description of Reference Plant Geometry (Browns Ferry)	5-1
	5.2 Description of Standard Problem and Objectives	5-2
	5.3 Discussion of Major Phenomenology	5-3
	5.4 Methods of Analysis	5-4
	5.5 Numerical Results and Sensitivity Studies	5-8
	5.6 Considerations of Loads and Likelihood of Containment Failure	5-13
	5.7 Conclusions and Recommendations	5-14
Chapter 6	BWR MARK II CONTAINMENT (SP-5)	6-1
	6.1 Description of Reference Plant Geometry (Limerick)	6-1
	6.2 Description of Standard Problem and Objectives	6-1
	6.3 Discussion of Major Phenomenology	6-2
	6.4 Methods of Analysis	6-3
	6.5 Numerical Results and Sensitivity Studies	6-4
	6.6 Considerations of Loads and Likelihood of Containment Failure	6-6
	6.7 Conclusions and Recommendations	6-7
Chapter 7	BWR MARK III CONTAINMENT (SP-6)	7-1
	7.1 Description of Reference Plant Geometry (Grand Gulf)	7-1
	7.2 Description of Standard Problem and Objectives	7-2
	7.3 Discussion of Major Phenomenology	7-3
	7.4 Methods of Analysis	7-9
	7.5 Numerical Results and Sensitivity Studies	7-13
	7.6 Considerations of Loads and Likelihood of Containment Failure	7-13
	7.7 Conclusions and Recommendations	7-14

		<u>Page</u>
Chapter 8	DIRECT HEATING EFFECTS (SP-A)	8-1
	8.1 Description of Reference Plant Geometry	8-1
	8.2 Description of Standard Problem and Objectives	8-1
	8.3 Discussion of Major Phenomenology	8-2
	8.4 Methods of Analysis	8-2
	8.5 Numerical Results and Sensitivity Studies	8-2
	8.6 Considerations of Loads and Likelihood of Containment Failure	8-7
	8.7 Conclusions and Recommendations	8-8
Chapter 9	RELATED ACTIVITIES	9-1
	9.1 IDCOR/NRC Comparisons	9-1
	9.2 International Comparison Calculations	9-6
	9.3 NRC Source Term Reassessment	9-7
Chapter 10	CONCLUSIONS AND RECOMMENDATIONS	10-1
	10.1 Conclusions	10-1
	10.2 Specific Recommendations for Further Study	10-1
Chapter 11	REFERENCES	11-1
Appendix A	CONSENSUS SUMMARY ON DIRECT HEATING	A-1
Appendix B	CORIUM/CONCRETE INTERACTION IN THE MARK I CONTAINMENT DRYWELL AND LOCAL LINER FAILURE	B-1
Appendix C	EX-VESSEL STEAM EXPLOSIONS IN THE MARK II CONTAINMENT	C-1

## TABLES

<u>Table</u>	<u>Title</u>	<u>Page</u>
2.1	Parametric Variations Considered	2-6
2.2	Corium Composition	2-7
2.3	Reactor Cavity Concrete Composition and Characteristics	2-8
2.4	Conditions of Corium Ejection	2-9
2.5	Containment Structural Heat Sinks for Zion	2-10
2.6	Results of Sensitivity Studies	2-11
3.1	SP-2 Base Case Specifications	3-8
3.2	SP-2 Sensitivity Study Specifications	3-9
3.3	SP-2 Base Case Pressure and Temperatures	3-10
4.1	MARCH 2.0 Chronology for CLWG Ice Condenser Containment Standard Problem	4-12
4.2	Case Descriptions and Summary of HECTR Results	4-13
4.3	Summary of BCL Results for Ice Condenser PWR Standard Problem	4-14
4.4	Ice Condenser PWR Standard Problem	4-15
5.1	BWR 4 Reactor Vessel and Core Parameters	5-15
5.2	Containment Design Parameters	5-16
5.3	Containment Heat Sinks	5-17
5.4	Specifications for Comparison Calculations Base Case	5-18
5.5	Summary of BWR Mark I Sensitivity Studies	5-19
5.6	Comparison of CORCON-1/MARCON Results: TQUV1	5-20
5.7	Comparison of CORCON-1/INTER Results: TQUV3	5-21
5.8	Summary of the Major Modeling Differences for Six TQUV High Temperature Debris Calculations	5-22

TABLES (Continued)

<u>Table</u>	<u>Title</u>	<u>Page</u>
6.1	Mark II Standard Problem Definitions	6-8
6.2	Specifications of Concrete	6-9
6.3	Passive Heat Sinks for Mark II Plant Problem	6-10
6.4	Comparison of Results for Mark II Standard Problem	6-11
7.1	Grand Gulf Containments Geometric Data	7-16
7.2	Initial Conditions	7-17
7.3	Hydrogen Source Terms	7-18
7.4	Case A Results	7-19
7.5	Case B Results	7-20
7.6	Case C Results	7-21
7.7	Case 1 Results	7-22
7.8	Case 2 Results	7-23
7.9	Case 3 Results	7-24
7.10	Case 4 Results	7-25
8.1	SP-2 Pressures and Temperatures with Direct Heating	8-9
9.1	Percent of Zircaloy Reacted in TMLB' Sequence	9-8
9.2	Comparison of Hydrogen Production in CLWG Standard Problem SP-6 (Mark III) Calculations vs. IDCOR Calculations	9-9
9.3	IDCOR Sensitivity Results for Mark III T1QUV	9-10

## FIGURES

<u>Figure</u>	<u>Title</u>	<u>Page</u>
2.1	Schematic Illustration of Zion Reactor Containment Building	2-12
2.2(a)	Representation of the Reactor Vessel Situated Within the Reactor Cavity	2-13
2.2(b)	Plan View and Typical Dimensions of Reactor Cavity and Keyway	2-14
2.3	Pressure Versus Time (Non-adiabatic Case) for Two Quench Times	2-15
3.1	General Configuration of the Surry Containment Design	3-11
3.2	Plan View of Geometry of Surry Lower Reactor Cavity	3-12
3.3	Section A-A of Figure 3.2 Lower Reactor Cavity	3-13
3.4	SP-2 Pressures for the "High" Steam Spike Sensitivity Study	3-14
3.5	SP-2 Temperatures for the "High" Steam Spike Sensitivity Study	3-15
4.1	Reactor Building Elevation	4-16
4.2	Plan-Upper Compartment	4-17
4.3	Ice Condenser Bed	4-18
4.4	MARCH Ice Condenser Containment Model	4-19
4.5	HECTR Ice Condenser Containment Model	4-20
4.6	Reference Containment Steam Source Following Vessel Breach	4-21
4.7	Reference Containment Hydrogen Source Following Vessel Breach	4-22
4.8	HECTR Calculated Pressure Response Without Hydrogen Burning	4-23

FIGURES (Continued)

<u>Figure</u>	<u>Title</u>	<u>Page</u>
4.9	HECTR Calculated Temperature Response in the Lower Compartment	4-24
4.10	HECTR Calculated Ice Remaining Without Hydrogen Burning	4-25
4.11	MARCH Calculated Pressure Response Without Burning	4-26
4.12	MARCH Calculated Atmosphere in Dead End Volume Without Burning	4-27
4.13	MARCH Calculated Atmosphere Composition in Lower Compartment Without Burning	4-28
4.14	MARCH Calculated Atmosphere Composition in Ice Condenser Upper Plenum Without Burning	4-29
4.15	MARCH Calculated Atmosphere Composition in Upper Compartment Without Burning	4-30
5.1	Mark I Containment	5-23
5.2	BWR Standard Problem: TQUV-1	5-24
5.3	BWR Standard Problem: TQUV-1A	5-25
5.4	BWR Standard Problem: TQUV-2	5-26
5.5	BWR Standard Problem: TQUV-3	5-27
5.6	BWR Standard Problem: TQUV-3A	5-28
5.7	BWR Standard Problem: TQUV-4	5-29
5.8	Brown's Ferry TQUVCC01	5-30
5.9	TQUVCC01: Pressure vs. Time	5-31
5.10	TQUVCC01: Compartment Pressure vs. Time	5-32
5.11	TQUVCC01: Compartment Temperature vs. Time	5-33
5.12	TQUVCC01: Compartment Pressure vs. Time	5-34
5.13	TQUVCC01: Compartment Temperature vs. Time	5-35
5.14	TQUV: Compartment Temperature vs. Time	5-36
5.15	TQUV: Compartment Pressure vs. Time	5-37
5.16	Brown's Ferry TQUVCC	5-38

FIGURES (Continued)

<u>Figure</u>	<u>Title</u>	<u>Page</u>
6.1	Mark II Primary and Secondary Containments	6-12
6.2	Comparison of Containment Pressure for the TQUV Sequence (Limestone Concrete)	6-13
6.3	Comparison of Containment Temperature for the TQUV Sequence (Limestone Concrete)	6-14
6.4	Comparison of Containment Pressure for the TQUV Sequence (Basalt Concrete)	6-15
6.5	Comparison of Containment Temperature for the TQUV Sequence (Basalt Concrete)	6-16
7.1	Cutaway View Showing Reactor Pedestal Support Structure and the Cavity Beneath the Reactor Vessel for Plant III	7-26
7.2	The Safety/Relief Valve Discharge is Into the Portion of the Pressure Suppression Pool Lying Outside of the Drywell	7-27
7.3	Case-C: 100 lb/min Through 9 Spargers Pressure and Average Heat Flux in the Containment	7-29
7.4	Case-C: 100 lb/min Through 9 Spargers Flame Height, Oxygen and Steam Concentrations	7-30
7.5	Case C: 100 lb/min Through 9 Spargers Inner Wall Peak Heat Fluxes	7-31
7.6	Case C: 100 lb/min Through 9 Spargers Outer Wall Peak Heat Fluxes	7-32
7.7	SNL-1 Case C: 100 lb/min Through 9 Spargers Heat Flux vs. Time	7-34
7.8	SNL-1 Case C: 100 lb/min Through 9 Spargers Temperature vs. Time	7-35



FIGURES (Continued)

<u>Figure</u>	<u>Title</u>	<u>Page</u>
7.9	Compartment 4: Pressure vs. Time	7-37
7.10	Compartment 7: Temperature vs. Time	7-38
7.11	Compartment 4: Temperature vs. Time	7-39
7.12	Surface 27: Net Total Heat Flux vs. Time	7-40
7.13	Surface 27: Temperature vs. Time	7-41
7.14	Pressure in the Wet Well	7-42
7.15	Max and Min Temperature in Wet Well	7-44
7.16	Heat Flux to the Inner Wall	7-45
7.17	Heat Flux to the Inner Wall vs. Time	7-46
7.18	Temperature of the Inner Wall	7-47
8.1	SP-2 Pressure and Temperature as a Function of Core Fraction Involved in Direct Heating	8-10
8.2	Calculated SP-2 Pressures for the "Low" and "High" Steam Spikes and for the Nominal Direct Heating Scenario	8-11
8.3	Calculated SP-2 Temperatures for the "Low" and "High" Steam Spikes and for the Nominal Direct Heating Scenario	8-12
9.1	Containment Pressure vs. Time for TMLB' with a Dry Reactor Cavity for an Ice Condenser Plant	9-11
9.2	Drywell Pressure and Temperature vs. Time for Mark I Sequences Dominated by Core-Concrete Interactions; CLWG vs. IDCOR	9-12

## EXECUTIVE SUMMARY

This report documents the work performed by the Containment Loads Working Group (CLWG) and provides the NRC staffs' current interpretation of the significance of that work with respect to specific loading mechanisms in selected containment designs.

The CLWG was formed in July 1983 under SARP auspices. The Group is composed of expert analysts from BCL, BNL, LANL, ORNL, SNL, Purdue University, University of Wisconsin, Factory Mutual Research Corporation, and NRC (RES and NRR).

The central objective of the Group was to develop an updated evaluation of containment loads (temperature and pressure history) and associated challenges to containment integrity, due to severe (core melt) accidents. Such loads result from thermal-hydraulic phenomena following the release of the molten core materials (corium) from the reactor vessel. These evaluations, together with the results of the Containment Performance Working Group (CPWG),\* can provide a basis for assessing modes and likelihoods for containment failure. In this summary the staff has compared containment loads estimated by the CLWG to containment pressure capabilities estimated by the CPWG. This provides a basis for reaching some conclusions regarding the significance of containment loading mechanisms for certain classes of accidents in the various types of reactor containments.

### CLWG Approach

The overall approach used by the CLWG is based on a standard problem methodology. The CLWG management team (NRC) selected a specific reactor to represent each one of the six containment designs deployed in the U.S. as follows:

<u>Containment Type</u>	<u>Reactor Name</u>
Large Dry	Zion
Subatmospheric	Surry
Ice Condenser	Sequoyah
Mark I	Browns Ferry
Mark II	Limerick
Mark III	Grand Gulf

\* NUREG-1037, Containment Performance Working Group Report, Draft dated May, 1985.

This selection was made to overlap with previous assessments (i.e., the Reactor Safety Study (WASH-1400) and the Zion-Indian Point Study (NUREG-0850), etc.) and thus afford a basis for evaluating progress in understanding severe accident phenomena. At this point the representation achieved by this selection is qualitative. It is left for future studies to determine the extent of variability in response due to individual design variations within each type of containment. This plant-specific approach allowed the definition of each standard problem in the necessary detail. The standard problem methodology allowed relatively unambiguous comparisons among the proposed results by the various analysts participating. Efforts were made to understand differences and wherever possible to arrive at consensus conclusions as well as qualitative results.

For each reactor the CLWG management team defined a containment challenge mechanism and associated standard problem as follows.

<u>Standard Problem</u>	<u>Containment Type</u>	<u>Challenge Mechanism</u>
SP-1	Large Dry	Steam Spike
SP-2	Subatmospheric	Concrete Attack
SP-3	Ice-Condenser	Hydrogen Burn
SP-4	Mark I	Concrete/Liner Attack
SP-5	Mark II	Concrete Attack
SP-6	Mark III	Diffusion Flames

The above selection is an attempt to represent a principal containment loading mechanism for each containment type as dictated by prevalent phenomenology. The emphasis was distributed for more thorough coverage while an adequate understanding can still be developed, on this basis, for any combination. The in-vessel aspects of the severe accident sequences were considered parametrically as follows:

- (a) Quantity, composition and temperature of corium released at times of vessel failure.
- (b) Quantity and timing of hydrogen release.
- (c) Vessel breach size.
- (d) Primary system and containment pressures.

Although they are most likely unrealizable, cases of 100% core release at vessel failure (the presence of core melting incoherencies is widely recognized) and hydrogen production corresponding to 100% metal oxidation were included in the specifications of the standard problems. Similar attempts to bound the specifications over generously assigned uncertainty ranges were also made with regard to metals available for ex-vessel oxidation and core thermal state. In all cases all of the active containment heat removal and spray systems were assumed to be in-operative.

In general the specifications for the standard problems called for conditions typical of either a station blackout (a high primary system pressure at vessel failure) or a large loss-of-coolant accident (a low primary system pressure at vessel failure). These scenarios encompass the major thermal-hydraulic phenomena associated with severe accidents.

Consideration of in-vessel steam explosions was left for the Steam Explosion Review Group (SERG, see NUREG-1116). Ex-vessel steam explosions were reviewed by the CLWG and found not to be a source of significant loads for these plants. These findings are reported in more detail in the main text.

Another mechanism which came to be known as "direct heating" gained some advocacy during the CLWG proceedings. It is relevant only to molten corium dispersal to the containment atmosphere following release from a high pressure system. It is evaluated in this summary as a special problem (SP-A).

After completion of the work summaries of each CLWG problem results were prepared and reviewed by the participating analysts. The documentation in the CLWG report is based primarily on these summaries. It is hoped that, in addition to providing numerical estimates, it will be of future use regarding the analytical methodology and overall technical approach.

### Probabilistic Aspects

By definition the standard problem approach is mechanistic (deterministic). However, because of the parametric variations mentioned above and other sensitivity studies and because of phenomenological uncertainties, as reflected by the particular set of assumptions, models and model parameters utilized, a range of potential loads, rather than a single value,\* was arrived at for each standard problem. In a sense this may be taken to represent an uncertainty range for the estimated loads. Available time and resources, as well as the CLWG's technical direction, were not conducive to a thorough evaluation of the likelihood of each calculated outcome. Still an attempt has been made to supplement the results with degrees of expectation. Each standard problem presented a different kind of challenge in this regard. The basis for these judgments will be presented together with the results on a case by case basis.

### Results for SP-1

The standard problem SP-1 was focused on the loads resulting from the so-called steam-spikes in a large dry containment such as that of the Zion plant. The phenomena involve rapid quenching of the melt as it is being released into the reactor cavity. Corium-concrete interactions, even if they were present, could

\* For monotonically increasing loads reference to the values at an appropriately selected time (typically a few hours) is made here.

not alter the loading history due to the steam spike within the first few hours. On the other hand energy release due to metal/water reactions was taken into account. In the presence of a steam-spike, hydrogen burn events could not be sustained (steam inerting) and no such events were considered in the calculations.

Quenching of a whole-core melt in a fully-flooded cavity would yield a pressure increment of 2.3 bar (35 psi).<sup>\*</sup> If a 4 bar (60 psia) pressure already existed as a result of primary system boil-off (i.e., station blackout) a steam spike of 6.3 bar (95 psia) would result. Steam blowdown from an initially pressurized primary system at 157 bar (2,300 psi) could contribute another 1 bar (15 psi). Hence, even under the worst possible conditions a pressurization to 7.3 bar (107 psia) is predicted. This is an upper bound value and still well below the 10.2 bar (150 psia) containment pressure capability estimated by the CPWG. In fact, as a result of finite boil-off times and passive heat sinks significant reductions (15 to 30 psi) in these values were calculated when steam generation is water limited. The CLWG results lead one to conclude that steam-spike-induced failure of the Zion containment at the time of vessel failure should be considered an event of very low probability.

The long-term containment response is driven by decay heat and depends on water availability. If core debris cooling in the reactor cavity does not become water limited containment pressurization would continue at the rate of 10 psi/hr yielding failure at 16 hrs. If the cavity dries out pressurization will continue due to gases released from corium-concrete interactions. The time of failure in this case would be considerably longer.

#### Results for SP-2

Subatmospheric containments are very closely related to "large dries." They are of somewhat smaller volume and they are built for a somewhat lower design pressure. It is expected, therefore, that the steam-spike behavior will be similar to that determined under SP-1. There are cavity designs, however, both for large dries as well as subatmospheric containments, that preclude the flow of containment building water into them. Thus, except for high pressure scenarios that involve the dumping of accumulator water (wet cavity case) following reactor vessel melt-through (containment sprays are assumed inoperative), steam-spike phenomenology is also precluded for sequences without ECCI and containment spray operation. Corium-concrete interactions would then dominate (dry cavity case) the containment loading process. The Surry reactor was selected to exemplify this kind of behavior. Both the wet and dry cavity cases were considered.

For the wet cavity case the accumulator water was sufficient to quench a whole-core melt producing, at most, a pressure increment of 2 bar (30 psi). Thus, with steam blowdown from an initially pressurized primary system at 156 bar (2,300 psi)

<sup>\*</sup> The numbers in this summary generally represent the essence of the results and should be considered approximate values.

together with an assumed initial containment pressure of 2 bar (30 psi) a steam spike of 5 bar (73 psia) is obtained. Even assuming, arbitrarily, that the corium melt contained a sufficiently large quantity of steel (by melting reactor vessel internals) to vaporize all the accumulator water a peak pressure of less than 7.3 bar (107 psia) would result. This upper bound is well below the 9.2 bar estimated by the CPWG to be required for failure. The CLWG results lead one to conclude that steam-spike-induced failure of the Surry containment is an event of very low probability. Since water cannot return to the cavity eventual dry-out leading to corium-concrete interactions should be expected. The pressure build up due to this process is much slower than that due to a steam spike. The two-phases are, therefore, relatively uncoupled.

For the dry cavity cases any pressurization within the first few hours would correspond to whatever small amounts of water were assumed to be present in the cavity, and whatever small quantities of steam is assumed to exist within the primary system at the time of vessel failure. Pressures below 2.7 bar (40 psia) are indicative of this behavior. Any pressure loads due to the basaltic concrete decomposition develop slowly over a time scale of 10s of hours and containment failure levels are not approached for a few days.

However, further consideration of this scenario by some analysts subsequent to the initial calculations indicate that it is possible that over such a long time frame, continuing steam condensation might lead to steam de-inerting and, as a consequence, to hydrogen burns. The conclusion is, however, that containment failure within the first few hours is quite unlikely.

### Results for SP-3

With its extensive pressure suppression capability an ice-condenser containment is not susceptible to steam spikes. However, this capability may lead to de-inerting and thus to potential challenges by hydrogen burns. This has been recognized already and electric-powered igniters have been installed in operating plants. As long as these igniters remain operational and the hydrogen is well mixed controlled burning of a reasonable rate of in-vessel hydrogen production and release (as well as reasonable quantities of ex-vessel hydrogen), and suppression of the resulting energy by the ice-bed will occur. However, the loss of the mixing function provided by the air returns can result in detonable mixtures. The most likely potential for challenge, therefore, exists if power to the igniters and air return fans is lost. Station blackout (TMLB) would represent such a situation. The Sequoyah power plant was selected for the calculations.

The results indicate that, for the assumptions in these analyses, the loading pattern is generally characterized by intermittent, sharp, pressurization of the containment. These spikes correspond to hydrogen burns. Their timing depends upon meeting conditions for self-ignition, and their amplitude depends upon the spatial hydrogen distribution at the time of ignition and the flame propagation requirements. As the waiting period for ignition increases not

only the quantities of accumulated hydrogen increase, but also its distribution is biased towards the containment dome. As a consequence the quantity of energy release in the burn increases and the ice-bed becomes less effective in suppressing the resulting pressures. This whole process is aggravated as the magnitude of the steam spike in the lower compartment increases. This is because the resulting high steam flows through the ice bed and into the upper dome favor inerting of the lower compartments and ignition within the upper containment dome (sweeps hydrogen to upper dome). Burn spikes of up to 4.8 to 6.8 bar (70 to 100 psi) have been calculated and possibilities for detonations were raised under such conditions. Such loads, compared to the CPWG estimated failure pressure of the Sequoyah containment at 4.4 bar (65 psia), would represent a significant challenge. Calculations based on a low steam spike assumption resulted in burn spikes of 3.4 to 4.8 bar (50 to 70 psi), still significant with regard to containment failure.

The CLWG results lead one to conclude that a station blackout accident (as it is currently perceived to lead to high pressure scenarios and including loss of igniters) in the Sequoyah plant would most likely cause an early containment failure. This conclusion, can be modified by primary system failure prior to core melt (see SP-A) and by ensuring proper functioning of igniters and air returns fans (e.g., with a dedicated battery). Clearly more work needs to be done to improve our understanding in these areas for this containment type.

#### Results for SP-4

With its extensive pressure suppression capability the Mark I containment is not susceptible to steam spikes, even if contact with a significant quantity of water was to occur. Because of inerted operation hydrogen burns are also irrelevant. This standard problem, therefore, is focused on the consequences of corium-concrete interactions on the drywell floor. In addition to the pressurization resulting from the generation of non-condensibles one should be concerned about high drywell temperatures and concomitant penetration seal degradation. The Browns Ferry power plant was selected for the specifics. The drywell was considered completely free of water. Parametric ranges were defined on the quantity of the metallic component (e.g., unreacted zirconium) available for oxidation on the drywell floor (by the steam released from the concrete), and the extent of the melt spreading outside the pedestal area.

The results indicate that because of the relatively small gas volume in comparison to all other containments non-condensable pressures build rapidly. They reach the estimated 9 bar (132 psia) ultimate capability of the containment within 2 hours from the start of core concrete interaction. However, based on results from the CPWG studies it appears that significant leaks could develop before the ultimate capability pressures are reached and catastrophic failure might therefore be prevented.

In competition with the above overpressure failure mechanism is the thermal loadings on the drywell boundaries (particularly at penetration seals). The drywell atmosphere was calculated to heat briefly up to the range of 650° down in the range of 500° to 700°F. The integrity of the seals could be uncertain under such thermal loading conditions. It would take temperatures significantly above 1000°F to challenge the integrity of the drywell liner. However, the possibility of early melt-through of the drywell liner, by direct contact with the melt, in the neighborhood of the floor-drywell wall junction has also been suggested.

The CLWG results lead one to conclude that Mark I failure within the first few hours following core melt would appear rather likely.

#### Results for SP-5

The Mark II containment is also inerted and hydrogen burns can be of no consequence. This standard problem, therefore, is very similar to that considered for the Mark I case (SP-4) with one major exception. Here, as the melt spreads on the diaphragm floor, it can flow through the numerous downcomer openings into the suppression pool. Thus only a fraction of that exiting the vessel will be available for corium-concrete interactions. A corresponding reduction in containment loads would be expected. The standard problem considered this fraction parametrically. The Limerick power plant was selected for the specifics.

Some calculated results indicate that the ultimate containment capability of 10.5 bar (155 psia) could be approached within 2 to 3 hours (for a limestone concrete cavity floor). Other calculations do not predict early failure. For a basaltic concrete floor the pressurization rate is considerably lower. As in the Mark I case high drywell temperatures again raise the possibility of penetration seal failures.

Based on these results we conclude that while early failure of the Limerick containment appears rather unlikely, additional work remains to be done before this judgment can be adequately sharpened.

#### Results for SP-6

This problem dealt with the Mark III containment. The geometrical arrangement of the Mark III drywell is such that the effects of corium-concrete interactions will be similar to those in Mark I containments. Because of the much larger volume of the Mark III, however, pressurization rates will be slower than those reported for the Mark I or Mark II (SP-4 and SP-5). On the other hand the Mark III containment is not inerted and the potential consequences of hydrogen burns must be considered. In fact all owners of BWR Mark III plants are now required to install deliberate ignition devices to control potential releases of H<sub>2</sub> to containment. The Grand Gulf power plant was selected to provide the specifics for this problem.



First let us consider the global effects of  $H_2$  combustion assuming the  $H_2$  ignition devices are operable. The extent of burning would be limited by the quantities of oxygen available. In this limit the required quantity of hydrogen would correspond to oxidation of nearly 65% of all the zirconium in the cladding. Resulting peak pressures of 2 bar (30 psia) can thus be calculated as an upper bound assuming that the  $H_2$  is burned continuously as it is released to the wetwell. Such loads are well below the estimated 5 bar (75 psia) capability of the Mark III containment and the likelihood of containment overpressure failure through this mechanism is thus extremely low. However, if the  $H_2$  release rates are sufficiently high, standing flames can be produced in the wetwell above the suppression pool. Local heat fluxes in the vicinity of the flames can produce high local temperatures which could result in degradation of seals. Seal degradation could result in loss of drywell integrity allowing the fission products released from the fuel to bypass the suppression pool where they would normally be scrubbed. Thus, seal degradation is an important consideration. The Mark III standard problem was, therefore, focused on local thermal effects due to standing flames in the wetwell.

Localized heating can result from diffusion flames developed near the suppression pool surface as the hydrogen is discharged from the primary system, through the SRVs, to the wetwell air space. Such localized heating can affect the integrity of penetration seals which are expected to degrade at temperatures around 330°F. The position of the flames above the SRVs (assumed to release the hydrogen) and the rate and duration of the hydrogen source to them were considered parametrically. Peak gas temperature were found to be moderated by large gas entrainment rates to levels around 1,370°K (2,000°F). The wall (and seal) temperatures depend on position and the heat flux delivered. In general, values in the range of  $10^3$  to  $10^4$  BTU/hr ft<sup>2</sup> were determined. Evaluations of consequent seal degradation and leak area development have been carried out by the CPWG. They conclude that important seals (including the drywell and containment personnel airlocks) retain their integrity under these conditions.

#### Results for SP-A

There was no standard problem per se defined in connection with the direct heating issue. The concern developed while addressing standard problems SP-1 and SP-2, hence, it was examined in this frame work. The relevant phenomenology involves forceful expulsion of the melt from a pressurized reactor vessel and massive dispersion of the molten corium into the containment atmosphere. Under such conditions any metallic component in the melt could be subjected to oxidation and additional direct heating of the containment atmosphere from this source will occur.

The resulting containment loads will depend principally on the quantities of melt actually dispersed and the amounts of metallic components oxidized. In the case of a whole-core dispersal and 100% oxidation of all cladding, a peak pressure of 12 bars (176 psia) and a peak temperature of 1,000°K (1340°F) can be calculated. If oxidation of steel is included this value is even higher. In general, rather extreme assumptions had to be utilized to produce loads of sufficient magnitude to challenge a large dry containment. On the other hand the quantification of the dispersal (i.e., via distorted pathways)\* and oxidation processes, as well as of the availability of metallic components for oxidation, are uncertain. As a result it did not become possible to arrive at a consensus conclusion regarding the relative likelihood of loads for any case of material involvement below the one specified.

Examination of the attainability of the initial condition invoked for direct heating provides an alternative and potentially more promising approach to this problem. Although the CLWG did not deal as a whole with the aspect of the analysis, calculations were developed which indicated that, due to strong natural circulation currents of the high pressure steam, temperature gradients within the primary system components were rather modest. Since the structural properties of steel and steam generator tube material degrades rapidly above 1,300°F, it was concluded that primary system failure and depressurization could occur prior to core melt. Clearly, steam generator tube failures would also imply a path to the outside. If these initial results were to be confirmed it would be possible to conclude that only low pressure scenarios are relevant to containment capability evaluations. This approach will be examined in parallel with realistic assessments of the flow paths to containment supported by relevant experiments.

#### Concluding Remarks

Based on the above results several areas are indicated in which reduction of uncertainties would appear beneficial. Perhaps the most important one, as it may affect all reactor types and containments, is that associated with melt release at high pressure (direct heating problems). Since initial evaluations indicate that primary system failure, and hence depressurization, could be possible prior to core melt, a high priority in this area is to address whether a high pressure scenario persisting to core melt is physically realizable. The second important topic, affecting principally the ice-condenser plants, is that of hydrogen combustion. This is a rather complex topic and it may be resolved in a number of contributing subproblems including: hydrogen generation, release, ignition, burning, and possibly transition to detonation. Finally, some residual uncertainties in corium-concrete interactions should be mentioned. They concern the long-term temperature evolution of the melt and affect not so much the development of pressure loads as they do the so-called "vaporization release" (source term) and the containment temperature (seal integrity). This problem is of principal interest to Mark I containments.

\* The IDCOR program has initiated a study to examine in detail the geometry of the flow paths to containment for core debris for all plants.

## SUMMARY OF TABLES

### SP-1 (Zion)

Containment Capability:	149 psia*
Upper Bound Spike:	107 psia
Early Failure Physically Unreasonable	
Best Estimate Pressure Rise: (Including heat sinks)	10 psi/hr
Best Estimate Failure Time: (Unlimited water in cavity)	16 hrs

### SP-2 (Surry)

Containment Capability:	134 psia*
Upper Bound Spike:	107 psia
Early Failure Physically Unreasonable	
Best Estimate Failure Time: (Dry cavity)	Several Days

### SP-3 (Sequoyah)

Containment Capability:	65 psia, 330°F*
Upper Bound Loading:	70-100 psia
Lower Bound Loading:	50-70 psia
Thermal Loads:	500° - 700°F
Early Failure Quite Likely	

### SP-4 (Browns Ferry)

Containment Capability:	132 psia, 330°F*
Upper Bound Loading:	132 psia in 40 min.
Lower Bound Loading:	132 psia in 2 hours
Thermal Loads:	500° - 700°F
Early Failure Quite Likely	

SP-15 (Limerick)

Containment Capability: 155 psia, 330°F\*  
Upper Bound Loading: 145 psia in 2-3 hours  
Lower Bound Loading: 100 psia in 3 hours  
Thermal Loads: 550° - 700°F  
Early Failure Rather Unlikely  
(Upper bound too conservative)

SP-6 (Grand Gulf)

Containment Capability: 75 psia\*  
Upper Bound Loading: 30 psia  
Wall Fluxes:  $10^3 - 10^4$  BTU/hr ft<sup>2</sup>  
Penetration Seal Temperature: 345°F\*  
Pressurization Failure from Diffusion Flames Physically Unreasonable  
Seal Failure Unlikely

SP-A (Based on SP-1 Results)

Containment Capability: 150 psia\*  
Upper Bound Loads: 176 psia  
Thermal Loads: 1340°F  
Early Failure Quite Likely  
(100% core dispersal with  
100% clad oxidation  
- No seal oxidation  
- No early depressurization  
- Unobstructed flow)

\*From NUREG-1037, Containment Performance Working Group Report,  
Draft Dated May 1985.

## Chapter 1 INTRODUCTION

### 1.1 Origin and Objectives of the CLWG

Containment loads from core melt accidents arise as a consequence of primary system failure and the thermal-hydraulic-material interactions following release of the corium melt debris into the containment space. The phenomena and mechanisms involved in these interactions have been under intensive study following the TMI accident. These may be summarized as follows:

- (a) Steam Spike - The term refers to pressure generated due to rapid quenching of the corium melt. For this process to occur the melt must come into intimate contact with substantial quantities of water. The steam spike would be augmented by release of primary system steam in the high pressure scenario.
- (b) Concrete Attack - The term refers to concrete decomposition and associated gas generation due to contact of high temperature melt with the containment floor. The consequence is penetration of the floor and generation of both combustible and non-combustible gases with the associated pressure generation. For this to occur the corium must remain unquenched on the concrete floor, implying absence of water, or possibly isolation of the water from the melt by formation of crusts. In the absence of water, high temperature gas evolution and radiation heating would result also in a thermal loading of the containment atmosphere and perhaps even of its boundaries. The presence and oxidation of metallic components within the melt by steam released from the concrete may play an important role of the overall behavior affecting the temperature of the melt and thus the rate of concrete attack.
- (c) Hydrogen Burn - In contact with oxygen in the containment atmosphere the hydrogen generated from metal-water reactions and concrete decomposition can burn at various rates depending on the composition of the atmosphere at ignition. With increasing rates of this chemical reaction we can have: diffusion flames, deflagrations and detonations. On the other hand, at a sufficiently high steam content the mixture is inerted and burning cannot be initiated or sustained. The consequences range from localized thermal effects (diffusion flames), to global pressurization and heating of the containment atmosphere (global burn or deflagration), to shock waves as well as pressurization and heating effects (detonations).

- (d) Direct Heating - The term refers to the direct heating of the containment atmosphere through intimate contact with the corium melt. For this process to occur large scale dispersal of corium within the containment volume must occur. Ejection at high pressure has been suggested as the specific mechanism initiating such phenomena. The intensity of heating may be augmented by the heat of reaction from the large scale oxidation of any metallic components during the dispersal process. This process is particularly relevant to PWRs because they are not equipped with an automatic de-pressurization system, although in this case energy redistribution by natural circulation may cause primary system failure and de-pressurization prior to the melt release event.

The realistic evaluation of the loads that can evolve from these phenomena for particular severe accident sequences is an important component of assessing the risk from commercial nuclear power generation. An adequate appreciation of these loads together with an understanding of the containment response to them provides the basis for assessing the likelihood and timing of containment failure and hence of the potential for and magnitude of any radioactivity release to the environment. The results of this process are particularly sensitive to the timing of failure, with significant reduction in the release of radioactive material occurring by natural deposition, condensation and plate-out processes as the failure is delayed into the several hours time frame. The CLWG was formed as part of a coordinated NRC effort to develop a comprehensive reevaluation of the source terms and risk taking into account progress made since the previous such evaluation was made in the Reactor Safety Study (WASH-1400).

The CLWG was formed in July 1983 under SARP auspices. The Group was composed of expert analysts from BCL, BNL, LANL, ORNL, SNL, Purdue University, University of Wisconsin, Factory Mutual Research Corporation and NRC (including both the office of Research and Regulation). The objective of the Group was to develop an updated evaluation of containment loads (temperature and pressure history) and the associated challenges to containment integrity. These evaluations, together with results from the Containment Performance Working Group (CPWG), provide a basis for assessing the modes and likelihood of containment failure. These results have been used in the Severe Accident Risk Reduction Program (SARRP) to help define containment trees which were combined with new estimates of fission product release to develop improved severe accident source terms. These improved source terms are described in NUREG-0956.

## 1.2 The CLWG Standard Problem Approach

The overall approach was based on a standard problem methodology. The CLWG management team (NRC) selected a specific reactor to represent each of the six containment designs deployed in the U.S. as follows:

<u>Containment Type</u>	<u>Reactor Name</u>
Large Dry	Zion
Subatmospheric	Surry
Ice Condenser	Sequoyah
Mark I	Browns Ferry
Mark II	Limerick
Mark III	Grand Gulf

These specific selections were made to maximize overlap with previous assessments, e.g., the Reactor Safety Study (WASH 1400) and the Zion-Indian Point Study (NUREG-0850), etc. and thus afford a basis for evaluating progress in understanding severe accident phenomena. At this point the representation achieved by this selection is qualitative. It is left to future studies to determine the extent of variability in response due to individual design variations within each type of containment. It is hoped that the insights developed through the CLWG effort and the results recorded in this report will enormously facilitate the task of assessing this variability. On the other hand, by considering all six types of containment, the coverage is believed to be comprehensive.

This plant-specific approach allowed the definition of each standard problem in the required detail. This forced a sense of realism not only in the narrow parameter sense but also in the overall attitude of addressing phenomena, sequences and issues. Furthermore, together with a common definition of initial conditions and primary system inventory released into the containment at vessel failure, the specification was sufficiently complete to allow reasonably unambiguous comparisons among the results obtained by the CLWG members. On this basis efforts were made to understand differences and, whenever possible, to arrive at consensus conclusions as well as qualitative results. Prior to its complete definition and issuance each standard problem was introduced by a member of the NRC management team to the whole CLWG for review and discussion.

The principal focus of the CLWG was on containment events following release of the melt from the primary system. In keeping with the above philosophy the in-vessel aspects of the severe accident sequences were specified parametrically as follows:

- (a) Quantity, composition and temperature of corium released,
- (b) Quantity and timing of hydrogen release,
- (c) Vessel breach size, and
- (d) Primary system and containment pressures.

In general these choices were made to reflect the so-called "high" and "low" pressure scenarios. They correspond to the Station Blackout and Loss of Coolant Accident scenarios respectively and are believed to encompass, for CLWG purposes, the range of thermal-hydraulics phenomenology of containment events in core melt accidents. The intentional enveloping nature of these parametric specifications should be kept in mind in considering the CLWG results. For example, the presence of core melting incoherencies is widely recognized yet due to remaining uncertainties releases including up to 100% of the core inventory were specified. Similar attempts to bound the specifications over generously assigned uncertainty ranges were made on matters of hydrogen production and release, metals available for ex-vessel oxidation and core thermal state. In all cases all active containment heat removal and spray systems were assumed to be permanently inoperative.

Depending on the conditions and the containment type one or more of the loading mechanisms mentioned in the previous section may become operative while others may be simply impossible. For example the MARK I type containments are inerted thus hydrogen burn becomes irrelevant. On the other hand these loading mechanisms may appear singly or in combinations of simultaneous or sequential events. For example, a large steam spike in a large dry containment requires sufficient water to assure quenching.

This means an absence of concrete attach (the water precludes it) and, due to high partial steam pressures (from the steam spike) there will be no hydrogen burn because of the inerting effect of the steam. On the other hand, in an ice condenser containment, a steam spike may be quenched by the ice bed but, in the process, conditions may develop that lead to a subsequent large scale hydrogen burn.

Based on these types of consideration, existing knowledge from previous studies and engineering judgment, the standard problems were specified to address the major challenge mechanism(s) for each reactor and containment type. This association is summarized in the Table below:

<u>Standard Problem</u>	<u>Containment Type</u>	<u>Challenge Mechanism</u>
SP-1	Large Dry	Steam Spike
SP-2	Subatmospheric	Concrete Attack
SP-3	Ice-Condenser	Hydrogen Burn
SP-4	Mark I	Concrete Attack
SP-5	Mark II	Concrete Attack
SP-6	Mark III	Diffusion Flames
SP-A	All Types	Direct Heating



The direct heating challenge mechanism was separated out not only to avoid repetition (affects all containment types) but also because both the likelihood of the high pressure scenario as well as the extent of dispersal leading to direct heating are highly uncertain and contested topics at this time. A special subcommittee was formed to consider approaches for estimating the potential effects from direct heating. The large dry and sub-atmospheric containments are quite similar and, depending on conditions, both may be subject to steam spikes and concrete attack. The table entry shown above indicates that the emphasis was distributed for more thorough coverage while an adequate understanding can still be developed, on this basis, for any load combination. Finally, two special studies considered localized liner-melt attack in Mark I, and steam explosion effects in Mark II.

By definition the standard problem approach is mechanistic (deterministic). However, because of the parametric variations mentioned above and because of phenomenological uncertainties (as reflected by the particular set of assumptions, models and model parameters utilized) a range of potential loads rather than a single value\* was arrived at for each standard problem. In a sense this may be taken to represent an uncertainty range. Available time and resources, as well as the Group's own technical direction, were not conducive to a thorough evaluation of the likelihood of each calculated outcome. Still an attempt has been made to supplement the results with degrees of expectation. Each standard problem presented a different kind of challenge in this regard. The basis for the judgments will be presented together with the results on a case-by-case basis.

### 1.3 Factors not Considered by the CLWG

As noted above the CLWG focused attention on major thermal-hydraulic phenomena and the resulting pressure-temperature loads associated with release of the primary system inventory of corium melt, steam and hydrogen into the containment. Although it may be obvious, a number of peripheral items, not taken within the scope of the Group's efforts, will be mentioned here to more clearly delineate the area of responsibility.

- (a) Containment performance was not coupled to the calculation of loads. An important aspect of this coupling, which is receiving considerable attention recently, is the possibility of local containment integrity degradation allowing sufficient venting to prevent a catastrophic failure. The outcome would depend upon the load rise time and the mode, timing and extent of local failures. Clearly, for very slowly rising pressure loads, even small cracks might be capable of providing adequate release while, at the other extreme, rapid pressure loads well in excess of the containment ultimate capability would not be

\* For monotonically increasing loads reference to the values at the appropriately selected time (typically a few hours) is made here.

arrested by anything short of catastrophic failure. The actual behavior in each case may be evaluated by considering the results of the CLWG jointly with those of the CPWG.

- (b) Local heating effects by fission product deposition directly upon the containment boundary were ignored. Such effects may be important for the in-vessel portion of the core melt sequence. However, with the exception of the Mark I local liner attack made possible by the particular geometry involved, there seems to be no basis for concern at this level of detail.
- (c) Long term behavior (beyond several hours) was not explicitly quantified. This is in keeping with the principal objective of evaluating the early response. In most cases, however, at least a scoping of long term effects may be gained by studying the CLWG results.

#### 1.4 Structure of This Report

The principal contents of this report are found in the next seven chapters corresponding to the seven standard problems. All are presented in a similar format that includes: description of relevant geometry, specifications of the standard problem, method of analyses utilized, numerical results and sensitivity studies, likelihood considerations of the various loads, and conclusions and recommendations. Each one of these chapters was written on the basis of the information developed during the CLWG meeting and associated documentation (i.e., presentation viewgraphs, informal reports by individual investigators, etc). The chapters describing the various standard problems have, in fact, been extracted from the consensus summaries provided by each team assigned to that particular standard problem. The group assigned to that problem and the principle authors of the summary are given at the beginning of each chapter. The editor has exercised some judgment in modifying the format of the material provided in the consensus summaries to maintain a consistent structure for this report.

The approach in writing these summaries is not to fully document all the results obtained, and certainly not their bases; but rather to convey a distillation of the understanding and conclusions as they developed during this effort. In many cases individual organizations and investigators will be publishing their own results in considerably more detail. The reader is referred to these publications for further elaboration on the details. Three special studies smaller in scope and effort were also completed and they are summarized in the Appendix.

In parallel with the CLWG effort a joint NRC/IDCOR program also came into being. The purpose of this program was to provide a basis of communication for recent developments in the area of severe accidents by the NRC and U.S. Industry. Much of the information developed by the CLWG was presented in the NRC/IDCOR meetings and was extremely helpful in forming the basis for NRC personnel and contractors to more meaningfully interact with the IDCOR group. A brief summary of the results of these interactions is given in Chapter 9. An international program comparing the analyses of various analysts on two standard problems has been in progress since the Spring of 1984. The status of this effort is also described in Chapter 9. This Chapter also includes further discussions of the interfacing of the CLWG program with NRC's source term reassessment effort.

The report concludes with Chapter 10 providing the conclusions from an overall perspective of this effort and recommendations for future work.

## 2.1 Description of Reference Plant Geometry (Zion)

The PWR large dry containment concept relies on a large internal volume ( $2.7 \times 10^6 \text{ ft}^3$ ) and a high design pressure based on the large LOCA taken as the design basis accident. This capability has proved beneficial in severe accident considerations. The Zion facility was selected to represent this containment type. The general arrangement of the Zion containment building is shown in Figure 2.1. Of principal interest to this standard problem is the reactor cavity geometry because it is in this environment that the initial thermal interactions, following the release of the molten corium from the vessel, will occur. The geometry of a Zion type cavity is shown in Figures 2.2(a) and 2.2(b). There are two important aspects of this geometry regarding the response to a postulated core melt release: (a) the overall dimensions and geometry are such that entrainment and expulsion of core debris could occur if significant steam supply, either from a vessel failure at high pressure or from extensive fuel coolant interactions, was to develop and (b) the cavity would remain flooded if a significant quantity of water was to be released to the containment floor (i.e., from the RWST). Both of these aspects are reactor specific. That is cases exist where the cavity design is of such large dimensions and/or the geometry involves significant dead end regions that corium sweep-out, even in the presence of large steam supply, may be rather limited. On the other hand cases also exist where, because of floor curbs and other obstructions, cavity flooding would be absent even with the RWST on the containment floor. However, the release of the accumulator water (passive system) should be considered if vessel failure from a high primary system pressure were to be postulated.

## 2.2 Description of Standard Problem and Objectives

The overall objective of this problem is to develop an updated technical position on near-term (few hour duration) containment pressure-temperature loading following reactor vessel failure. Technical areas of interest include: high, low and best estimate pressure loadings, and sensitivity analyses using the parameters with important bearing on containment loads. The particular objective of SP-1 was to determine containment loads without significant limitations on the availability of water to contact the melt released from the vessel, i.e., from a "steam spike" standpoint. Hence the choice of the Zion type of containment was made. The primary parameter variations were, therefore, corium mass and temperature as shown in Table 2.1. The particular variations in composition of the various masses considered are shown in Table 2.2. In addition variations on the initial

\* CLWG analysts are: Williams, Bergeron, Haskin, Powers, Berman (SNL); Ginsberg Green, Pratt, Theofanous, Nurbaksh (BNL/Purdue); Corradini, (UW). Consensus summary author is Theofanous (Purdue).

water quantity, the type of concrete and primary system pressure were also considered parametrically. The concrete characteristics are given in Table 2.3. The primary system pressures considered were representative of two so-called high pressure scenario, and the low pressure scenario. An intermediate pressure was also considered as a parametric variation. The vessel breach radius is thought to depend upon whether the failure occurs at low or high pressure. This association was specified as shown in Table 2.4. The reactor primary system (RPS) volume and pressure at the time of failure are also given in this table.

Two containment conditions were considered for this problem. The one specified an adiabatic containment at an initial pressure of 0.4 MPa (partial pressure, air=0.1 MPa, steam=0.3 MPa) and an initial temperature of 407°K. The water temperature in the reactor cavity was specified at 397°K. The other specified a non-adiabatic condition with heat sinks as given in Table 2.5. Since the consideration of the sinks requires the time of exposure to an elevated pressure-temperature (P-T) environment (pre-heating), the particular P-T history estimated for a TMLB transient (see NUREG-850) was specified.

### 2.3 Discussion of Major Phenomenology

Even upper bound estimates of hydrogen generation and concrete attack indicate that they could not influence the containment pressure in the first hour by more than 1-2 psia. The primary aspect of the phenomenology therefore involves steam generation due to corium quench and continued decay heating. As a conservative estimate of the energy release from oxidation of metallic compounds (steel and zinc) we assumed oxidation of 30% of the available quantities, yielding ~24,000 MJ (megajoules) of energy. This quantity of energy corresponds roughly to 20% of the available quench energy and just about equals the sensible heat required to bring the cavity, if it were full of water, to boiling.

For the three water depths specified in the problem (3.2m, 1.5m and 0.5m) the corresponding water masses are: 133.4 Mg, 66.7 Mg and 22.2 Mg respectively. The initial steam mass in the containment is 233.3 Mg. If all the cavity water was to be vaporized and be added to the containment atmosphere we would obtain (on an equilibrium, adiabatic basis) pressures of ~100, ~73, and ~58 psia respectively. These are upper limit values and would be obtained only if there is enough energy to vaporize all the water. The corresponding energy levels required are 280,000, 139,000 and 46,000 MJ respectively. The associated rough estimates of the sensible energies are 20,000, 10,000, and 3,000 MJ respectively.

One possibility of having to consider only a portion of the available energy as discussed above, is when the interaction process becomes water-limited. Another possibility mentioned by some is if the corium arrives to the cavity floor above it by the formation of a solid crust. The group felt that for the low pressure scenario the occurrence of such isolating crusts could not be excluded. The resulting low pressures (i.e., assuming only 10% of the corium mass quenching) should, however, be viewed as a "low" estimate in a likelihood sense.

For the standard problem we have the following energy balance:

+ 198,000 MJ	Quench (initial corium) energy
+ 24,000 MJ	Oxidation energy
+ 81,000 MJ	Decay heat for 45 min.
- 20,000 MJ	Sensible heat
<u>= 283,000 MJ</u>	

For a full cavity this amount of energy would be just about sufficient to deplete all the water (280,000 MJ required). The peak adiabatic pressure obtained would be ~100 psia (see above). In the pressure range 50-100 psi the heat removal capability from the quenching corium on the cavity floor would correspond to ~250 W/cm<sup>2</sup> for a total of 109 MW. Hence total quenching would be obtained at ~43 min. These estimates are also consistent with counter-current flow limitations in the reactor cavity tunnel communicating to the containment. For the half full cavity specified in some of the standard problems all water would be vaporized for a maximum pressure of ~73 psia and the corium would continue to attack the basemat.

The significance of these long quench times is that there would be time for heat losses into the passive heat sink to occur. However, it is also possible that the quenching occurs at a much shorter time scale. This would require the persistence of small scale steam explosions. Large scale, energetically significant, steam explosions are limited by the quantities of fuel that can exist in premixture conditions in the reactor cavity geometry, even in the stratified regime. The reason for this is that the fuel enters the cavity at a rate that is too great for immediate quenching. That is, water and possibly fuel would be flooded out of the cavity at a certain high quenching rate this (for the case of water flooding) is estimated at a equivalent cavity floor flux of ~350 W/cm<sup>2</sup>. However, unsteady periodic behavior (including water expulsion and return as well as possibly fuel expulsion which may result, for example, from high pressure blowdown from the vessel) may hasten the quenching to times even shorter than those implied by some return water flooding limits. At present these considerations can be represented by an uncertainty range on the quench times from a few tens of seconds up to a few tens of minutes. The implications of this uncertainty are addressed below.

As a result of the consideration of the phenomena described above we arrive at the following visualization of the process involved in the standard problem. The sequences of events originates with vessel failure and release of the specified corium quantity into the reactor vessel. The timing of the release would vary, depending on the primary system pressure, from a few seconds for the high pressure system to a few tens of seconds for the low pressure case. The magnitude of explosive corium-coolant interactions would be limited by the extent of premixtures obtainable in the reactor cavity. In any case we consider that complete quenching will occur with a time uncertainty from ~1 minute to a few tens of minutes.

#### 2.4 Methods of Analysis

The calculations were performed by the teams from SNL, BNL/Purdue, BCL and Wisconsin. SNL used the CONTAIN code, BNL/Purdue used hand calculations and a home-made computer program of a system of such programs called CLAS, BCL used MARCH 2.0, and Wisconsin used hand calculations. The agreement among all these calculations was excellent.

#### 2.5 Numerical Results and Sensitivity Studies

The standard problem results for the non-adiabatic case, for the two quench times mentioned above are given in Figure 2.3. It is noted that the effect of quench time on final system pressure is negligible. The effect of forced turbulent convection during a fast quench was also explored using the CONTAIN code. The effect was negligible.

The set of complete sensitivity results obtained (adiabatic case) is given in Table 2.6. It is noted that these pressures should be reduced appropriately using the results of Figure 2.3 to take into account the important effect of the passive heat sinks.

As already noted the timing of quench is quite uncertain. The results of all calculations indicate, however, that the impact of this uncertainty is negligible. The passive heat sinks are important. The mechanisms and quantities (of sinks) are well defined and the losses should be taken into account even for upper bound estimates. The degree of metal oxidation is also uncertain but the effect as shown in Table 2.6 is also very small. Thus the "low" estimate can only be associated with a spatial (say 10%) quench with resulting pressures significantly lower than those shown in Table 2.6. As discussed above this kind of behavior must be viewed only as providing a low bound and its actual expectation remains unquantified.

## 2.6 Considerations of Loads and Likelihood of Containment Failure\*

The standard problem SP-1 was focused on the loads resulting from the so-called steam-spikes in a large dry containment such as that of the Zion plant. The phenomena involve rapid quenching of the melt as it is being released into the reactor cavity. Except for the quantities of the molten corium available for release and the quantities of water in the cavity available for quench, which were examined parametrically, all aspects of the calculation were found to be straightforward. Hence, they could be characterized with relatively negligible uncertainty. As a matter of fact, as already demonstrated in NUREG-0850, the problem can be reduced to equilibrium thermodynamics which can be carried out by hand calculations. Corium-concrete interactions, even if they were present, could not alter the loading history due to the steam spike within the first few hours. On the other hand energy release due to metal/water reactions was taken into account. In the presence of a steam-spike, hydrogen burn events could not be sustained (steam inerting) and no such events were considered in the calculations.

Quenching of a whole-core melt in a fully water-flooded cavity would yield a pressure increment of 2.3 bar (35 psi). If a 4 bar (60 psia) pressure already existed as a result of primary system boil-off (i.e., station blackout) a steam spike of 6.3 bar (95 psia) would result. Steam blow-down from an initially pressurized primary system at 157 bar (2,300 psi) could contribute another 1 bar (15 psi). Hence, even under the worst possible conditions a pressurization to 7.3 bar (107 psia) is predicted. This is an upper bound value and still well below the 10.2 bar (150 psia) containment pressure capability estimated by CPWG. In fact, as a result of finite boiloff times and passive heat sinks significant reductions (15 to 30 psi) in these values were calculated when steam generation is water limited.

## 2.7 Conclusions and Recommendations

The CLWG results, therefore, lead one to conclude that steam-spike-induced failure of the Zion containment at the time of vessel failure should be considered an event of relatively low probability.

\* Considerations of the likelihood of containment failure from the various load sources described in this report have been provided by the NRR staff and is based on extended discussions with staff consultants and staff members involved in containment loads and performance activities.



TABLE 2.1  
PARAMETRIC VARIATIONS CONSIDERED

<u>Case No.</u>	<u>Corium Mass (kg)</u>	<u>Corium Temperature (°K)</u>	<u>Water Depth* (m)</u>	<u>Concrete Type</u>	<u>PSP** (MPa)</u>
Base	138,400	2,533	1.5	Limestone	0.4
A.1	106,133	3,033	3.2	Limestone	17
B.1	46,133	2,033	3.2	Limestone	17
C.1	46,133	3,033	0.5	Basaltic	17
D.1	106,133	2,033	0.5	Basaltic	17
E.1	46,133	3,033	3.2	Basaltic	7
F.1	106,133	2,033	3.2	Basaltic	7
G.1	106,133	3,033	0.5	Limestone	7
H.1	46,133	2,033	0.5	Limestone	7
A.2	46,133	3,033	3.2	Limestone	0.1
B.2	106,133	2,033	3.2	Limestone	0.1
C.2	106,133	3,033	1.5	Limestone	0.1
D.2	46,133	2,033	1.5	Limestone	0.1

\* For the low depth cases a water quantity of 90,000 kg dumps onto corium following its release from the vessel.

\*\* Primary System Pressure (PSP) at time of vessel failure.

TABLE 2.2  
CORIUM COMPOSITION

<u>Case No.</u>	<u>UO<sub>2</sub> Mass* (kg)</u>	<u>Steel Mass** (kg)</u>	<u>Zr Mass*** (kg)</u>	<u>Total Mass (kg)</u>
Base	90,000	22,000	22,000	138,400
A.1,D.1,F.1,G.1	90,000	7,333	7,333	106,133
B.2,C.2				
B.1,C.1,E.1,H.1	30,000	7,333	7,333	46,133

\* Decay heat level = 30 MW (~1%)

\*\* Fe 85 w/o, Cr 10 w/o, Ni 5 w/o

\*\*\* 50% oxidized

TABLE 2.3

REACTOR CAVITY CONCRETE COMPOSITION AND CHARACTERISTICS

	<u>Base Case (Limestone)</u>	<u>Parametric (Basalt)</u>
CaCo <sub>3</sub>	80 w/o	2 w/o
Ca(OH) <sub>2</sub>	15 w/o	6 w/o
SiO <sub>2</sub>	1 w/o	53 w/o
Free H <sub>2</sub> O	3 w/o	4 w/o
Al <sub>2</sub> O <sub>3</sub>	1 w/o	19 w/o
CaO	----	16 w/o
k(w/cm°C)	0.015	0.015
Cp (J/gm°C)	1.7	1.7
p (g/cm <sup>3</sup> )	2.4	2.4

TABLE 2.4

CONDITIONS OF CORIUM EJECTION

	<u>Type 1</u>	<u>Type 2</u>
RPS* Pressure (mPa)	17	0.4
Vessel Hole Radius (cm)	14.5	46.
RPS Volume (m <sup>3</sup> )	340**	340

\* Reactor Primary System (RPS)

\*\* Saturated Steam plus 455 kg H<sub>2</sub>

TABLE 2.5

CONTAINMENT STRUCTURAL HEAT SINKS FOR ZION

<u>Wall No.</u>	<u>Area (ft<sup>2</sup>)</u>	<u>Thickness (ft)</u>	<u>Layer Composition</u>
1	54447.	0.00033/0.02083/1.0	Paint/Steel/Concrete
2	15016.	0.00033/0.02083/1.0	Paint/Steel/Concrete
3	15500.	1.5	Concrete
4	2000.	0.02083/1.0	Steel/Concrete
5	36000.	1.0	Concrete
6	7000.	0.75	Concrete
7	16000.	0.02083/1.0	Steel/Concrete
8	54860.	0.02083	Steel
9	89300.	0.00033/0.03125	Paint/Steel
10	1060.	0.05208	Steel
11	1147.	0.4375/1.0	Steel/Concrete
12	1400.	0.0533/1.0	Steel/Concrete
13	185.63	0.87583/1.0	Steel/Concrete
14	54.3	0.02083/1.0	Steel/Concrete
15	440.	0.0625/1.0	Steel/Concrete
16	603.94	0.6073/1.0	Steel/Concrete
17	180.93	1.0026/1.0	Steel/Concrete
18	14862.	0.02083/1.0	Steel/Concrete
19	3712.	0.02083/1.0	Steel/Concrete
20	32000.	0.03125	Steel

TABLE 2.6

RESULTS OF SENSITIVITY STUDIES

<u>Alternative Case</u>	<u>No Zr - H<sub>2</sub>O Reaction</u>	<u>100% Zr - H<sub>2</sub>O Reaction</u>
Base	5.78	6.62
A.1	5.58	5.82
B.1	4.33	4.61
C.1	4.74	5.02
D.1	4.67	4.91
E.1	4.05	4.33
F.1	3.98	4.22
G.1	4.88	5.12
H.1	3.64	3.91
A.2	3.77	4.04
B.2	3.70	3.94
C.2	4.43*	4.43*
D.2	3.36	3.63

\* Water supply is limiting.

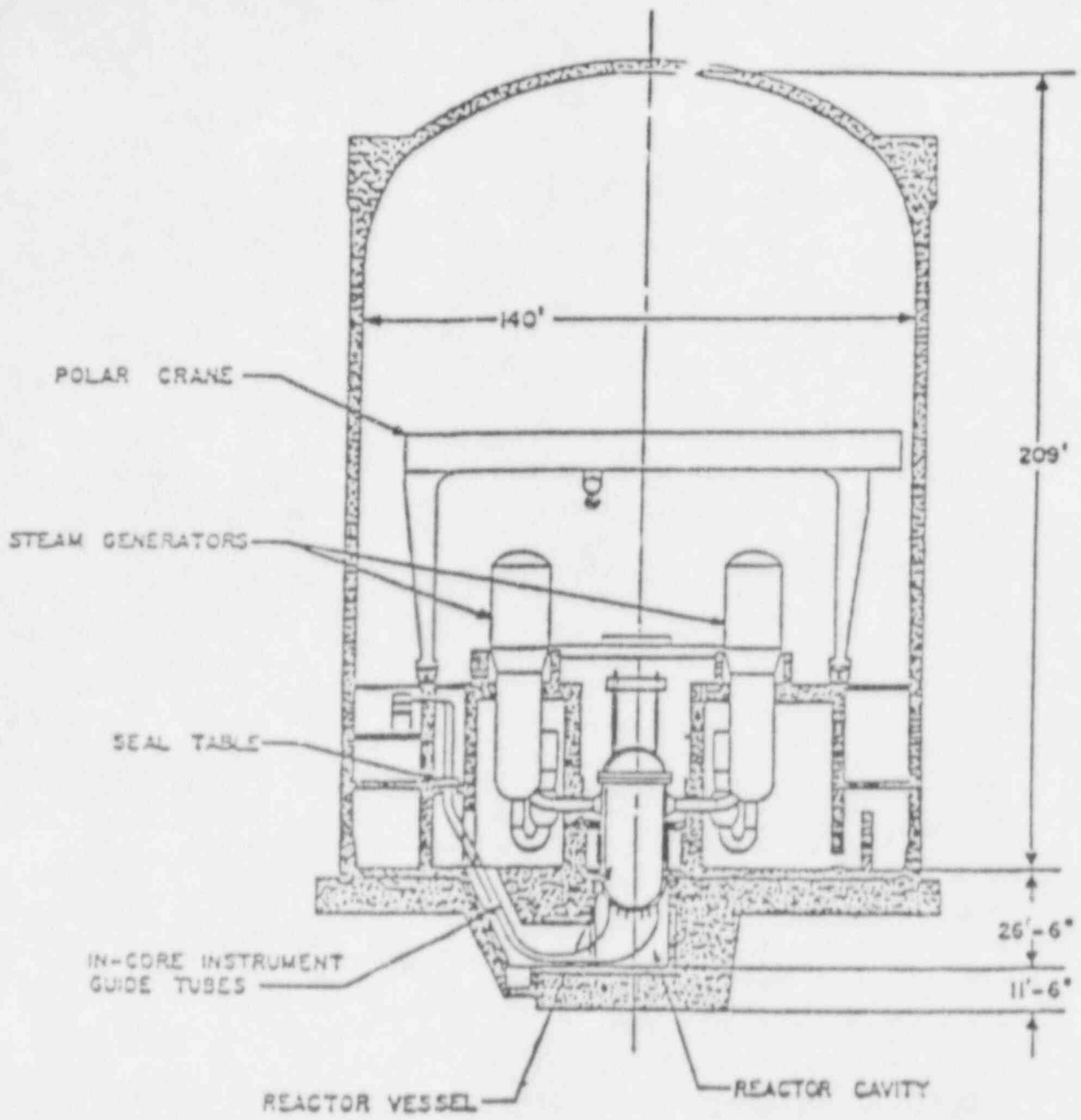


Figure 2.1 Schematic Illustration of Zion Reactor Containment Building.

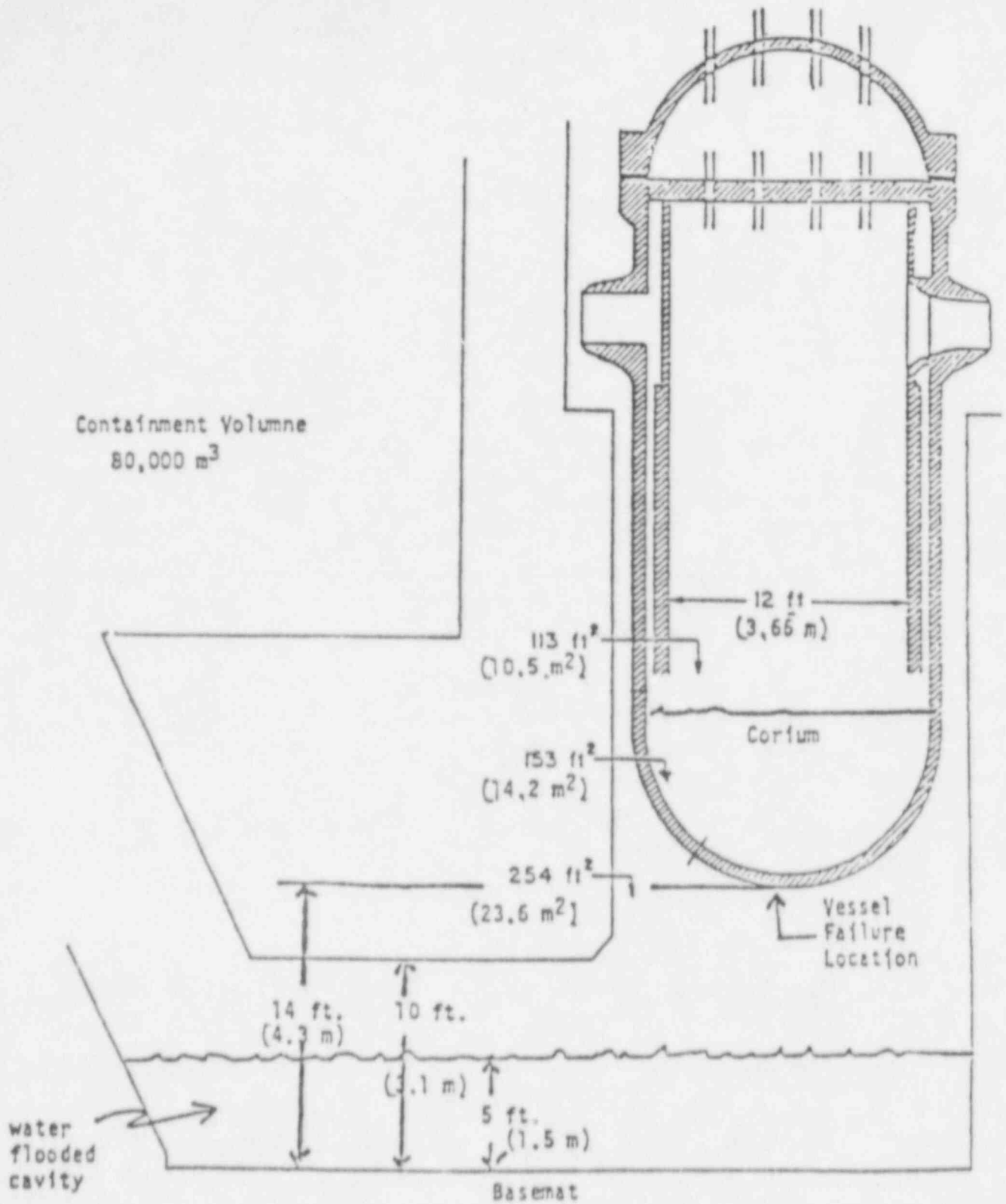


Figure 2.2 (a) --- Representation of the reactor vessel situated within the reactor cavity.



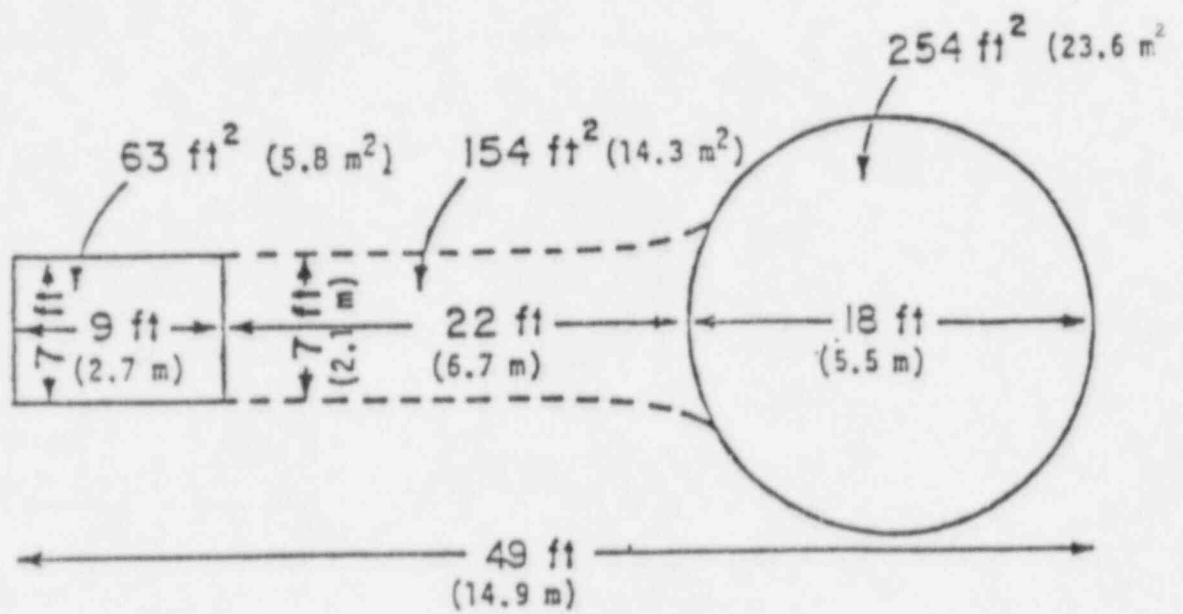


Figure 2.2 (b) - Plan view and typical dimensions of reactor cavity and keyway.

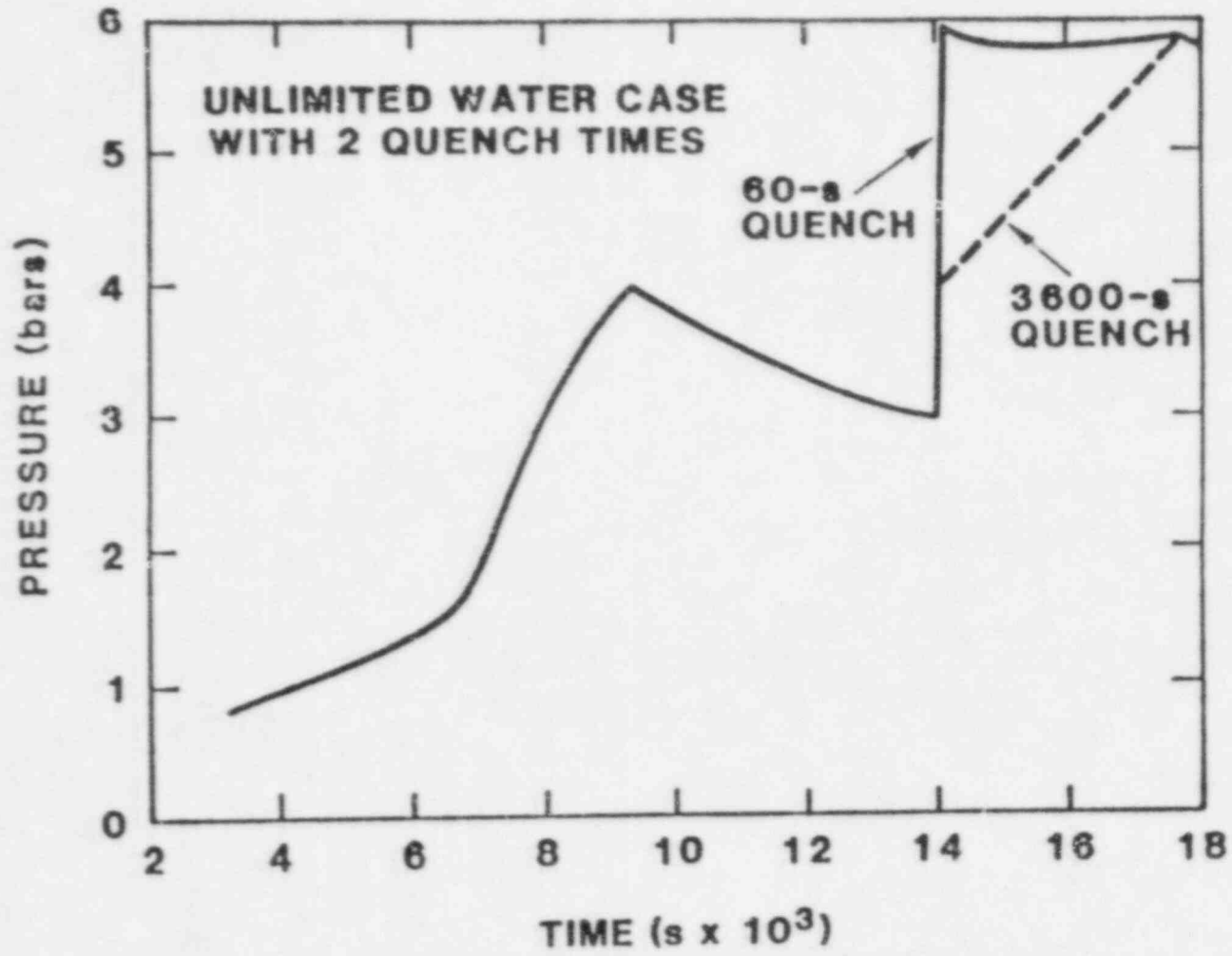


Figure 2.3 Pressure Versus Time (Non-adiabatic Case) for Two Quench Times.

## Chapter 3 PWR SUBATMOSPHERIC CONTAINMENT (SP-2)\*

### 3.1 Description of Reference Plant Geometry (Surry)

The free volume of a subatmospheric containment is considerably smaller than that of a large dry containment. The Surry facility was selected to represent this containment type. The containment volume at Surry is  $1.8 \times 10^6$  ft<sup>3</sup> compared to  $2.6 \times 10^6$  ft<sup>3</sup> for the Zion design used in SP-1. The containment design pressure is, however, not much different (45 psig for Surry versus 47 psig for Zion).\*\* The general arrangement of the Surry containment building is shown in Figure 3.1. The Surry cavity geometry is shown in Figures 3.2 and 3. The same general considerations apply to this design concept with regard to possible entrainment and expulsion of core debris and cavity water flooding and retention as was described for SP-1.

### 3.2 Description of Standard Problem and Objectives\*\*\*

SP-2 represents a TMLB<sup>1</sup> sequence leading to core melt and vessel failure at high pressure. The principal features of the standard problem specifications are the initial containment conditions prior to vessel failure, the mass of molten debris released to the cavity, the temperature and composition of the released debris, the water level in the reactor cavity, the various geometric features of the containment building. Table 3.1 provides the most important of the standard problem parameter specifications for the base case, while Table 3.2 gives the parameter variations specified for the sensitivity studies.

For the base case, the analysts were requested to provide "high" and "low" estimates that were to bound the range within which the actual containment loads (i.e., pressures and temperatures) might reasonably be expected to fall, and they were also requested to provide "central" estimates. For the "high" case, results were to include the quantities of steam H<sub>2</sub>, CO, and CO<sub>2</sub> added to the atmosphere, as well as the extent of basemat attack after one and three hours. For the sensitivity study, it was requested that the combination of governing phenomena assumed for the "high" case be used throughout, and that peak pressures and temperatures during the first hour after vessel failure be reported.

\* CLWG analysts are: Corradini (UW); Cybulskis (BCL); Bergeron, Berman, Haskin, Powers, Williams (SNL); Ginsberg, Greene, Pratt, Theofanous, Nurbaksh (BNL/Purdue). Consensus summary authors are Bergeron and Williams (SNL).

\*\* NUREG-1037

\*\*\* The summary provided by SNL included a considerable amount of material concerning direct heating effects. Because of the generic nature of this subject the details of that analysis has been included as a separate topic in Chapter 8.

### 3.3 Discussion of Major Phenomenology

As noted above, subatmospheric containments are very closely related to "large dries." They are of somewhat smaller volume and they are built for a somewhat lower design pressure. It is expected, therefore, that the steam-spike behavior will be similar to that determined under SP-1. There are cavity designs, however, both for large dries as well as subatmospheric containments, that preclude the flow of containment building water into them. Thus, except for high pressure scenarios that involve the dumping of accumulator water (wet cavity case) following reactor vessel melt-through (containment sprays are assumed inoperative), steam-spike phenomenology is also precluded for sequences without ECCI and containment spray operation. Corium-concrete interactions would then dominate (dry cavity case) the containment loading process. Both the wet and dry cavity cases were considered.

### 3.4 Methods of Analysis

For the SP-2 analyses, BCL employed MARCH 2 and BNL employed MARCH 1.1. The UW results (reported for the base case only) were performed using adiabatic calculations. SNL results were based upon calculations performed with the CONTAIN code, although many of the actual numerical results cited were obtained using a much simpler adiabatic code, DHEAT, which had been validated by performing detailed comparisons with CONTAIN calculations over the full range of parameter values of interest. Sources of gases due to core-concrete interactions were calculated by MARCH/INTER (BCL), MARCH/INTER or CORCON (BNL), and CORCON (SNL). Differences between INTER and CORCON, as well as differing input assumptions, led to substantial variations in the amounts of these gases that were calculated to be produced. However, in no cases did the core-concrete interactions drive the peak pressures and temperatures during the periods of interest and the SNL calculations typically omitted core-concrete interactions once this fact had been established.

### 3.5 Numerical Results and Sensitivity Studies

The CLWG spent a considerable amount of time evaluating the consistency of different calculations of steam spike loads (i.e., without direct heating) and evaluating the importance of non-adiabatic effects for steam spike calculations. Most of this work was performed in connection with Standard Problem 1 (SP-1) and will not be discussed extensively here. Salient conclusions that are relevant to the SP-2 results include the following:

- (a) Adiabatic steam spike calculations can conveniently be characterized in terms of a single parameter, e.g., the mass of steam added to the containment. For equivalent assumptions concerning this parameter, there was good agreement among the results obtained by different analysts.

- (b) With some qualifications, non-adiabatic calculations can be characterized in terms of two parameters, with the second parameter being a time parameter. Again, with equivalent assumptions different analysts obtained equivalent results.
- (c) For steam addition times of 1 minute or less, non-adiabatic effects reduced the pressure increase only slightly, i.e., by  $\leq 7\%$  with respect to the adiabatic case.
- (d) A consensus was reached that "high" steam spike calculations should be performed assuming rapid quench of 100% of the core, with 30% of the metallic zirconium present reacting with water. The heat of reaction of the zirconium is assumed to be available for steam generation.

Peak pressures and temperatures that were reported for the base case are summarized in Table 3.3. Not all analysts reported results of all cases. The BNL and the BNL results included no direct heating, the UW results included 10% direct heating in the "high" case, and the SNL results included significant direct heating for the "central" and, especially, the "high" cases. The MARCH assumptions used by BCL and BNL for the "high" case appear to correspond reasonably well to the CLWG consensus position for maximum steam spike calculations that was noted above.

The tabulated results indicate that there are differences between the BCL and BNL "high" results that appear significant (almost 0.1 MPa), even though the problems analyzed are nominally quite similar, in terms of the data given. The difference between these two results is very much less than the difference with respect to the SNL "high" results. From other SNL calculations of steam spikes, it is apparent that this difference in results has little to do with the difference in calculational tools; rather, it is almost entirely due to the inclusion of substantial direct heating in the SNL calculations. The UW "high" results are significantly increased by even the small amount of direct heating assumed. The UW "central" results are based upon steam generation only and are thus more nearly comparable to the BCL and BNL "high" results.

The sensitivity studies presented by BCL, BNL, and SNL were performed using calculational techniques and input parameters similar to those employed for the "high" base case results summarized in Table 3.3. Thus, the BCL and BNL results did not include direct heating while the SNL results did. Results for the base case show that it is necessary to include an examination of the impact of direct heating upon the sensitivity study. As in the case of the base case analyses, it is necessary to include an examination of the impact of direct heating upon the sensitivity study. As in the case of the base case analyses, it is probably more representative of the CLWG state of understanding

to employ direct heating parameters based upon the recommendations of the Direct Heating Subcommittee than to employ the results of any one analytical team. Calculations of this kind are presented in Chapter 8. However, it is also of interest to summarize the results obtained when the problem is restricted by specifying no direct heating, and the results will be considered here.

In addition to the sensitivity study with direct heating, SNL also performed the study with direct heating eliminated. These calculations were run for the limiting cases of 0% and 100% zirconium-water reaction as part of a parameter study, and thus none of the calculations were exactly comparable to those performed by BCL and BNL which included metal-water reactions as calculated by the HOTDROP module of MARCH. However, the SNL results showed that including 30% zirconium-water reaction would increase the base case pressures by about 0.04 MPa, and the pressures in the sensitivity study cases would be increased by only 0.01-0.02 MPa in two instances and there would be no effect in the other six cases. Hence, the zirconium-water reactions are not a major factor in the steam spike sensitivity study calculations and the SNL results without zirconium-water reactions will be presented here along with the BCL and BNL results.

In Figures 3.4 and 3.5 the pressures and temperatures, respectively, obtained in the three sets of analyses are presented graphically. In each figure, the first bar on the left represents the base case while the remaining eight bars represent the results for the sensitivity study cases specified in Table 3.2. As might be expected, the four cases where the vessel fails at low primary system pressure (cases 3, 4, 7 and 8) give substantially lower pressures than do the high-pressure cases. In large part, this result follows from the fact that only the (very limited) amount of water in the cavity is available for steam generation in the low-pressure cases, since the accumulator water is assumed to have dumped and boiled off before vessel failure. It also reflects the smaller release of steam and gas upon vessel failure.

There is one major qualification that must be made to the conclusion that the low-pressure cases are much less severe. BCL noted that, for all four low-pressure cases, flammable conditions were calculated to exist within the containment, but hydrogen burning was not included in the results given. If the hydrogen is assumed to burn efficiently, the BCL calculations indicate that pressures could be at least as high as any shown in Figure 3.4 and temperatures would be much higher than any of those in Figure 3.5. On the other hand, the occurrence of flammable conditions for these scenarios can not be taken to be rigorously established, because of limitations in the definition of SP-2 and limitations in the analyses. For example, none of the analysts took into account outgassing of unlined concrete within the containment, which might reduce or eliminate flammability of the atmosphere.

Among the high-pressure cases, the high-temperature corium releases yielded more severe results than did the lower-temperature releases, which is hardly surprising. In at least one set of calculations (SNL's), the difference would have been considerably greater were it not for the fact that steam generation was water limited; that is, the total water available (cavity plus accumulator water) was inadequate to completely quench the large mass of hot corium.

In comparing the results obtained by different analysts, it is seen that the quantitative trend of the pressures from case to case shows good agreement between the three sets of results. Quantitatively, there is good agreement for several of the cases but significant differences (up to 0.15 MPa) arise in some instances, notably the most severe cases. In calculating the temperatures shown in Figure 3.5, the SNL results were obtained using the adiabatic DHEAT code, which assumes the containment atmosphere is saturated unless direct heating is involved. The MARCH calculations assumed superheating in some cases, presumably due to superheated gases released from the RCS. Hence, it is not surprising that the SNL temperatures tend to be the lowest. Actually, however, the SNL and BNL temperatures are very similar. The BNL temperatures are significantly higher in some instances.

No effort has been made to identify in detail the reasons for the differences in the results obtained by the different analysts. It is worth noting that the differences between the BCL and BNL results, which were obtained using similar calculational tools, are comparable in magnitude to the differences between the BCL and SNL results, which were obtained using similar calculational tools, are comparable in magnitude to the differences between these results and the SNL results, which were obtained using quite different calculational tools. This fact suggests that the differences reflect different input assumptions at least as much as they reflect differences in calculational approach. Such a conclusion, if valid, is all the more striking in view of the fact that the range of input assumptions was heavily restricted by the definition of the problem, which corresponds closely to the CLWG consensus "high" steam spike case with direct heating postulated to be absent. (It should be noted that the present problem is dominated by sources of steam and energy released to containment over a short time, which minimizes the dependence upon calculational approach.)

### 3.6 Considerations of Loads and Likelihood of Containment Failure\*

For the wet cavity case the accumulator water was sufficient to quench a whole-core melt producing, at most, a pressure increment of 2 bar (30 psi). Thus, with steam blowdown from an initially pressurized primary system at 157 bar (2,300 psi) together with an assumed initial containment pressure of 2 bar (30 psi) a steam spike of 5 bar (73 psia) is obtained. Even assuming, arbitrarily, that the corium melt contained a sufficiently large quantity of steel (by melting reactor vessel internals) to vaporize all the accumulator water a peak pressure of less than 7.3 bar (107 psia) would result. This upper bound is well below the 9.2 bar (135 psia) estimated by the CPWG to be required for failure. The CLWG results, therefore, lead one to conclude that steam-spike-induced failure of the Surry containment is an event of vanishingly small probability. Since water cannot return to the cavity eventual dry-out leading to corium-concrete interactions should be expected. The pressure build up due to this process is much slower than that due to a steam spike. The two-phases are, therefore, relatively uncoupled.

For the dry cavity cases any pressurization within the first few hours would correspond to whatever small amounts of water were assumed to be present in the cavity, and whatever small quantities of steam is assumed to exist within the primary system at the time of vessel failure. Pressures below 2.7 bar (40 psia) are indicative of this behavior. Any pressure loads due to the basaltic concrete decomposition develop slowly over a time scale of 10s of hours and containment failure levels are not approached for a few days.

However, further consideration of this scenario by some analysts subsequent to the initial calculations indicate that it is possible that over such a long time frame, continuing steam condensation might lead to steam de-inerting and, as a consequence, to hydrogen burns. The conclusion is that containment failure within the first few hours is quite unlikely.

### 3.7 Conclusions and Recommendations

- (a) Results obtained by different analysts for SP-2 peak pressures and temperatures agree reasonably well when equivalent input assumptions are used even if different calculational techniques are employed. However, the limited sensitivity to calculational approach should not be overgeneralized; other containment loading problems can show a much greater dependence upon the sophistication of the calculation.

\* Considerations of the likelihood of containment from the various load sources described in this report have been provided by the NRR staff and is based on extended discussions with staff consultants and staff members involved in containment loads and performance activities.



- (b) Results obtained by different analysts differ widely for high pressure ejection scenarios, but do not differ greatly for the low pressure ejection scenarios. The large differences among the high pressure results primarily reflect the different beliefs about the appropriate input assumptions, especially with respect to direct heating. Even with direct heating defined out of the problem, the steam spike results showed significant (about 0.15 MPa) differences in some cases. Obtaining closer agreement will require more care in identifying and defining significant parameters in addition to direct heating.
- (c) There is at least an implied consensus that neither steam spike nor direct heating effects will present a severe threat of massive structural failure in low pressure ejection scenarios for SP-2. (Significant leakage induced by pressure and/or temperature transients are not ruled out, however.)
- (d) There is a consensus that steam spike effects alone will not present a severe threat of massive structural failure in high pressure ejection scenarios, although some of the pressures calculated for certain (rather extreme) parameter choices specified in the sensitivity study do present quite substantial challenges, of the order of 0.7 MPa.

TABLE 3.1

SP-2 BASE CASE SPECIFICATIONSContainment before vessel failure:

Volume	50,971 m <sup>3</sup>
Pressure	0.19 MPa (absolute) (0.10 MPa steam; 0.09 MPa noncondensable)
Temperature	375 K
Water level in cavity	10 cm
Atmosphere was specified as being steam inerted	

Reactor Coolant System (RCS) conditions:

Pressure	15.7 MPa (absolute)
Volume (including pressurizer)	275.3 m <sup>3</sup>
Accumulators	
Pressure	4.6 MPa (gage)
Temperature	322 K
Water volume	78.58 m <sup>3</sup>

Corium specifications:

Total mass	114,556 kg
UO <sub>2</sub>	79,820 kg
Zirconium (total)	16,500 kg
Zirconium (un- oxidized)	11,550 kg
Steel	16,500 kg
Fraction of core released	100%

TABLE 3.2

SP-2 SENSITIVITY STUDY SPECIFICATIONS

<u>Case</u>	<u>Corium Composition</u>	<u>Corium Temperature K</u>	<u>Primary Pressure (MPa)</u>	<u>Water Depth (cm)</u>
1	Corium H	3000	15.7	33
2	Corium L	1800	15.7	33
3	Corium L	3000	6.5 (low)	33
4	Corium H	1800	6.5 (low)	33
5	Corium L	3000	15.7	5
6	Corium H	1800	15.7	5
7	Corium H	3000	6.5 (low)	5
8	Corium L	1800	6.5 (low)	5

Notes:

1. Corium H is 79,820 kg UO<sub>2</sub>; 81,500 kg steel (45.8 weight percent); 16,500 kg zirconium (assume 90% of the zirconium will oxidize in-vessel); total mass of 177,820 kg.
2. Corium L is 79,820 kg UO<sub>2</sub>; 56,500 kg steel (37.0 weight percent); 16,500 kg zirconium (assume 60% of the zirconium will oxidize in-vessel); total mass of 152,820 kg.
3. For the primary system pressure of 15.7 MPa, the accumulators will dump onto the corium. The vessel hole equivalent radius is 0.145 m.
4. For the primary system pressure of 6.48 MPa, the accumulator water has already boiled off. The vessel hole equivalent radius is 0.46 m.
5. All other initial conditions are as specified in the base case.

TABLE 3.3

SP-2 BASE CASE PRESSURE AND TEMPERATURES

	<u>BCI</u>	<u>BNL</u>	<u>UW</u>	<u>SNL</u>
"High" P (MPa)	0.50	0.41	0.64	1.13
T (K)	425	408	---	915
"Central" P (MPa)	---	---	0.54	0.72
T (K)	---	---	---	545
"Low" P (MPa)	---	0.38	(0.26*)	0.48
T (K)	---	404	---	415

\*Performed for a low pressure sequence, and thus not directly comparable to other results.



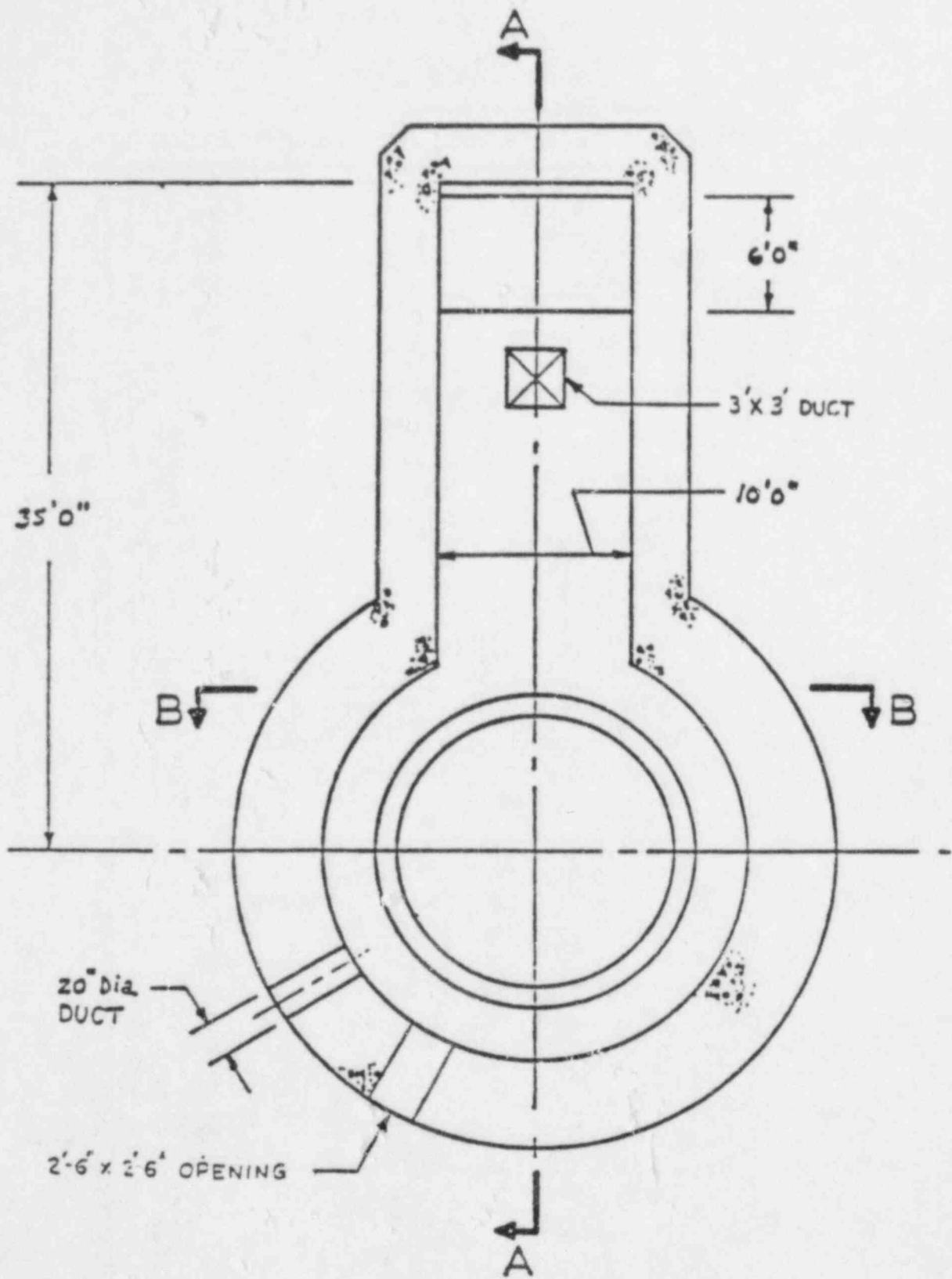


Figure 3.2 - Plan View of Geometry of Surry Lower Reactor Cavity

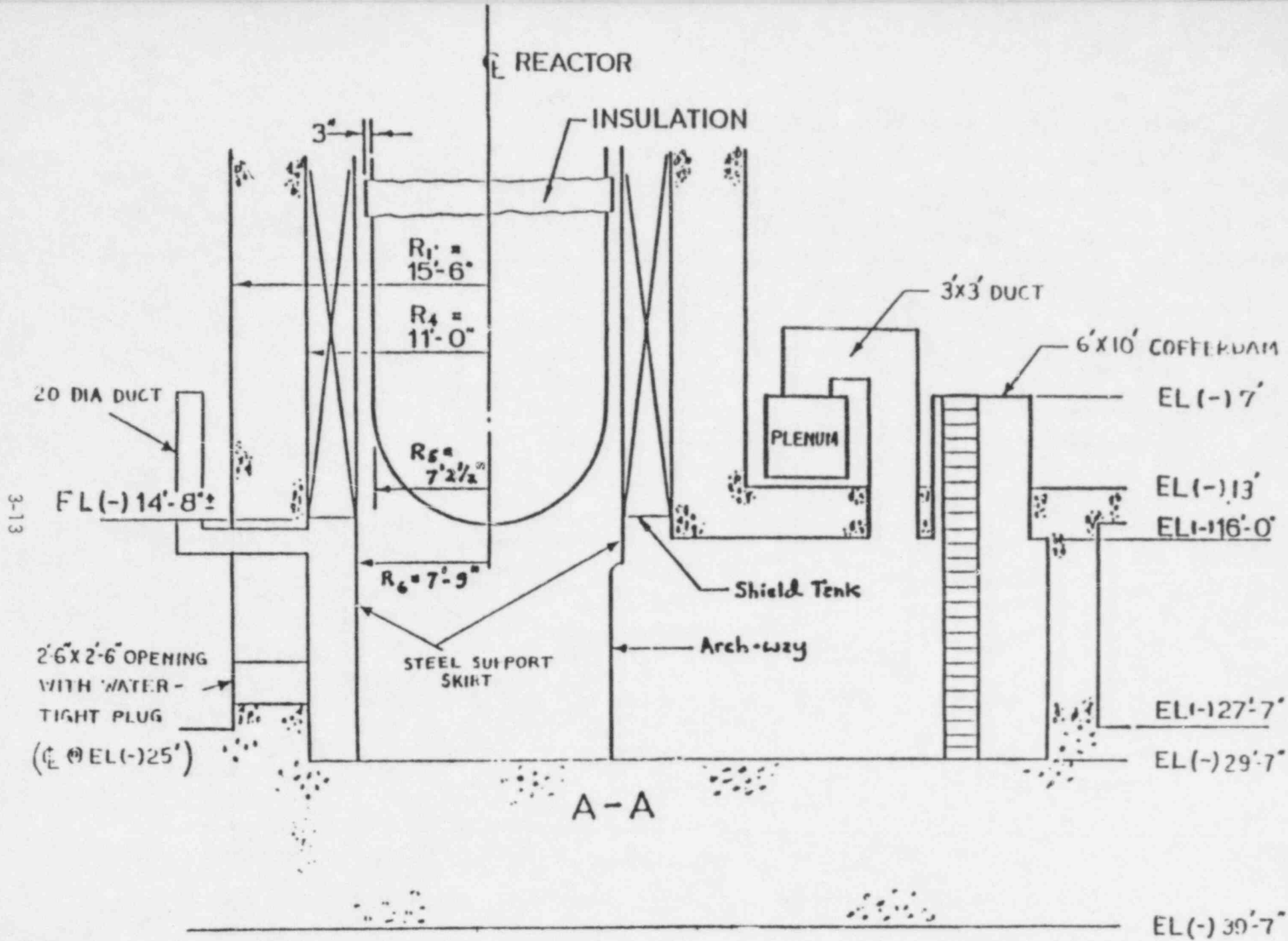


Figure 3.3 - Section A-A of Figure 3.2 Lower Reactor Cavity

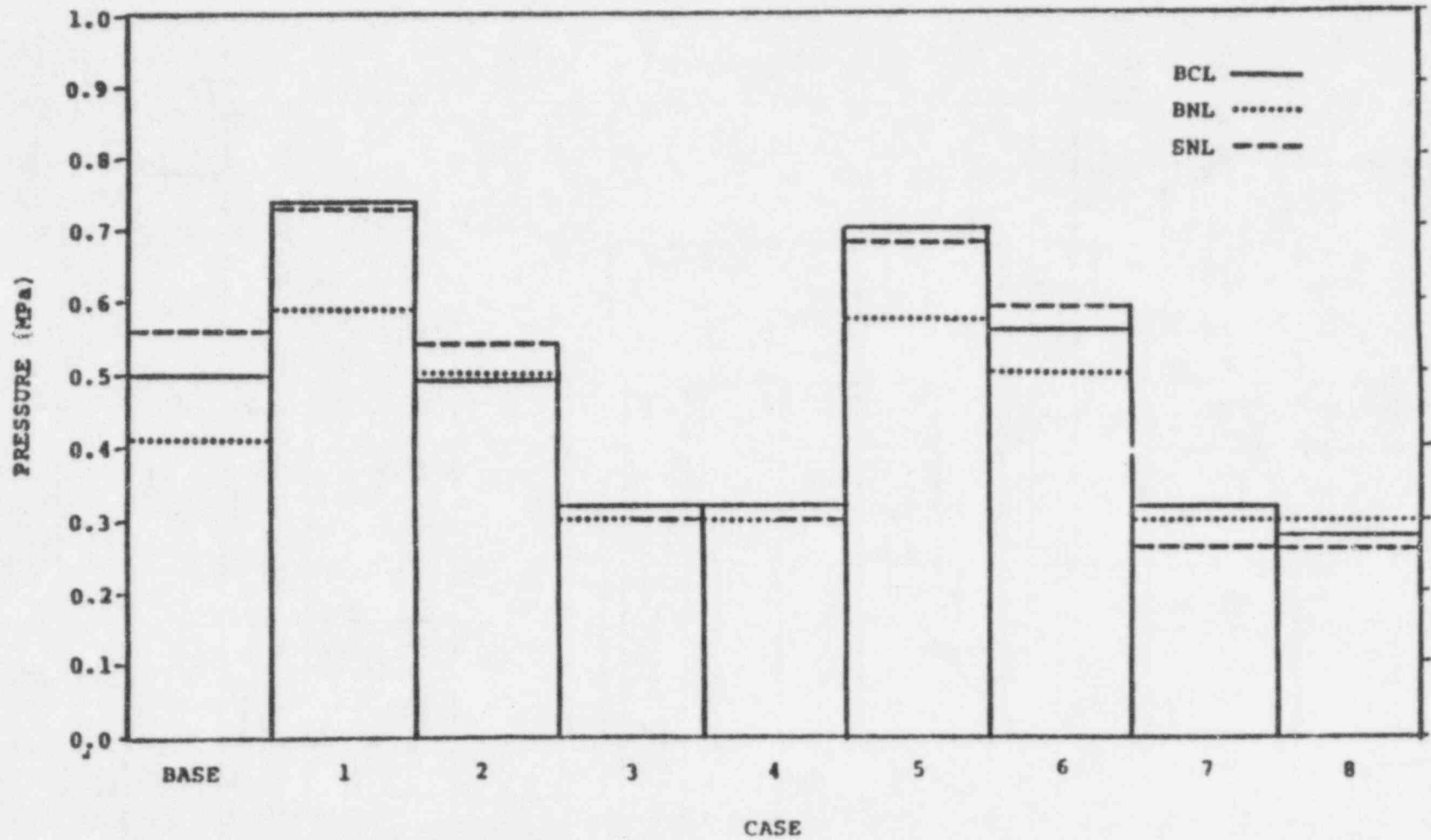


Figure 3.4 -- SP-2 pressures for the "high" steam spike sensitivity study (no direct heating)



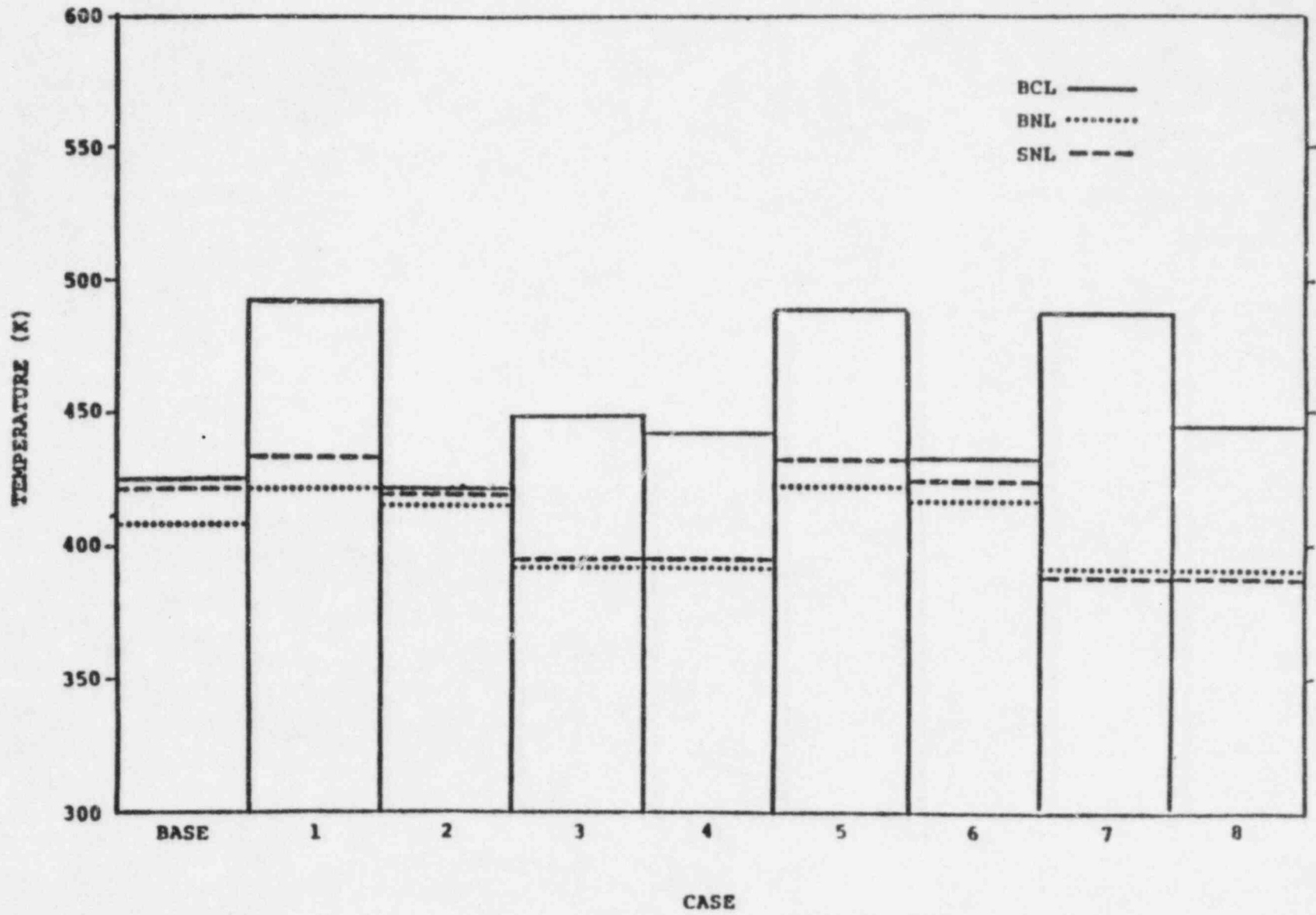


Figure 3.5 - SP-2 temperatures for the "high" steam spike sensitivity study (no direct heating)

#### 4.1 Description of Reference Plant Geometry (Sequoyah)

Ice condenser containments are smaller than the large dry and subatmospheric designs. They also have substantially lower design pressures and pressure capabilities. This is due to the use of ice beds to provide a passive energy absorption capability. These beds are designed to mitigate the consequences from design basis accidents. The Sequoyah plant was selected for analysis in this standard problem. The general configuration of the Sequoyah design is shown in Figures 4.1 and 4.2. A section of an ice bed is shown in Figure 4.3.

#### 4.2 Description of the Standard Problem and Objectives

The TMLB accident sequence was selected as the basis for analysis in the ice condenser containment design. Based on earlier analyses, e.g., BMI-2104 and others, which had indicated a potential vulnerability of this design to hydrogen burns, the CLWG standard problem analyses focused on the loadings due to this source. In the TMLB sequence the hydrogen igniters typically provided in containments of this type would not be operable due to the assumed loss of electric power, thus a variety of hydrogen ignition assumptions could logically be investigated for this sequence. In the initial set of calculations undertaken as part of this standard problem, ignition was assumed whenever the hydrogen concentration in any compartment of the containment reached preselected levels; specifically, hydrogen concentrations of 8, 12, and 30 v/o were assumed for ignition. The occurrence of ignition was still subject to other constraints, such as the availability of oxygen and absence of inerting due to diluents. Later calculations sought a somewhat more mechanistic basis for the occurrence of ignition, and were tied to the timing of the failure of the vessel head, with the release of the hot corium being the source of ignition either immediately upon release from the primary system or at some time later. Additional calculations were performed in which ignition was assumed at low hydrogen levels, e.g., 4.1 v/o, as well as without any hydrogen burning.

In the analyses conducted for the purposes of this standard problem no assumptions were made regarding the pressure or temperature levels at which the containment would fail. The analyses were performed as if the containment had infinite strength in order to develop a picture of the magnitude of the loads that would be predicted under the variety of modeling assumptions discussed above.

\* CLWG analysts are: Cybulskis (BCL); Bergeron, Berman, Haskin, Behr, Camp, Powers (SNL); Ginsberg, Greene, Pratt, Theofanous, Nurbaksh (BNL/Purdue). The consensus summary authro is Cybulskis (BCL) with significant contributions by Haskin, Behr, Camp (SNL).

### 4.3 Discussion of Major Phenomenology

As noted above, the passive energy absorption capability of the ice beds makes the containment relatively immune to steam spike loads from severe accidents. If a severe accident such as a station blackout were to result in a core melt the hydrogen generated during the melt would be released and, under certain circumstances, might burn in a way that would threaten containment integrity. While hydrogen is generated under similar circumstances in the large dry and subatmospheric cases (SP-1 and SP-2) the smaller volume and lower containment pressure capability make the ice condenser design more vulnerable to failure by hydrogen combustion. These designs are, therefore, required to have hydrogen igniters to mitigate challenges from design basis accidents. In the station blackout case, however, the igniters are inoperative. But the steam from primary system blowdown and the steam spike phenomena in core melt accidents inerts the lower compartment atmosphere initially. However, steam inerting may be lost in some compartments because of condensation in the ice condenser. In this case the hydrogen can be swept by steam flow to areas where combustion could threaten containment.

### 4.4 Methods of Analysis

MARCH 2 analyses were used to determine the in-vessel hydrogen generation and release to the containment for the purposes of the subsequent assessment of the effect on the containment of resulting hydrogen burns. The input for the MARCH 2 analyses used the Sequoyah plant design as the model and the actual input parameters utilized were similar to those of the BMI-2104 calculations for this type of design. One point of difference from the earlier calculations was the use of revised values for the volume of water on the containment floor before spillover into the reactor cavity and the volume of the reactor cavity; the revised values were provided by TVA, the owner of the Sequoyah plant.

Using the MARCH 2 calculated rates of hydrogen generation and release to the containment, Sandia National Laboratories and Battelle's Columbus Laboratories conducted independent calculations of the occurrence and effects of subsequent hydrogen burns in the containment. The specific approaches used by each of the two laboratories will be described later. The analyses performed by the two laboratories included consideration of: various hydrogen ignition criteria, effects of varying the in-vessel hydrogen production, effects of the timing and rate of hydrogen release from the primary system, and variations in the magnitude of the steam spike due to the debris-water interaction following vessel bottom head failure. The variations in each of these parameters that were considered are discussed below.

#### 4.4.1 Approach Taken by Battelle

All of Battelle's calculations for the Ice Condenser PWR Standard Problem were performed with the MARCH 2 code. Thus the MARCH calculations were used not only to define the in-vessel hydrogen generation and release to the containment, but also to evaluate the subsequent behavior of the hydrogen in the containment. The BURN subroutine in MARCH is used to determine flammability, flame speed, flame propagation between compartments, etc.; this subroutine was basically developed by Sandia and has been adapted for incorporation into the MARCH code. The ignition and burning criteria incorporated into the BURN subroutine are very similar to those in Sandia's HECTR code. The MACE subroutine in MARCH describes the containment response, including the effects of hydrogen burning as defined by the subroutine BURN. The MACE routine determines mass and energy transfers between compartments on the assumption that the pressures in the various containment compartments are equal. This approximation is believed to be a valid one except for extremely rapid transients, e.g., detonation. The pressure equilibrium assumption is somewhat unique to the MARCH code and is not widely used.

In the MARCH analyses the ice condenser containment was modeled as a four compartment system. The four compartments modeled were: the dead end spacers in the lower compartment, the upper plenum of the ice condenser, and the operating floor and dome volume. The containment compartmentalization is illustrated in Figure 4.4. In MARCH the ice condenser itself is modeled in the junction between two compartments, in the present case between the main volume of the lower compartment and the upper plenum of the ice condenser. The performance of the ice condenser is described by specifying the exit temperature from the ice condenser; the values used in MARCH are based on the experimental results with a segment of a full scale system. Only one way flow through the ice condenser is permitted in MARCH with the implication of sufficient leakage from the upper to the lower compartments to permit pressure equilibration.

#### 4.4.2 Approach Taken by Sandia

Sandia's analyses utilized the in-vessel hydrogen generation and release to the containment as predicted by MARCH as input to the HECTR code, the latter described hydrogen burning and the resulting response of the containment. The HECTR code was specifically developed for addressing issues related to hydrogen burning during severe reactor accidents and represents a much more detailed treatment of the problem than afforded by the MARCH code. Some of the key features of HECTR of interest to the evaluation of the Ice Condenser PWR Standard Problem are noted below.

Mass and energy transfers in HECTR are based on pressure driven as well as buoyant flows, accounting for flow resistances and one way ice condenser doors, including time required for these doors to close. HECTR is capable of modeling series as well as parallel flow paths among compartments; for the ice condenser containment this included consideration of the flow from the lower to the upper compartment that bypassed the ice bed. The ice region is explicitly modeled by four compartments in the HECTR calculations, and a heat transfer correlation is used to predict the rate of heat transfer from steam to ice and the associated steam condensation rate.

In the HECTR analyses the ice condenser containment was modeled by nine interconnected volumes. These included: the dead spaces in the lower compartment, the main area of the lower compartment, the lower plenum of the ice condenser, four volumes in the ice bed, the upper plenum of the ice condenser, and the operating floor and dome volume. This compartmentalization is illustrated in Figure 4.5. Bypass of the ice condenser through the floor drain return lines was considered, as was the finite time required to close the ice condenser one way doors.

It was noted previously that the hydrogen ignition and flame propagation criteria in HECTR and the BURN subroutine in MARCH have a common origin and are very similar. Once hydrogen burning is initiated, the HECTR modeling includes radiation heat transfer from burning gases to structures in the compartment; MARCH does not include such a radiation heat transfer model.

#### 4.4.3 Differences Between MARCH and HECTR Modeling of Ice Condenser Containments

It has been noted that there are a number of differences between the MARCH and HECTR treatments of ice condenser containments. Some of the principal differences and the implications of these differences on the predicted results will be discussed in this section.

The MACE routine in MARCH which treats containment behavior is basically limited to series flow paths; this means that all the flow from the lower compartment to the upper compartment passes through the ice condenser. HECTR models series as well as parallel flow paths; for ice condenser containments this includes consideration of some flow from the lower compartment to the upper compartment through the floor drains, thus bypassing the ice bed.

MARCH treats the ice condenser as a heat exchanger in the junction between two compartments. The performance of the ice condenser is described by specifying the exist steam temperature from the ice bed; the values incorporated into MARCH are based on the large scale experiments conducted in the course of the development of this containment concept. In the

analyses conducted here this model results in the condensation of essentially all the steam passing through it. HECTR explicitly models the ice condenser by a series of compartments, including a steam condensation model that takes into account the rate of heat transfer between the fluid stream and the ice. In the event of large steam spikes the HECTR model permits more steam to pass through the ice bed without condensing than does the MARCH model.

The transfer of mass and energy between compartments in MARCH is, with some exceptions, based on the assumption of pressure equilibration among compartments. This is believed to be a reasonable approximation except for very rapid transients, e.g., detonation. This approximation has been adopted in order to improve the efficiency of the computations and is somewhat unique to MARCH. HECTR models transfers between compartments due to pressure as well as buoyancy differences, accounting for flow resistances, one way ice condenser doors, the finite time required for these doors to close, etc.

The above key differences between the MARCH and HECTR treatments of the ice condenser containment are believed to be the reasons for the differences in the predicted results. In comparing the pressures predicted by the two codes in the absence of any burning (see Figures 4.8 and 4.11 below) it can be seen that the HECTR modeling leads to higher containment pressures than does the MARCH treatment. This difference is consistent with the above discussion of differences. The higher pressures predicted by HECTR prior to burning are also manifested when burning takes place. The HECTR burn pressures start from a higher level than do those in MARCH. Also, the higher preexisting pressures imply that a larger amount of hydrogen must be accumulated in any compartment to reach a given volumetric concentration of hydrogen.

#### 4.5 Numerical Results and Sensitivity Studies

##### 4.5.1 Results from MARCH 2 Analyses of In-Vessel Accident Progression

MARCH 2 analyses were used to predict the in-vessel hydrogen generation and its release to the containment. The MARCH calculations for this standard problem were very similar to those conducted for BMI-2104, with the exception of some updated input on the volume of water on the containment floor before overflow into the reactor cavity. The in-vessel modeling (MARCH subroutine BOIL) options and assumptions in the base case calculation were identical to those of BMI-2104. At the time of vessel bottom head failure approximately 50% of the Zircaloy cladding was predicted to have reacted with steam to generate hydrogen. Most of the hydrogen generated in-vessel was retained in the reactor coolant system up to the time of vessel failure and was released rapidly upon failure together with the contained quantity of high pressure steam.

Table 4.1 gives the accident event times for a representative MARCH analysis for the TMLB sequence as obtained by Sandia. Figure 4.6 gives the corresponding steam source to the containment, and Figure 4.7 presents the hydrogen input into the containment. As illustrated in Figure 4.6, the steam input into the containment consists of two components; the first is the release of the high pressure steam stored within the primary coolant system, and the second is the result of the interaction of the core debris with the accumulator water in the reactor cavity. The hydrogen source also is made up of two components; the hydrogen produced in-vessel during the core melting phase, and the hydrogen generated during the debris-water interaction. Figure 4.7 illustrates that the former is substantially larger than the latter under the conditions of this analysis.

#### 4.5.2 Results from Analysis of Containment Response Without Hydrogen Burning

Before presenting specific results of the hydrogen burning analyses, it may be instructive to consider the predictions of containment conditions without burning; this may be useful background in the understanding of analyses with hydrogen burning. Figures 4.8 and 4.9 give the containment pressures and temperatures for the foregoing case as calculated by HECTR without any hydrogen burning. Figure 4.10 illustrates the ice remaining in the ice condenser as a function of time. Figure 4.11 illustrates the containment pressure response in the absence of any burning as calculated by MARCH. Note that this particular calculation was carried out for a long time into the accident sequence; our principal interest is in the time period of a few hours following reactor vessel failure, or perhaps to about 300 minutes on this figure. Vessel head failure is predicted at about 150 minutes, with a containment pressure of about 30 psia immediately after head failure. The predicted containment pressure is relatively low even though the failure of the vessel head is followed by rapid debris quench due to the effectiveness of the ice condenser. Comparison of Figures 4.8 and 4.11 shows the difference between the MARCH and HECTR predictions of the containment responses in the absence of burning. The different treatment of ice condenser heat transfer as well as consideration of flows that by pass the ice result in considerable higher short term pressure predictions by HECTR in comparison with the MARCH results. The longer term responses predicted by the two codes are not comparable. Figures 4.12-4.15 present the composition histories of the four compartments in terms of the mole fractions of steam, hydrogen, and oxygen. Nitrogen is the other constituent of the containment atmosphere that is not explicitly shown in these figures; after the onset of the corium-concrete interaction there may also be some carbon monoxide and carbon dioxide present. In these figures, Volume 1 represents the dead end spaces in the lower compartment, Volume 2 is the main area, area of the lower compartment, Volume 3 represents the upper plenum of the ice condenser, and Volume 4 is the dome region and operating floor. Figure 4.12 indicates that the dead end compartments would be expected

to be nonflammable due to low hydrogen concentration, but possibly also due to high steam concentration later in time. Figure 4.13 illustrates that the main volume of the lower compartment would be inerted essentially throughout the time period of interest by the very high steam concentrations predicted. Figure 4.14 shows very high hydrogen concentrations in the upper plenum of the ice condenser immediately following vessel failure. The high hydrogen flows are seen to temporarily reduce the oxygen level in this compartment, but there is significant overlap between high hydrogen and near normal oxygen concentrations. The oxygen level is seen to build up again after the debris quenching process has run its course. The steam concentration in the upper plenum of the ice condenser is maintained at very low levels due to the assumption of essentially complete condensation in the ice condenser which is inherent in MARCH. Figure 4.15 indicates that flammable conditions would be established in the upper compartment shortly after head failure and maintained for the time during of interest. It should be emphasized that the results presented in the foregoing figures are based on no burning, and that the assumption of burning at any stage in the calculation would alter the subsequent observations. These figures do illustrate the types of composition changes that are predicted in the analyses with burning considered, and lend insight on the reasons why certain compartments are flammable at some times and not at others.

#### 4.5.3 Results from Hydrogen Burning Analyses

Tables 4.2 and 4.3 summarize the specific cases evaluated by Sandia and Battelle, respectively. Table 4.4 compares the results of the two sets of calculations for a number of key cases. Some general observations on the results of the Ice Condenser PWR Standard Problem will be given here. A discussion of the differences between the MARCH and HECTR predictions will be given in a later section.

The calculations performed for the TMLB sequence in an ice condenser containment design indicate that the lower portions of the containment will be inerted with respect to hydrogen burning for major portions of the accident sequence. The upper portions of the ice condenser, particularly the upper plenum, and the dome region of the containment would be expected to contain flammable compositions shortly after head failure as well as thereafter. Since, by definition, electric power is not available in this sequence, hydrogen igniters would not be available to control the buildup of high concentrations of hydrogen. Thus ignition could effectively be a random event. The discharge of the hot core debris from the reactor vessel at the time of vessel head failure is often cited as a likely source of ignition. In the analyses considered here, however, the lower compartment was typically found to be inerted by high steam concentrations at the time of head failure. Thus the hot core debris would not necessarily be an effective ignition source unless some of the debris found their way into the upper compartment without first being cooled.



For the above reasons, a variety of ignition criteria were examined during these analyses; these included ignition on hydrogen concentration, on vessel breach, and at various time delays after vessel breach. Given ignition, a number of burns were typically predicted. Burning was typically predicted to start in the upper portions of the ice condenser compartment and, as long as the burning was confined to the ice condenser, very low containment pressure loads were found. In essentially all the cases considered, however, the burning was eventually predicted to propagate from the ice compartment to the upper dome region. When the latter occurred, substantial pressure rises were calculated.

Some of the sensitivities of the predicted containment loads on the variables considered in the analyses are discussed below. The predicted peak containment pressure loads were found to increase with the extent of in-vessel hydrogen production. This is an expected observation since the greater in-vessel production would lead to correspondingly higher hydrogen concentrations in the various compartments of the containment.

The predicted peak containment pressures were found to be sensitive to the timing of ignition, with delays in the timing of ignition leading to higher peak pressures. This again is an expected result, since the longer the time to ignition, the more time for hydrogen to build up in the upper portions of the containment. The peak containment pressures were also found to increase with the magnitude of the steam spike following reactor vessel breach. The larger the steam spike the more of the hydrogen can be swept into the upper compartment; the large containment loads are always associated with burns that propagate into the upper compartment. Increases in preburn pressures were obviously also reflected in the ultimate values predicted.

The dead end spaces of the lower compartment were generally predicted to be nonflammable, or have hydrogen concentrations barely into the flammable range. Thus minimal burning would be predicted in this part of the containment under the conditions of the present analyses. Since most of the containment penetrations are believed to be located in these areas, it may be inferred that overtemperature challenges to containment penetrations do not constitute a major threat to containment integrity.

The hydrogen concentrations in local regions were predicted to reach detonable proportions in a number of the cases considered. Neither HECTR nor MARCH can treat hydrogen detonations and are limited to the assumption of deflagration type behavior. Thus the possible implications of hydrogen detonations, should they occur, have not been addressed in the present studies.

#### 4.5.4 Sensitivity Studies

In the base case MARCH 2 calculation approximately 50% of the Zircaloy cladding was predicted to have reacted with steam during the in-vessel phase of the accident to produce hydrogen. For purposes of investigating sensitivities of the containment response, additional cases were considered in which the reaction of the Zircaloy was arbitrarily forced to completion in the primary system, as well as some cases in which the in-vessel modeling assumptions were changed to produce less than the base case extent of Zircaloy reaction.

In a normal MARCH calculation the failure of the reactor vessel bottom head is assumed to be a large opening. For transient accident sequences such as the one considered here, a normal MARCH calculation typically predicts that very little of the hydrogen generated in-vessel is released to the containment prior to bottom head failure; thus bottom head failure is typically followed by the release to the containment of a large quantity of hydrogen. Such rapid releases of hydrogen to the containment could have an undue influence on the prediction of the effects of hydrogen burning. As part of the standard problem analyses some alternative assumptions regarding the timing and rate of hydrogen release to the containment were also considered. Specifically, the situation where the collapse of the molten core into the vessel bottom head leads to the early failure of the head via a small hole, such as may be associated by the melting of a penetration, was considered. In the MARCH analyses this situation was actually modeled by the opening of the relief valve at the time of the start of core collapse; this permitted the release of the hydrogen from the primary system to start prior to the general failure of the head and the release of the core debris to the reactor cavity.

In a typical analysis of the TMLB sequence the failure of the vessel bottom head is followed by the discharge of the accumulator water and the subsequent interaction of the core debris with this water. The large steam spikes that are typically associated with the latter interactions can result in the rapid transport of hydrogen from the lower compartment to the upper compartment of the ice condenser containment. The subsequent burning of the hydrogen in the upper compartment can pose serious challenges to containment integrity. In addition to such a large steam spike which was considered in the base case MARCH analysis, alternate cases were considered in which only minimal interaction between the core debris and water in the reactor cavity were assumed. In these cases the debris were assumed not to fragment, but remain as a coherent mass; this assumption leads to the early attack of the concrete by the core debris, with heat transfer to the overlaying water layer by film boiling and radiation.

#### 4.6 Consideration of Loads and Likelihood of Containment Failure\*

With its extensive pressure suppression capability an ice condenser containment is not susceptible to steam spikes. However, this capability may lead to de-inerting and thus to potential challenges by hydrogen burns. This has been recognized already and electric-powered igniters have been installed in operating plants. As long as these igniters remain operational and the hydrogen is well mixed controlled burning of a reasonable rate of in-vessel hydrogen production and release (as well as reasonable quantities of ex-vessel hydrogen), and suppression of the resulting energy by the ice-bed will occur. Loss of the mixing function provided by the air return fans can result in detonable mixtures. The most likely potential for challenge, therefore, exists if power to the igniters and air return fans is lost. Station blackout (TMLB) would represent such a situation. The Sequoyah power plant was selected for the calculations.

The results indicate that, for the assumptions on these analyses, the loading pattern is generally characterized by intermittent, sharp, pressurization of the containment. These spikes correspond to hydrogen burns. Their timing depends upon meeting conditions for self-ignition, and their amplitude depends upon the spatial hydrogen distribution at the time of ignition and the flame propagation requirements. As the waiting period for ignition increases not only the quantities of accumulated hydrogen increase, but also its distribution is biased towards the containment dome. As a consequence the quantity of energy release in the burn increases and the ice bed becomes less effective in suppressing the resulting pressures. This whole process is aggravated as the magnitude of the steam spike in the lower compartment increases. This is because the resulting high steam flows through the ice bed and into the upper dome favor inerting of the lower compartments and ignition within the upper containment dome (sweeps hydrogen to upper dome). Burn spikes of up to 4.8 to 6.8 bar (70 to 100 psi) have been calculated and possibilities for detonations were raised under such conditions. Such loads, compared to the CPWG estimated failure pressure of the Sequoyah containment at 4.4 bar (65 psia), would represent a significant challenge. On the other hand, calculations based on a low steam spike assumption resulted in burn spikes of 3.4 and 4.8 bar (50 to 70 psi), still significant with regard to containment failure.

---

\* Considerations of the Likelihood of containment failure from the various load sources described in this report have been provided by the NRR staff and is based on extended discussions with staff consultants and staff members involved in containment loads and performance activities.

The CLWG results, therefore, lead one to conclude that a station blackout accident (as it is currently perceived to lead to high pressure scenarios and including loss of igniters) in the Sequoyah plant would most likely cause an early containment failure. This conclusion, can be modified by primary system failure prior to core melt (see SP-A) and by ensuring proper functioning of igniters (e.g., with a dedicated battery). Clearly more work needs to be done to improve our understanding in these areas for this containment type.

#### 4.7 Conclusions and Recommendations

Based on the analyses of the Ice Condenser PWR Standard Problem discussed above, the following observations can be made:

For the accident sequence considered, ignition of the hydrogen-air mixtures is effectively a random event; ignition is not assured even after vessel breach due to steam inerting of the lower compartment and lower portions of the ice condenser.

Assuming the availability of an ignition source, burning was typically found to start in the ice condenser, but generally was predicted to eventually propagate to the upper plenum of the ice condenser.

When burning was confined to the ice condenser compartment, the resulting overall pressures were small; propagation of the burning to the upper compartment lead to the prediction of large pressure rises.

The calculated peak pressure loadings were found to be sensitive to the timing of ignition, with longer delays to ignition leading to higher predicted peak pressures.

The predicted peak pressures in the containment were found to increase with increasing extent of in-vessel Zircaloy oxidation.

The predicted peak containment pressures were found to increase with increasing magnitude of the ex-vessel steam spike following vessel breach.

Locally detonable compositions were found to be possible under the conditions and assumptions of these analyses; the effects of possible detonations were not considered in the present analyses.

A number of differences between the approaches used by the two groups analyzing this problem were noted. These differences lead to differences in the specific values in the loadings predicted, but the overall trends in predicted behavior were found to be very similar.

TABLE 4.1

MARCH 2.0 CHRONOLOGY FOR CLWG ICE CONDENSER  
CONTAINMENT STANDARD PROBLEM

	<u>EVENT</u>	<u>TIME(S)</u>
1.	STM GEN DRY	3885
2.	CORE UNCOVER	5550
3.	START MELT	7350
4.	CORE SLUMP	8640
5.	START HEAD HEATUP	8745
6.	BOTTOM HEAD FAIL	9465

TABLE 4.2 CASE DESCRIPTIONS AND SUMMARY OF HECTR RESULTS

Case No.	In-Vessel Zr Oxd. Spike	Steam Type <sup>a</sup>	Ignition Limit MHZ	Number of Burns by Compartment									Peak Loadings Pressure (Comp.#) F(psa)	Peak Temp. Comp.# F	Preburn Drive Conditions psia	Peak Burn Rate MHZ		
				1	2	3	4	5	6	7	8	9						
Q.00	49.4#	High	VB+5s	4.1	2	3	0	0	1	0	0	1	4	87 (1-3,6-9)	2060 (2)	523	78	4.1
Q.00o	49.4#	High	Nonmech.	10.0	1	8	0	0	1	0	0	2	2	97 (all)	2540 (2)	1130	44	6.8
Q.01	49.4#	High	DlexIC	8.0	1	7	0	0	1	0	1	2	6	106 (1,2)	2470 (2)	961	48	8.0
Q.02	49.4#	High	DI all	8.0	1	10	0	0	1	0	1	9	17	83 (all)	1660 (2)	968	44	5.1
Q.02o	49.4#	High	Nonmech.	12.0	1	8	0	0	1	0	0	2	4	95 (all)	2720 (2)	1590	44	6.6
Q.03o	49.4#	High	Nonmech.	30.0	0	1	0	0	0	0	0	0	1	51 (all)	3220 (2)	302	--	--
Q.05	49.4#	High	VB	4.1	2	9	0	0	3	0	0	4	9	90 (all)	3320 (2)	695	67	4.1
Q.06	49.4#	High	None	100.0	0	0	0	0	0	0	0	0	0	48 (all)	327 (4)	293	--	--
Q.07	49.4#	High	VB	8.0	2	3	0	0	0	0	0	1	1	90 (all)	3330 (2)	397	68	4.1
Q.08	49.4#	High	VB+5s	8.0	1	2	0	0	0	0	0	1	3	78 (all)	1890 (2)	395	33	6.1
Q.09	49.4#	High	VB+10s	8.0	1	2	0	0	0	0	0	2	2	100 (all)	2170 (9)	462	36	8.0
Q.10	49.4#	High	VB+20s	8.0	1	2	0	0	0	0	0	1	1	123 (1,2)	2250 (8)	440	43	11.0
R.00	49.4#	Low	VB+5s	8.0	1	2	0	0	0	0	0	1	3	71 (all)	1890 (2)	394	33	6.1
S.01	99.8#	Low	VB+5s	8.0	1	3	0	0	1	0	0	2	2	102 (1,2)	3180 (2)	1480	35	8.7
S.02	99.8#	Low	VB+1hr	8.0	1	1	0	0	1	0	0	1	1	212 (1,2)	3800 (1)	2800	36	22.7
T.01	39.4#	High	VB+5s	8.0	2	2	0	0	0	0	0	0	1	87 (1,2)	2130 (2)	386	66	4.1
U.00	39.4#	Low	VB+5s	8.0	1	2	0	0	0	0	0	0	3	59 (all)	2130 (2)	350	32	4.6
U.01	39.4#	Low	None	100.0	0	0	0	0	0	0	0	0	0	37 (all)	300 (4)	251	--	--
V.00	48.3#	High	VB+5s	8.0	0	0	0	0	0	0	0	0	1	152 (1,2)	2560 (1)	451	36	14.5
V.01	48.3#	High	DI all	8.0	1	8	0	0	0	0	0	5	8	96 (1-3,6-9)	2790 (2)	478	34	8.0

<sup>a</sup>DlexIC --Deliberate Ignition except in Ice Compartments and lower plenum  
 DI all --Deliberate Ignition in all compartments  
 VB --Vessel Breach  
 Nonmech. --Nonmechanistic Ignition

TABLE 4.3 SUMMARY OF BCL RESULTS FOR ICE CONDENSER  
PWR STANDARD PROBLEM

STEAM SPIKE	IGNITION THRESHOLD, % $H_2$	IGNITION TIME/TYPE (1)	BURN IN COMP No (2)	PEAK PRESSURE, PSIA
HIGH	NONE	NONE	---	30
HIGH	8	DI	3,4	76
HIGH	10	NM	3,4	80
HIGH	30	NM	3,4	78
LOW	8	DI	3,4	53
LOW	10	NM	3,4	48
LOW	30	NM	3,4	60
HIGH	8	VB	3,4	76
HIGH	8	VB+5 SEC	3,4	77
HIGH	8	VB+20 SEC	4,3	82
HIGH (3)	8	VB	3,4	135
HIGH (4)	8	VB	3,4	70
HIGH (4)	8	DI	3,4	68

- (1) DI = IGNITION UPON REACHING 8 %  $H_2$ , SIMULATING DELIBERATE IGNITION.  
 NM = NON-MECHANISTIC, ASSUMED IN THE ABSENCE OF IGNITION SOURCES.  
 VB = IGNITION AT VESSEL BREACH, OR IF INDICATED, AT SOME DELAY AFTER VESSEL BREACH.
- (2) COMPARTMENT NUMBER IN WHICH BURNING IS FIRST PREDICTED TO TAKE PLACE, FOLLOWED BY COMPARTMENT NUMBER TO WHICH THE BURNING IS PREDICTED TO PROPAGATE.
- (3) FOR THIS CASE, 100% ZIRCALOY OXIDATION IN-VESSEL ASSUMED; IN ALL OTHER CASES, APPROXIMATELY 49% IN-VESSEL OXIDATION CALCULATED.
- (4) IN THESE TWO CASES SMALL OPENING IN VESSEL, PRIOR TO VESSEL BREACH ASSUMED, ALLOWING EARLIER RELEASE OF  $H_2$  FROM PRIMARY SYSTEM.

TABLE 4.4 ICE CONDENSER PWR STANDARD PROBLEM

## SUMMARY OF ICE CONDENSER PWR STANDARD PROBLEM RESULTS

IN-VESSEL Zr OXIDE, %	STEAM SPIKE	IGNITION THRESHOLD v/o H <sub>2</sub>	IGNITION TIME/TYPE (1)	PEAK PRESSURE, PSIA	
				MARCH	HECTR
49	HIGH	NONE	NONE	30	48
49	HIGH	8	DI	76	104
49 <sup>(2)</sup>	HIGH	8	DI	68	95
49	HIGH	8	VB	76	88
49 <sup>(2)</sup>	HIGH	8	VB	70	150
49	HIGH	8	VB+5 SEC	77	77
49	HIGH	8	VB+20 SEC	32	122
49	HIGH	10	NM	80	95
49	LOW	8	DI	53	
49	LOW	8	VB+5 SEC		70
49	LOW	10	NM	48	
100	HIGH	8	VB	135	
100	LOW	8	VB+5 SEC		101
39	HIGH	8	VB+5 SEC		86
39	LOW	8	VB+5 SEC		58
49	HIGH	4.1	VB+5 SEC		86

- (1) DI = IGNITION ON 8 v/o H<sub>2</sub> SIMULATING DELIBERATE IGNITION.  
 VB = IGNITION ON VESSEL BREACH, PLUS INDICATED DELAY.  
 NM = NON-MECHANISTIC, ASSUMPTION ONLY.

- (2) LEAKAGE FROM PRIMARY SYSTEM AT CORE COLLAPSE, BEFORE GROSS HEAD FAILURE.



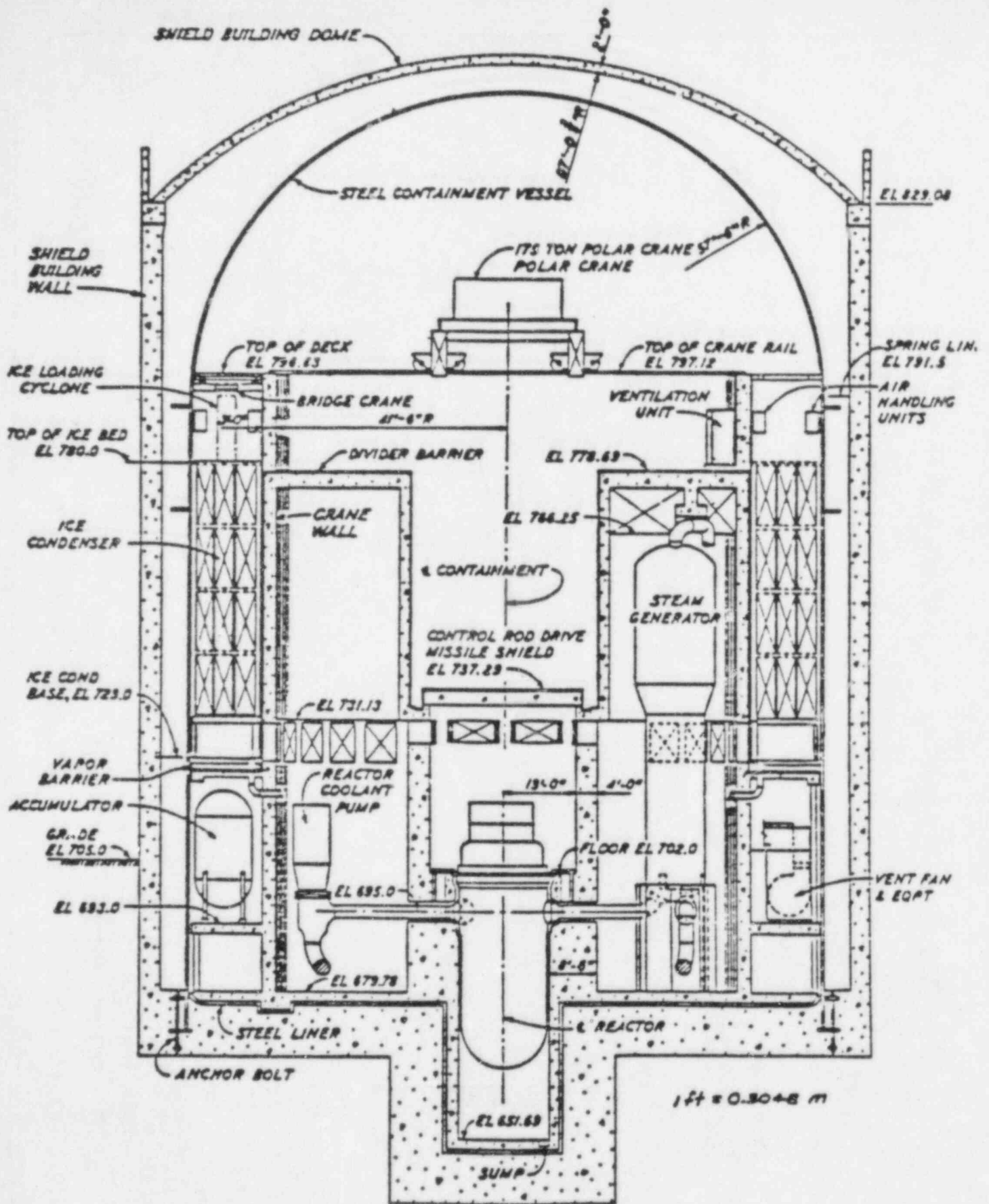


Figure 4.1 Reactor Building Elevation

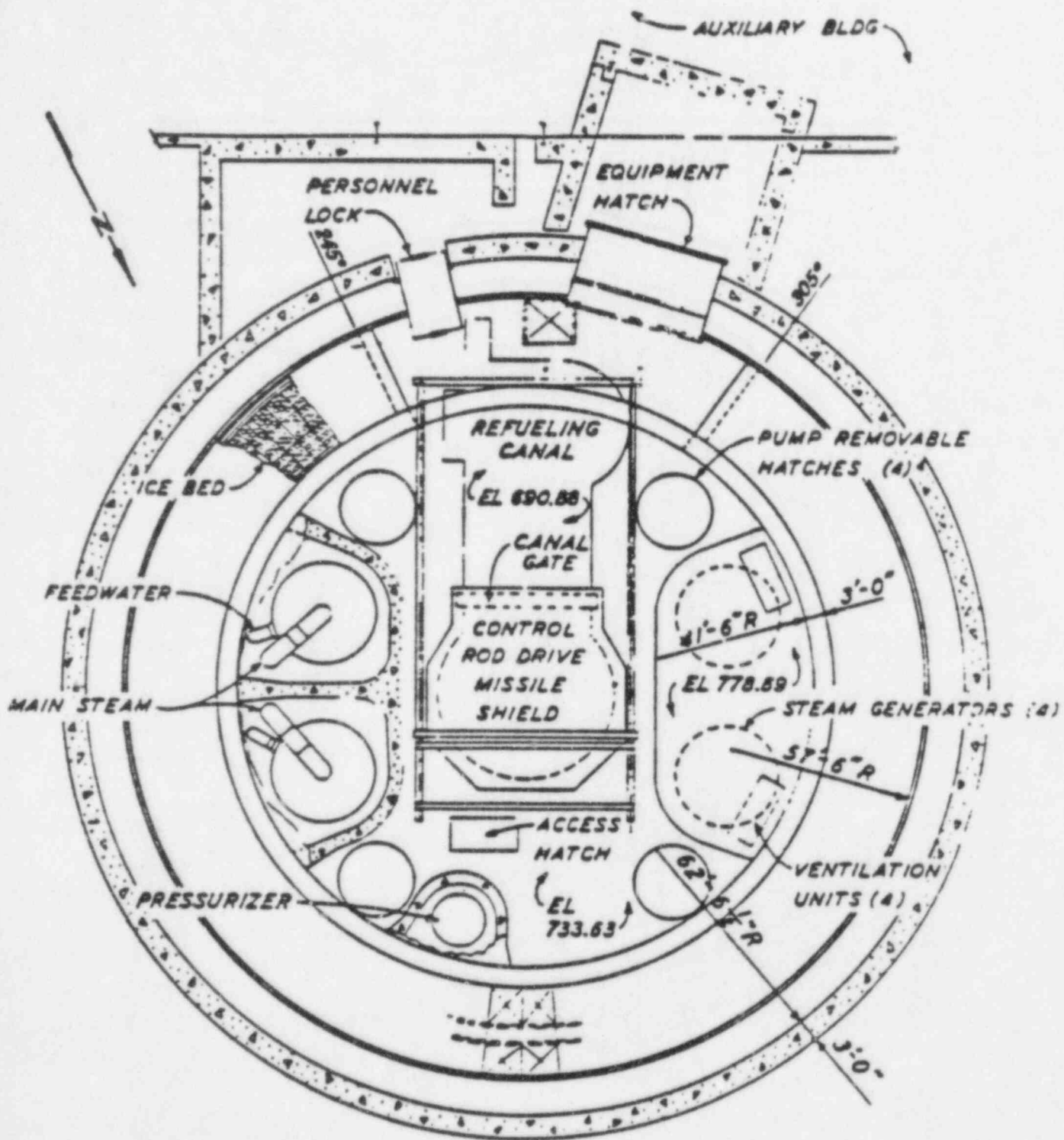


Figure 4.2 Plan-Upper Compartment

# Ice condenser

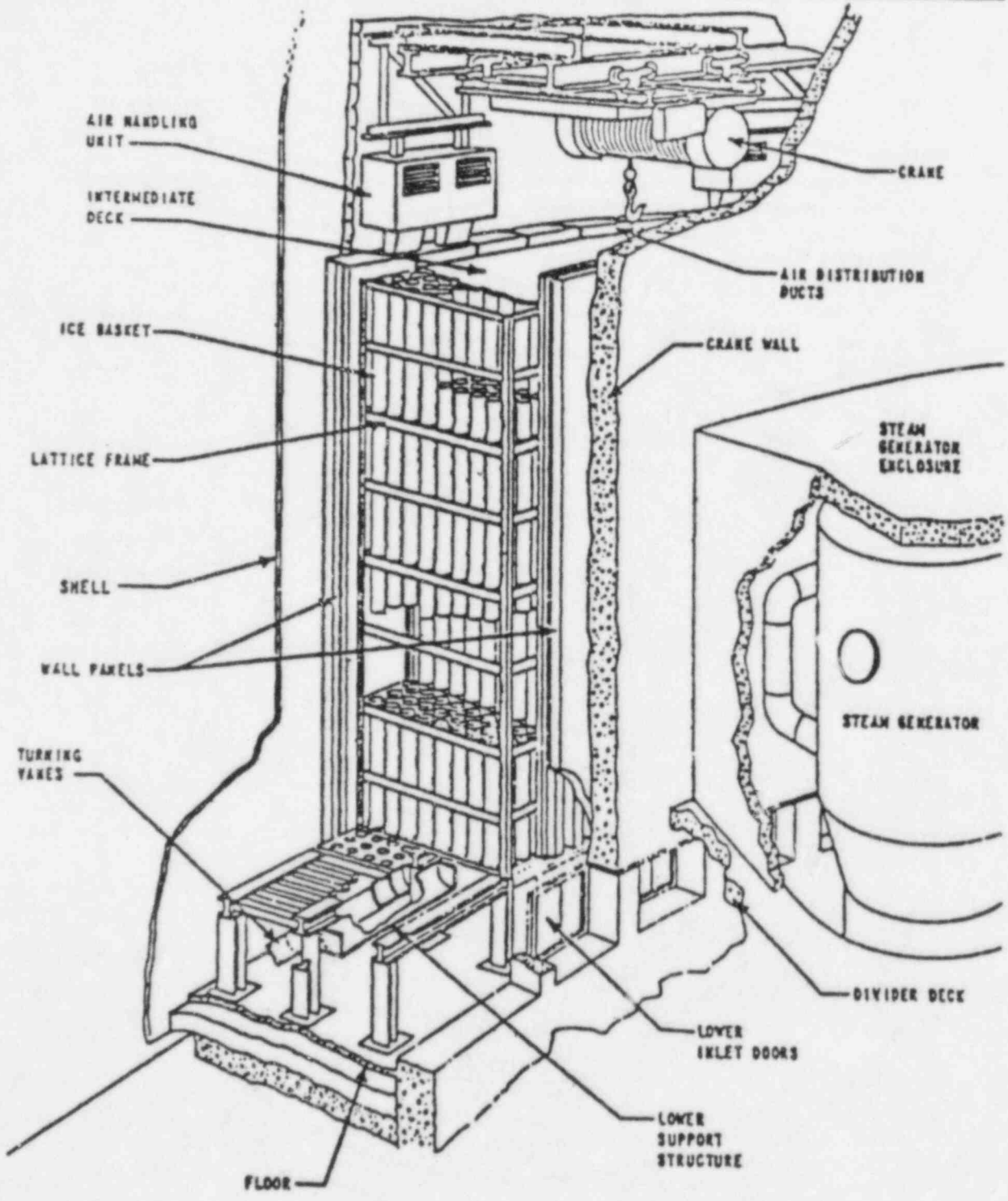


Figure 4.3 - Ice Condenser Bed

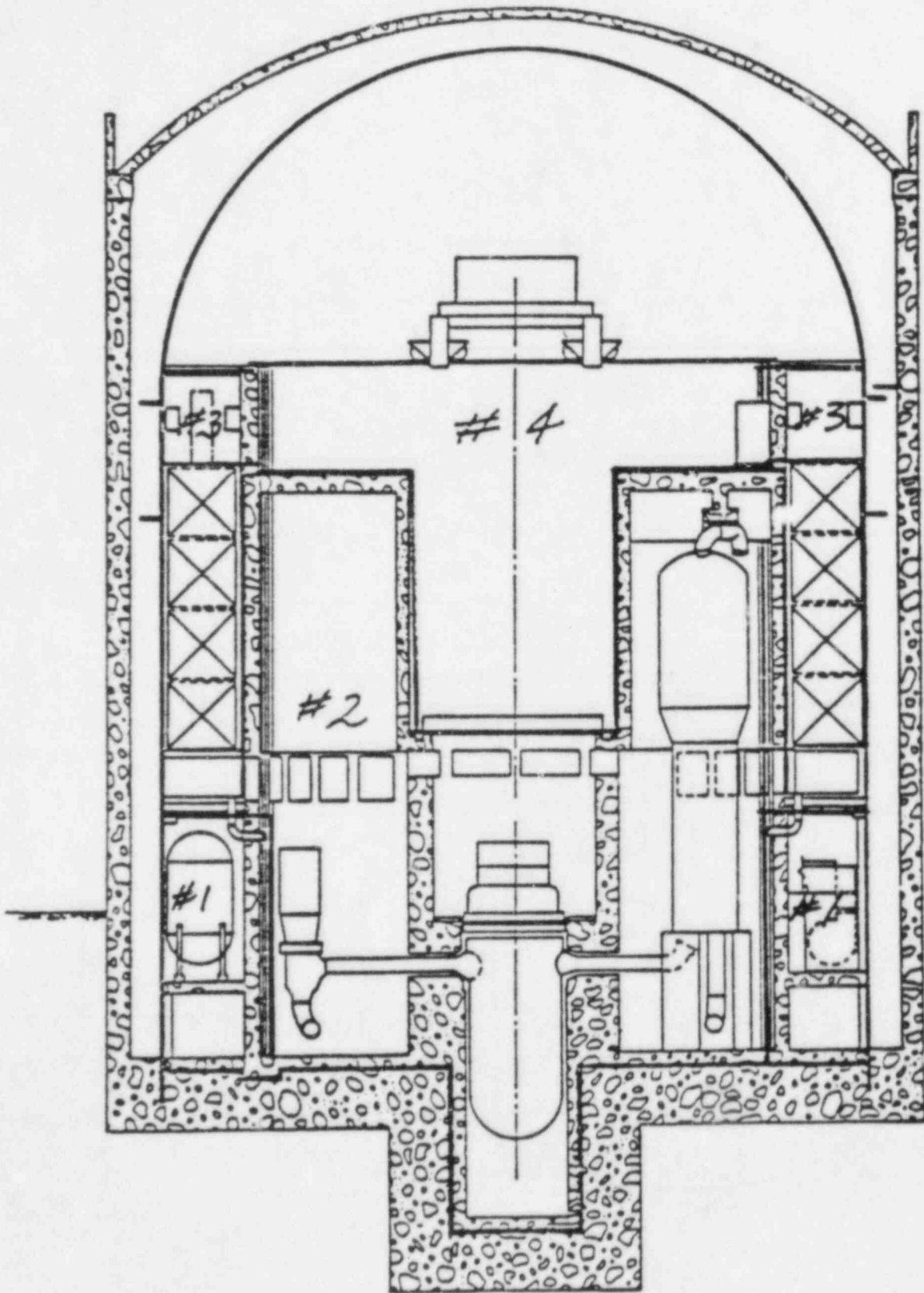


Figure 4.4 MARCH Ice Condenser Containment Model

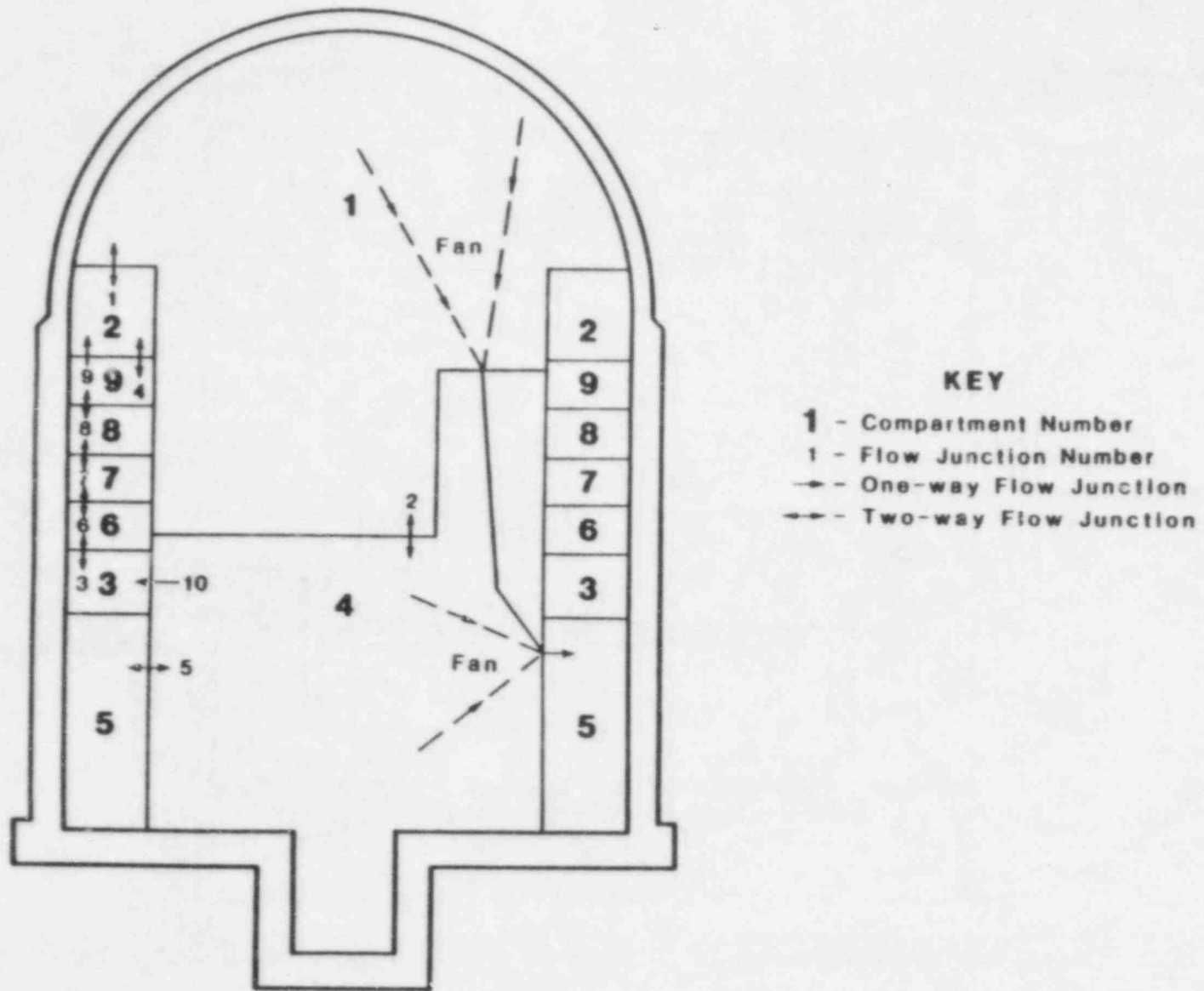


FIGURE 4.5 HECTR ICE CONDENSER CONTAINMENT MODEL

clwg sp#6 case.q.06

MARCH Input

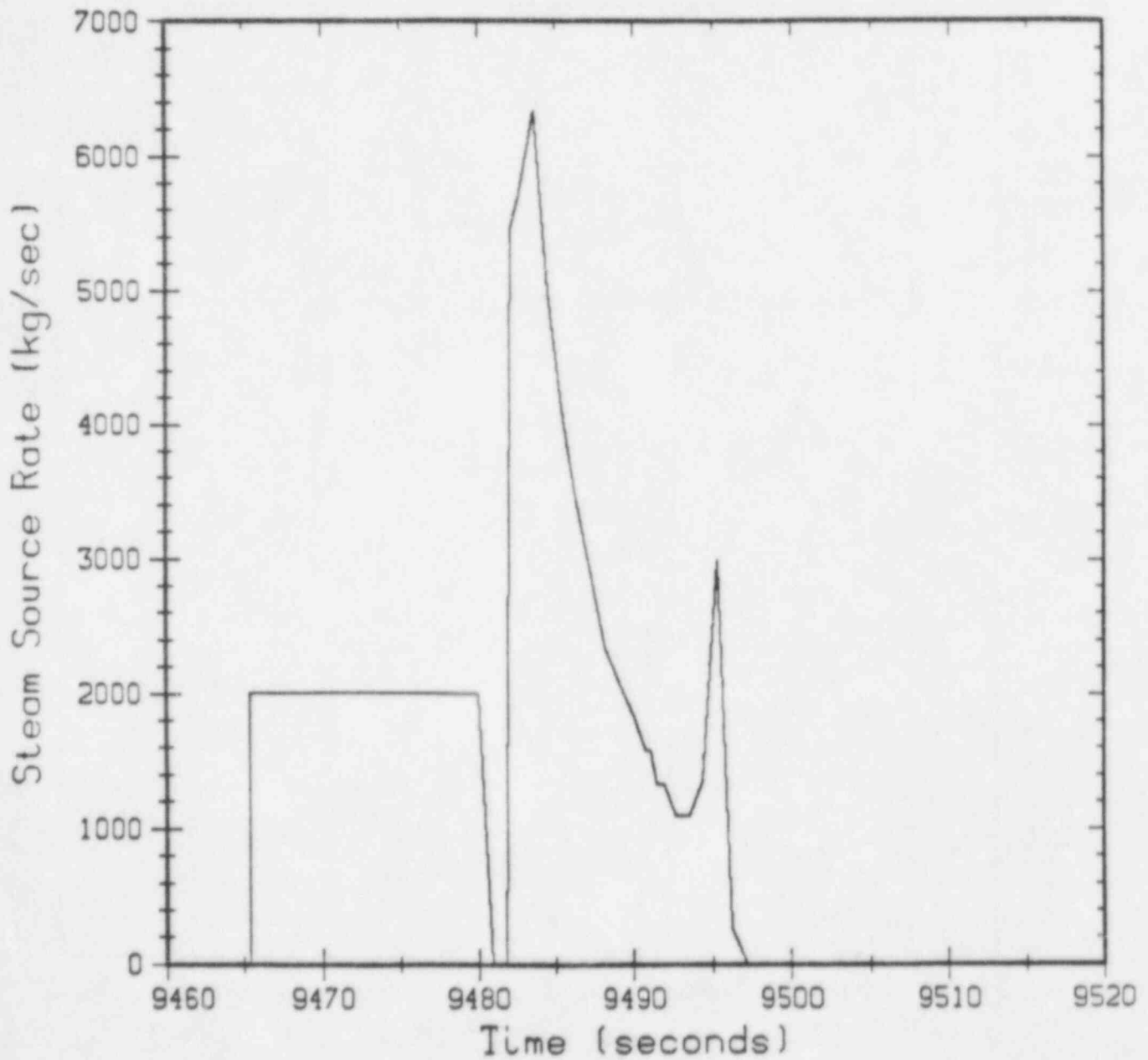


FIGURE 4.6 REFERENCE CONTAINMENT STEAM SOURCE FOLLOWING VESSEL BREACH

clwg sp#6 case q.06

MARCH Input

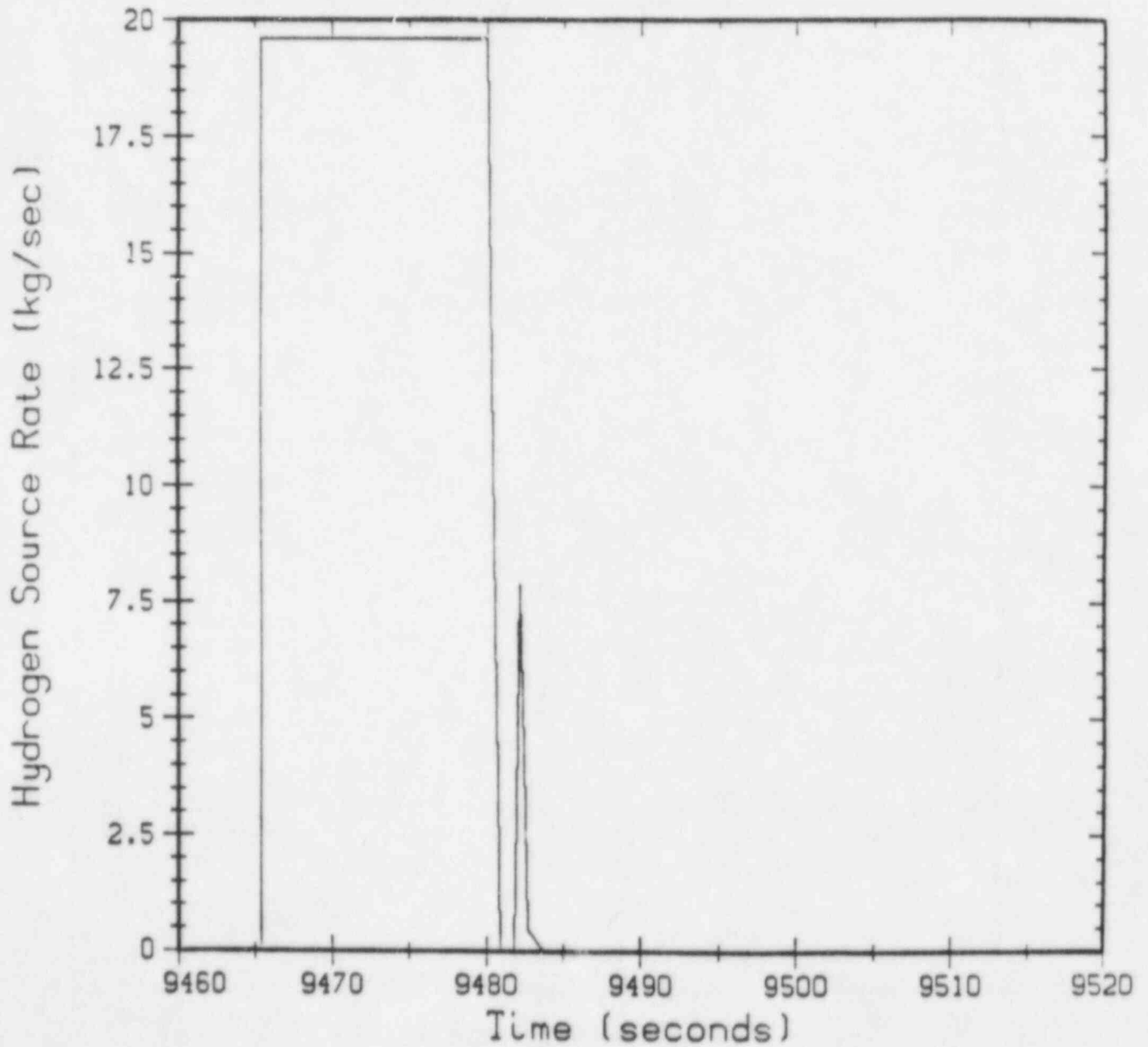


FIGURE 4.7 REFERENCE CONTAINMENT HYDROGEN SOURCE FOLLOWING VESSEL BREACH

clwg sp#6 case q.06  
Compartment 1

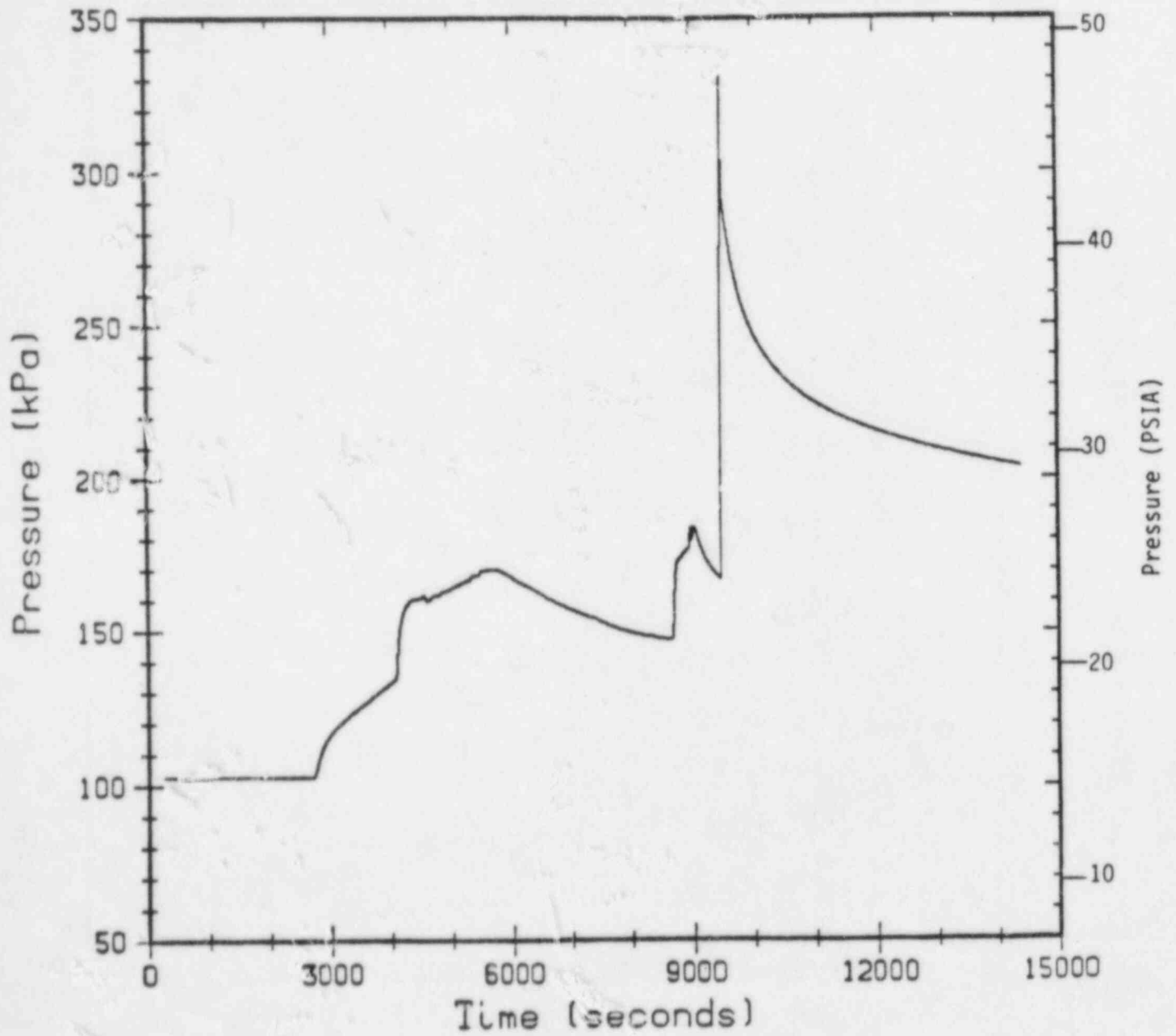


FIGURE 4.3 HECTR CALCULATED PRESSURE RESPONSE WITHOUT HYDROGEN BURNING



clwg sp#6 case q.06  
Compartment 4

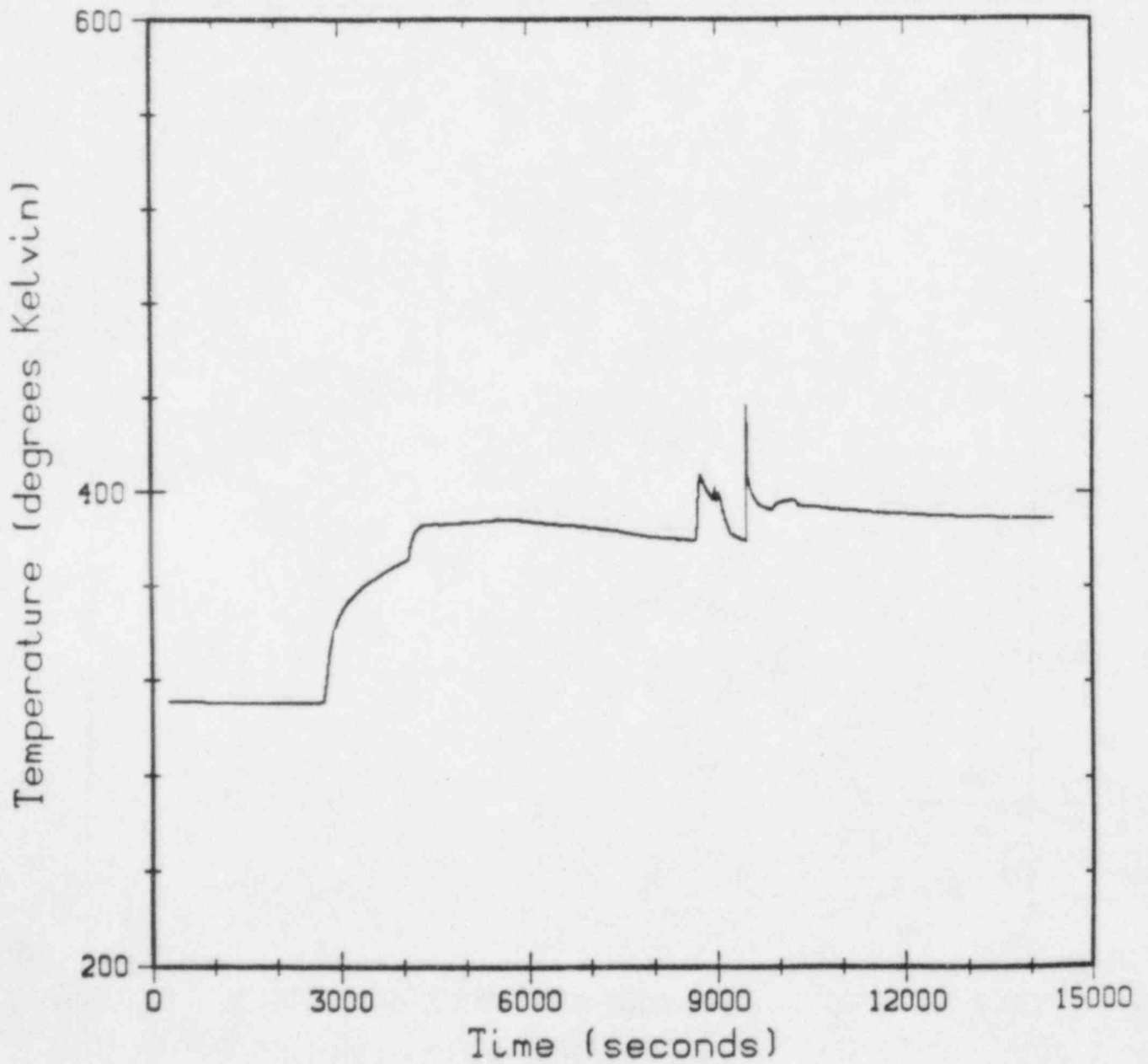


FIGURE 4.9 HECTR CALCULATED TEMPERATURE RESPONSE IN THE LOWER COMPARTMENT

clwg sp#6 case q.06  
Ice Remaining

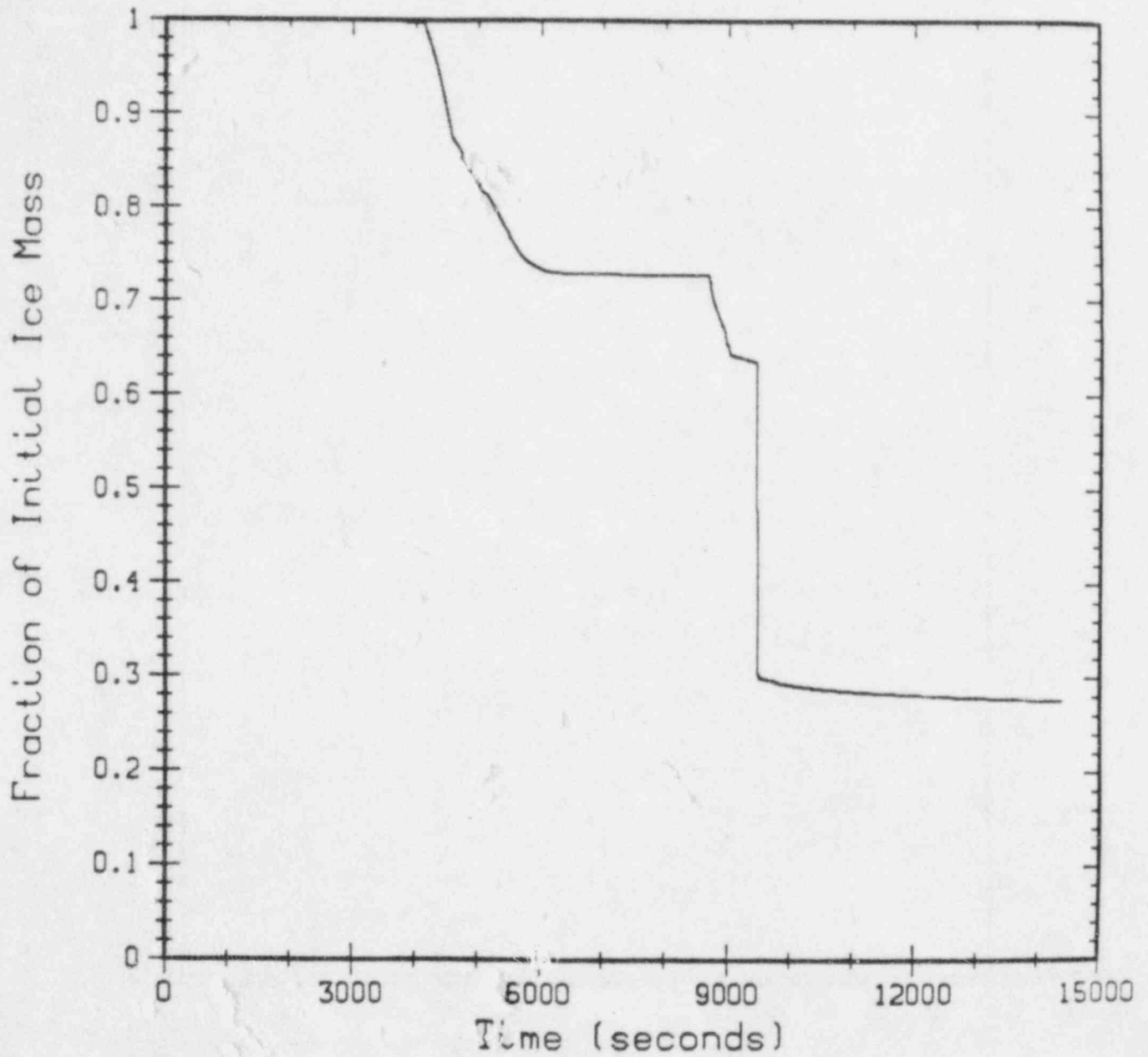


FIGURE 4.10 HECTR CALCULATED ICE REMAINING WITHOUT HYDROGEN BURNING

TMLB4V11

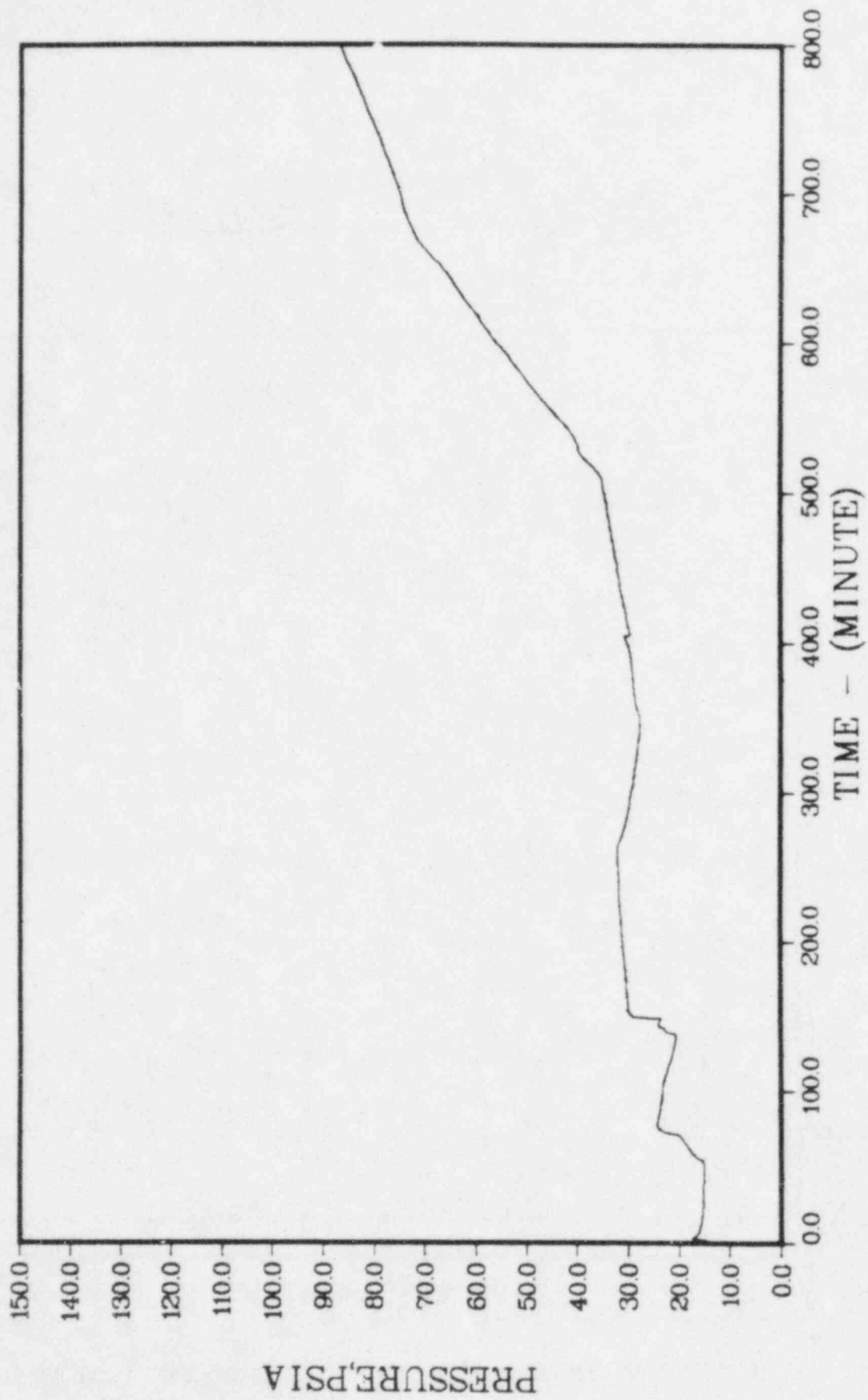


FIGURE 4.11 MARCH CALCULATED PRESSURE RESPONSE WITHOUT BURNING

TMLB4V11

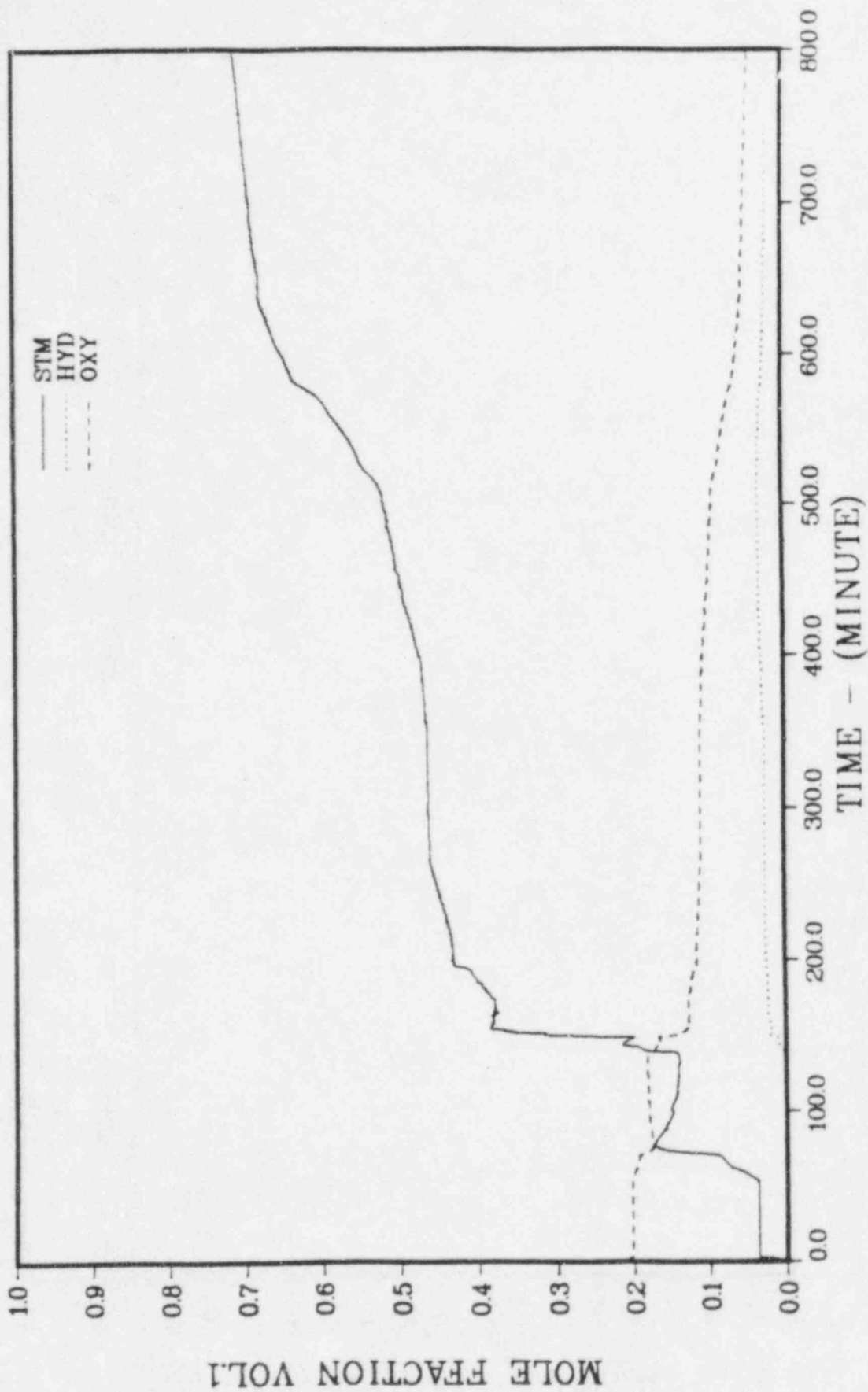


FIGURE 4.12 MARCH CALCULATED ATMOSPHERE COMPOSITION IN DEAD END VOLUME WITHOUT BURNING

TMLB4V11

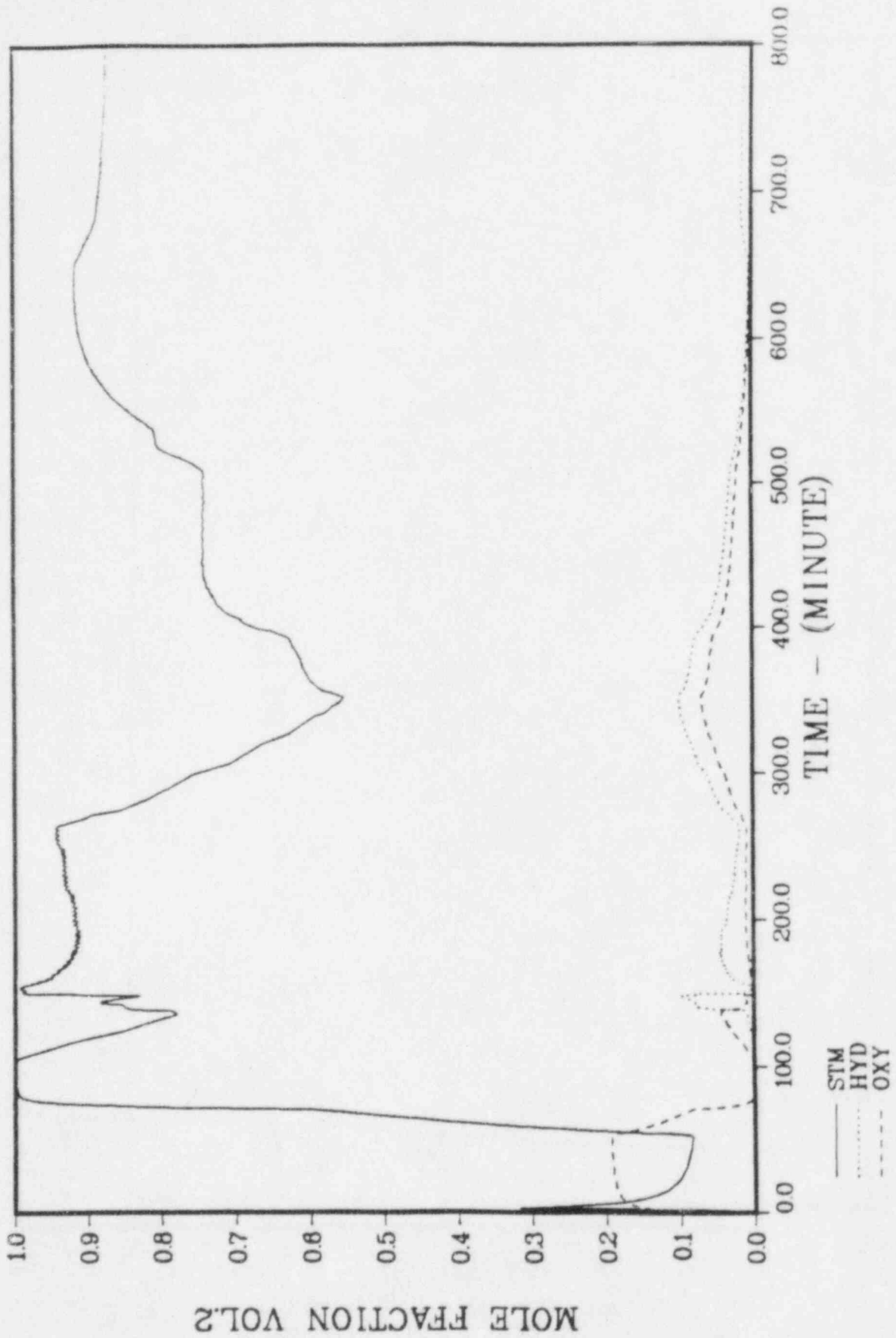


FIGURE 4.13 MARCH CALCULATED ATMOSPHERE COMPOSITION IN LOWER COMPARTMENT WITHOUT BURNING

# TMLB4V11

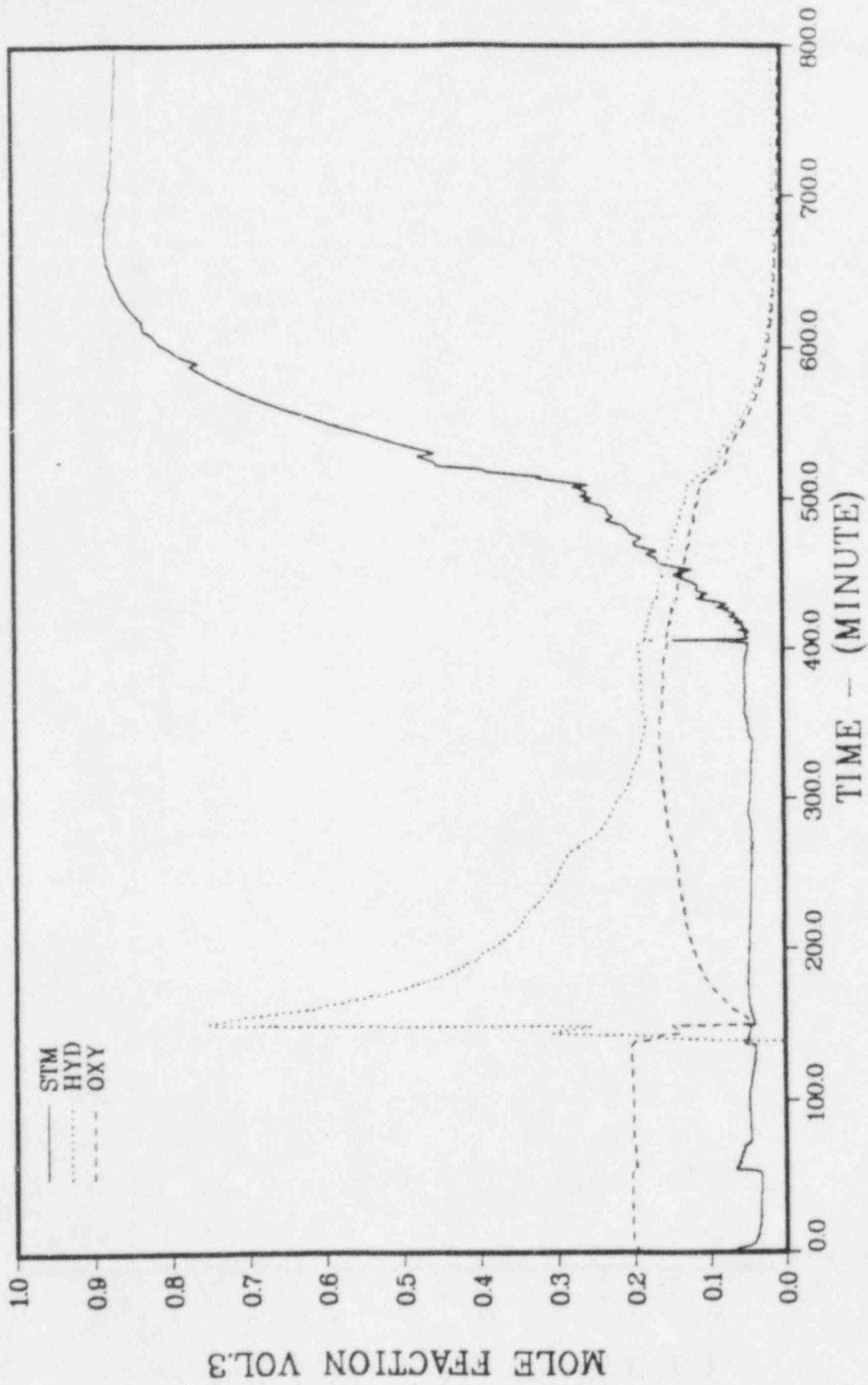


FIGURE 4.14 MARCH CALCULATED ATMOSPHERE COMPOSITION IN ICE CONDENSER UPPER PLENUM WITHOUT BURNING

# TMLB4V11

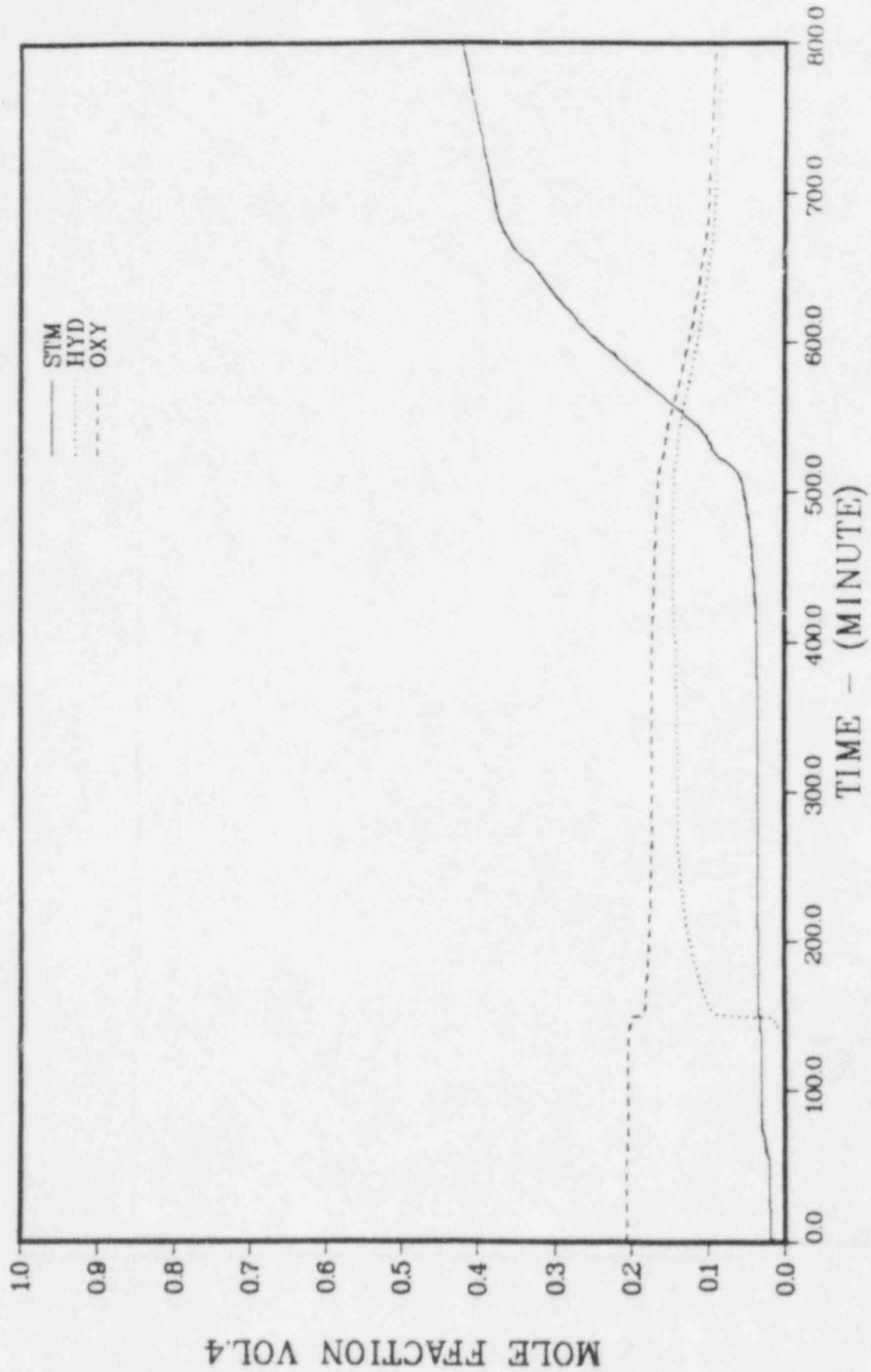


FIGURE 4.15 MARCH CALCULATED ATMOSPHERE COMPOSITION IN UPPER COMPARTMENT WITHOUT BURNING

## Chapter 5 BWR MARK I CONTAINMENT (SP-4)\*

### 5.1 Description of the Reference Plant Geometry (Browns Ferry)

The Mark I containment system consists of the drywell, the pressure suppression pool, the vent system connecting the drywell and pressure suppression pool, a containment cooling system, isolation valves, and various service equipment. Figure 5.1 shows the arrangement of the drywell and pressure suppression pool.

The drywell is a steel pressure vessel with a spherical lower portion and a cylindrical upper portion. It is designed for an internal pressure of 0.531 MPa (62 psig) at a temperature of 138°C (281°F). Normal environment in the drywell during plant operation is an inert atmosphere of nitrogen at atmospheric pressure and a temperature of about 57°C (135°F).

The vent system consists of 8 circular vent pipes which connect the drywell to the pool. The pressure suppression pool is a toroidal shaped steel pressure vessel located below the drywell. The pool contains about 3823 m<sup>3</sup> (235,000 ft<sup>3</sup>) of water and has an air space above the water pool of 3370 m<sup>3</sup> (119,000 ft<sup>3</sup>). Inside the pool extending around the circumference of the torus, is a 1.45 m (4.75 ft) diameter vent header. The 8 drywell vents connect to this vent header. Projecting down from the vent header are 96 downcomer pipes which terminate 1.22 m (4 ft) below the surface of the water.

The torus which contains the pressure suppression pool is designed to essentially the same requirements as the drywell liner, i.e., a maximum internal pressure of 0.531 MPa (62 psig) at 138°C (281°F), but neither the drywell nor the torus is designed to withstand the stresses which would be created by a significant internal vacuum. To ensure that a significant vacuum cannot occur in the drywell, vacuum breaker valves are installed, which will open to permit flow from the pressure suppression pool airspace into the drywell whenever the suppression pool pressure exceeds the drywell pressure by more than 3447 Pa (0.5 psi). Additional vacuum breaker valves with the same setpoints are installed to permit flow from the reactor building into the pressure suppression pool airspace, to prevent a significant vacuum there.

The specific design parameters for the standard problem are listed in Tables 5.1, 5.2 and 5.3.

\* CLWG analysts: Perkins, Greene, Pratt (BNL); Haskin, Gasser, Behr, Shaffer Smith (SNL); Cybulskis, Wooton (BCL); Hodge (ORNL); Theofanous (University of California); Cunningham, Barrett (NRC). Consensus summary authors: Perkins, Greene, Pratt (BNL).



## 5.2 Description of the Standard Problem and Objectives

The "base case" accident sequence is a TQUV-type sequence in which the all main steam system is isolated and reactor vessel injection capability is lost at the time of a reactor trip from 100% power. Because of mass loss out of the SRV's and the lack of coolant injection, the core eventually becomes uncovered. In this sequence, automatic ADS actuation will not occur, and manual actuation is assumed not to occur, so that the RCS remains at high pressure. The uncovered core becomes molten and the debris falls into the reactor vessel lower plenum where, eventually, the corium attacks the reactor vessel bottom head.

When the reactor vessel head fails, the corium falls onto the dry concrete floor of the drywell and the corium-concrete reaction begins. As steam is liberated from the concrete, previously unoxidized zirconium in the corium is oxidized, releasing large amounts of energy. If sufficient quantities of unreacted zirconium and steam are available, the drywell temperature may increase quickly to values significantly above the design temperature.

The comparison calculations are to be performed for a Mark I plant and the standard problem conditions are listed in Table 5.4. The output of interest here is the pressure and temperature (assuming both are spatially uniform) history of the drywell atmosphere as a function of time after vessel failure.

It is apparent that the details of this standard problem provide information on the condition of the corium leaving the reactor vessel, but do not provide a specific description of how the corium disperses on the drywell floor. This is done to allow the analysts to use (and document) their best judgment on how this dispersal will occur.

The TQUV sequence is concerned with failure to provide any ECCS makeup following an initiating event. A loss of all feedwater has been chosen to illustrate the event sequence. Upon a loss of feedwater, vessel water level starts to decrease because of a mismatch between the coolant inventory loss in the form of steam and the supply of feedwater. As the vessel water level decreases to Level 4, the reactor is scrammed and runback of the recirculation pump is initiated. At this point, the control rods are automatically inserted into the core, terminating full-power operation.

Because there is no ECCS makeup flow, the vessel water level continues to decrease due to boil-off from stored heat and fission product decay. At the Level 2 setpoint, the recirculation pumps are tripped and the MSIVs start to close. This isolates the reactor from the power conversion system. Soon afterwards, the vessel pressure reaches the SRV setpoints and excess vessel pressure is relieved by SRV steam discharges into the suppression pool.

Based on MARCH 1.1B calculations, with no HPCI, RCIC, LPCI mode of RHR, or core spray, the core would uncover at about 33 minutes and core melt would start at about 70 minutes. The core melt/slump vessel failure sequence is highly uncertain and very sensitive to modeling assumptions. Without Control Rod Drive (CRD) flow, MARCH predicts that the core will melt, slump, and fail the vessel head within about two hours with as much as 1700 pounds of hydrogen being generated. It should be noted that, with CRD flows, substantially more H<sub>2</sub> is predicted to be generated but core damage is delayed for three or more hours and for most sequences core melt is prevented. While the TQUV sequence with CRD flow may be at least as likely as one without CRD flow, the net effect of delaying or preventing core melt makes it less interesting as a containment loading problem and it has not been examined as part of the standard problem.

After the core melts and slumps, MARCH predicts the vessel will be breached within about 30 minutes. There is a large uncertainty as to the condition and location of the core debris after vessel failure but for the purposes of the standard problem, it is assumed that a large fraction of the fuel (80%) along with all the zirconium and most of the lower head (140,000 lbs) is uniformly distributed on the drywell floor. Sensitivity studies are then used to investigate key parameters.

### 5.3 Discussion of Major Phenomenology

The standard problem addresses the issue of drywell temperature loadings during ex-vessel interactions of the corium with concrete. The concern is that the integrity of the drywell would be compromised by high temperatures and/or high pressures shortly after vessel failure. Previous results by Yue and Cole indicate that for a TQUV sequence the containment would fail almost immediately after vessel failure due to drywell containment temperatures in excess of 1300°F. A loss of drywell integrity in Mark I BWR containment designs is potentially important because radionuclide releases would occur directly into secondary buildings bypassing the suppression pool and potential pool scrubbing.

The approach taken has been to define a set of physically consistent initial conditions appropriate to the base case under consideration and for the Mark I containment type. This was done by reference to appropriate experimental evidence and by use of simple hand calculations. Table 5.4 defines the initial masses, composition and temperature of the corium. It was left up to the individual analyst to define the dispersal and final deposition of the corium. These initial conditions were then used to calculate the subsequent corium-concrete interactions.

Spreading of the corium melt specified within the Mark I pedestal area would produce a collapsed pool 85 cm deep. With gas fluidization (bubbling) from corium-concrete interactions (CCI), the pool depth will be even greater. It is clear that such a deep pool will remain molten and rapidly spread through the two pedestal access doors into the ex-pedestal (annular) space. An even spreading over the whole available area would produce a pool 22 cm deep (collapsed level). This is still a rather deep layer but based on the scoping estimates of heat losses for the Mark I design, it appears that spreading over the entire drywell floor area is unlikely. Based on these heat loss estimates, the maximum spreading case has been taken to be 5 meters in radius for standard problem purposes. This represents about 50% of the drywell floor. The calculations neglect the effect of the transient spreading of the corium.

There are two major variations of the TQUV base case: a high temperature case (at the fuel melting point) and a low temperature case (at the melting point of steel). It is mechanistically assumed that for the low temperature case, the core debris could not flow and would remain confined within the pedestal wall. Conversely, the high temperature case is expected to spread rapidly into the annular space surrounding the pedestal. These two cases produce dramatically different results but most of this difference is due to the debris temperature difference and not to geometric differences.

In the Mark I containment, there are a number of sumps in the drywell floor (two-1 m deep sumps are immediately under the vessel inside the pedestal wall). The corium would therefore be rather deep above these sumps and the temperature of a deep corium pool will respond differently than a shallow pool during core/concrete interactions. The calculations for the shallow pool configuration are unlikely to be representative of the thermal response of the corium in the sumps. Additional calculations were therefore performed for a deep pool assuming all of the corium to be retained inside the pedestal wall. These are limiting calculations as the pool depth is overestimated. The corium stays hot much longer in the deep pool configuration but after 5 hours the total quantities of gases released are nearly the same as when the corium is spread across the entire floor area (shallow pool configuration).

#### 5.4 Methods of Analysis

The CLWG Standard Problem specification for the Mark I BWR is dominated by the calculation of the interaction of molten core debris and the concrete drywell floor. Several models currently exist and are in widespread use with which to make this calculation. Among these models are the INTER model (Ref. 10), CORCON-MOD 1 (Ref. 12), and CORCON-MOD 2 (Ref. 3) computer codes. For the present calculations, the BCL staff made use of the INTER model which is incorporated in MARCH 2. The BNL staff used the CORCON-MOD-1 code in a stand alone configuration and input the results manually to the MACE subroutine in MARCH 1.1B while the Sandia staff used an integrated code called MARCON, which consists of MARCH 2 and a pre-released version of CORCON-MOD 2. A description and comparison of these core-concrete interaction models follows.

#### 5.4.1 CORCON-MOD 1

CORCON-MOD 1 is a general model describing the thermal and chemical interactions between molten core debris and structural concrete. The major components of the system are the concrete cavity, the molten debris pool, and the gas atmosphere and surroundings above the pool. The geometry of the system is formulated as a two-dimensional, axisymmetrical system, although specific geometries not available as code-supplied options may be user-input.

The code offers three default concrete compositions or the user may input any specific concrete composition. The core debris is assumed to be molten and consist of metallic and oxidic phases, primarily  $UO_2$ ,  $FeO$ ,  $ZrO_2$ , steel, and Zr. The metallic and oxidic phases are assumed to separate into unmixed overlying layers. Mixture layers and an overlying water layer are not available in CORCON-MOD 1.

A gas atmosphere exists above the pool as well as structural surroundings, with which mass and energy exchange with the molten pool may occur.

Thermodynamic and transport properties as well as phase transition criteria for the molten debris pool are internally calculated at each time step. Mass and energy transfer between the various layers of core debris, as well as between the debris and the surroundings, occur instantaneously and are assumed to be in equilibrium. Models are included for heat transfer across the melt-concrete interface, between pool layers, and from the pool to the atmosphere and surroundings. The interaction between the pool and concrete is driven by the local temperature difference between the two and varies around the periphery of the pool. The pool-concrete interface is treated as an incompressible gas film composed of concrete decomposition gases. Heat transfer across this film is calculated by appropriate convective heat transfer models.

The erosion of concrete is modeled as one-dimensional, steady-state ablation. As the concrete is heated it decomposes, releasing  $H_2O$  and  $CO_2$  into the pool or gas film and molten concrete slag into the pool. The molten oxide slag is transported to the oxide layer, diluting the layer density and eventually resulting in an inversion of the oxide and metallic pool layers.

The concrete decomposition gases that bubble through the pool,  $H_2O$  and  $CO_2$ , oxidize the metallic layer, resulting in the release of chemical energy and production of  $H_2$  and  $CO$ .

Convective heat transfer within the pool is enhanced by the bubbling of concrete decomposition gases. Internal heat transfer is modeled by either gas injection across liquid-liquid interfaces or gas agitation along liquid-liquid interfaces. Energy sources in the pool consist of chemical reactions or decay heat generation.

For the calculations performed at BNL, it was intended to maximize the thermal attack on the concrete by eliminating convective and radiative energy transfer from the pool surface to the containment atmosphere and structural surroundings. This was accomplished by setting the pool surface-to-atmosphere convective heat transfer coefficient to zero and the emissivity of the drywell structures to a very small value. The results of the CORCON-MOD 1 calculations are in the form of core debris temperature and integrated gas release and are shown for the parametric sensitivity cases studies in Figures 5.2-5.7. The summary of the parametric variation for each case are listed in Table 5.5.

#### 5.4.2 CORCON-MOD 2

The CORCON-MOD 2 computer code was used by the Sandia staff for their CLWG calculations. The CORCON code was integrated into MARCH 2, replacing INTER, and is called MARCON. CORCON-MOD 2 is the second generation core-concrete interactions code in the CORCON series, which has several changes and additional models not present in CORCON-MOD 1. Among these are the addition of debris crusting and freezing and coolant layer boiling models not present in MOD 1. In addition, the heat transfer and viscosity models in the code were improved. Chemical reactions have been added to the gas films and the atmospheric heat transfer coefficient has been replaced by an experimentally verified relationship.

In addition, MARCON models surface radiative heat transfer from the core debris surface to a "well-mixed" reactor cavity aerosol atmosphere and radiation from the atmosphere to unlined structural concrete, which is allowed to outgas. In the BNL calculations, thermal radiation from the surface of the debris was intentionally suppressed to maximize the concrete ablation attack rate. This difference in system modeling represents the single greatest difference between the Sandia and BNL calculations; the remainder of the differences stem from differences in modeling between CORCON-MOD 1 and -MOD 2, principally the gas film chemical reactions and crusting model.

A comparison of the integrated gas generation rates and concrete erosion rates calculated by both CORCON-MOD 1 (BNL) and MARCON (Sandia) for the high debris temperature, limestone concrete case (TQUV-1) is presented in Table 5.6. The results presented are cumulative values after three hours of calculated core-concrete interaction.

It is clear in Table 5.6 that CORCON-MOD 1 calculates approximately 30% more concrete erosion and thus 30% more concrete decomposition gases for this case than MARCON. This is a direct result of the surface heat flux boundary condition imposed by the two calculations. The BNL calculation imposed a zero heat flux condition at the debris-containment atmosphere interface with the intention to maximize the rate of attack on the concrete and the generation rate of concrete decomposition gases. The Sandia calculation allowed direct radiative heating of the containment atmosphere from the molten debris surface, resulting in lower rate of attack on concrete but more severe containment response due to the direct heat flux to the drywell atmosphere. The other significant difference between the two calculational procedures is the nearly total chemical reduction of  $H_2O$  and  $CO_2$  to  $H_2$  and  $CO$  in the MARCON calculation. The reason for this is that CORCON-MOD 2 in MARCON accounts for metal/gas chemical reactions in the gas film as well as in the molten debris pool, resulting in almost total reaction; CORCON-MOD 1 allows metal/gas reactions in the molten debris pool only.

#### 5.4.3 INTER

The third core-concrete interaction model used in these standard problem calculations (BWR MARK 1: TQUV) was the INTER model as coded in MARCH 2. The INTER code was originally written by Sandia laboratories, not as a predictive code for analyzing core-concrete interactions, but more as a tool useful to perform parametric sensitivity studies of various core-melt accidents to explore the impact of varying such parameters as concrete type and core debris temperature.

Nevertheless, since no other model of core-concrete interactions was available, the INTER model was integrated into the MARCH 1.0 system in essentially the identical form as originally written. It has since, with minor modifications, been integrated into MARCH 2 as well. A complete description of INTER is available in Ref. 10 with supplemental descriptions of its use in MARCH available in Ref. 2 and 8.

Modifications made to the version of INTER coded in the MARCH 2 code include an internal calculation of fission product decay heat, radiation heat transfer from the top of the debris, boiling of a water coolant layer, addition of a concrete heat sink above the debris, and treatment of a solidified debris layer. Prior to the start of the standard problem calculations, a comparison was made between INTER and CORCON to identify differences between the two codes and errors in the modeling of dominant process in core-concrete interactions. A number of differences/errors were discovered during this comparison and they include:

The drywell temperature will reach a peak of 650 to 850°F within one hour after vessel failure. Then the temperatures will drop into the range of 500 to 700°F over the next several hours.

The pressure loading calculations for the base case are shown in Figure 5.9 and show a much wider range of behavior. Two limiting calculations have been chosen from each of the three lab's calculations to emphasize the extent of the uncertainty range. It should be emphasized that the base case is itself a limiting case (maximum Zr oxidation, maximum debris temperature and maximum debris spreading) so that none of the calculations represent a best-estimate of containment response for the TQUV sequence. Rather, the calculations show the effect of various modeling approximations for a hypothetical severe accident sequence. The differences between the six various cases and summarized in Table 5.8. Note that curve 2 from BNL and curve 3 from SNL utilize essentially the same modeling assumptions but show significantly different results (approaching a difference of 50 psi at the end of the calculation). This difference has two contributions which may be indicative of the limits of the "state-of-the-art" in containment modeling. The first contribution of about 20 psi occurs immediately after vessel failure. For as yet unidentified reasons, the SNL MARCON calculations show a higher pressure spike after vessel failure, which comes to an equilibrium about 20 psi higher than either BNL or BCL calculates. This 20 psi difference is maintained for about one hour when MARCON calculates a layer flip of the debris and begins to generate considerably more non-condensable gases. This change in gas generation rate accounts for an additional 30 psi difference which is maintained through-out the remainder of the transient. The BCL calculations (5 and 6) with substantially different modeling generally tend to confirm the broad range of expected behavior. Without the highly energetic FeO/Zr reaction (Case 5) the BCL calculations agree reasonably well with the BNL Case 2 and predicts containment over pressure failure about 2 hours after vessel failure. With the FeO/Zr reaction (Case 6), the BCL calculations show a much more rapid rise in pressure and containment over pressure failure is predicted within one hour.

It should be noted that BCL assumed containment failure at 132 psi while BNL and SNL continued the calculations beyond this point for purposes of comparison. Thus the BCL comparisons (5 and 6) are terminated at the failure point. BNL's Case 1 is also terminated but for different reasons. After 2 hours, Case 1 calculations indicate that the debris drops below the "ablation point" and CORCON stops executing. The BNL calculations were not carried out past this point, but it is clear what would happen: with the debris frozen below the concrete ablation temperature, the debris would continue to radiate decay heat to the structures and the containment temperature would rise at a rate similar to the IDCOR calculation (Section 9) for the long-term blackout. For this frozen debris situation the resulting temperatures would eventually exceed 1000°F.

It is not at all clear which of the six models give a best-estimate of the containment loading for the base case calculation. But five of the six calculations indicate that pressure capability of the containment will be reached within 1 hour and (may be reached within 40 minutes) after vessel failure. Thus, for this extreme case (high temperature debris maximum H<sub>2</sub> generation and maximum debris dispersal), the thermal loading problem also becomes a pressure loading problem and it is a race between the two possible failure mechanisms.

As mentioned in the previous section, the base case should not be considered to be a best-estimate of the TQUV accident sequence. Rather it represents an extreme standard problem which provides the basis for comparisons between the various participants. Since there is considerable uncertainty in the accident conditions as well as design variations from plant to plant, the standard problem also addresses a series of sensitivity calculations as discussed in the following subsections. In order to emphasize the separate effect of each parameter variation, only one set of calculations are shown (those from BNL). Calculations from the other labs show similar separate effects but there is considerable variation in the absolute result.

#### 5.5.1 Debris Temperature

The rate of core/concrete interaction is very sensitive to the debris temperature at the time of vessel failure. The debris temperature calculated by MARCH is, in turn, sensitive to several input parameters including time-step size and clad oxidation, particularly during the core slump phase of the calculation. More detailed phenomenological modeling and experimental evidence must be developed in order to define a best-estimate debris temperature. The standard problem approach was to investigate the limit on debris temperature (the UO<sub>2</sub> melting temperature, 4130°F, and the stainless steel melting temperature, 2700°F). It is the consensus of the participants that neither of these limits can be precluded at this time. However, we believe that the best-estimate lies closer to the lower limit since the vessel would fail rapidly even for small amounts of molten material in the lower head. Note that the assumption of a large fraction of the core and lower vessel head forming a low temperature debris gives similar results to IDCOR's approach (Section 9) which allows an initially small fraction of the core to be released at high temperature and the remainder of the core to be released gradually.

The temperature and pressure loadings for the two limiting cases are shown in Figure 5.10 and Figure 5.11 for the drywell compartment. For the high temperature limiting case the compartment pressure is calculated to exceed the threshold pressure 2¼ hours after vessel failure. However the compartment temperature is well above the seal design temperature (280°F for



Brown's Ferry) during this period rising to a peak of 660°F within 2 hours. The combination of high temperatures and pressures is expected to cause degradation of drywell seals and allow gases and fission products to leak from the primary containment. This leakage may have a net positive effect in that even a small amount of leakage may limit the pressure rise and prevent catastrophic over-pressure failure.

### 5.5.2 Concrete Composition

The specific core/concrete reactions and the gases evolved from these reactions are very sensitive to the concrete composition. The sensitivity study (Table 5.5) specified two concrete compositions (representing limestone and basalt) plus two variations in the free water content. Figure 5.12 shows the predicted pressure response for the two nominal compositions with the high temperature limiting case. At these limiting temperatures the attack on basaltic concrete is predicted to generate considerably less non-condensable gas with the pressure estimated to be 35 psi less than the limestone case after 5 hours.

The early containment temperature response for basaltic concrete is sensitive to the free water content while there is only a slight effect on the limestone concrete as shown in Figure 5.13. The high water-content concrete is taken to be twice the nominal content but it is not clear whether such a high water content (6% and 8% for limestone and basalt, respectively) is physically possible.

### 5.5.3 Debris Dispersal

The Mark I lower pedestal region would tend to confine the initial debris dispersal to a 6m diameter area immediately beneath the reactor vessel. However, there are doorways in the pedestal which, for the high temperature case, would allow molten debris to flow outward into an angular region about 13m in diameter. It is assumed that the high temperature debris will spread out and attack the entire drywell floor area but the low temperature debris will remain confined to the pedestal region as previously noted. However, in order to assess the importance of the debris spreading assumption, a (non-mechanistic) high temperature confined (ignoring parths through the access doors) case was also run.

The pressure and temperature response for the high temperature spread and confined cases are shown in Figures 5.14 and 5.15. Note that the spread case initially has a much higher gas generation rate and results in a correspondingly more rapid pressure rise. However, for the confined case, the debris remains at a higher temperature and maintains a much more aggressive attack on the concrete. After about one hour the gas generation rate for the spread case is less than that for the confined case and the pressure rise rate has moderated until after 5 hours; the pressure for the confined case is nearly as high as the spread case.

#### 5.5.4 Upward Heat Transfer

Preliminary calculations with CORCON indicated that with a transparent atmosphere, the dispersed debris would rapidly lose heat to the cooler structures above and would cool below the concrete ablation temperature within about one hour after vessel failure. This case presents a problem for the CORCON-MOD 1 code in that there is no further core-concrete interactions and the code terminates the calculation. After the debris cools to the concrete ablation temperature, there will be very little non-condensable gas generation and the predominant energy exchange will be radiation to the structures and convection from the structures to the drywell atmosphere. This limiting case has not been analyzed past this point but it should be noted that this result is essentially in agreement with preliminary results from IDCOR for the TQUV sequence. As shown in IDCOR (9) under these conditions, the decay heat will be radiated to the drywell resulting in a gradual rise in the drywell temperature with little or no corresponding rise in pressure. Since the drywell wall is insulated, the temperatures will rise over a period of several hours until the containment fails by over-temperature.

However, there are several points that argue against the possibility of a frozen low temperature debris layer rapidly stopping core/concrete reactions:

- (a) There are a considerable number of structural barriers to preclude uniform spreading over the entire floor as well as to limit radiative view factors to upper structures. Thus, spreading over 50% of the drywell floor (5 m radius) has been taken as the limiting case with the highest non-condensable gas generation rate.
- (b) CORCON calculations indicate that the debris freezes rapidly and will have little opportunity to spread if it is released from the vessel in a confined configuration.
- (c) The large amount of aerosols generated from the core/concrete attack will limit radiation to structures and may provide a thermal blanketing effect.

With these several factors to consider, the BNL approach has been to make assumptions which tend to maximize the rate of non-condensable gas generation in an effort to investigate the limiting pressure loading on the containment. Thus, along with the limiting core debris temperature, 2277C (4130°F) specified in the standard problem, the BNL approach assumes a uniform spreading of the debris across the entire drywell floor and a thermal blanketing effect from the aerosols. "Direct heating" of the containment atmosphere may provide still higher pressure loading if a significant fraction of the sensible heat and chemical energy in the debris is transferred directly to the atmosphere during debris dispersal. Due to the structural confinement in the pedestal region, this is believed to be a low likelihood scenario for BWRs.

### 5.5.6 Heat Losses

There are three sources of energy in the containment after vessel failure: 1) chemical energy from the oxidation reactions, 2) sensible energy from the debris, and 3) decay heat from radionuclides. The first two are very sensitive to temperature and dominate the early containment response for the high temperature limiting case. As shown in Figure 5.16, the steel heat sinks (the steel shell and "miscellaneous steel") tend to ameliorate large spikes in temperatures, but they do very little to affect long-term behavior. However, for the maximum spread case, sufficient heat may be lost by concrete decomposition and thermal radiation to cool the debris down to the concrete ablation temperature. At this point upward radiation may be sufficient to remove the decay heat and prevent further concrete decomposition. As mentioned in the previous section, freezing of the core debris is prevented from occurring via the thermal blanketing (emissivity = 0) assumption. This assumption forces concrete decomposition to continue indefinitely, so the containment will continue to pressurize due to the addition of non-condensable gases and energy from the decay heat and oxidation reactions.

### 5.6 Considerations of Loads and Likelihoods of Containment Failure\*

With its extensive pressure suppression capability the Mark I containment is not susceptible to steam spikes, even if contact with a significant quantity of water was to occur. Because of inerted operation hydrogen burns are also irrelevant. This standard problem, therefore, is focused on the consequences of corium-concrete interactions on the drywell floor. In addition to the pressurization resulting from the generation of non-condensibles one should be concerned about high drywell temperatures and concomitant penetration seal degradation. The Browns Ferry power plant was selected for the specifics. The drywell was considered completely free of water. Parametric ranges were defined on the quantity of the metallic component (e.g., unreacted zirconium) available for oxidation on the drywell floor (by the steam released from the concrete), and the extent of the melt spreading outside the pedestal area.

The results indicate that because of the relatively small gas volume in comparison to all other containments non-condensable pressures build rapidly. They reach the estimated 9 bar (132 psia) ultimate capability of the containment within 40 minutes to 2 hours from the start of core concrete interaction. However, based on results from the CPWG studies it appears that significant leaks could develop over the 82 to 117 psia pressure range such that catastrophic failure might be prevented.

\* Considerations of the likelihood of containment failure from the various load sources described in this report have been provided by the NRR staff and is based on extended discussions with staff consultants and staff members involved in containment loads and performance activities.

In competition with the above overpressure failure mechanism is that due to thermal loadings on the drywell boundaries (particularly at penetration seals). The drywell atmosphere was calculated to heat briefly up to the range of 650° to 850°F and settle down in the range of 500° to 700°F for the most part. The integrity of the seals would be uncertain under such thermal loading conditions. It would take temperatures significantly above 1000°F to challenge the integrity of the drywell liner. However, the possibility of early melt-through of the drywell liner, by direct contact with the melt, in the neighborhood of the floor-drywell wall junction has been suggested.

The CLWG results, therefore, lead one to conclude that Mark I failure within the first few hours following core melt would appear rather likely.

## 5.7 Conclusions and Recommendations

For a wide range of possible containment conditions following vessel failure, the TQUV accident poses severe loads which threaten the structural integrity of the containment. For the limiting high temperature case, the diverse methods of analysis give a fairly consistent result for the thermal loading (a peak atmospheric temperature of 560°F to 850°F in the drywell and then dropping to 500°F to 700°F as the debris cools). The pressure loading results are less consistent but all three calculations indicate that the ultimate pressure capability of the containment (132 psia) will be reached from 40 minutes to two hours after vessel failure for the limiting high temperature case. For lower temperature debris the pressure/temperature buildup in the drywell is much slower than for the high temperature case but the containment would eventually be threatened by a combination of temperature and pressure loading.

Table 5.1 BWR4 Reactor Vessel and Core Parameters

Number of assemblies	764
Fuel rods per assembly	62
Water rods per assembly	2
Fuel rod diameter (inch)	0.483
Fuel pellet diameter (inch)	0.410
Water rod diameter (inch)	0.591
Core equivalent diameter (inch)	187.1
Core hydraulic diameter (ft)	0.0459
Length of active fuel [including 6 inches of natural uranium at top and bottom of fuel column] (inch)	150
Core flow area (ft <sup>2</sup> )	108.7
Reactor vessel internal diameter (inch)	251
Mass of UO <sub>2</sub> (lb)	351,440
Mass of Zr in cladding (lb)	95,536
Cladding thickness (inch)	0.032
Mass of Zr in channel boxes (lb)	48,846
Channel box wall thickness	0.080
Number of control rods	185
Mass of stainless steel and inconel in core (lb)	26,980
Mass of stainless steel structures beneath core (lb)	66,750
Mass of stainless steel in control rods (lb)	32,750
Mass of stainless steel in top guide assembly (lb)	15,200
Volume of liquid in reactor vessel (ft <sup>3</sup> )	11,922
Volume of steam in reactor vessel (ft <sup>3</sup> )	10,122
Volume of liquid in recirculation loops (ft <sup>3</sup> )	1,320
Volume of steam in steam lines (ft <sup>3</sup> )	1,218
Volume of liquid in feedwater line (ft <sup>3</sup> )	1,233
Total reactor coolant volume (ft <sup>3</sup> )	25,815
Weight of reactor vessel bottom head (lb)	207,500
Diameter of bottom head (ft)	20.915
Thickness of bottom head (ft)	0.713
Safety/relief valve rated capacity (lb/hr) at 1143 psia and fluid density of 2.608 lb/ft <sup>3</sup>	838,900
Safety/relief valve setpoint (psia)	1,120
Safety/relief valve blowdown per actuation (psi)	50

Table 5.2 Containment Design Parameters

Drywell design pressure (psia)	70.7
Drywell design temperature (°F)	281
Drywell volume (ft <sup>3</sup> )	70.7
Wetwell design pressure (psia)	281
Wetwell pool volume (ft <sup>3</sup> )	138,700
Wetwell free volume (ft <sup>3</sup> )	119,000
Predicted failure pressure (psia)*	132
Predicted failure location*	Intersection of spherical and cylindrical sections of drywell
Initial drywell temperature (°F)	135
Initial drywell pressure (psia)	15.3
Initial wetwell temperature (°F)	104
Initial wetwell pressure (psia)	14.7

\*L.G. Greiman, et al., "Reliability Analysis of Steel Containment Strength," NUREG/CR-2442, June 1982.

Table 5.3 Containment Heat Sinks

Heat Sink	Material	Area (ft <sup>2</sup> )	Thickness (ft)	Left Side	Right Side
Drywell Liner	Steel	18684	0.094	Drywell	Insulated*
Drywell Floor	Concrete	1640	4.73	Drywell	Insulated
Upper Reactor Pedestal	Concrete	4130	2.29	Drywell	Drywell
Lower Reactor Pedestal	Concrete	1814	3.5	Drywell	Drywell
Wetwell Liner (above pool)	Steel	17050	0.0625	Wetwell	Insulated
Drywell Misc. Steel	C Steel	41525	.0417	Drywell	Drywell
Wetwell Misc. Steel	C Steel	2520	.0417	Wetwell	Wetwell

\*Drywell liner is separated from 3 ft of concrete by 2 1/4" polyester foam and 1/8" fiberglass laminate at 400°F; this will be compressed to 1"=.083 ft.

Table 5.4 Specifications for Comparison Calculations  
Base Case

Mass of corium exiting vessel (lb)	535,000
a. UO <sub>2</sub> (lb)	280,000
b. Steel (lb) (% oxidized)	140,000 15
c. Zirconium (lb) (% oxidized)	115,000 13
Temperature of corium exiting vessel. (°F)	4130
Concrete type (details in Table 2)	Limestone
Vessel, containment specifications	
RCS pressure at vessel failure (psia)	1120
H <sub>2</sub> released up to time of vessel failure (lb)	1170*
Hole size in vessel lower head (inches)	6
Containment conditions at vessel failure:	
a. Drywell temperature (°F)	150
b. Pool temperature (°F)	133
c. Pressure (psia)	35

\*The H<sub>2</sub> release directly correlated with the amount of zirconium and steel oxidized. They are displayed because of this correlation, and do not represent independent variations for these sensitivity studies.



Table 5.5 Summary of BWR Mark I Sensitivity Studies

Case Number	1	1a	2	3	3a	4
Corium Spread (m)	5		3	5		3
Debris Temperature (°F)	4130		2700	4130		2700
Concrete Type	L		L	B		B
Free H <sub>2</sub> O (%)	3	6	3	4	8	4
Steel in Corium (lb)	140K		140K	140K		140K

Table 5.6 Comparison of CORCON-1/MARCON Results: TQUV1  
(after 3 hours)

	CORCON-1 (BNL)	MARCON (Sandia)
Axial Erosion (m)	0.47	0.42
Radial Erosion (m)	0.49	0.38
CO (kg-moles)	707	724
CO <sub>2</sub> (kg-moles)	251	27
H <sub>2</sub> (kg-moles)	324	332
H <sub>2</sub> O (kg-moles)	116	13
Total Gas Generation (kg-moles)	1398	1096

Table 5.7 Comparison of CORCON-1/INTER Results: TQUV3

	CORCON-1 (BNL)	INTER (BCL)
Axial Erosion (m)	1.20	1.64
Radial Erosion (m)	0.61	0.60
CO (kg)	700	1000
CO <sub>2</sub> (kg)	250	300
H <sub>2</sub> (kg)	2000	2732
H <sub>2</sub> O (kg)	4500	8691
Containment Failure Time (min)	360	309
Temperature, Metal (K)	1530	1223
Temperature, Oxide (K)	1530	1707

Table 5.8 Summary of the Major Modeling Differences for Six TQUV High Temperature Debris Calculations

Curve Number	Calculator	Codes Used		Modeling Assumptions
		T/H	Core/Concrete	
1	BNL	MARCH 1.1B	CORCON 1	Upward radiation to structures. No degassing of pedestal concrete.
2	BNL	MARCH 1.1B	CORCON 1	No upward radiation. No degassing of pedestal concrete.
3	SNL	MARCH 2	CORCON 2	No upward radiation. No degassing of pedestal concrete.
4	SNL	MARCH 2	CORCON 2	Upward radiation to drywell atmosphere H <sub>2</sub> O degassing of pedestal concrete.
5	BCL	MARCH 2	INTER	Upward radiation to structures. No degassing of pedestal concrete. No FeO/Zr reaction.
6	BCL	MARCH 2	INTER	Upward radiation to structures. No degassing of pedestal concrete. Rapid FeO/Zr.

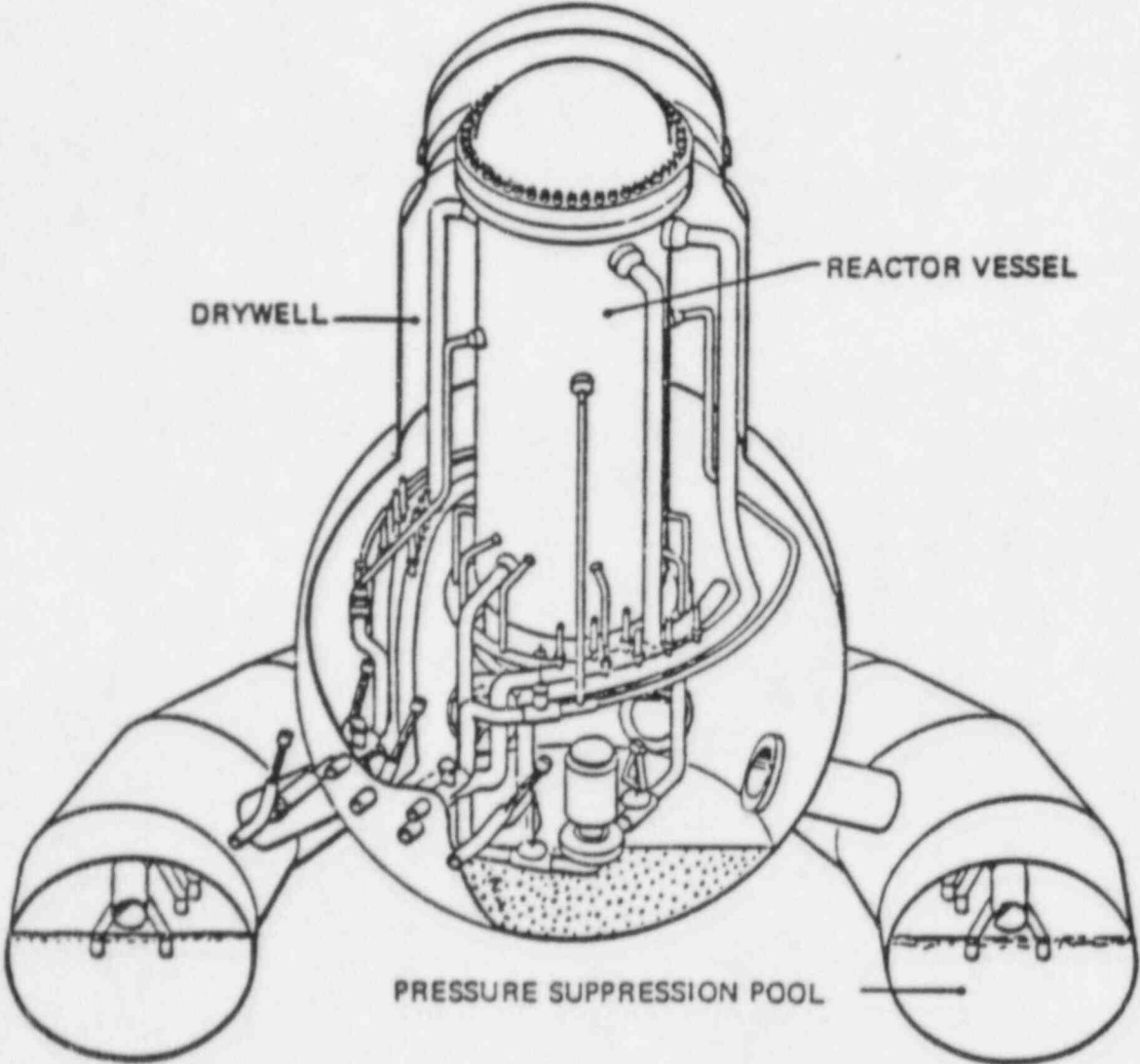
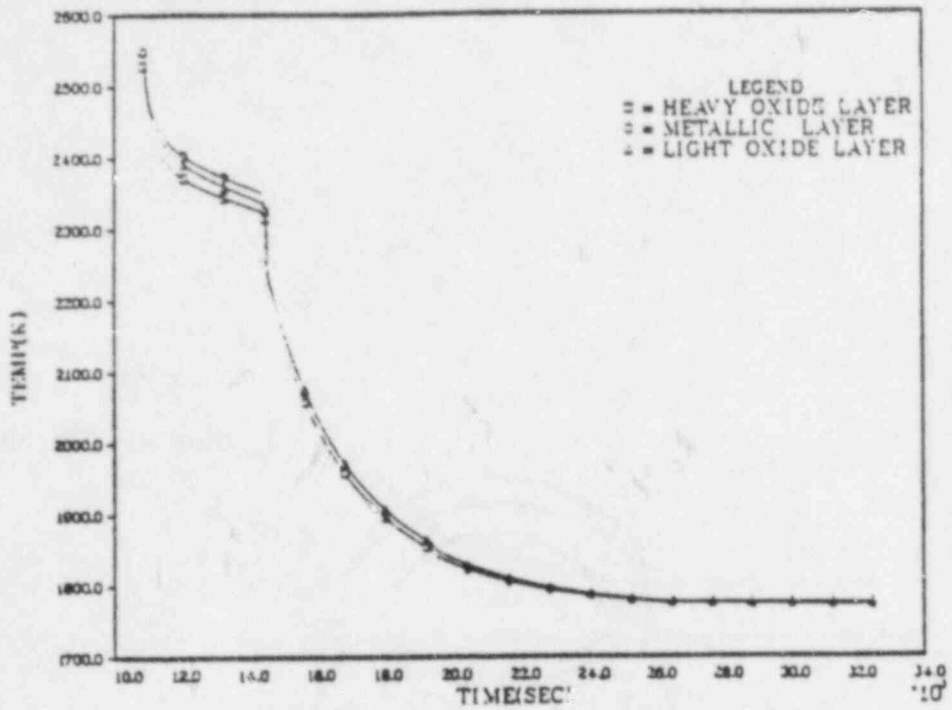


Figure 5.1 MARK I Containment

BWR STANDARD PROBLEM: TQV-1  
LAYER TEMPERATURES



BWR STANDARD PROBLEM: TQV-1  
GAS GENERATION

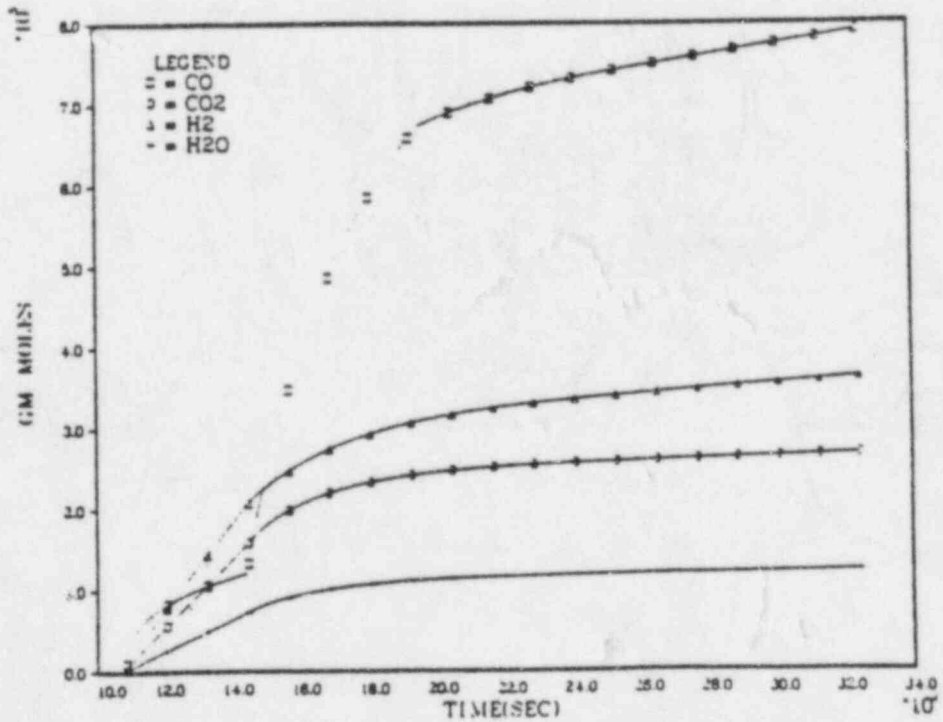
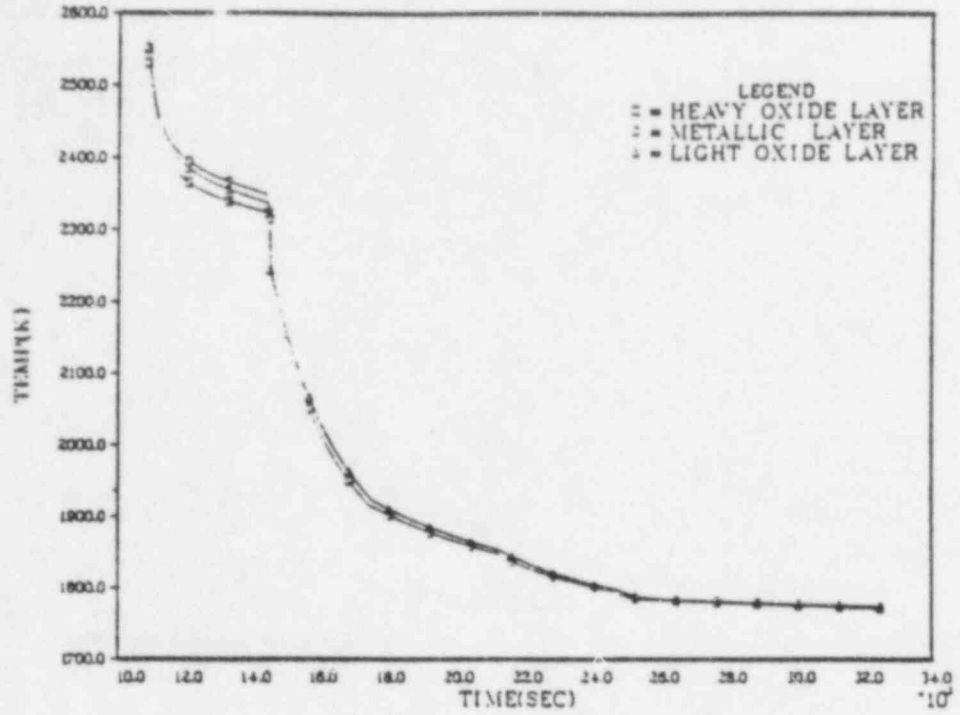


Figure 5.2  
5-24

BWR STANDARD PROBLEM: TQV-1A  
LAYER TEMPERATURES



BWR STANDARD PROBLEM: TQV-1A  
GAS GENERATION

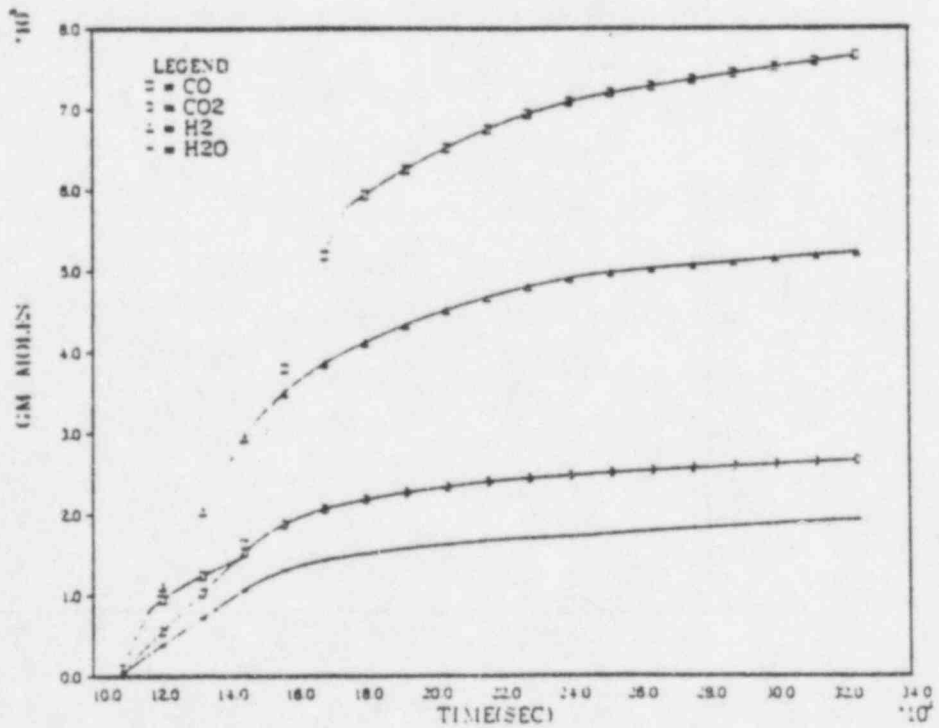
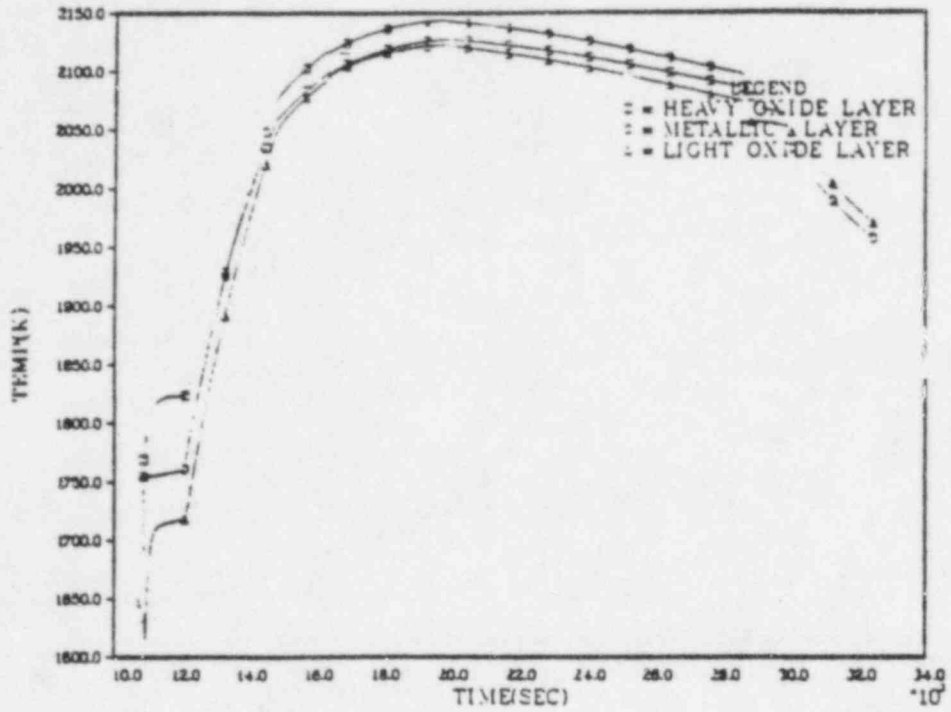


Figure 5.3

BWR STANDARD PROBLEM: TQUV-2  
LAYER TEMPERATURES



BWR STANDARD PROBLEM: TQUV-2  
GAS GENERATION

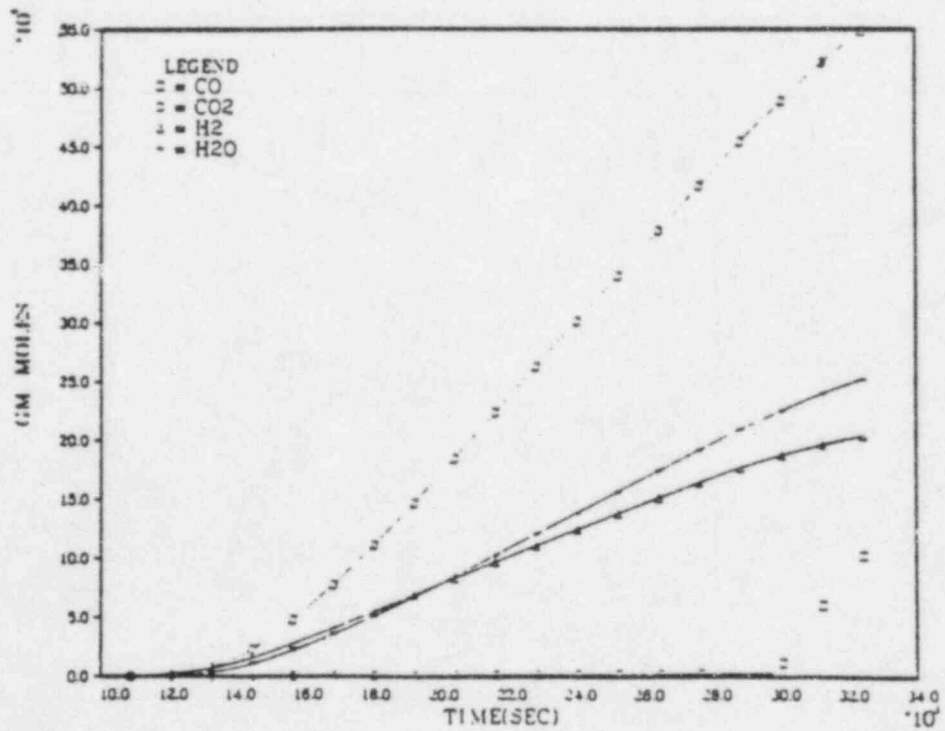
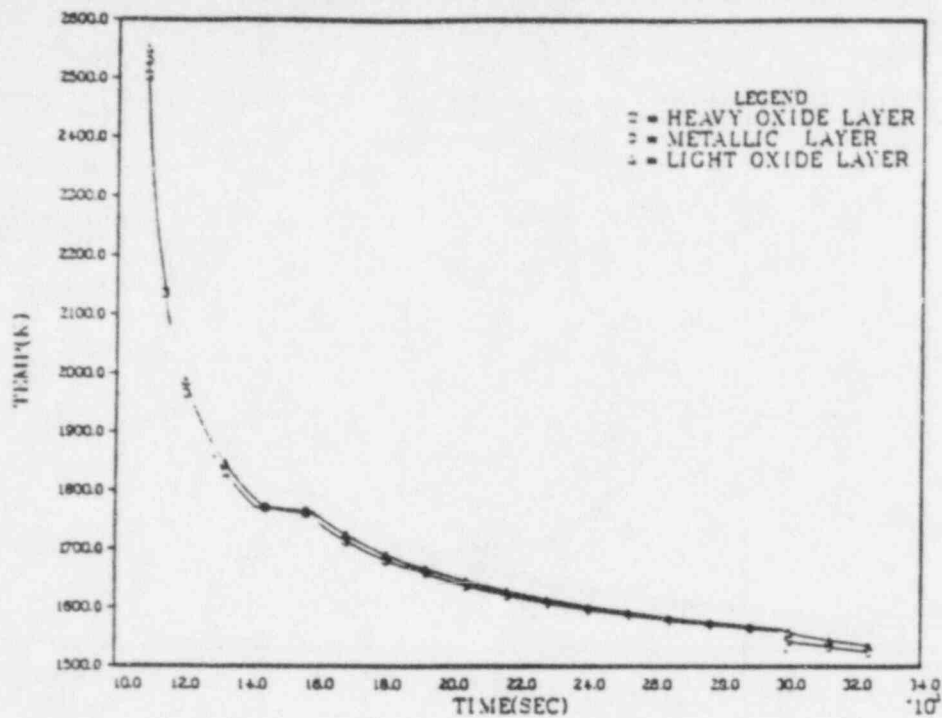


Figure 5.4



BWR STANDARD PROBLEM TQV-3  
LAYER TEMPERATURE



BWR STANDARD PROBLEM: TQV-3  
GAS GENERATION

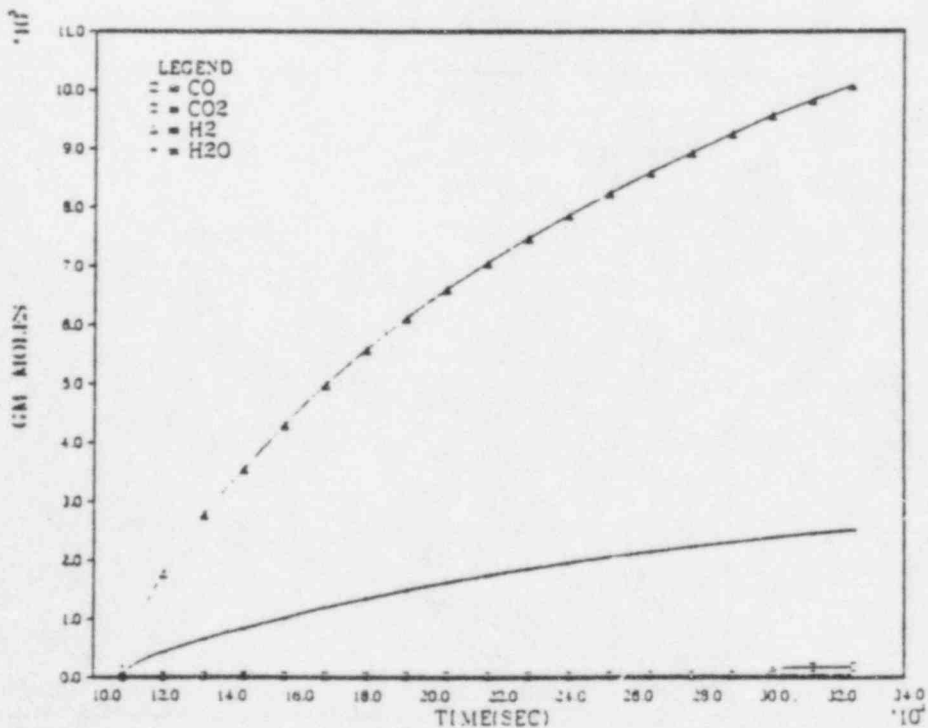
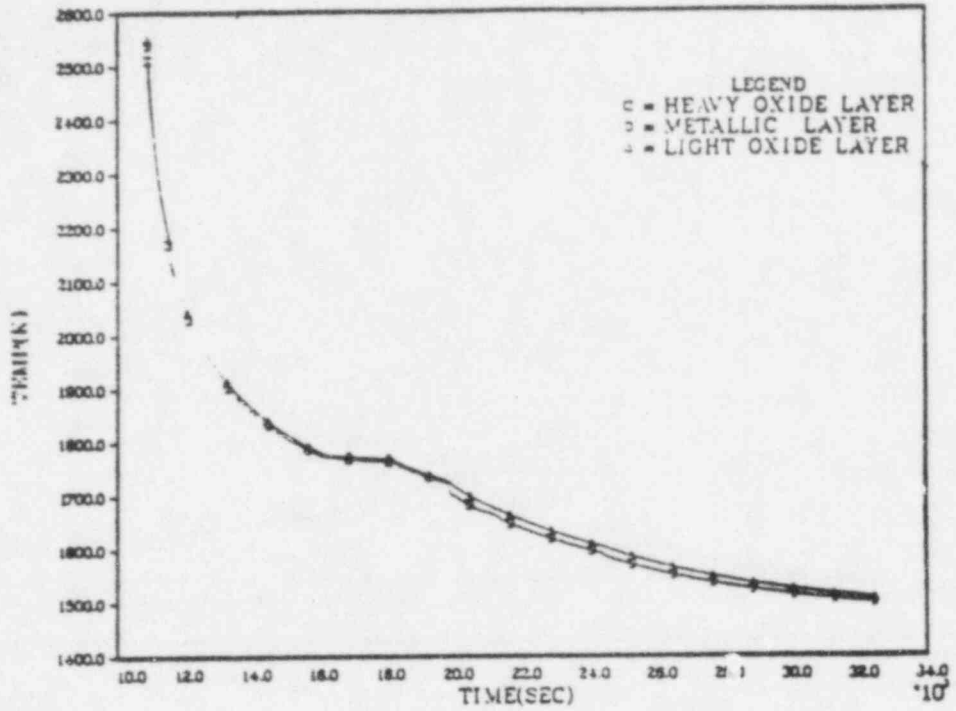


Figure 5.5

BWR STANDARD PROBLEM: TQV-3A  
LAYER TEMPERATURES



BWR STANDARD PROBLEM: TQV-3A  
GAS GENERATION

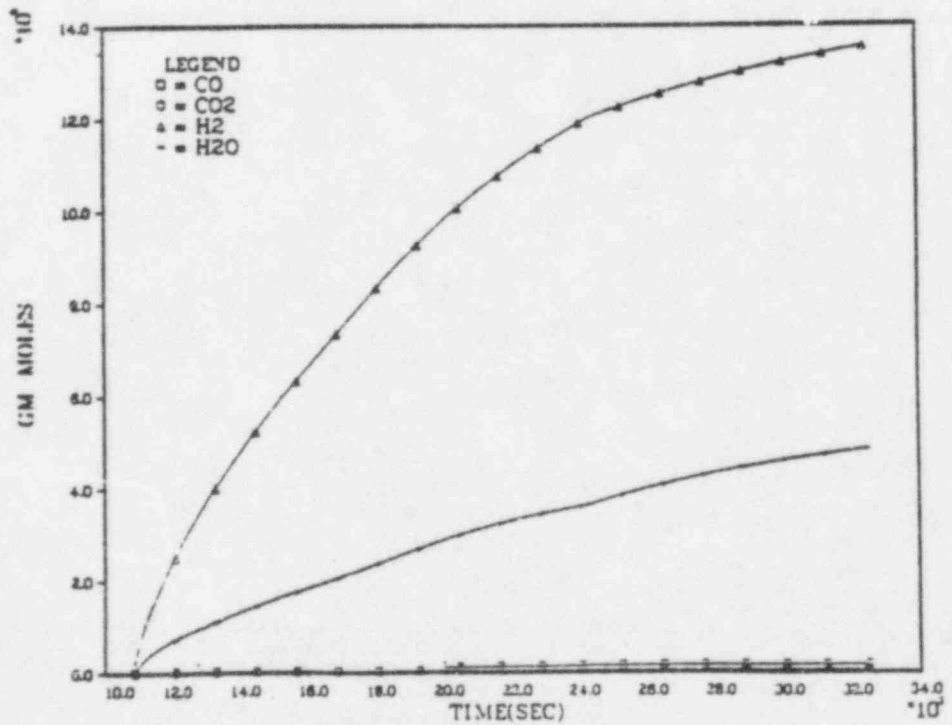
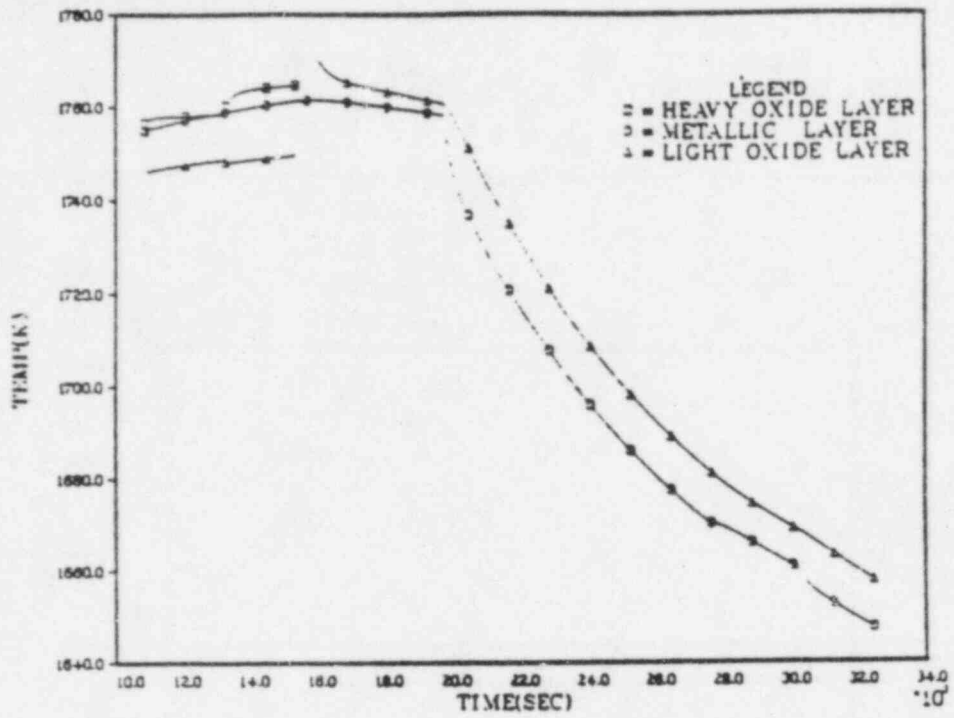


Figure 5.6

BWR STANDARD PROBLEM: TQV-4  
LAYER TEMPERATURES



BWR STANDARD PROBLEM: TQV-4  
GAS GENERATION

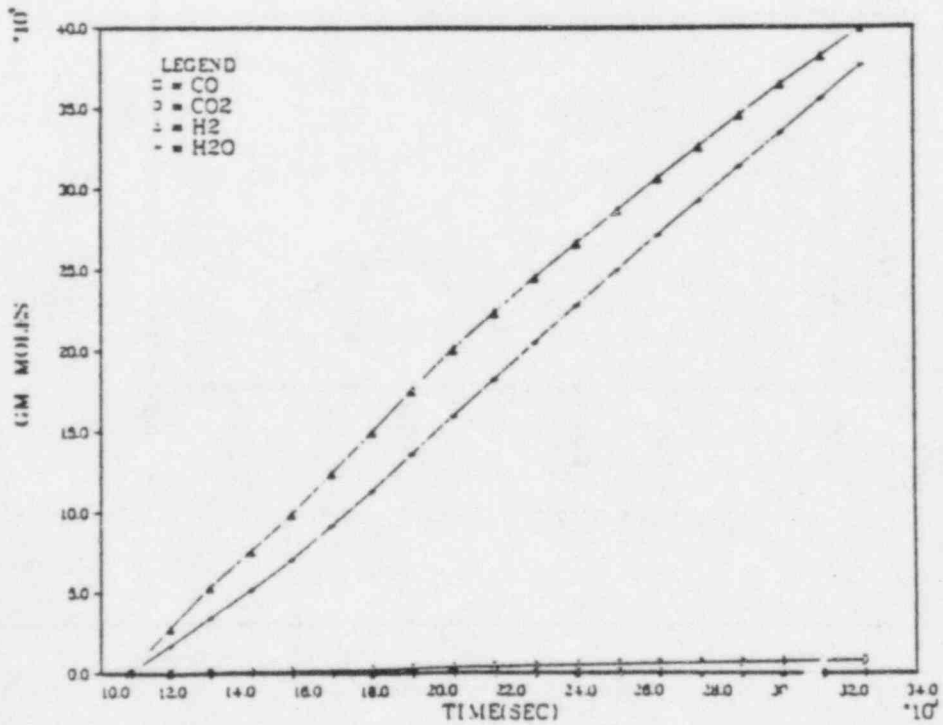


Figure 5.7

# BROWN'S FERRY TQUVCC01

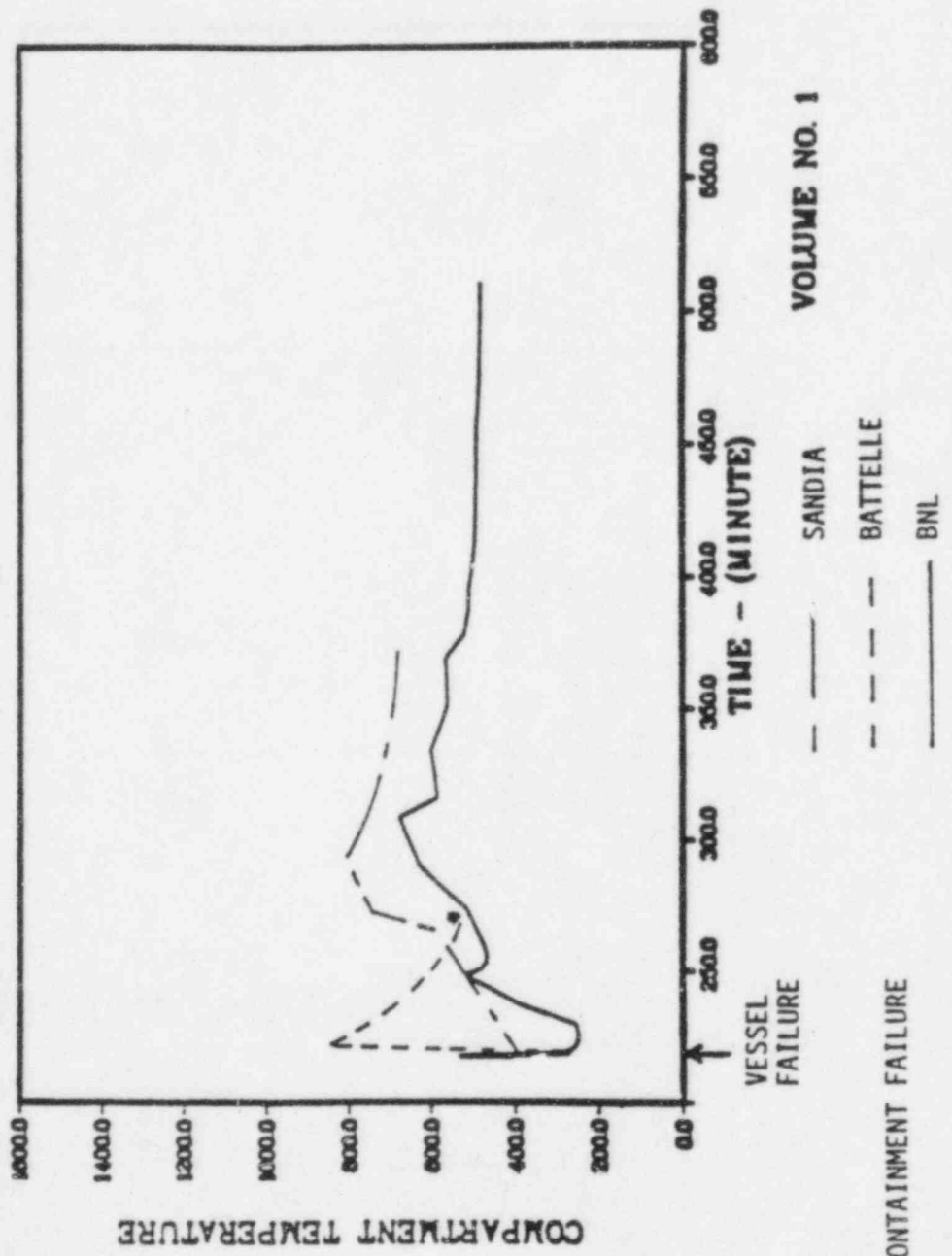


Figure 5.8 Brown's Ferry TQUVCC01

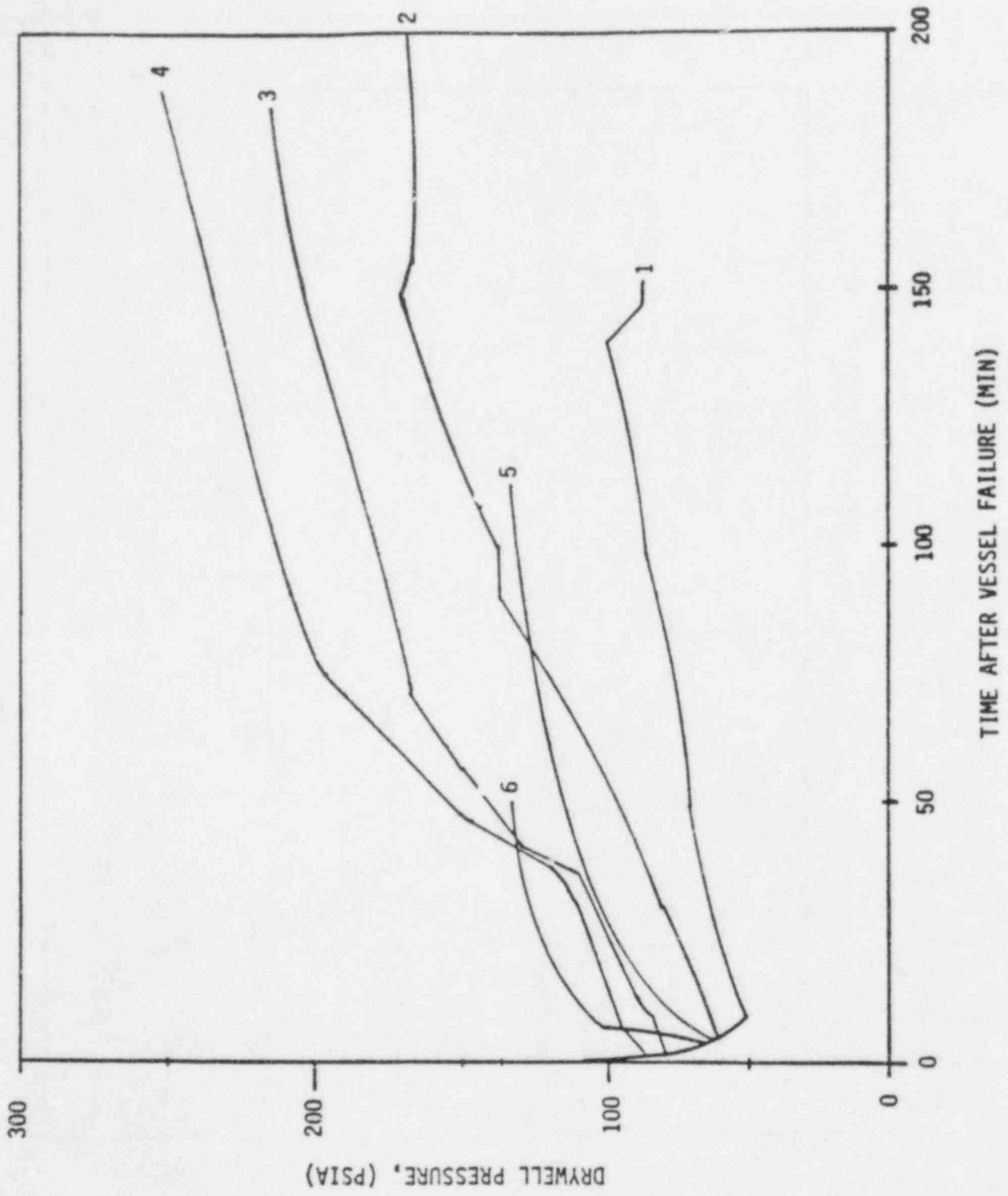


Figure 5.9 TQUVCC01: Pressure vs. Time

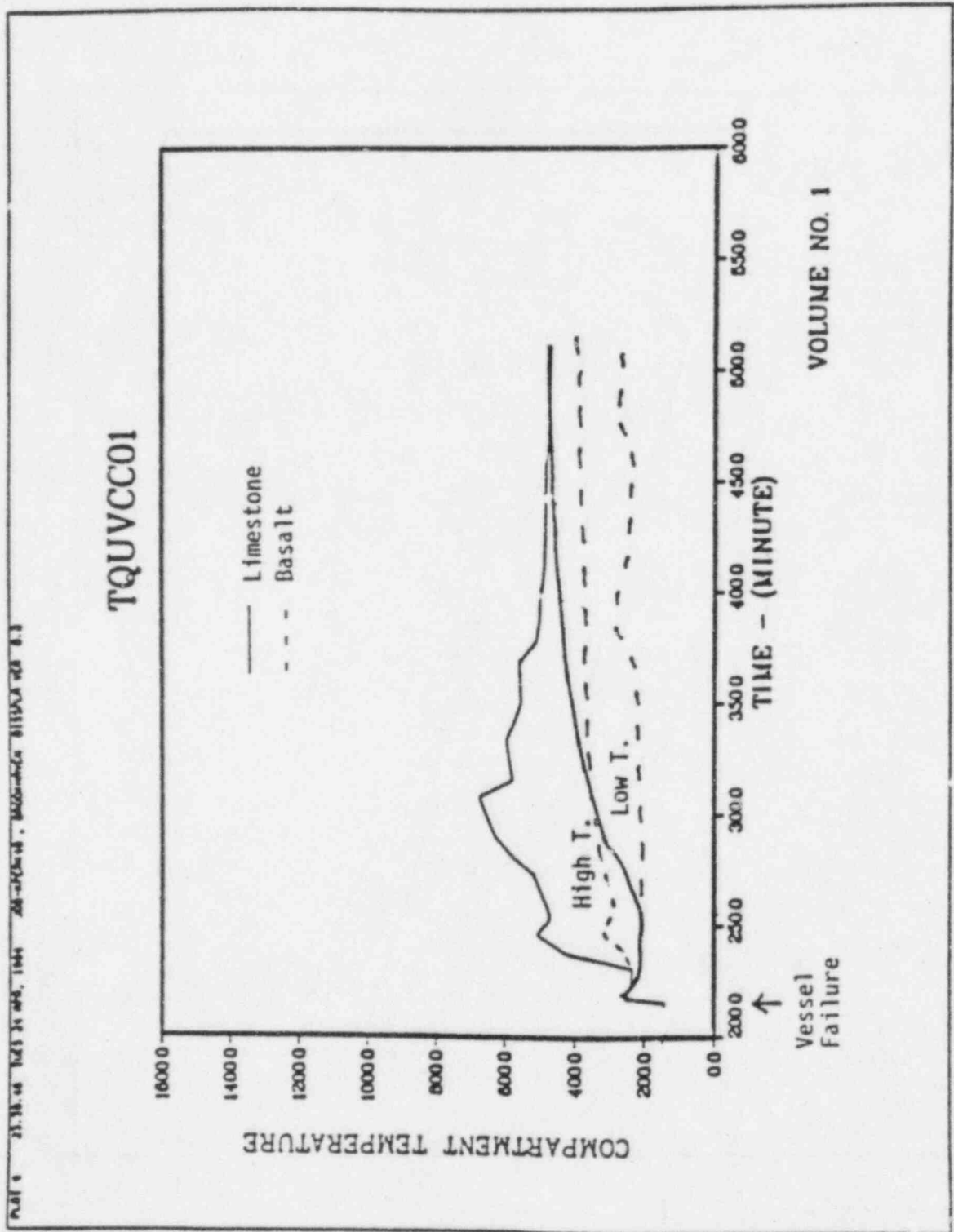


Figure 5.10 TQUVCC01: Compartment Pressure vs. Time

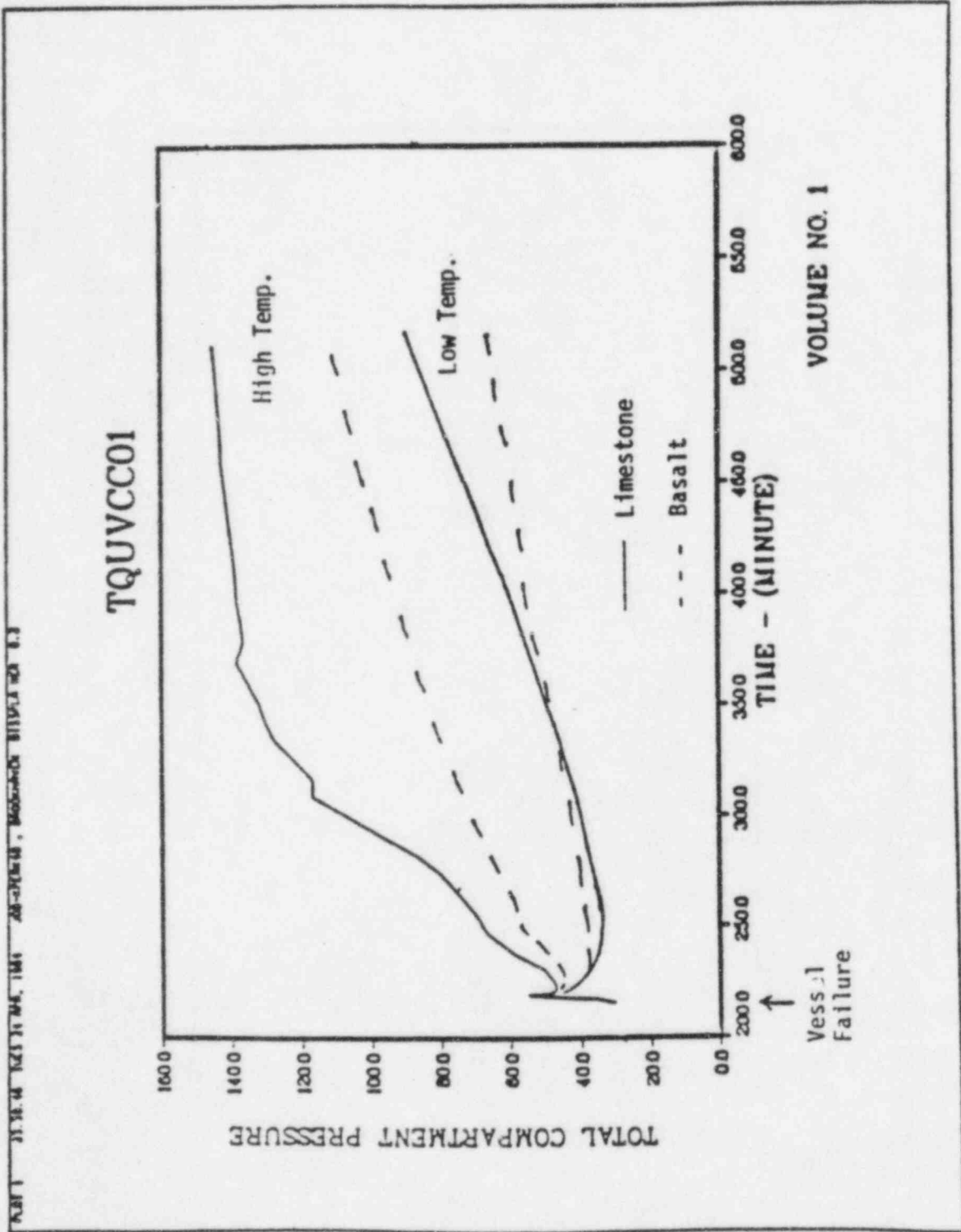


Figure 5.11 TQUVCC01: Compartment Temperature vs. Time

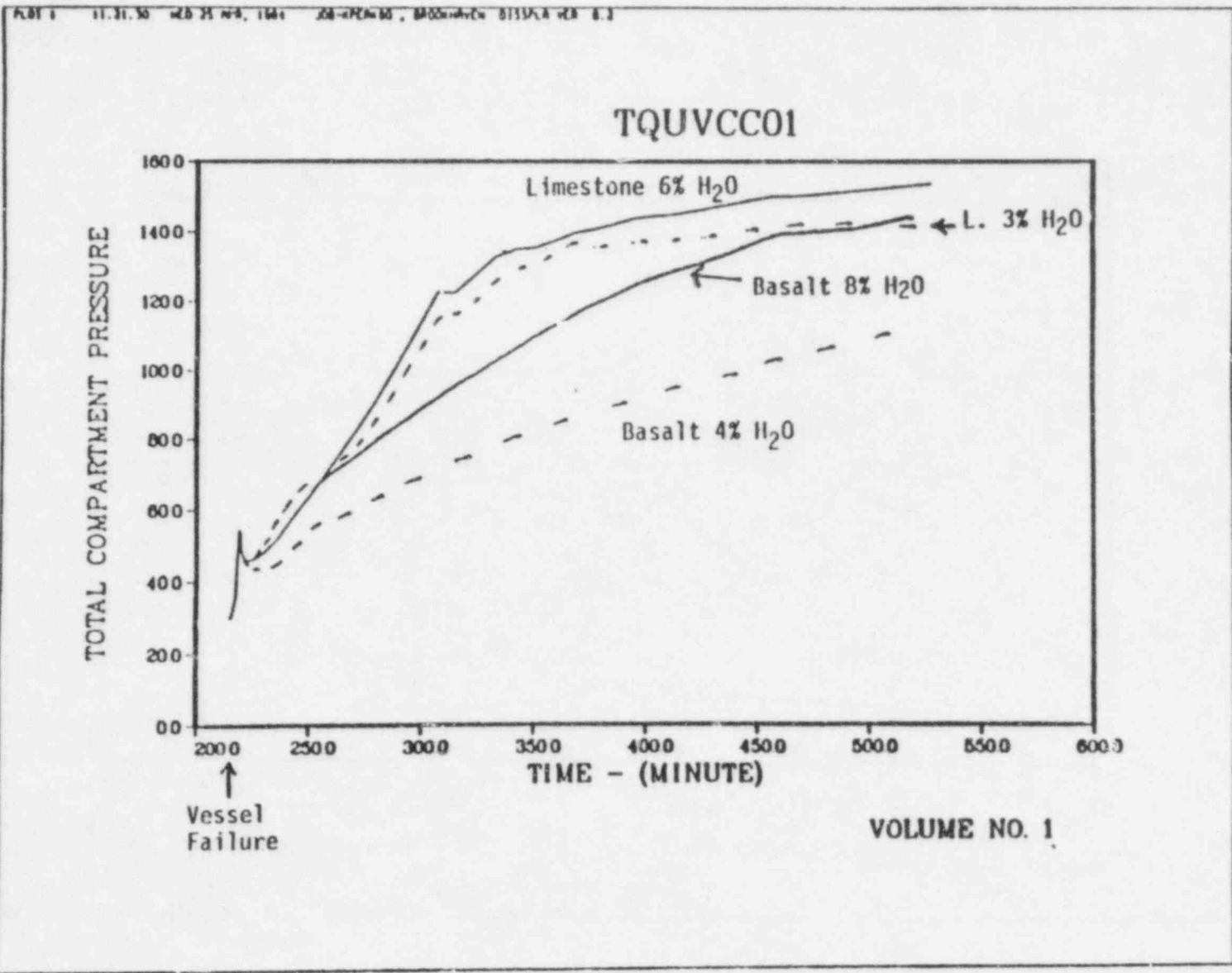


Figure 5.12 TQUVCC01: Compartment Pressure vs. Time



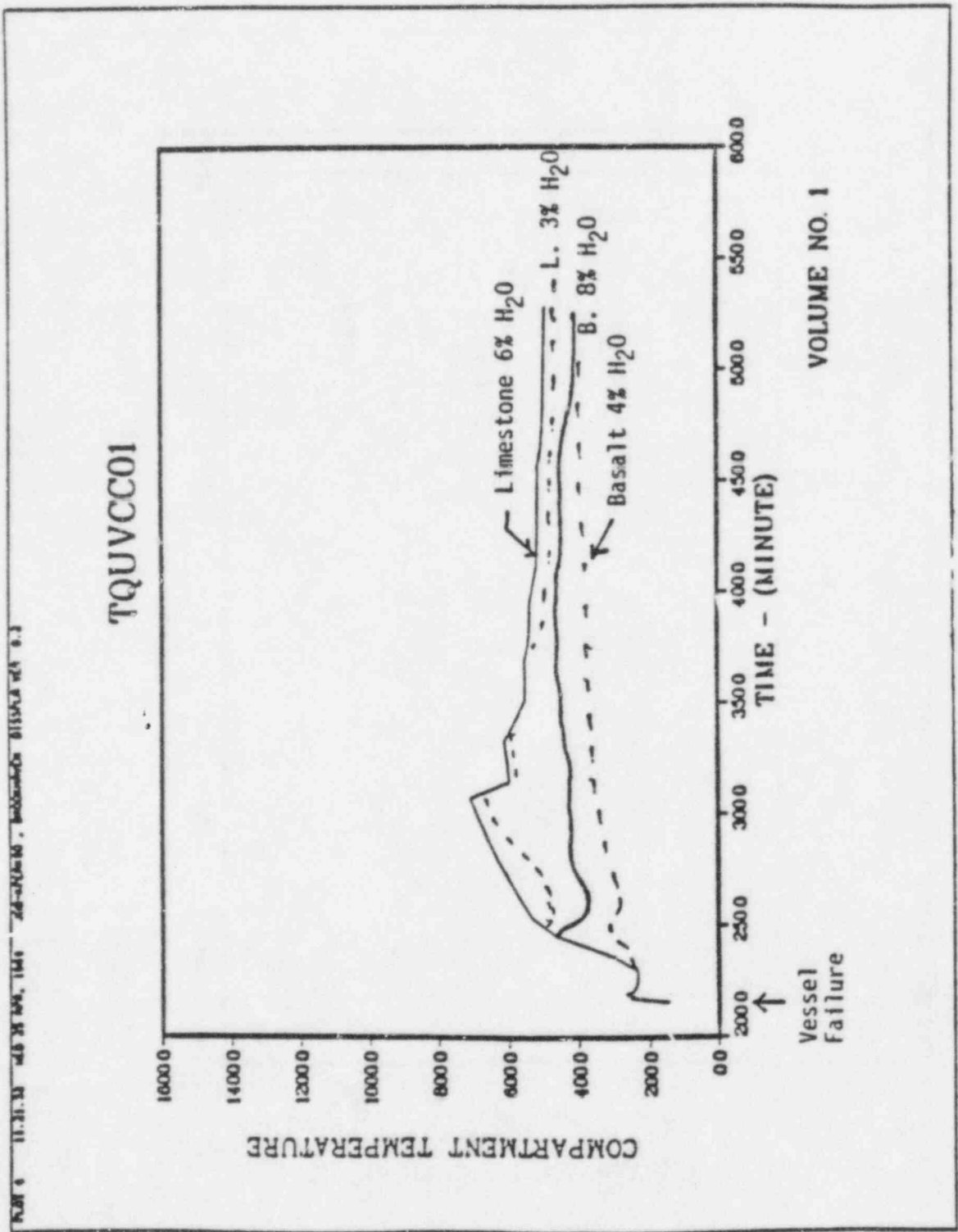


Figure 5.13 TQUVCC01: Compartment Temperature vs. Time

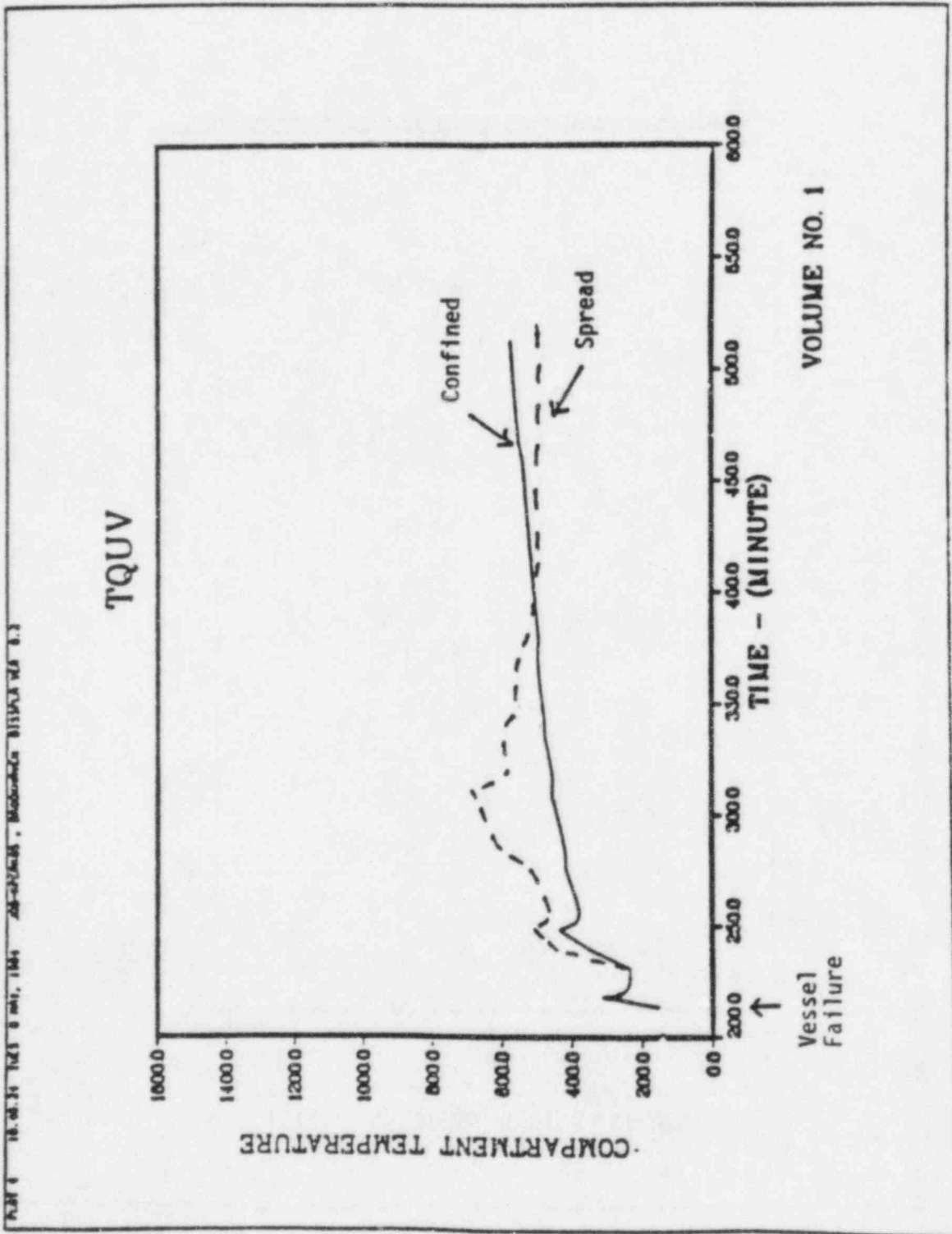


Figure 5.14 TQUV: Compartment Temperature vs. Time

ART 1 18.00.31 1425 8.00.144 28-02-00000. MASSACHUSETTS BOSTON 02111

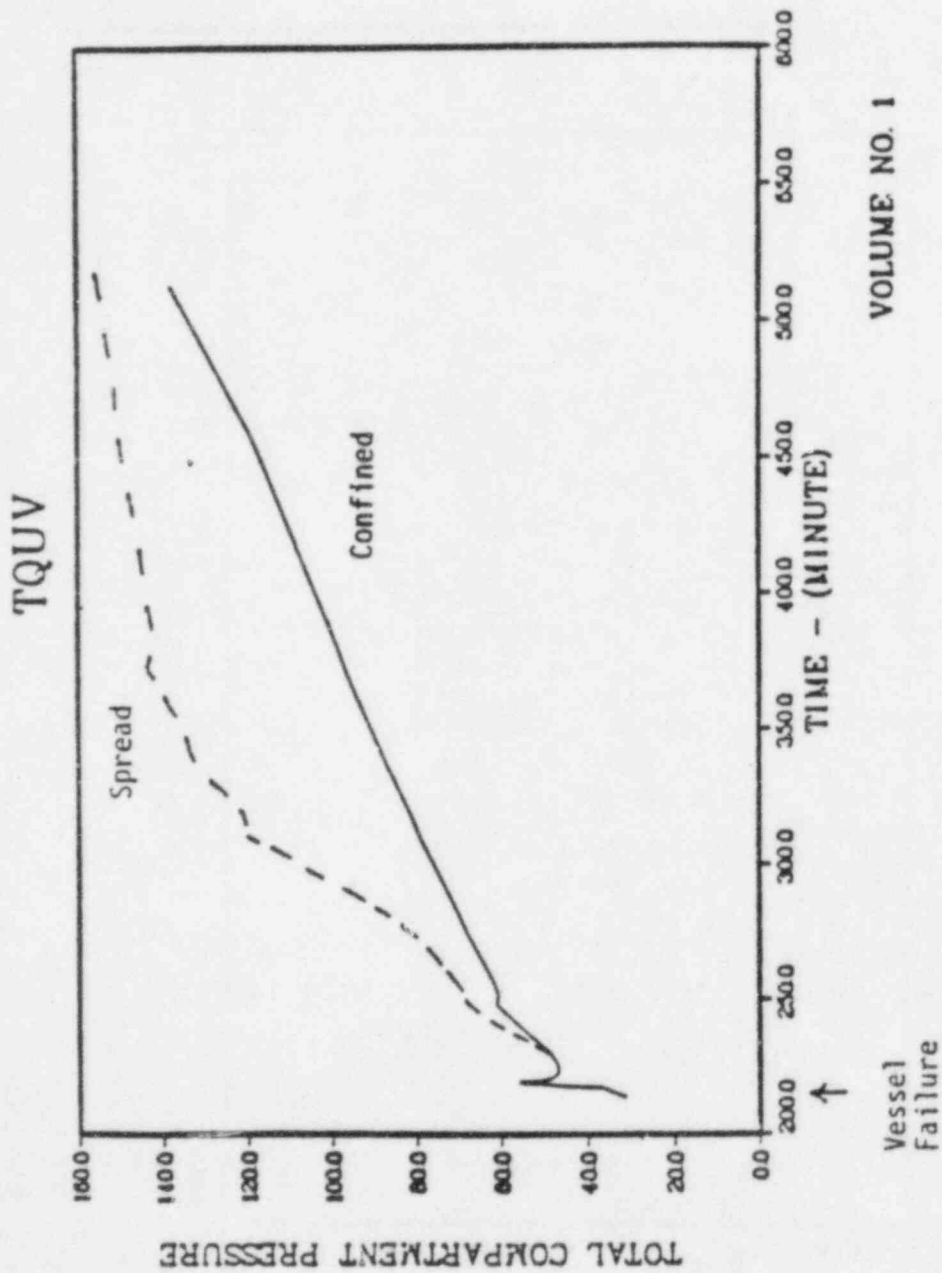
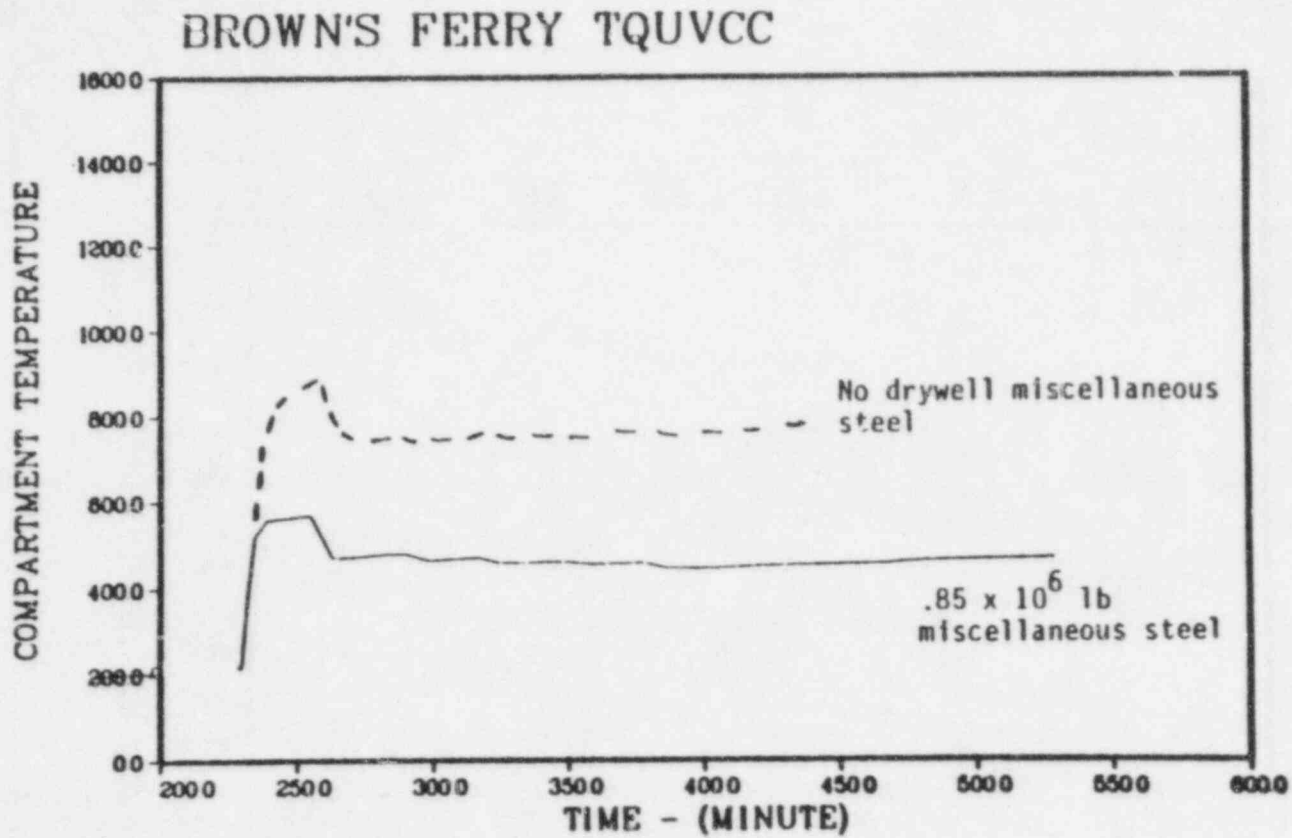


Figure 5.15 TQUV: Compartment Pressure vs. Time

5-38



VOLUME NO. 1

Figure 5.16 Brown's Ferry TQUVCC

## Chapter 6 BWR MARK II CONTAINMENT (SP-5)\*

### 6.1 Description of Reference Plant Geometry (Limerick)

The primary containment of the Mark II plant is made up of the drywell and wetwell compartments as shown in Figure 6.1. The primary system is enclosed in the upper or drywell compartment. The suppression pool is located below in the wetwell. Steam released from a break in the primary system during an accident would be released to the drywell and conveyed into the suppression pool by multiple vertical steel downcomer pipes. The downcomers penetrate the diaphragm floor which separates the drywell and wetwell. The suppression pool condenses steam and maintains the containment pressure and temperature below the design limit.

The reactor vessel is supported on a concrete pedestal extending down to the concrete basement of the primary containment. A horizontal diaphragm floor passes through the pedestal. Vent valves in the downcomers allow flow from the top of the wetwell back into the drywell. The reference plant does not have any downcomers within the pedestal region immediately below the reactor vessel.

The advantages of the Mark II containment configuration over that of the Mark I are:

- (a) More volume in the drywell and wetwell to accommodate steam and non-condensable gases.
- (b) Simpler vent configuration from the drywell to the wetwell via straight pipes.
- (c) More containment construction materials (concrete and steel) which serves as heat sinks during accidents.

### 6.2 Description of Standard Problem and Objectives

The definitions of the BWR Mark II standard problem are given in Table 6.1, which includes a base case (Case 5) and eight additional cases in which key parameters have been varied. The accident sequence defined as the standard problem is a TQUV-type sequence in which all reactor vessel injection capability is lost at the time of a reactor trip from 100% power. Because of mass loss out of the SRV's and the lack of coolant injection, the core eventually becomes uncovered. It is assumed that the automatic depressurization system (ADS) is not actuated so that the core melts and the vessel fails at high RCS pressure. When the reactor vessel bottom

\* CLWG analysts: Yang, Pratt, Greene (BNL); Cybulskis (BCL); Haskin (SNL); Hodge (ORNL); Cunningham, Barrett (NRC). Consensus summary authors: Yang, Pratt (BNL).

head fails, the corium falls onto the dry concrete floor of the drywell and the corium-concrete reaction begins. Steam and non-condensable gases are released from the concrete. The previously unoxidized zirconium will be oxidized, releasing a large amount of energy. The drywell pressure and temperature may increase quickly to values significantly above the design values. Two types of concrete, namely the limestone and basalt types, are considered for the standard problem. The concrete specifications are given in Table 6.2.

There were 15 passive heat sinks specified consisting of concrete, steel liner and miscellaneous steel as shown in Table 6.3. Among all the heat sinks, 5 are located in the drywell region, 4 in the suppression chamber and 4 in the suppression pool. Since the MARCH code does not model the heat sinks in the suppression pool and they do not contribute to the transient containment pressure and temperature response, these sinks in the pool were not included in the analysis by BCL and BNL. However, SNL employed all the 15 passive heat sinks. For the large amount of miscellaneous steel (848500 pounds in the drywell and 51500 pounds in the suppression chamber), a uniform thickness (i.e., 0.5 inches by SNL and 0.25 inches by BCL and BNL) is assumed.

### 6.3 Discussion of Major Phenomenology

The quantities and configurations of the interacting corium and concrete materials are important factors on containment loading. The Mark II drywell floor is significantly larger than the Mark I drywell floor. It is, therefore, unlikely that the melt will uniformly distribute over the whole area because of solidification of the corium. In addition, the presence of the downcomers will allow any molten corium to pour through the diaphragm floor into the suppression pool. Consequently, the bulk of the Mark II sample problem will involve solid corium (of non-uniform thickness) interacting with concrete. At present, the physical phenomena cannot be modeled by INTER or CORCON-MOD 1 (refer to Appendix D). In the standard problem base case, it is assumed the corium spread is about 5 meters. This area covers a portion of the annular space outside the pedestal walls. It is felt that this limited distribution of core debris may not be consistent with the high pressure failure of the reactor vessel.

The radiative heat transfer from the top of the corium into the containment space would affect the containment temperature response. The absorption and reflection of thermal radiation from aerosol, steam, CO<sub>2</sub> and structures are not modeled by the MARCH code. In performing the MARCH/CORCON analysis, BNL has assumed that energy associated with the radiative heat transfer could be added to the corium-concrete reaction. Thus, the overestimated corium-concrete reaction could balance, at least partially, the lack of radiation into the atmosphere. The MARCON code developed by SNL includes an upward radiative model. The MARCON code predictions are also included in this appendix.

## 6.4 Methods of Analysis

Various codes and/or combinations of codes have been used by the different groups. BCL used the MARCH 2 code to perform the standard problem. The MARCH 2 code contains the INTER subroutine, which predicts the corium-concrete reaction. The present publicly available version of the INTER subroutine has several errors related to the treatment of free water mass balance, rebar enthalpy and Zr-H<sub>2</sub>O heat of reaction. BCL reported that these errors have been modified to perform the standard problem computation. BNL used MARCH 1.1 code and the CORCON-MOD 1 code concurrently. The initial conditions of the corium-concrete interactions obtained from the MARCH 1.1 calculations were input to CORCON-MOD 1. The outputs from CORCON-MOD 1, involving the flow rates and temperature of the steam, hydrogen, carbon dioxide and carbon monoxide, were fitted as polynomial equations by the least-square method. These polynomial equations were incorporated into a version of the MARCH 1.1 code, which bypassed the INTER model. SNL performed their analyses by using the MARCON code, which is a direct coupling of the MARCH 2 and CORCON-MOD 2 codes. In the version of MARCON used by SNL to analyze the standard problem, the CORCON-MOD 2 code delivers energy to the drywell atmosphere in two ways. First, the gases generated in the attack of molten debris upon concrete convectively transfer heat from the pool to the atmosphere. And secondly, heat is transferred from the molten pool surface directly to the atmosphere by radiation. The assumption is made in the latter mechanism that sufficient aerosols, steam, and CO<sub>2</sub> are present in the atmosphere to render it opaque to radiation. In addition, it is assumed that the drywell atmosphere is well mixed by natural convection and by the gases generated in the molten pool, and that the aerosol particles are in thermal equilibrium with the atmosphere. The code has been modified to include radiative heat transfer from the drywell atmosphere to the containment passive heat structures as well.

A rather simplistic model was developed by SNL and is included in the MARCON code in an attempt to assess the magnitude of the contribution to containment response due to degassing of the concrete heat structures in containment. The model allows for the outgassing of both steam and CO<sub>2</sub>, depending on concrete composition. To allow for diffusional delays, the steam (from free and bound water), for example, is assumed to come out of the concrete linearly over a specified (input) temperature range. In this analysis, it was assumed that steam begins to outgas at 200°F and is completely removed by 500°F (to allow for the presence of bound water). The model has some inherent problems, the most serious one being the difficulty of accounting for the energy involved in phase changes and chemical reactions. Without completely removing the finite difference solution used for the heat structures in MARCH and incorporating a solution that includes volumetric heat sources and sinks and convective terms, the problem cannot be solved rigorously. However, an approximation can be made by adjusting the concrete heat capacity to account for these effects.

Comparative studies made by BNL and BCL staff have shown that the differences in CORCON and INTER predictions are caused by different modeling of corium-concrete interactions. Major differences involve the treatment of decay heat, free water, simultaneous Zr and Cr reaction, and FeO/Zr reaction. These modeling differences yield different release of gases and energy from the concrete and, hence, different containment response. In general, the INTER code predicts a higher gas release rate, in particular for H<sub>2</sub> and steam. The energy (i.e. temperature) associated with the gases predicted by the INTER code is also much higher during the first three hours of corium-concrete interactions. A detailed discussion of the CORCON-MOD 1, CORCON-MOD 2, and INTER codes are given in Appendix D for the Mark I standard problem. The same discussion applies to Mark II.

## 6.5 Numerical Results and Sensitivity Studies

The predicted containment pressure for the TQUV base case (Case 5 of Table 6.1) involving the limestone concrete is shown in Figure 6.2. It is noted that the BCL calculations predict a large pressure increase following the vessel failure. The pressure exhibits another sharp increase at about 88 minutes after vessel failure. At about 112 minutes, the containment fails at the assumed ultimate failure pressure of 145 psia. The BNL calculations predict a slower increase in containment pressure. The BNL calculations result in most of the gases (CO<sub>2</sub>, H<sub>2</sub>, steam and CO) being released within the first three hours. Since no significant mass and energy are added to the containment after about three hours, the containment pressure gradually approaches a stable site. The BNL predictions show that the peak pressure is about 130 psia, which is 15 psia below the estimated failure pressure. The SNL calculations indicate that there is a large pressure rise immediately after the vessel failure which results in an initial containment pressure 18 psia higher than the BNL or BCL calculations. During the first 80 minutes, the SNL calculations predict a higher rate of pressure rise. This is due to the radiation and degassing models in the MARCON code used by SNL. According to SNL's calculations, the heat transfer rate by radiation and convective from the debris surface to the drywell atmosphere would be as high as 60% to 70% of the total heat transfer to the atmosphere. The gas enthalpy rate from the degassing model is relatively small. At about 80 minutes after the vessel failure, the pressure curve assumes a smaller slope. This change in pressure slope corresponds to a reduction in the drywell temperature predicted by the MARCON code as shown in Figure 6.3. At three hours after the vessel failure, the peak containment pressure is 136 psia and is 9 psia below the assumed containment failure pressure.



The corresponding containment temperature is shown in Figure 6.2. The drywell temperature predicted by BNL using the MARCH/CORCON code shows gradual variation with time (similar to the behavior of containment pressure). The BCL and SNL predictions indicate a large variation in the temperature in the drywell region. The variation, according to SNL's calculation, is strongly related to the debris surface temperature which controls the radiative and convective heat transfer to the atmosphere. For example, the sudden reduction of drywell temperature at 80 minutes is caused by the reduction of debris surface temperature as the heavy oxide layer on the bottom changes place with the metallic layer above it. For the temperature in the wetwell region, there is a remarkable agreement between the BCL and BNL predictions prior to the containment failure. It is surprising SNL predicted that the wetwell temperature remains nearly constant throughout the entire transient.

The predicted containment pressure for the TQUV base case involving the basalt concrete (Case 7 of Table 6.1) are compared in Figure 6.4. The basalt concrete is characterized by the release of a large amount of steam relative to the non-condensable  $\text{CO}_2$  and  $\text{CO}$ . Since the steam is condensable, it is expected that the containment pressure would increase at a slower rate. This is reflected by both BNL and SNL predictions shown in Figure 6.4. The pressure evaluated at three hours after the vessel failure is about 100 psia by the BNL calculation and 110 psia by the SNL calculation. The BCL prediction also shows that containment failure at 145 psia has been delayed to about 160 minutes after the vessel failure. The difference between the predicted pressures by the MARCON and CORCON codes becomes smaller when the radiation model is removed from the MARCON code as shown in Figure 6.3. This difference is probably caused by the computation method of the two codes. The drywell and wetwell temperatures are compared in Figure 6.5. There is a large difference between the predicted drywell temperatures by the various codes. The wetwell temperatures, on the other hand, exhibit a remarkable agreement between BCL and BNL for the period prior to the containment failure.

The final comparisons are presented in Table 6.4 for the two base cases (i.e., Case 5 for the limestone concrete and Case 7 for the basalt concrete). The comparisons include the drywell pressure at 0, 2, and 3 hours after the vessel failure and the peak drywell temperature.

All the participants performed parametric studies according to Table 6.1. The following conclusions are generally observed:

- (a) Type of concrete - Higher drywell temperatures and pressures are encountered with the limestone concrete while the deepest vertical penetration is found with basalt concrete.

- (b) Free H<sub>2</sub>O - A higher percentage of free H<sub>2</sub>O leads to higher drywell temperatures and pressures, and higher vertical concrete penetration for both types of concrete.
- (c) Corium temperature and spread - The higher temperature corium which spreads further leads to higher drywell temperatures and pressures but lower concrete penetration.
- (d) Steel in corium - Reducing the steel in the corium reduced the pressure slightly and reduced the drywell peak temperature but increased the concrete penetration.
- (e) Pool loss - A higher percentage of pool loss implies less corium-concrete interactions and reduces the containment temperatures and pressures. The suppression pool remains at a subcooled state during the entire transient.

#### 6.6 Considerations of Loads and Likelihood of Containment Failure\*

The Mark II containment is also inerted and steam spikes can be of no consequence. This standard problem, therefore, is very similar to that considered for the Mark I case (SP-4) with one major exception. Here, as the melt spreads on the diaphragm floor, it can flow through the numerous downcomer openings into the suppression pool. Thus, only a fraction of that exiting the vessel will be available for corium-concrete interactions. A corresponding reduction in containment loads would be expected. The standard problem considered this fraction parametrically. The Limerick power plant was selected for the specifics.

The calculated results indicate that the ultimate containment capability of 10.5 bar (155 psia) could be approached within 2-3 hours (limestone concrete). For a basaltic concrete the pressurization rate is considerably lower, yielding only 100 psia at 3 hours. As in the Mark I case high drywell temperatures, in the range of 550 to 700°F prevail, raising again the possibility of penetration seal failures.

Based on these results we conclude that early failure of the Limerick containment is rather unlikely although additional work remains to be done before this judgment can be adequately sharpened.

\* Considerations of the likelihood of containment failure from the various load sources described in this report have been provided by the NRR staff and is based on extended discussions with staff consultants and staff members involved in containment loads and performance activities.

## 6.7 Conclusions and Recommendations

Based on the comparative studies presented in this report, it appears that a range of uncertainty can be assigned to the containment pressure and temperature. The predictions from the INTER code by BCL represent the upper bound of the uncertainty and CORCON code by BNL results the lower bound. The MARCON results (with some uncertainty of modeling radiation and degassing) obtained by SNL lie within the bound. The differences between the two codes (INTER and CORCON) are caused by the modeling of the complex corium-concrete reaction. The major uncertainties involve the different treatment of decay heat, free water, and certain chemical reactions. The uncertainty is larger for the basalt concrete, smaller for the limestone concrete. The uncertainty of pressure prediction covers the estimated containment failure pressure of 145 psia. Thus, using the failure pressure as a criterion in the computer code, a threat to the containment integrity is predicted by BCL using the INTER code and is not predicted by BNL and SNL using the CORCON and MARCON codes, respectively. However, it must be pointed out that the comparative study should not be used to reach final conclusion regarding the failure of containment due to over-pressurization. A more comprehensive study of the corium-concrete chemistry and corium heat transfer are needed for the assessment of the uncertainties.

The comparative study also indicates that the temperature in the drywell is higher than the design temperature for a long period of time. Thus, the heating of the drywell region could present a potential threat to the containment integrity.

Table 6-1 Mark II Standard Problem Definitions

Case	5	5A	5B	5C	5D	6	7	7A	8
Corium Spread, m	5	5	5	5	5	3	5	5	3
Debris Temperature, F	4130	4130	4130	4130	4130	2700	4130	4130	2700
Concrete type	L	L	L	L	L	L	B	B	B
Free H <sub>2</sub> O, %	3	6	3	3	3	3	4	8	4
Steel in Corium, lb <sub>m</sub>	140K	140K	85K	140K	140K	140K	140K	140K	140K
Pool Losses, %	0	0	0	25	50	0	0	0	0

KEY

L - Limestone  
B - Basalt

Table 6.2 Specifications of Concrete

	Limestone		Basalt	
Ca(OH) <sub>2</sub>	15%	15%	18%	18%
Ca CO <sub>3</sub>	80%	77%	1%	1%
Al <sub>2</sub> O <sub>3</sub>	1%	1%	20%	20%
SiO <sub>2</sub>	1%	1%	57%	53%
Free H <sub>2</sub> O	3%	6%	4%	8%

Table 6.3 Passive Heat Sinks for Mark II Plant Problem

Sink	Location	Area (ft <sup>2</sup> )	Concrete Thickness (ft)	Steel Liner Thickness (in)	Mass (lb)
1	D	4142	2	-	-
2	D	1850	3.5	-	-
3	W	2345	3.9	-	-
4	W	2642	1.9	-	-
5	P	1185	3.9	-	-
6	P	1121	1.5	-	-
7	D	10595	4.5	0.38	-
8	D	4163	7.0	0.38	-
9	W	9100	4.5	0.38	-
10	P	4219	4.5	0.38	-
11	P	4902	9.0	-	-
12	D	4544	1.5	-	-
13	W	4418	1.5	-	-
14*	D				8485000
15*	W				51500

Key

D - Drywell, W - Wetwell, P - Suppression pool

\*Sinks 14 and 15 denote miscellaneous steel in drywell and wetwell chambers, respectively.

Table 6.4 Comparison of Results for Mark II Standard Problem

	P <sub>0</sub>	P <sub>2</sub>	P <sub>3</sub>	T <sub>p</sub>
	psia			°F
Limestone Base Case				
MARCH/INTER (BCL)	70	15* <sup>1</sup>	15	800
MARCH/CORCON (BNL)	70	112	123	630
MARCON (SNL)	88	130	136	830
Basalt Base Case				
MARCH/INTER (BCL)	70	130	15* <sup>2</sup>	720
MARCH/CORCON (BNL)	70	90	98	480
MARCON (SNL)	88	103	110	660
MARCON (No RHT) (SNL)	88	97	104	400

\*<sup>1</sup> - Containment fails at 112 minutes. Peak containment pressure is 145 psia.

\*<sup>2</sup> - Containment fails at 158 minutes. Peak containment pressure is 145 psia.

Subscripts: 0 - Evaluated immediately after vessel failure.  
 2 - Evaluated at 2 hours.  
 3 - Evaluated at 3 hours.  
 P - Peak value.

Units: Pressure in psia, temperature in °F.

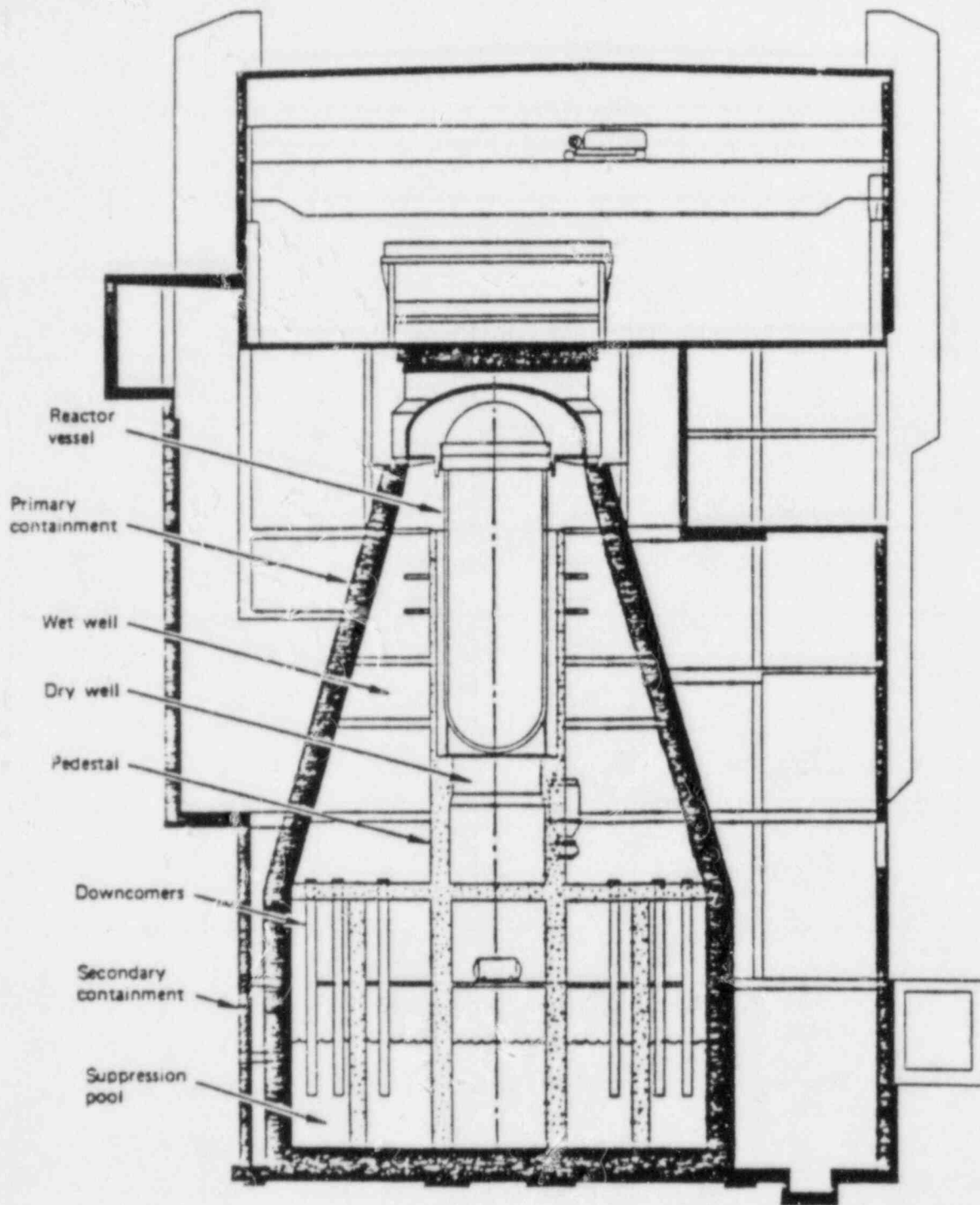


Figure 6.1 Mark II primary and secondary containments.

LIMERICK



BWR Mark II TQUV5 (Limestone Concrete)

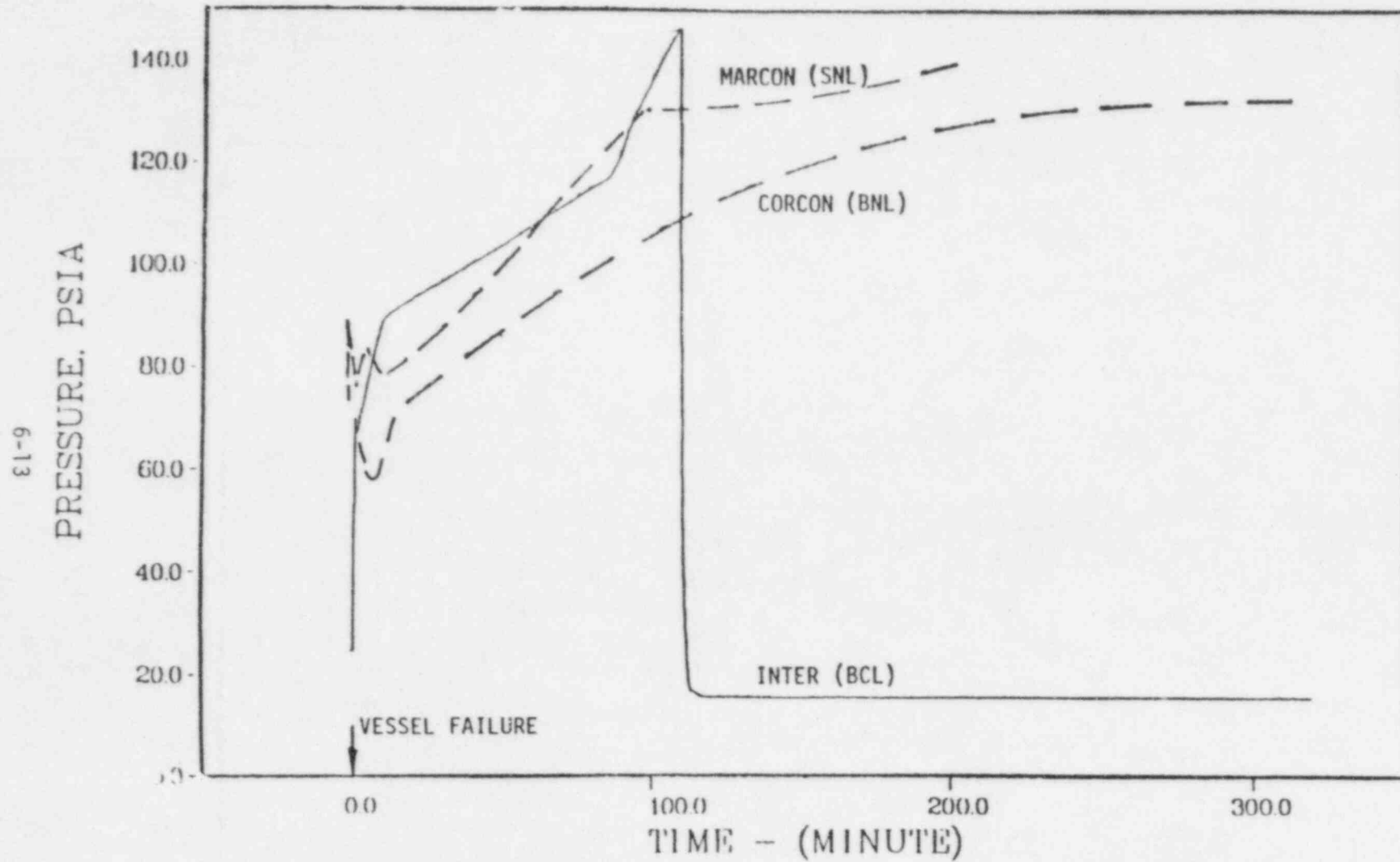


Figure 6.2 Comparison of containment pressure for the TQUV sequence (limestone concrete)

BWR Mark II TQV5 (Limestone Concrete)

6-14

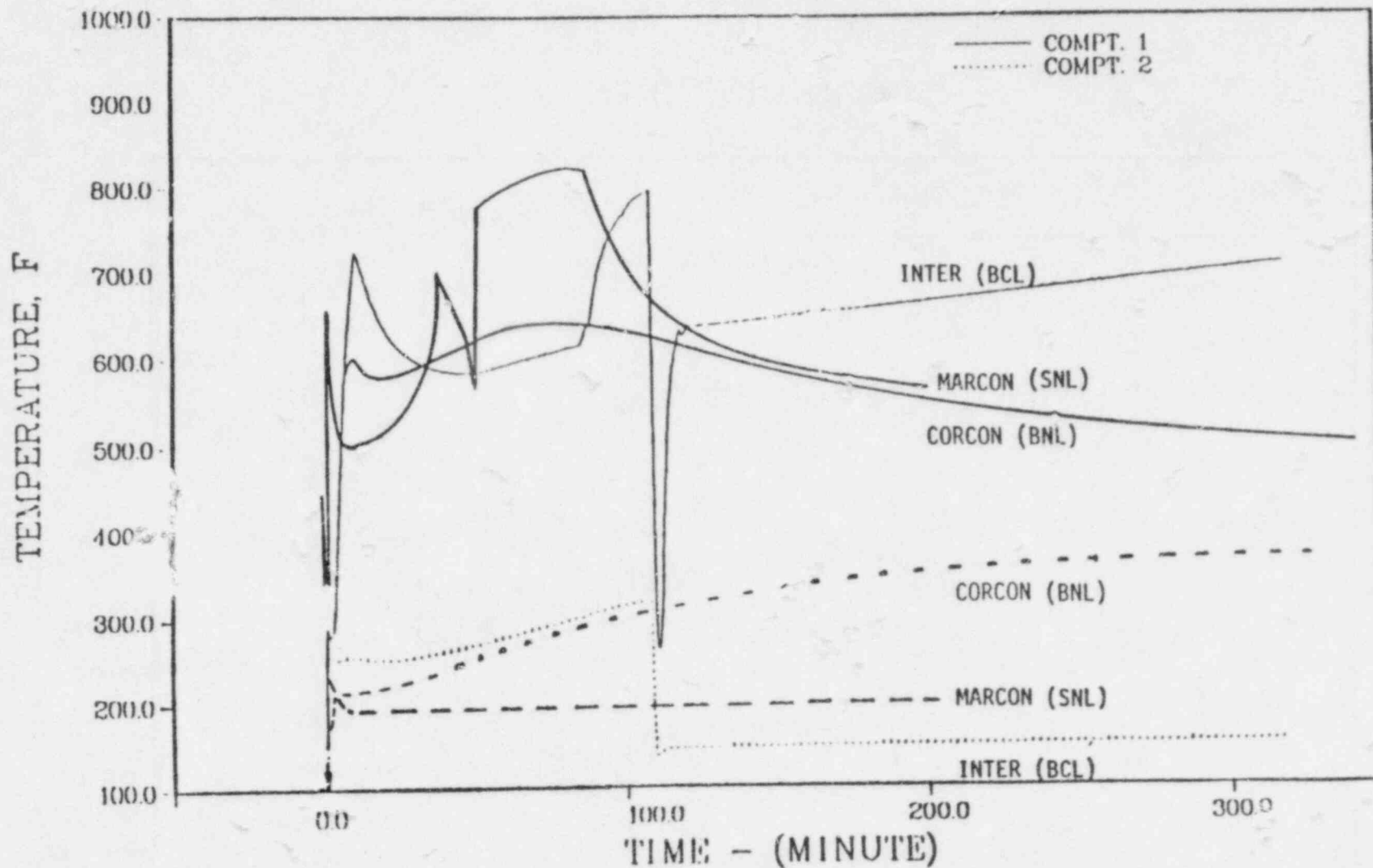


Figure 6.3 Comparison of containment temperature for the TQV sequence (limestone concrete)

BWR MARK II TQV7 (Basalt Concrete)

61-9

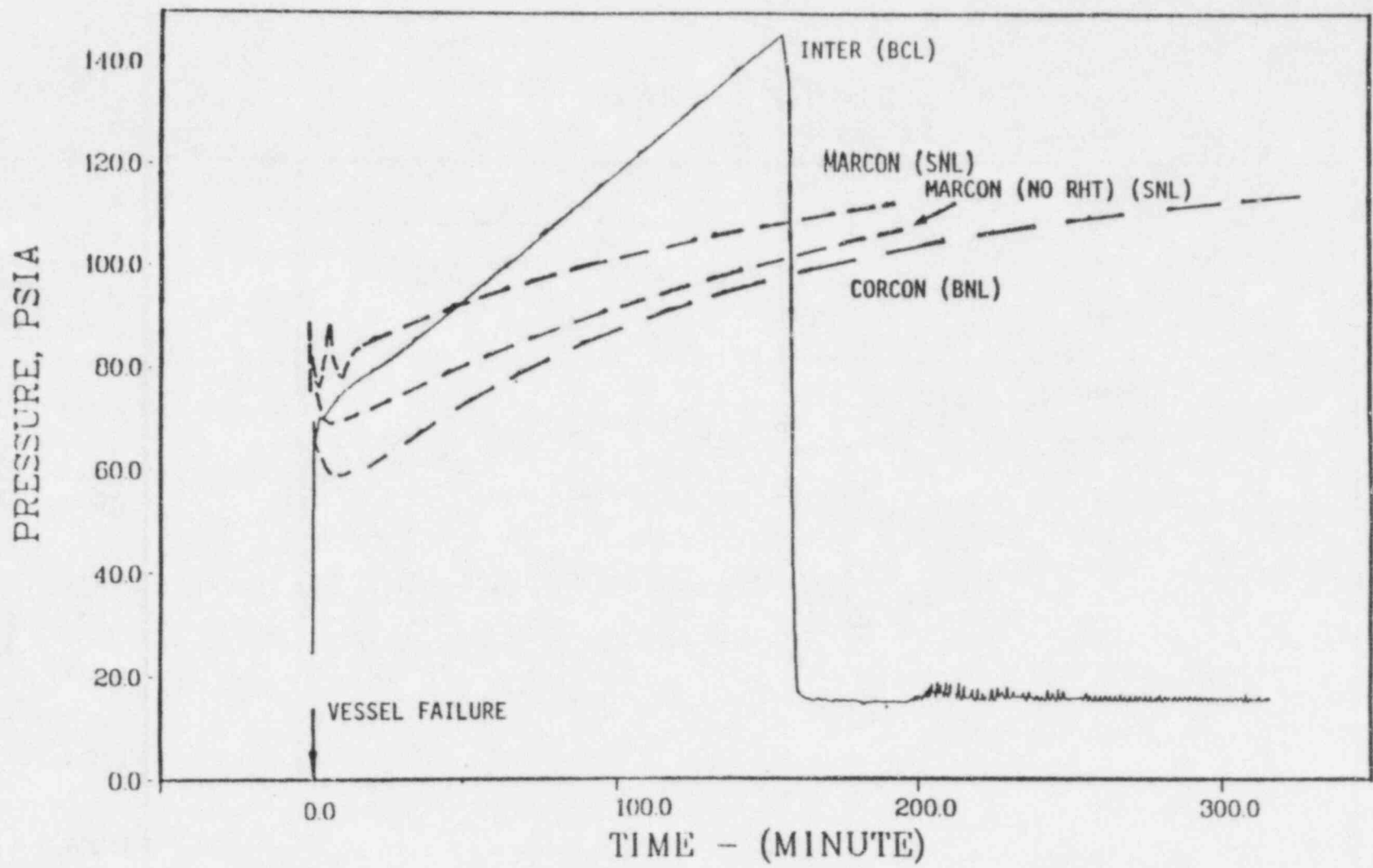


Figure 6.4 Comparison of containment pressure for the TQV7 sequence (basalt concrete).

BWR Mark II TQV7 (Basalt Concrete)

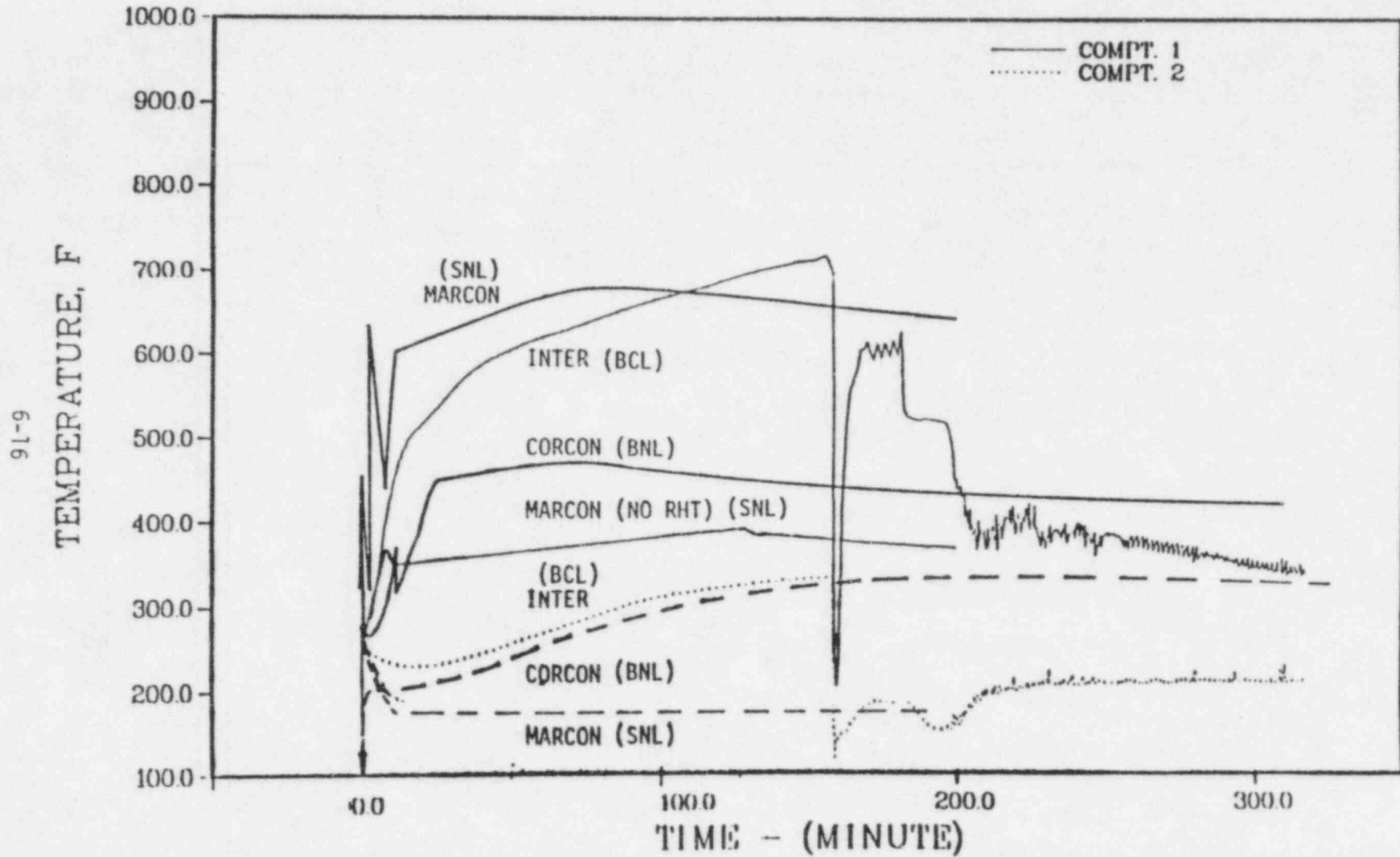


Figure 6.5 Comparison of containment temperature for the TQV sequence (basalt concrete)

## 7.1 Description of Reference Plant Geometry

The reference plant has a BWR Mark III containment, as shown in Figure 7.1. Because of the way in which the problem is formulated (see Section 7.2), a description of the primary system and drywell is not necessary. Therefore, only the outer containment (the region outside of the drywell) will be described here.

During most severe accidents, hydrogen, steam and fission products will enter the outer containment through the suppression pool. Gases can enter the suppression pool either through vent holes in the drywell wall or directly from the primary system through a set of spargers, depending on the particular accident scenario (see Figure 7.2). Some bypass of the suppression pool might occur, but was not considered for this problem.

The spargers are located approximately 12-15 ft. below the surface of the suppression pool, depending on the amount of water dumped from the upper pool. A heat exchanger is provided that, when operating, should maintain the temperature of the pool below about 160°F. As long as the pool remains relatively subcooled, it may be expected that most of the steam will be condensed in the suppression pool.

Directly above the suppression pool is an annular region that extends upward approximately 98 ft. This region contains most of the equipment and penetrations that are located in the outer containment. The region is divided by grates and floors and includes various rooms and equipment.

Numerous igniters are located in this region, with the lowest set positioned about 20 ft. above the suppression pool. Above the annular region is the relatively open dome region which also contains igniters.

The Mark III containment design used for these analyses was based on the Grand Gulf design, which has a steel-lined concrete shell with a failure pressure of approximately 72 psia. Other Mark III designs exist with an air gap between a free-standing steel shell and a concrete outer shell. The Grand Gulf containment has both a spray system and a drywell purge system. Both of these systems were assumed inoperative for these analyses. The major geometrical parameters are shown in Table 7.1. Some of this information was provided to the CLWG by the General Electric Company; the remainder was supplied by the NRC. Some discrepancies may be present in the calculations presented later on, because some of the numbers changed while the work was in progress. Also, for cases where

\* CLWG analysts: Zalosh, Ural (FMRC); Camp, Dingman, Shepard, Cummings, Hickox (SNL); Travis (LANL); Telford (NRC). Consensus summary author: Camp (SNL).

the containment was significantly subdivided, the individuals performing the calculations were required to exercise judgment regarding the placement of the miscellaneous heat sinks within containment.

## 7.2 Description of Standard Problem and Objectives

The basic problem considered was one of a standing diffusion flame located above the suppression pool. The problem represents a parametric treatment of hydrogen release rates, rather than the examination of a particular accident sequence. Various hydrogen release rates were postulated, and information was requested from the group regarding gas temperatures, gas pressures, and heat fluxes to the wetwell and drywell walls. The calculations are intended to provide some insight into the integrity of penetrations through these walls during the course of an accident. However, no attempt was made to predict the response of particular penetrations, and any conclusions drawn regarding the penetrations will represent extrapolation of the calculations presented here.

There are three base cases and four sensitivity analyses that were performed by the group. Certain parameters and assumptions were maintained constant for all cases. Table 7.2 contains many of the important initial conditions. Some slight variations on these conditions may occur in the different analyses to be presented later. For all cases it was assumed that the sprays and drywell purge systems did not work, but that suppression pool cooling was maintained so that the pool temperature remained in the range of 150-160°F. The likelihood of this particular sequence of events occurring is not clear. If the accident is intended to represent a case with total loss of power, then the suppression pool should be expected to heat up. Otherwise, there is no clear reason why the other systems should not be working.

The hydrogen was injected into containment at the suppression pool temperature. All of the steam was assumed to be condensed in the suppression pool. The hydrogen release rates for the seven cases are shown in Table 7.3. The cumulative value of 3000 lb. of hydrogen released in several of the cases corresponds to approximately 68% oxidation of the zirconium, excluding the channel boxes. The hydrogen was assumed to be released within a circle with a radius of 5 ft. centered above the associated sparger.

The hydrogen was assumed to ignite as it entered the containment. Inerting criteria were left to the discretion of the analysts, with 5% oxygen generally used as the inerting level. The likelihood of the existence of stable diffusion flames was not examined here, rather, those conditions were postulated.

### 7.3 Discussion of Major Phenomenology

Diffusion flames involve conditions where the fuel and air are initially separated, and combustion occurs along an interface between the fuel and air where the mixture is flammable. The cases considered here involve buoyant plume-like diffusion flames with Froude numbers  $\ll 1$ . The important phenomena when considering diffusion flames in containments are: (1) flammability limits, (2) entrainment rates, (3) suppression pool behavior, (4) flame characteristics, (5) radiative heat transfer, and (6) convective heat transfer. The first two items appear to be the most important, while the other items may change in relative importance for different problems. Each of these topics will be discussed in more detail below.

#### 7.3.1 Flammability Limits

The flammability limits determine whether or not stable diffusion flames can exist. They are a function of the hydrogen and steam injection rates, the surrounding gas composition, and the temperature and pressure of the gases involved. For the cases considered, stable diffusion flames appear to be possible. The 1/20 scale experiments indicate that diffusion flames may be possible as long as the hydrogen injection rates is greater than about 25 lb./min. through nine spargers. Combustion would be expected to continue until the hydrogen injection rate decreases or the surrounding atmosphere becomes depleted of oxygen. Generally, it may be expected that combustion will terminate when the oxygen concentration falls to about 5%. Recent experiments at the Nevada Test Site by EPRI indicate that combustion may terminate earlier, when the oxygen concentration falls to about 8%.

#### 7.3.2 Entrainment Rates

If stable diffusion flames exist, then the single most important factor to consider is gas entrainment. Entrainment controls the local temperatures and the transport of hot gases throughout the containment. High entrainment rates lead to lower temperatures (due to thermodynamic mixing) in the region surrounding the flame and higher temperatures throughout the rest of the containment, because less heat is deposited locally.

Diffusion flames are fairly efficient air pumps. Based on small and medium scale experiments, the amount of air entrained in such a flame may be 5 to 15 times the amount of air actually needed to burn the fuel. This entrainment produces temperatures in the flame region that are usually much less than the adiabatic flame temperature.

Gas entrainment increases along the length of the flame. Thus, depending on how the combustion rate varies along the flame, the gas temperatures are higher at the bottom of the flame, and tend to drop off along the top half of the flame.

### 7.3.3 Suppression Pool Behavior

The behavior of the gases coming up through the suppression pool will influence the behavior of the diffusion flames. First, the bubble dynamics may be important, and second, the amount of steam remaining in the bubbles will influence subsequent combustion. With regard to the bubble dynamics, the coherence with which the hydrogen is released from the pool may be important. If the bubbles tend to coalesce or at least form a relatively contiguous flow field, then the flame can be treated as if driven by a single large fuel source. However, if the bubbles remain separated or in individual clusters, then the problem may be more typical of a case with many individual fuel sources, rather than one large one. The rise of the bubbles near the surface of the pool may be affected by large scale wave motion. Also, the bubble behavior will affect the pool surface, perhaps causing some water droplets to be thrown into the lower parts of the flame.

The amount of steam remaining in the bubbles will affect the flammability of the resulting plume and also the combustion characteristics of the flame, e.g., temperature. If the pool is significantly subcooled, then most of the steam will be condensed from the bubbles, depending on the bubble size and rise time. However, in our opinion there will probably remain in the bubbles a partial pressure of steam at least equal to the saturation pressure at the pool temperature.

The standard problem assumes that all of the hydrogen is released through the spargers. For some accidents hydrogen will come through the suppression pool vents instead of or in addition to the spargers. These cases may produce very different behavior than those considered in this study.

### 7.3.4 Flame Characteristics

Little data exist for large scale buoyant diffusion flames. Some experiments have been performed at 1/20 scale, and some 1/4 scale experiments are planned. Based on the 1/20 scale experiments, one should expect unsteady flames that are very sensitive to changes in flow currents. The most important characteristics of the flames to consider are the height of the flames, the temperature profiles within the flames, and the completeness of the combustion.

The actual flame geometry is important in determining local energy densities and heat fluxes to various locations within and around the flame zone. For a given hydrogen combustion rate, a different flame height will yield a different local energy density (temperature) and will produce different radiant heat fluxes to surfaces due to changing view factors between the surfaces and the flame. The flame height is typically a function of the source injection rate and composition, the composition of the surrounding



gas, and the entrainment rate. The flame height will increase with the source injection rate and as the gas mixture becomes less flammable, i.e., more steam or less oxygen. With an increase in source injection rate a flame will become taller and entrain more air, but not so much as to offset the increase in combustion rate, and some regions of the flame will become hotter (the peak temperatures near the bottom of the flame may not change much, but the flame will extend higher and the upper regions of the flame will become hotter). For a fixed injection rate the surrounding gas will become depleted of oxygen as time passes, and the flame may lengthen, tending to reduce some local temperatures, but this effect will be countered by the increase in the surrounding gas temperature as the containment heats up during the event. The change in temperature in the flame region with time will depend on the tradeoffs between the flame lengthening effects and the heatup of the surrounding gas.

The temperature profile within the flame region depends upon local values for combustion rate, entrainment rate, and the composition and state of the gases entering the local region. Normally, the highest temperatures will occur at or near the bottom of the flame, with temperatures that vary minimally over the bottom half of the flame and drop off significantly over the top half of the flame. Unfortunately, data applicable to these specific cases are limited, and thus, significant uncertainty exists regarding actual values. The uncertainties in the temperature profiles project into uncertainties in the local heat transfer rates. The 1/4 scale tests should provide data that help reduce the uncertainties.

The combustion completeness determines the combustion rate and, thus, influences most of the factors discussed previously. Generally, we feel that combustion in diffusion flames is virtually complete, with perhaps some decrease in the completeness near the end of the transient when the oxygen concentration nears the inerting level and the mixture is less flammable.

### 7.3.5 Radiative Heat Transfer

The heat transfer rates determine how much energy will be deposited locally, to structures and equipment near the flame, and how much will be transported throughout the rest of containment. Higher heat transfer rates will lead to higher surface temperatures in the regions near the flame. Radiative heat transfer is an important heat transfer mechanism when the gas temperatures are more than a few hundred degrees Fahrenheit. Radiative heat transfer may be more or less important than convective heat transfer, depending on the gas temperature, gas velocity, steam concentration, etc.

Most of the radiation will come from steam in the flame region and the hot plume above the flame. Some of the radiation will be absorbed by steam in the surrounding atmosphere, and some will be transmitted to surfaces which "see" the hotter regions. As long as the steam concentrations are fairly low (<20%), most of the radiation will be transmitted to the surfaces (>70%). The surrounding gases are not good absorbers of the radiation because of the spectral dependence of the emissivity, i.e., the radiation is emitted at a higher temperature than the temperature of the surrounding gas and the radiative bandwidths will be different.

Experiments have shown that as much as 15% of the energy released in the combustion process will be radiated from the flame region. This radiation will be emitted isotropically to surfaces, based on the view factors between the hot combustion gases and the surfaces, with some absorption (and a limited amount of reradiation) by the gases in between.

### 7.3.6 Convective Heat Transfer

Convective heat transfer is important near the flame and dominates the heat transfer in the cooler regions of containment. In the flame region and the plume above, gas velocities may be in excess of 25 ft./s; thus, turbulent forced convection would be expected (for this case the flame represents the forcing mechanism). However, it is possible that complex flow patterns will exist, perhaps including stagnation regions, such that a variety of convective heat transfer regimes will exist. For both radiative and convective heat transfer, the precise location of a surface relative to the flame and gas flow pattern is important. Calculations of such local effects would probably require excessively fine nodalization. Also, convective heat transfer correlations that have been validated for these scales and geometries do not exist. Thus, scoping calculations are the best that can be expected at this time.

### 7.3.7 Accident Progression and Timing

In any realistic accident involving core degradation and melting, hydrogen will probably not be released at fixed rates over long periods of time; rather, the accident will proceed in stages, with the possibility of diffusion flames igniting and extinguishing at various points during the event. For most severe accidents, one would expect the accident to progress along the following lines:

The first phase of the accident will involve core uncovering. If the accident is a LOCA, then the drywell will be pressurized and mass and energy will be transmitted into the outer containment via the horizontal vent holes that connect the portion of the pressure suppression pool within the drywell to the (larger) portion in the outer containment. All discharge from the drywell (except drywell leakage) would pass through the pressure suppression pool.

If the accident is a transient event, such as loss of all reactor vessel injection, the discharge from the reactor vessel as the core is uncovered will be through the safety relief valves (SRVs) and would enter the pressure suppression pool through the x-quencher spargers located near the floor of the pool on the wetwell side. In any case the suppression pool will begin to heat up, and there will be some pressurization and heatup of the outer containment. As long as suppression pool cooling systems are functioning, the heatup of the outer containment will be slight.

Following core uncover, the core temperature will begin to rise, and hydrogen production will follow. Hydrogen production should start off slowly, increase as the uncovered portions of the core heat up, and decrease as the reaction becomes steam starved when the water level is significantly below the bottom of the core. The effects of SRV operation is important, since the associated level swell serves to quench some uncovered portions of the core. Diffusion flames in the outer containment may be possible during any periods when the hydrogen production rate exceeds some minimum value (about 15 lb./min. through nine spargers based on the 1/20 scale tests), certainly not during the entire core degradation process.

The manner in which the BWR core melts and enters the lower plenum can significantly alter the hydrogen release profiles. As molten zirconium falls into water in the lower plenum, some amount of metal-water reaction is certain to take place. This assumes that less than 100% of the zirconium is reacted during the core degradation phase - a good assumption. The magnitude and rate of hydrogen generation during the core melting phase are governed by the way in which the core slumps and the type of reaction that occurs in the lower plenum. The BWR core may slump in a series of small pours in which the small amounts of material can be quickly quenched, producing little hydrogen in the lower plenum, but producing steam which may react while passing up through what is left of the core. This type of core slumping would produce significant amounts of hydrogen, but would generate it relatively slowly.

On the other hand, if the core relocation into the lower plenum is fairly rapid, with large fractions of the core slumping at one time, then fairly violent reactions including steam explosions are possible. In this case a large fraction of the unreacted metal (20-30% based on some experiments) may react in less than a second, producing a large burst of hydrogen that would greatly exceed the peak rates specified in the standard problem for a short period of time. The actual core slumping process represents a significant uncertainty and may fall somewhere between the two extreme cases mentioned above.

As significant portions of the BWR core relocate into the lower plenum and any initial reactions have taken place, the corium will begin to attack the lower vessel head and vessel penetrations, leading to vessel breach. Hydrogen generation during this period will depend on the presence of steam or water, and the length of time to vessel failure.

When vessel breach occurs, molten material will fall or be ejected onto the pedestal floor below. For cases where the reactor vessel remains at high pressure, significant amounts of material may be ejected out of the pedestal region into the rest of the drywell. Whether or not water is present will depend on the particular accident scenario. Water could be present if the accident involves a drywell break, if the control rod drive hydraulic system continues to operate after vessel failure, or if events occur in the outer containment that force water over the weir wall. The key parameter will be whether or not water is present. If water is present in significant quantities, then there is the potential for rapid oxidation of unoxidized metals. Otherwise, concrete attack may begin right away. Concrete attack will result in some combustible gas generation (hydrogen plus carbon monoxide), but the rate of generation will probably be below that necessary to sustain stable diffusion flames.

There are some other possibilities in addition to those mentioned above. If, for example, the accident is terminated late in the core degradation phase, the steam generated during the quenching process may result in a significant burst of hydrogen. Basically, any process resulting in the rapid coupling of hot, unoxidized metal with steam will rapidly produce hydrogen. However, it is clear that the highest hydrogen generation rates will only be sustained for short periods of time.

The behavior of the diffusion flames will vary during the course of the accident. The flames will change characteristics as the hydrogen release mechanism changes (from sparger flow to vent flow). It is likely that the flames will be intermittent, igniting and extinguishing more than once during the course of the accident. In any case, the flames will go out permanently when the oxygen concentration falls below about 5%. Assuming dry air, a total containment volume including the drywell of about  $1.65 \times 10^6$  ft.<sup>3</sup>, and an initial (pre-accident) temperature and pressure of 80.3°F and 14.7 psia, there are approximately  $4.0 \times 10^5$  moles of oxygen in containment. Ignoring the other gases injected into containment and assuming that all the steam condenses, approximately  $3.2 \times 10^5$  moles of oxygen could be consumed in the combustion process, corresponding to  $6.4 \times 10^5$  moles of hydrogen. This is a very conservative estimate, as the presence of steam and hydrogen would render the oxygen concentration lower than 5% much earlier. The total amount of hydrogen that could be burned (~2800 lb.) is slightly less than the total amount specified in some of the standard problem cases and corresponds to the oxidation of about 65% of the zirconium, excluding the channel boxes. For many severe accident scenarios, it appears that the containment will become inerted within the first few hours after the accident begins.

## 7.4 Methods of Analysis

In this section brief summaries of the individual calculational methods are provided. There are two methods based on correlations of experimental data (FMRC and SNL1), a method using a lumped-parameter computer code (SNL2), and a method based on a finite-difference code (LANL). The results from these calculations are provided in Section 7.5. More detailed discussions of these methods can be found in the individual reports provided elsewhere in the Containment Loads Working Group documentation.

### 7.4.1 FMRC Method

The FMRC approach has been to combine a global model for the containment building atmosphere with a local model for the diffusion flames in the wetwell. The global model uses energy and species mass balances to calculate average temperature, composition and pressure as a function of time as hydrogen is injected and continuously burned until the oxygen concentration is reduced to 5 vol. %. Heat losses from the bulk gas to the containment walls in the global model are calculated using empirical correlations for radiation, natural convection, and condensation. The containment wall heatup is calculated using lumped parameter heat conduction equations for the exposed steel and concrete.

The diffusion flame model is a generalization of recent data correlations for flame height, flame/plume centerline temperature and velocity distributions, and fraction of combustion energy released in the form of thermal radiation. The generalization accounts for changes in ambient gas temperature and composition as combustion products accumulate and oxygen is depleted in the containment. Heat fluxes to the drywell wall are calculated as the sum of the radiant heat flux emitted from the flame surface and the convective heat flux based on flame centerline temperature and velocity distributions. Heat fluxes to the wetwell outer wall are calculated as the sum of the radiant heat flux (accounting for flame-target view factors and a 70% transmissivity through the intervening steam-laden gas) and the background heat flux based on the containment atmosphere average temperature.

FMRC believes that this calculation procedures produces pressures, temperatures, and heat fluxes that are somewhat higher than would be expected with a more rigorous and detailed analysis. Therefore, the calculated results are categorized as "near-maximum" for purposes of a tabulated summary and comparison with other methods. The tabulated results also include approximate estimates of reasonable lower bound values. In the case of pressures and average temperatures, the lower bound is based on analogous global calculations but with isothermal containment walls to

provide a large heat sink effect. For drywell wall lower bound heat fluxes, the convective contribution due to the diffusion flame is entirely eliminated and the radiant heat flux is reduced by one third to account for that level of uncertainty in radiant energy fraction and nominal flame surface area. A similar reduction in radiant heat flux is also applied to the wetwell outer wall in order to provide a lower bound estimate.

FMRC recommendations for "best-guess" values would be to use the scaled experimental results from the 1/4 scale test facility. The tests are scheduled to be conducted within 3-6 months. In the interim, upper and lower bounds are all that can be reasonably expected from the FMRC calculations.

#### 7.4.2 SNL1 Method

The SNL1 analysis describes the local environment of a diffusion flame and its thermal effect on the wetwell and drywell walls. It concentrates on the flame over a single sparger and ignores the influence of other flames, any global flow patterns that might be set up in the containment and the overall heatup of the containment atmosphere. The analysis is intended to complement the HECTR analysis (SNL2), which models most of the processes, but cannot provide sufficient spatial resolution near the flame.

In order to calculate the heat flux from a hydrogen diffusion flame originating on the suppression pool, velocity and temperature conditions for empirical fire models were matches to those from a similarity solution for buoyant plumes. This allowed for computation of velocities and temperature rises as a function of height above the pool. These values are used to compute a convective heat transfer coefficient from an experimentally derived turbulent boundary layer correlation for forced convection. Direct radiative heat transfer from the flame is computed using an assumed fraction of the flame heat release, geometric view factors based on the radiant source (point, line, or volume), and average flame and ambient gas conditions (temperature and steam content). Radiation from the ambient gas and re-radiation from the walls are treated explicitly. Heat transfer to the concrete drywell and between walls is calculated using a transient one dimensional heat conduction model and an approximate numerical solution technique.

The results given for the BWR standard problem are conservative in that the fire and plume centerline velocity and temperature are used as an estimate for the gas velocity and temperature at the wall. While it is recognized that these values are overestimates, particularly for the drywell wall, using these values should insure that the computed temperatures and fluxes are upper bounds to what would be observed in a real accident. In order to obtain more realistic "best estimate" results, experimental data and more detailed, multi-dimensional calculations for the wetwell geometry are needed.

The flame-plume model used in this analysis is based on the results of experiments with small scale (10-100kW) fires on laboratory burners. There is a large uncertainty in extrapolating these data to the multi-megawatt fires considered in the present problem. In addition, the sparger-suppression pool system is a very different type of source than the simple burners used in laboratory experiments. The discrete distribution of bubbles and the unsteady motion of the pool surface may have a large influence on the fire environment. Other issues include the distribution of the source of the direct fire radiation and the influence of confinement on fire and plume entrainment.

Given the limitations discussed above, SNL1 results indicate that there is a potential for generating heat fluxes and temperatures large enough to damage equipment located in the wetwell.

To better assess the problem, a more detailed "best estimate" calculation should be developed and calibrated with the results of the upcoming 1/4 scale tests.

#### 7.4.3 SNL2 Method

The SNL2 calculations were performed using the HECTR computer code (Ref. 11). HECTR is a lumped-parameter containment analysis code developed for calculating the containment atmosphere pressure-temperature response to hydrogen burns. Four gases are modeled: steam, nitrogen, oxygen and hydrogen. To perform a HECTR calculation, the containment being modeled is divided into regions called compartments with flow between compartments occurring at junctions. Gases within each compartment are assumed to be instantaneously mixed. The pressure temperature and composition of gases are calculated by solving the mass, momentum and energy conservation equations for the compartments and junctions. The thermal response of surfaces and equipment in the containment is calculated using either one-dimensional finite difference slabs or lumped masses. Models are used to calculate hydrogen combustion, radiative heat transfer, convection heat transfer and steam condensation or evaporation.

The HECTR burn model was modified for these calculations to make it more representative of diffusion flame burning. Burning was only allowed in certain "flame compartments" which burned hydrogen at the same rate as it was injected into the compartment. Burning was stopped if the oxygen concentration in these compartments fell below 5%.

The temperature calculated by HECTR in the flame compartments represent average values for the entire flame region. Since radiative heat transfer varies with the fourth power of temperature, using this average temperature causes the radiative heat transfer to be too low for this problem. To account for this, energy was removed from the gases in the compartments

that were burning, and distributed to the gases in neighboring compartments and to surfaces near the flame. The distribution of the energy among the compartments and surfaces was based on the absorptivity of gases in the compartments and absorptivity and view factors of surfaces.

For the nine-sparger cases, the burning was assumed to occur within nine cylindrical compartments centered above the spargers. Each cylinder had a radius of 1.5 m and a height calculated from an experimental correlation. For the single-sparger cases, the flame was modeled as a stack of three truncated cones, with a radius at the base of 1.5 m and spreading .11 m horizontally per meter above the base. The height of the stack of compartments was calculated from an experimental correlation and the hydrogen was assumed to burn linearly along the flame. For both the single-sparger and nine-sparger cases, the flow loss coefficients were adjusted until the flow rate at the top of the flame compartments approximately equaled the flow rate predicted by more detailed flame models.

The HECTR results represent lower bounds for conditions in and near the flame because of the lumped-parameter approximation. HECTR is most useful for calculating bulk conditions in the containment, rather than details within the flame region. The calculations performed by the other participants in the working group are more suited for the flame region, but the HECTR results are useful for providing boundary conditions for these calculations. Future improvements planned for HECTR will allow it to calculate both bulk containment conditions and conditions in and near the flame.

#### 7.4.4 LANL Method

The HMS-Burn computer program simulates Hydrogen Mixing Studies and Burning in time-dependent, fully three-dimensional geometries. The code is capable of transporting and mixing four species ( $H_2$ ,  $O_2$ ,  $N_2$ , and  $H_2O$ ) in highly buoyancy driven flows due to thermal and species concentration gradients without the restrictions of the classical Boussinesq approximation.

Equations for mass, momentum, and energy conservation; wall heat transfer including convection and radiation effects; and chemical kinetics are written in finite-differences form for their numerical solution. The nonlinear finite-difference equations are then solved iteratively using a point relaxation method. Since the problem is only concerned with low-speed flows where the propagation of pressure waves need not be resolved, a modified Implicit Continuous-fluid Eulerian solution technique is used where the species densities are functions of the global or compartment pressure and not of the local pressure. The geometric region of interest is divided into many finite-size space-fixed zones called computational cells that collectively form the computing mesh. The finite-difference equations for all the unknown quantities such as velocities; wall, gas, and structure temperatures; species densities; pressure; and heat fluxes for the advanced time form a complex system of coupled, non-linear algebraic equations.



Generally, the detailed solutions for cases "B", "C" and "3" indicate a very sharp rise in the drywell wall heat flux shortly after hydrogen ignition followed by a decrease as the wall surface temperature increases. Maximum wall heat fluxes and temperatures are computed for the single flame case 3 on the wetwell wall of roughly 30,000 BTU/hr.-ft.<sup>2</sup> and maximum wall temperatures around 932°F.

## 7.5 Numerical Results and Sensitivity Studies

Tables 2.4 through 7.10 summarize the results of the calculations. In the tables the terms "maximum", "minimum", and "best-estimate" appear. These terms require some definition as used here. The "maximum" and "minimum" values do not correspond to theoretical bounds. Rather, they correspond to the highest and lowest values that the persons working the problem believe to be reasonably achievable. FMRC appropriately referred to the maximum values as "near maximum." The "best-estimate" values represent the best we can do at this time, but with the large uncertainties involved these values should not be weighted too heavily. Users of these results should note that the peak fluxes are present only for short periods of time; using the peak fluxes for the entire duration of the transient would be unduly conservative.

Figures 7.3 through 7.18 are presented to provide the reader with a qualitative picture of transient progression. Examples are provided for pressure rise, gas temperature rise, heat flux, and wall temperature. Case C was chosen for example purposes. However, the other nine-sparger cases behave qualitatively the same. The single-sparger cases exhibit enhanced local effects, i.e., higher local temperatures and heat fluxes. However, the trends are similar.

## 7.6 Considerations of Loads and Likelihood of Containment Failure\*

This problem dealt with the Mark III containment. The geometrical arrangement of the Mark III drywell is such that the effects of corium-concrete interactions will be similar to those in Mark I containments. Because of the much larger volume of the Mark III, however, pressurization rates will be slower than those reported for the Mark I or Mark II (SP-4 and SP-5). On the other hand the Mark III containment is not inerted and the potential consequences of hydrogen burns must be considered. In fact all owners of BWR Mark III plants are now required to install deliberate ignition devices to control potential releases of H<sub>2</sub> to containment. The Grand Gulf power plant was selected to provide the specifics for this problem.

\* Considerations of the likelihood of containment failure from the various load sources described in this report have been provided by the NRR staff and is based on extended discussions with staff consultants and staff members involved in containment loads and performance activities.

First let us consider the global effects of H<sub>2</sub> combustion assuming the H<sub>2</sub> ignition devices are operable. The extent of burning would be limited by the quantities of oxygen available. In this limit the required quantity of hydrogen would correspond to oxidation of nearly 65% of all the zirconium in the cladding. Resulting peak pressures of 2 bar (30 psia) can thus be calculated as an upper bound assuming that the H<sub>2</sub> is burned continuously as it is released to the wetwell. Such loads are well below the estimated 5 bar (75 psia) capability of the Mark III containment and the likelihood of containment overpressure failure through this mechanism is thus extremely low. However, if the H<sub>2</sub> release rates are sufficiently high, standing flames can be produced in the wetwell above the suppression pool. Local heat fluxes in the vicinity of the flames can produce high local temperatures and could result in degradation of seals in the vicinity of the flames. Seal degradation could result in loss of or drywell integrity allowing the fission products released from the fuel to by-pass the suppression pool where they would normally be scrubbed. Thus seal degradation is an important consideration. The Mark III standard problem was, therefore, focused on local thermal effects due to standing flames in the wetwell.

Localized heating can result from diffusion flames developed near the suppression pool surface as the hydrogen is discharged from the primary system, through the SRVs, to the wetwell air space. Such localized heating can affect the integrity of penetration seals which are expected to degrade at temperatures around 438°K (330°F). The position of the flames above the SRVs (assumed to release the hydrogen) and the rate and duration of the hydrogen source to them were considered parametrically. Peak gas temperatures were found to be moderated by large gas entrainment rates to levels around 1,370°K (2,000°F). The wall (and seal) temperatures depend on position and the heat flux delivered. In general, values in the range of 10<sup>3</sup> to 10<sup>4</sup> BTU/hr. ft.<sup>2</sup> were determined. Evaluations of consequent seal degradation and leak area development have been carried out by the CPWG. They conclude that important seals (including the drywell and containment personnel airlocks) retain their integrity under these conditions.

## 7.7 Conclusions and Recommendations

Despite the high degree of uncertainty regarding diffusion flame phenomena, there is reasonable agreement among the authors regarding the expected loads. Generally, the ranges of values given by the various groups overlap and are of the same order. The spread in the values is large, based on current uncertainties. Much of the uncertainty should be reduced, once the 1/4 scale tests at FMRC are completed. Our most important recommendation is that these data be factored into future consideration of diffusion flames after the results are available.

Regarding the specific results produced by this group, we can draw several conclusions. First, diffusion flames should pose no direct threat to containment due to overpressure. The concerns for diffusion flames are correctly confined to the response of equipment and containment penetration seals. Second, because of large amounts of gas entrainment, the peak gas temperatures will be well below theoretical maximum flame temperatures. However, gas temperatures on the order of 2000°F are possible, and the high entrainment rates will lead to some general heating of containment, producing temperatures well above ambient throughout the containment. Finally, peak heat fluxes may range from less than  $10^3$  BTU/hr./ft.<sup>2</sup> to in excess of  $3 \times 10^4$  BTU/hr./ft.<sup>2</sup>, depending on the scenario and the assumptions made.

We urge caution to those who attempt to extrapolate these results to examine the response of particular pieces of equipment or penetrations. First, one should examine the particular sequence and determine which, if any, of the cases considered here is most applicable. Second, it must be recognized that the response of the item in question may be different from the walls and surfaces considered here. The heat flux is dependent on the surface temperature, which in turn is dependent on the properties and geometry of the material involved

Table 7.1

Grand Gulf Containment Geometric Data  
(Volume  $1.38 \times 10^6$  ft<sup>3</sup>)

Region	Description	Mass (lbs)	Heat Transfer Surface Area (ft <sup>2</sup> )	Length Scale	
1	gratings	50,900	6,650 <sup>a</sup>	3/8"	
	I-beams, decks equipment	12,000	1,180 <sup>a</sup>	1/2"	
	Misc. steel	10,000	980 <sup>a</sup>	1/2"	
	Concrete floor	28,000	250	9"	
	Elev. 111' 7.5" to 134'	Containment concrete wall	4.578x10 <sup>6</sup>	8,720	3.5'
	Drywall cyla. wall	4.376x10 <sup>6</sup>	5,830	5'	
	Containment steel liner	88,840	8,720	1/4"	
2	gratings	109,760	14,340 <sup>a</sup>	3/8"	
	I-beams, decks	198,020	19,400 <sup>a</sup>	1/2"	
	HCU modules, equipment	187,950	18,410	1/4"	
	Misc. steel	150,000	14,690	1/2"	
	Concrete floor	259,410	2,310	9"	
	Concrete steam tunnel	1.7x10 <sup>6</sup>	2,000	4'	
	Elev. 134' to 143'	Containment concrete wall	1.843x10 <sup>6</sup>	3,510	3.5'
	Drywall cyl. wall	1.760x10 <sup>6</sup>	2,350	5'	
Containment steel liner	35,730	3,510	1/4"		
3	steel	3.933x10 <sup>6</sup>	192,660	1/2"	
	concrete	12.966x10 <sup>6</sup>	21,610	4'	
	upper pool water	1.588x10 <sup>6</sup>	3,370	8'	
	Elev. 143' to 208'10"	containment concrete wall	13.466x10 <sup>6</sup>	25,650	3.5'
	drywall clys. wall	8.116x10 <sup>6</sup>	10,820	5'	
containment steel liner	261,380	25,650	1/4"		
4	steel	415,570	40,710 <sup>a</sup>	1/2"	
	Elev. 208'10" to	containment concrete wall	18.590x10 <sup>6</sup>	35,410	3.5'
	299'7"	containment steel liner	360,980	35,410	1/4"

<sup>a</sup>Both sides of the structural/equipment material are accounted for in evaluating the heat transfer surface area

TABLE 7.2

INITIAL CONDITIONS  
(at start of H<sub>2</sub> Injection)

<u>Parameter</u>	<u>Value</u>
Gas Temperature	120 F
Pressure	17 psia
Steam Mole Fraction	0.19
H <sub>2</sub> Injection Temperature	155 F
Suppression Pool Temperature	155 F
Other Surfaces	120 F

Table 7.3  
Hydrogen Source Terms

Case	Location	Release Rate lbm/min	Duration min
A	8 non-adjacent SRVs plus 1 adjacent SRV	40	75
B	8 non-adjacent SRVs plus 1 adjacent SRV	75	40
C	8 non-adjacent SRVs plus 1 adjacent SRV	100	30
1	8 non-adjacent SRVs plus 1 adjacent SRV	50	30
2	8 non-adjacent SRVs plus 1 adjacent SRV	100	10
3	1 SRV	100	30
4	1 SRV	50	10

SRV = Safety Relief Valve

Table 7.4  
Case A Results

Parameter	FMRC	LANL	SNL1	SNL2
Peak Pres. (psia)				
Maximum	28	--	--	25
Minimum	21	--	--	20
Best Estimate	--	--	--	22
Peak Gas Temp. (F)				
Maximum	1832	--	--	2420
Minimum	---	--	--	458
Best Estimate	---	--	1832	1826
Peak Heat Fluxes (1000 BTU/hr/ft**2)				
Drywell Wall - 10'				
Maximum	8.0	--	5.7	7.9
Minimum	2.9	--	2.9	1.8
Best Estimate	---	--	--	--
Drywell Wall - 20'				
Maximum	6.2	--	2.9	6.3
Minimum	2.9	--	1.7	1.6
Best Estimate	---	--	--	--
Drywell Wall - 30'				
Maximum	5.6	--	2.3	5.7
Minimum	2.9	--	1.5	1.4
Best Estimate	---	--	--	--
Wetwell Wall - 10'				
Maximum	1.0	--	4.8	4.4
Minimum	0.7	--	1.6	0.6
Best Estimate	---	--	--	--
Wetwell Wall - 20'				
Maximum	0.73	--	3.0	4.1
Minimum	0.5	--	1.3	0.5
Best Estimate	---	--	--	--
Wetwell Wall - 30'				
Maximum	0.52	--	2.3	3.8
Minimum	0.3	--	1.1	0.5
Best Estimate	---	--	--	--

Table 7.5  
Case B Results

Parameter	FMRC	LANL	SNL1	SNL2
-----				
Peak Pres. (psia)				
Maximum	30	--	--	28
Minimum	--	--	--	21
Best Estimate	--	27	--	24
Peak Gas Temp. (F)				
Maximum	1832	--	--	2420
Minimum	---	--	--	624
Best Estimate	---	2372	1832	1826
Peak Heat Fluxes (1000 BTU/hr/ft <sup>2</sup> )				
Drywell Wall - 10'				
Maximum	12.	--	10.8	12.0
Minimum	3.8	--	5.1	3.2
Best Estimate	---	12.	--	--
Drywell Wall - 20'				
Maximum	8.8	--	3.8	8.9
Minimum	3.8	--	2.1	2.9
Best Estimate	---	6.	--	--
Drywell Wall - 30'				
Maximum	7.7	--	2.8	7.6
Minimum	3.7	--	1.7	2.5
Best Estimate	---	3.5	--	--
Wetwell Wall - 10'				
Maximum	1.9	--	6.7	7.0
Minimum	1.3	--	2.0	0.9
Best Estimate	---	1.5	--	--
Wetwell Wall - 20'				
Maximum	1.5	--	3.8	6.3
Minimum	1.0	--	1.5	0.8
Best Estimate	---	1.6	--	--
Wetwell Wall - 30'				
Maximum	1.1	--	2.9	5.7
Minimum	0.7	--	1.2	0.7
Best Estimate	---	1.7	--	--
-----				



Table 7.6  
Case C Results

Parameter	FMRC	LANL	SNL1	SNL2
-----				
Peak Pres. (psia)				
Maximum	32	--	--	29
Minimum	24	--	--	21
Best Estimate	--	25	--	25
Peak Gas Temp. (F)				
Maximum	1832	--	--	2420
Minimum	---	--	--	730
Best Estimate	---	2552	1832	1826
Peak Heat Fluxes (1000 BTU/hr/ft**2)				
Drywell Wall - 10'				
Maximum	14.	--	16.1	13.9
Minimum	4.3	--	7.2	4.4
Best Estimate	---	13	--	--
Drywell Wall - 20'				
Maximum	10.	--	4.7	10.1
Minimum	4.3	--	2.4	3.8
Best Estimate	---	6.5	--	--
Drywell Wall - 30'				
Maximum	9.0	--	3.2	8.9
Minimum	4.3	--	1.8	3.5
Best Estimate	---	3.5	--	--
Wetwell Wall - 10'				
Maximum	2.4	--	7.9	8.9
Minimum	1.6	--	2.3	1.1
Best Estimate	---	1.6	--	--
Wetwell Wall - 20'				
Maximum	2.1	--	4.6	7.9
Minimum	1.4	--	1.7	1.0
Best Estimate	---	1.7	--	--
Wetwell Wall - 30'				
Maximum	1.5	--	3.3	7.0
Minimum	1.0	--	1.3	0.9
Best Estimate	---	1.8	--	--
-----				

Table 7.7  
Case 1 Results

Parameter	FMRC	LANL	SNL1	SNL2
-----				
Peak Pres. (psia)				
Maximum	27	--	--	25
Minimum	--	--	--	20
Best Estimate	--	--	--	22
Peak Gas Temp. (F)				
Maximum	1832	--	--	2420
Minimum	---	--	--	496
Best Estimate	---	--	--	1826
Peak Heat Fluxes (1000 BTU/hr/ft**2)				
Drywell Wall - 10'				
Maximum	9.2	--	--	9.2
Minimum	3.2	--	--	2.3
Best Estimate	---	--	--	--
Drywell Wall - 20'				
Maximum	7.0	--	--	7.0
Minimum	3.2	--	--	2.0
Best Estimate	---	--	--	--
Drywell Wall - 30'				
Maximum	6.2	--	--	6.3
Minimum	3.2	--	--	1.7
Best Estimate	---	--	--	--
Wetwell Wall - 10'				
Maximum	1.3	--	--	4.8
Minimum	0.9	--	--	0.6
Best Estimate	---	--	--	--
Wetwell Wall - 20'				
Maximum	0.93	--	--	4.4
Minimum	0.6	--	--	0.5
Best Estimate	---	--	--	--
Wetwell Wall - 30'				
Maximum	0.67	--	--	3.8
Minimum	0.4	--	--	0.5
Best Estimate	---	--	--	--
-----				

Table 7.8  
Case 2 Results

Parameter	FMRC	LANL	SNL1	SNL2
-----				
Peak Pres. (psia)				
Maximum	28	--	--	28
Minimum	--	--	--	21
Best Estimate	--	--	--	24
Peak Gas Temp. (F)				
Maximum	1832	--	--	2420
Minimum	---	--	--	701
Best Estimate	---	--	--	1826
Peak Heat Fluxes (1000 BTU/hr/ft**2)				
Drywell Wall - 10'				
Maximum	14.	---	---	13.9
Minimum	4.3	---	---	4.4
Best Estimate	---	---	---	--
Drywell Wall - 20'				
Maximum	10.	---	---	10.1
Minimum	4.3	---	---	3.8
Best Estimate	---	---	---	--
Drywell Wall - 30'				
Maximum	9.0	---	---	8.9
Minimum	4.3	---	---	3.5
Best Estimate	---	---	---	--
Wetwell Wall - 10'				
Maximum	2.4	---	---	8.2
Minimum	1.6	---	---	1.0
Best Estimate	---	---	---	--
Wetwell Wall - 20'				
Maximum	2.1	---	---	7.0
Minimum	1.4	---	---	0.9
Best Estimate	---	---	---	--
Wetwell Wall - 30'				
Maximum	1.5	---	---	6.0
Minimum	1.0	---	---	0.7
Best Estimate	---	---	---	--
-----				

Table 7.9  
Case 3 Results

Parameter	FMRC	LANL	SNL1	SNL2
-----				
Peak Pres. (psia)				
Maximum	32	--	--	32
Minimum	24	--	--	22
Best Estimate	--	25	--	27
Peak Gas Temp. (F)				
Maximum	1832	--	--	2420
Minimum	---	--	---	539
Best Estimate	---	2732	1832	1826
Peak Heat Fluxes (1000 BTU/hr/ft**2)				
Drywell Wall - 10'				
Maximum	28.	--	31.4	31.4
Minimum	13.	--	--	3.8
Best Estimate	---	30	--	--
Drywell Wall - 20'				
Maximum	29.	--	33.0	33.0
Minimum	13.	--	--	4.8
Best Estimate	---	21	--	--
Drywell Wall - 30'				
Maximum	30.	--	31.1	31.1
Minimum	13.	--	--	5.7
Best Estimate	---	12.5	--	--
Wetwell Wall - 10'				
Maximum	4.0	--	11.1	5.7
Minimum	2.7	--	--	0.7
Best Estimate	---	4.0	--	--
Wetwell Wall - 20'				
Maximum	4.4	--	12.4	6.7
Minimum	2.9	--	--	0.8
Best Estimate	---	4.75	--	--
Wetwell Wall - 30'				
Maximum	4.5	--	10.8	7.6
Minimum	3.0	--	--	1.0
Best Estimate	---	5.5	--	--
-----				

Table 7.10  
Case 4 Results

Parameter	FMRC	LANL	SNL1	SNL2
-----				
Peak Pres. (psia)				
Maximum	24	--	--	25
Minimum	22	--	--	20
Best Estimate	--	--	--	22
Peak Gas Temp. (F)				
Maximum	1832	--	--	2420
Minimum	---	--	--	399
Best Estimate	---	--	1832	1826
Peak Heat Fluxes (1000 BTU/hr/ft**2)				
Drywell Wall - 10'				
Maximum	21.	--	23.8	23.8
Minimum	9.2	--	--	2.4
Best Estimate	---	--	--	--
Drywell Wall - 20'				
Maximum	22.	--	24.1	24.1
Minimum	9.2	--	--	3.2
Best Estimate	---	--	--	--
Drywell Wall - 30'				
Maximum	20.	--	19.7	19.7
Minimum	9.2	--	--	3.8
Best Estimate	---	--	--	--
Wetwell Wall - 10'				
Maximum	2.7	--	10.8	2.5
Minimum	1.8	--	--	0.3
Best Estimate	---	--	--	--
Wetwell Wall - 20'				
Maximum	3.0	--	10.5	3.2
Minimum	2.0	--	--	0.4
Best Estimate	---	--	--	--
Wetwell Wall - 30'				
Maximum	2.9	--	7.9	3.5
Minimum	1.9	--	--	0.4
Best Estimate	---	--	--	--
-----				

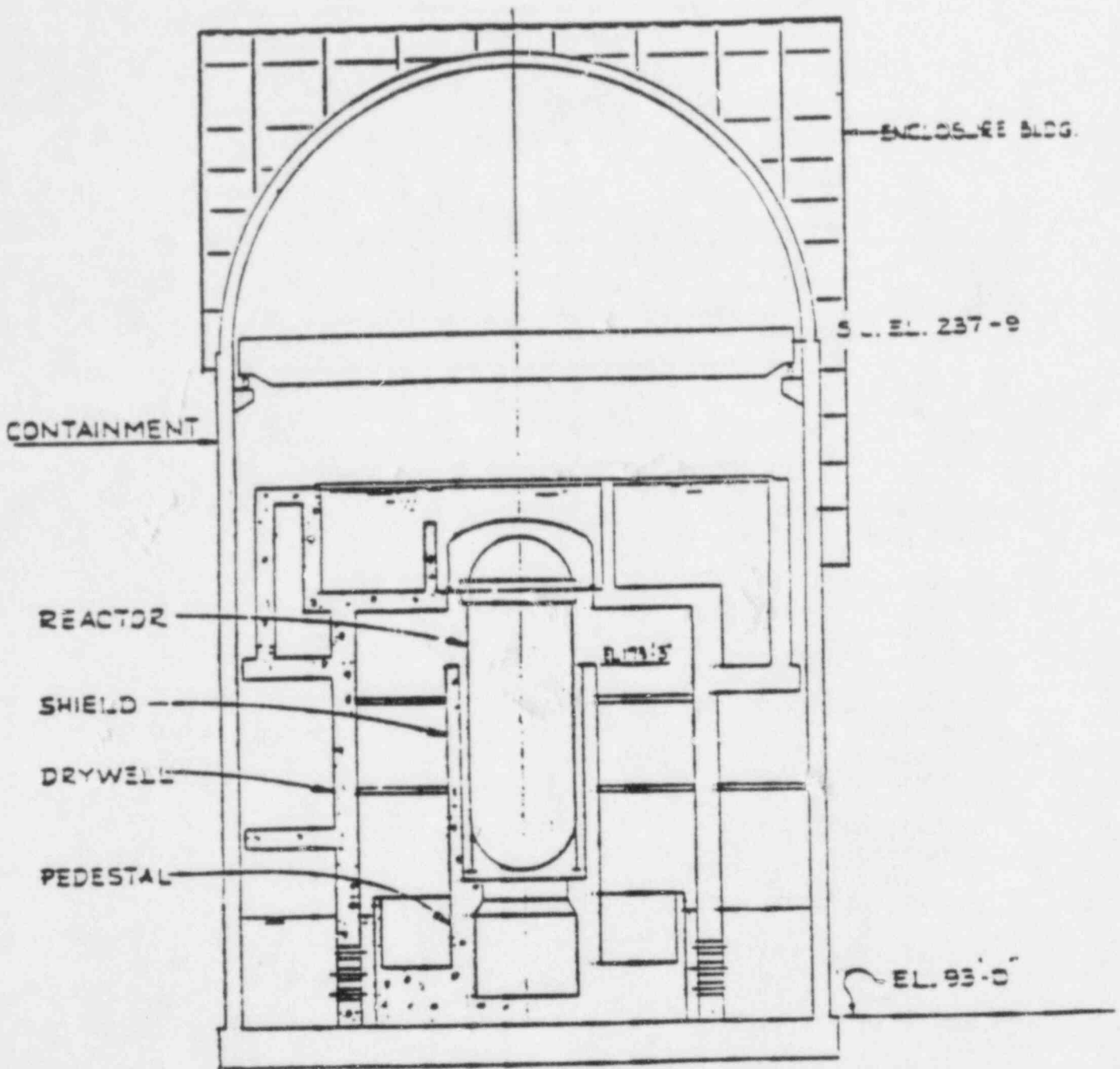


Fig. 7.1 Cutaway view showing reactor pedestal support structure and the cavity beneath the reactor vessel for Plant III.

GRAND GULF

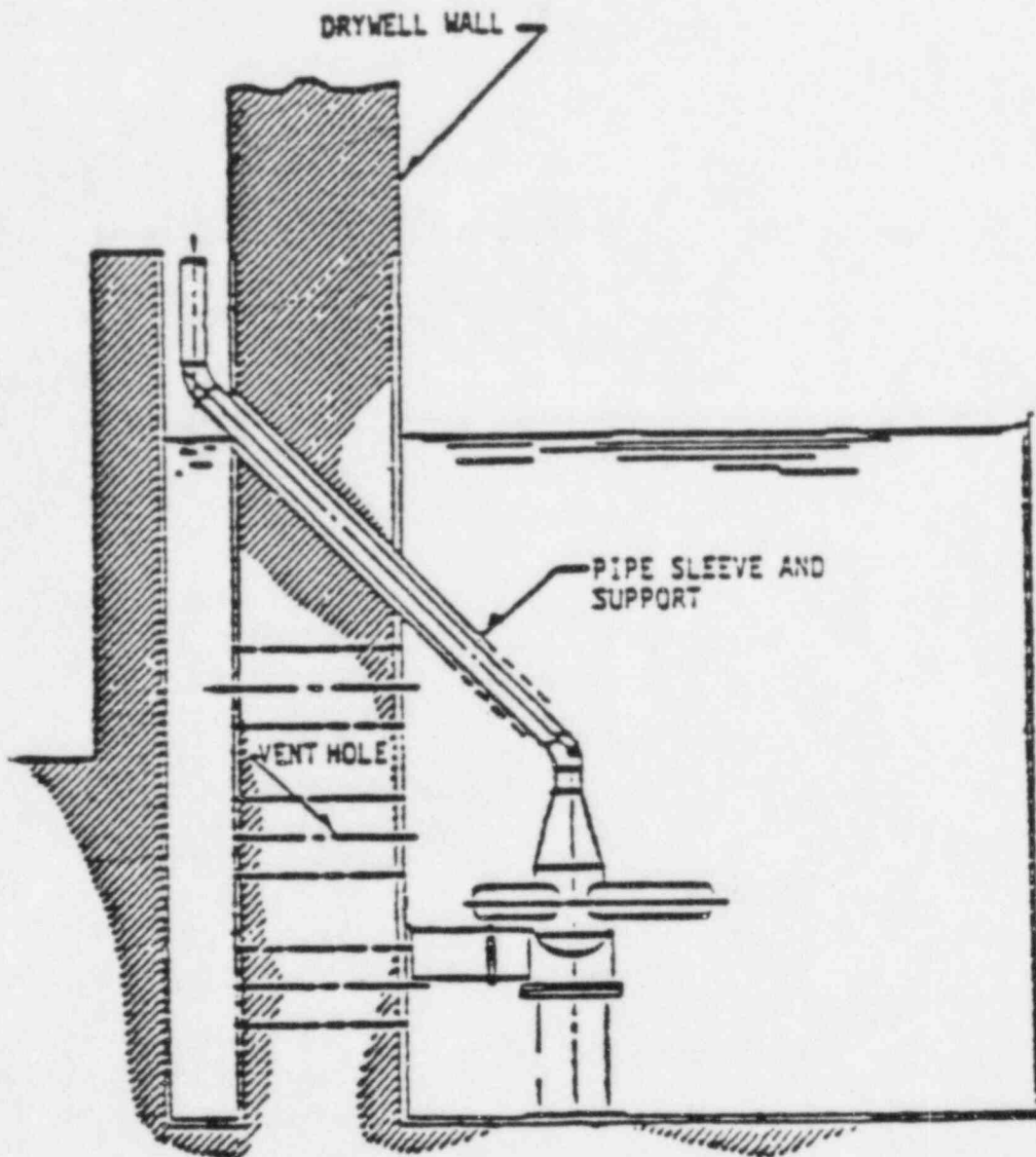


Fig. 7.2 The safety/relief valve discharge is into the portion of the pressure suppression pool lying outside of the drywell.

FMRC RESULTS

CASE C



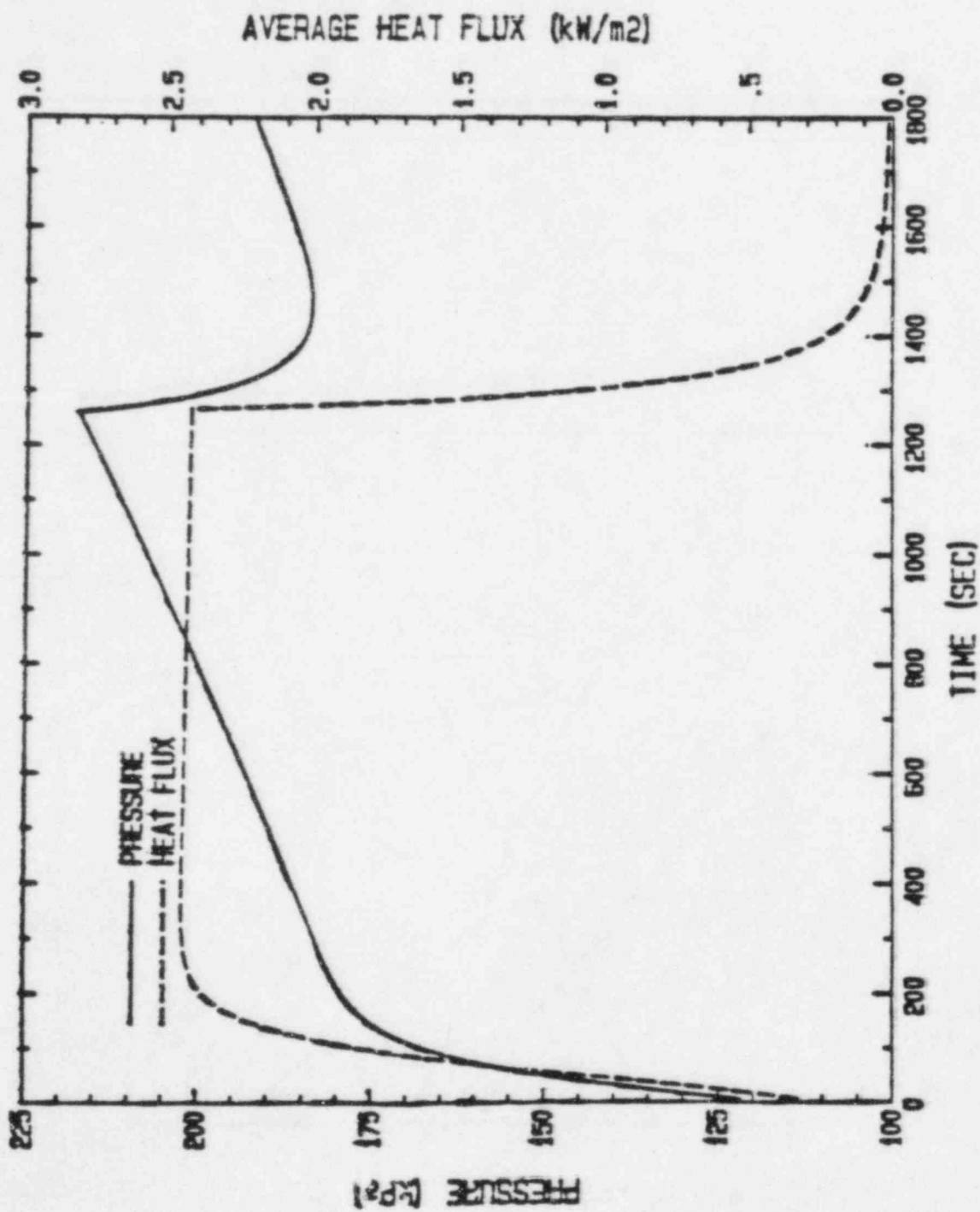


Figure 7.3 FMRC  
 CASE-C : 100 lb/min THROUGH 9 SPARGERS  
 PRESSURE AND AVERAGE HEAT FLUX IN THE CONTAINMENT

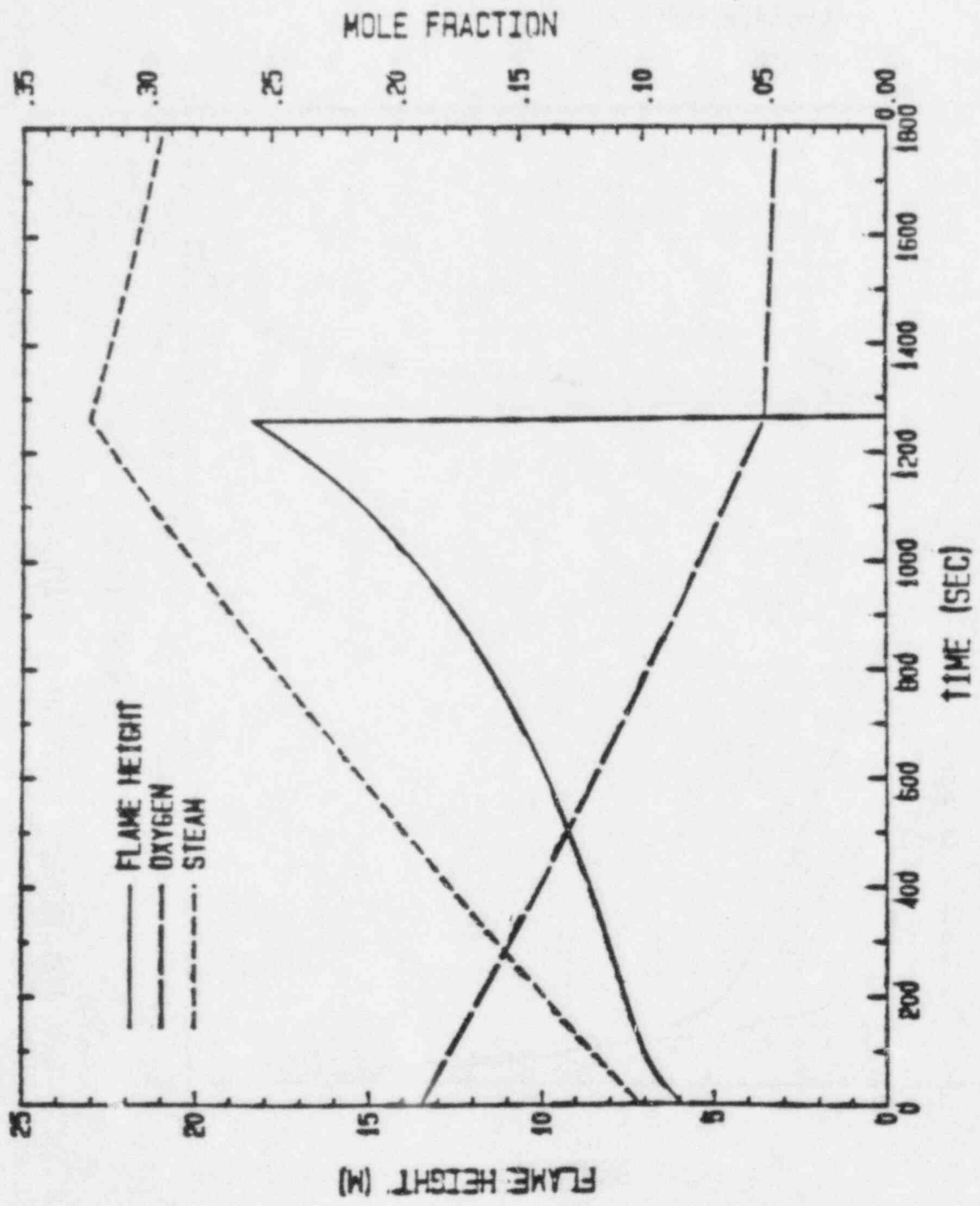


Figure 7.4 FMRC CASE-C: 100 lbm/min THROUGH 9 SPARGERS  
 FLAME HEIGHT, OXYGEN AND STEAM CONCENTRATIONS

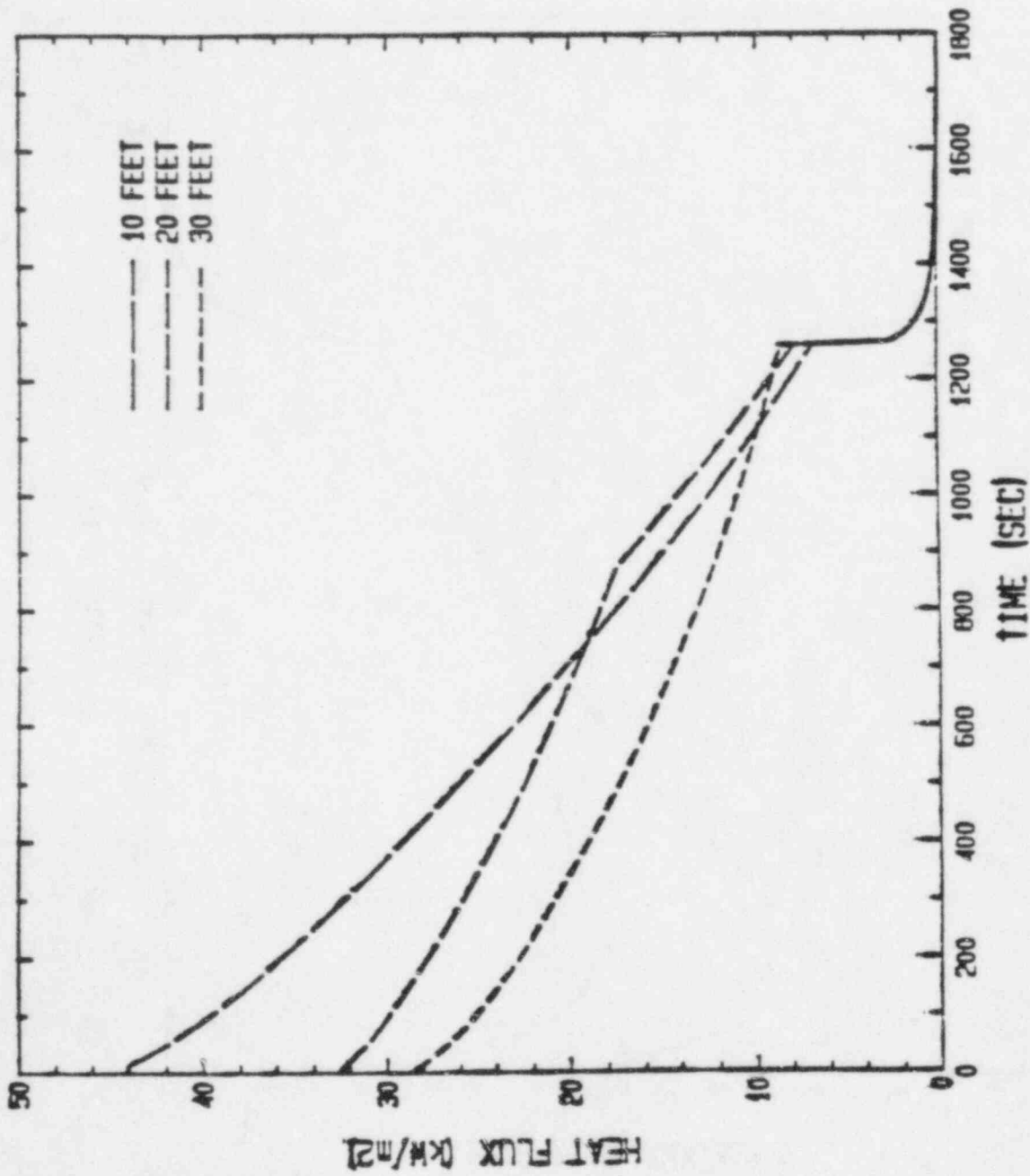


Figure 7.5 EMRC CASE C: 100 lb/min THROUGHGIL 9 SPANGFIB  
INNER WALL PEAK HEAT FLUXES

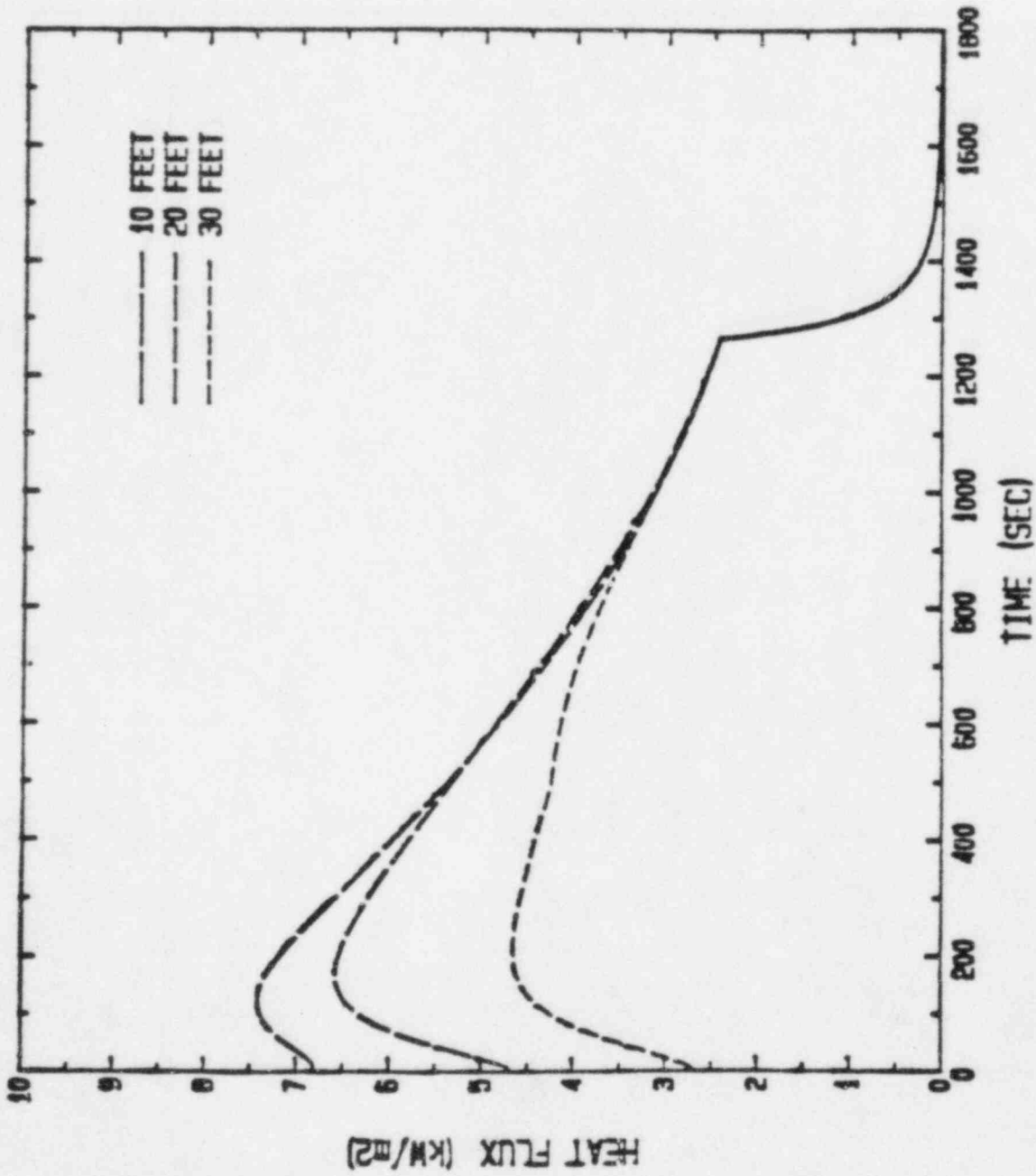


Figure 7.6 FMRC CASE C: 100 lb/min THROUGH 9 SPARGERS  
OUTER WALL PEAK HEAT FLUXES

SNL1 RESULTS

CASE C

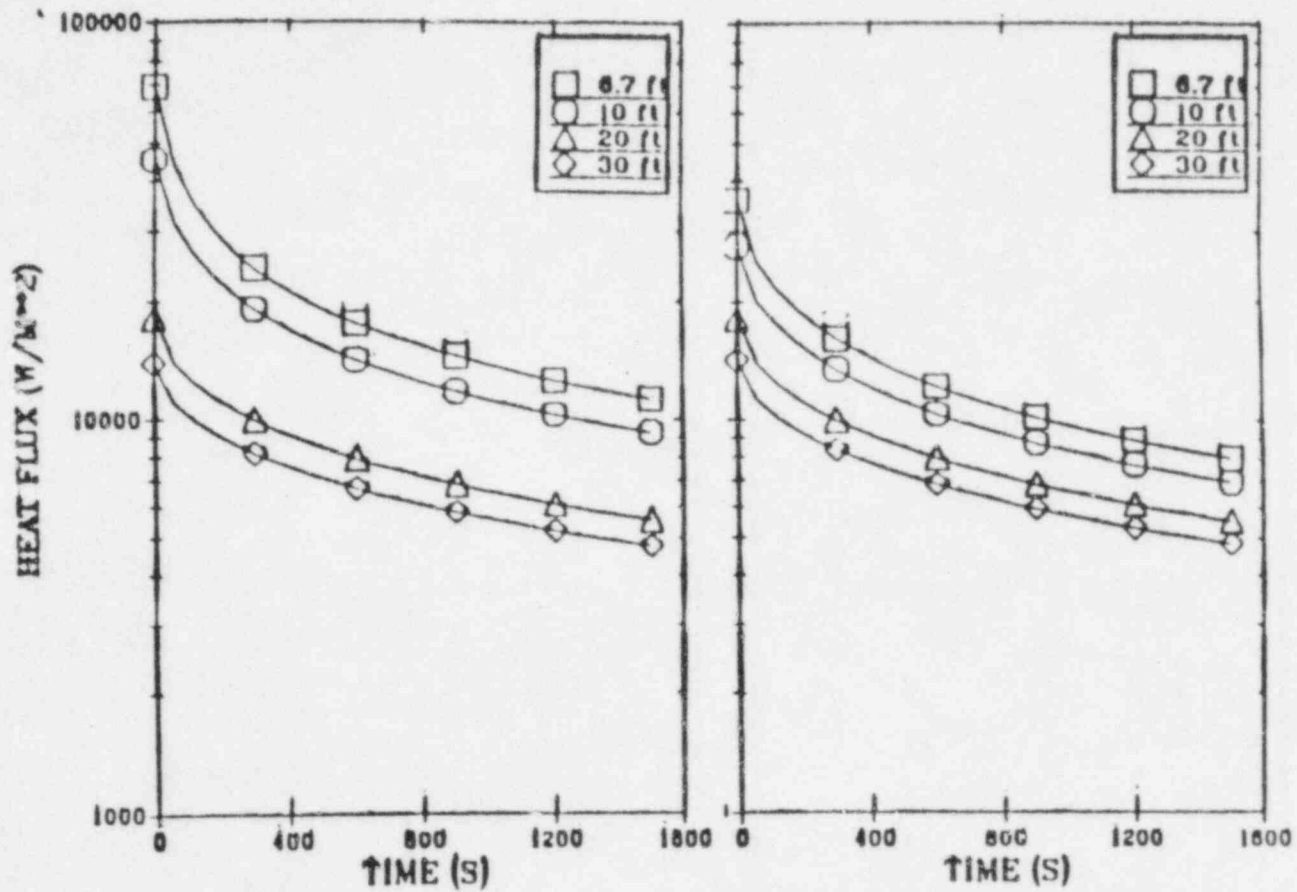


Figure 7.7  
 SNL-1 Case C: 100 lbm/min through 9 spargers. Heat Flux vs. Time  
 (Inner and outer wall heat fluxes at 10', 20', 30' and  $Z_P/2=6.7'$ .)

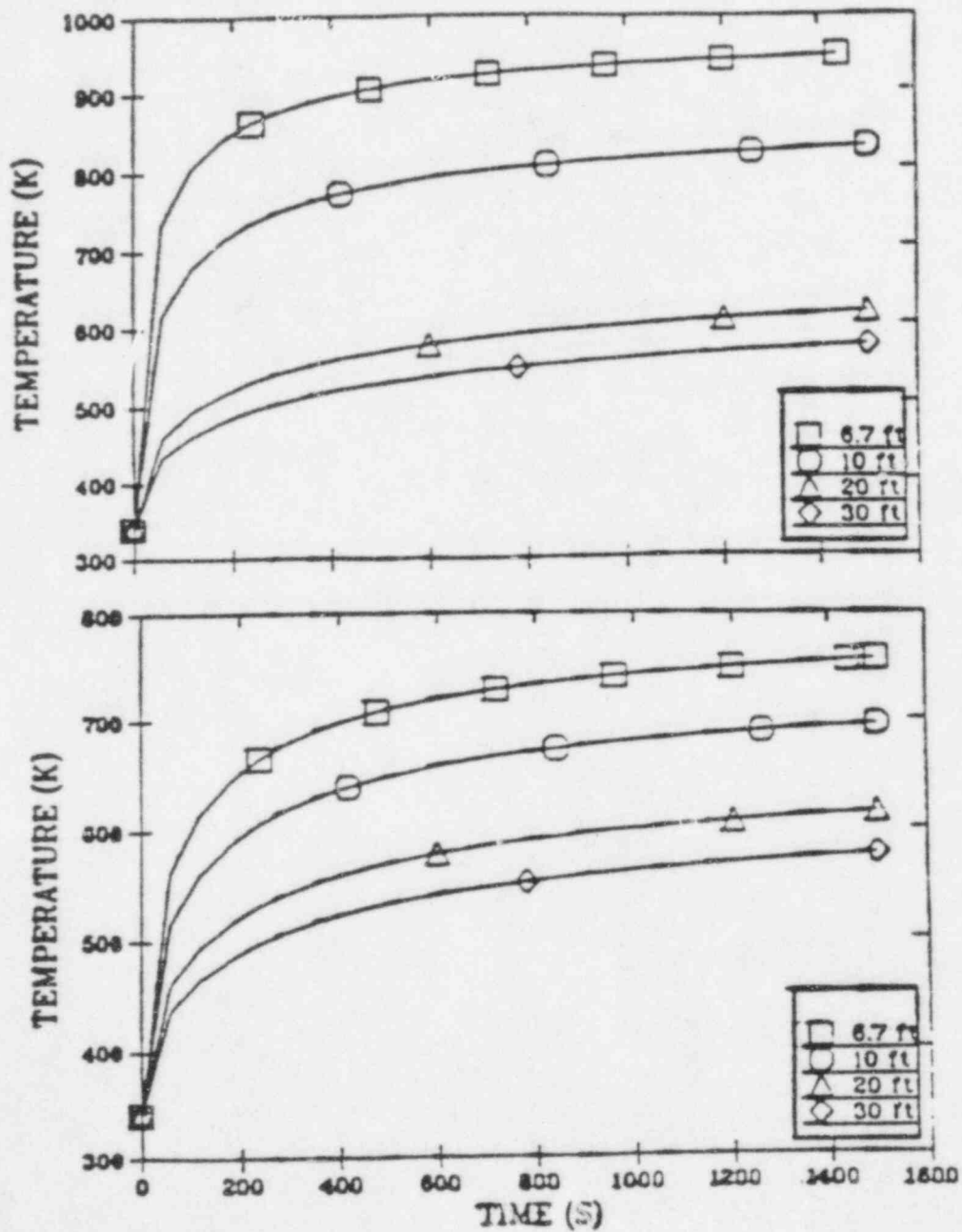


Figure 7.8

SNL1 Case C: 100 lbm/min through 9 spargers. Temperature vs. Time.  
 (Inner and outer wall surface temperatures at 10', 20', 30', and  $Z_F/2 = 6.7'$ .)

SNL2 RESULTS

(HECTR)

CASE C



### Compartment 4

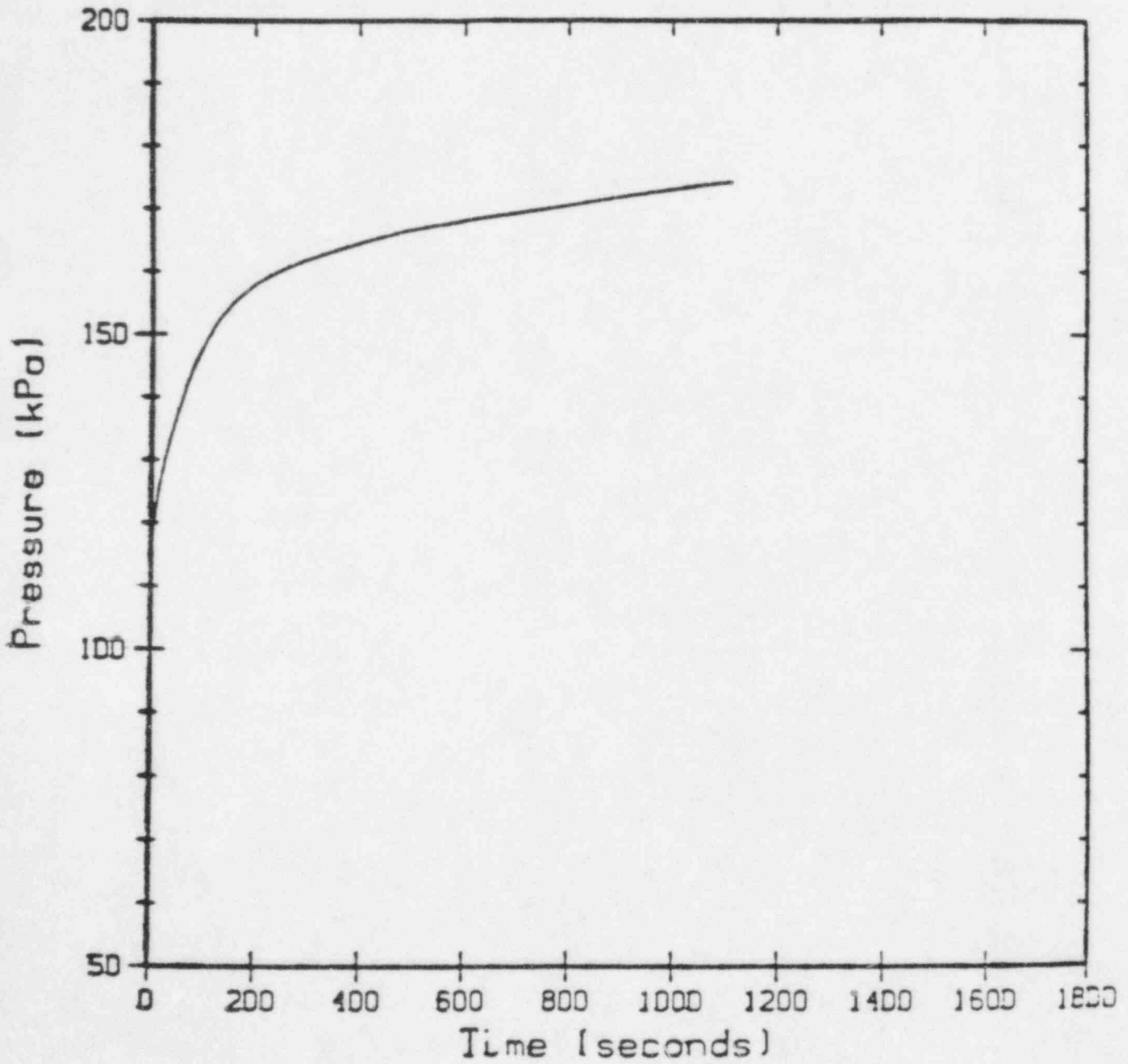


Figure 7.9

SNL2 Case C: Compartment 4: Pressure vs. Time

# Compartment 7

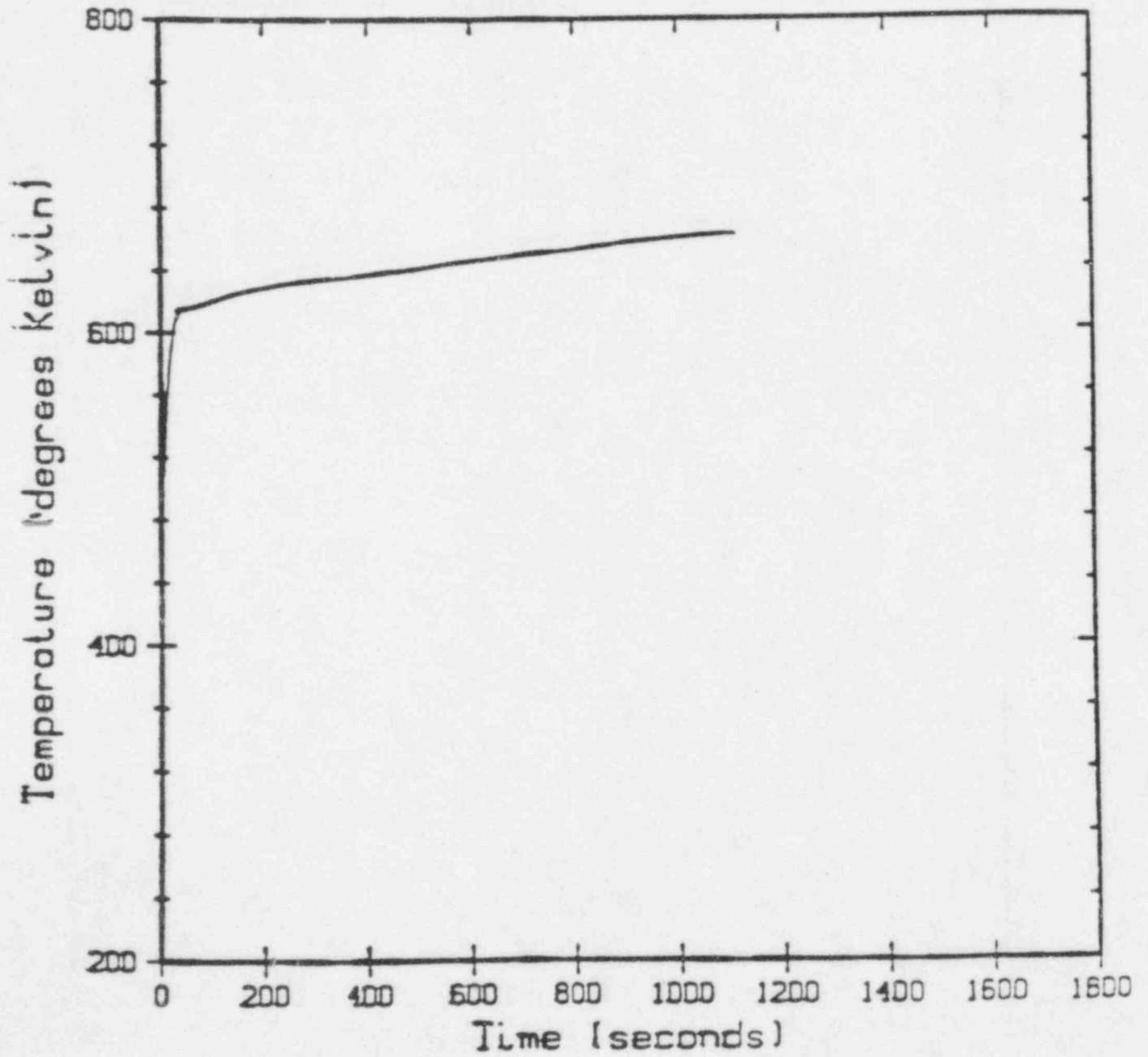


Figure 7.10

SNL2 Case C: Compartment 7: Temperature vs. Time

# Compartment 4

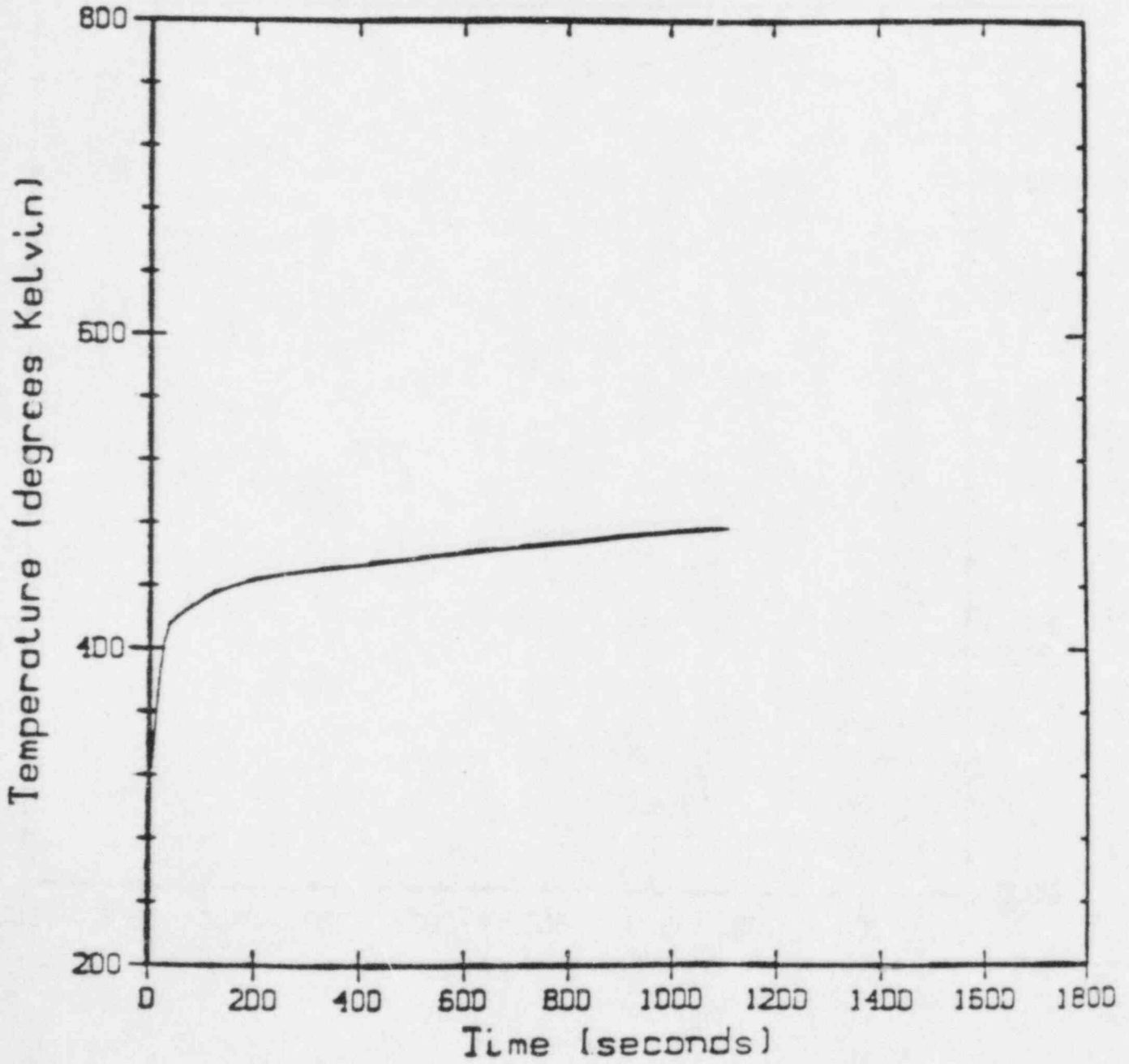


Figure 7.11  
SNL2 Case C: Compartment 4: Temperature vs. Time

Surface 27

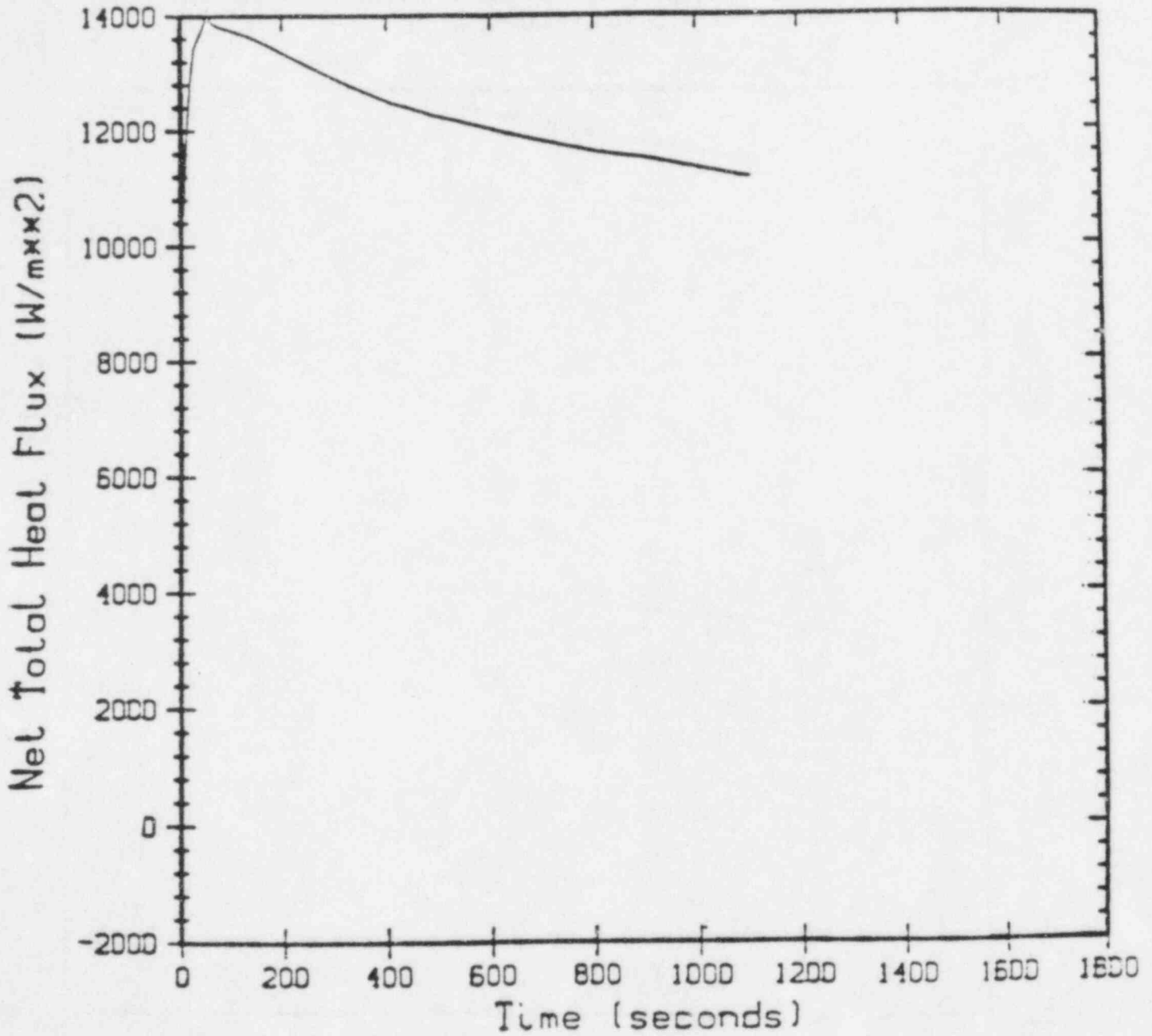


Figure 7.12  
SNL 2 Case C: Surface 27. Net Total Heat Flux vs. Time

Surface 27

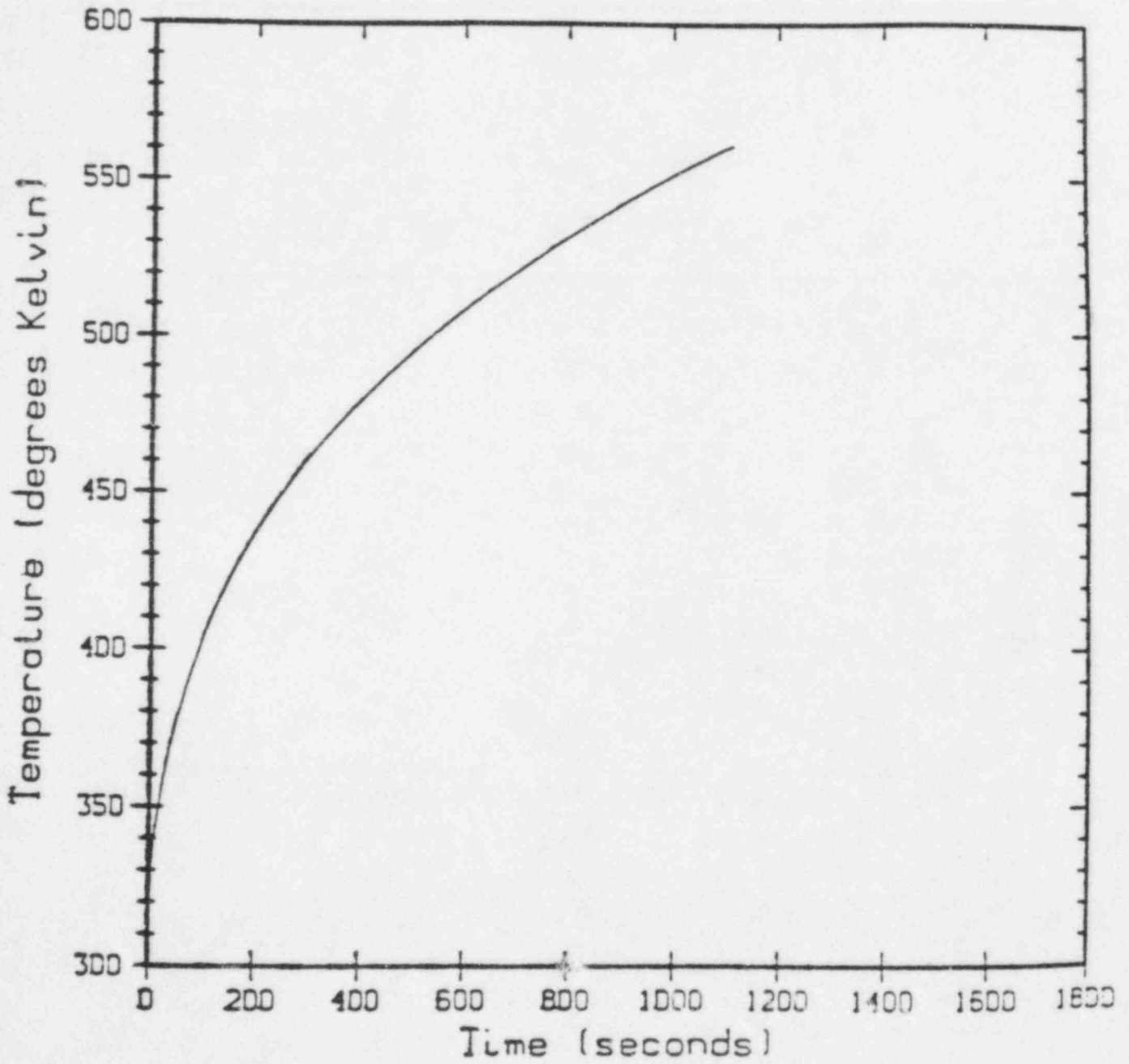


Figure 7.13  
SNL2 Surface 27: Temperature vs. Time

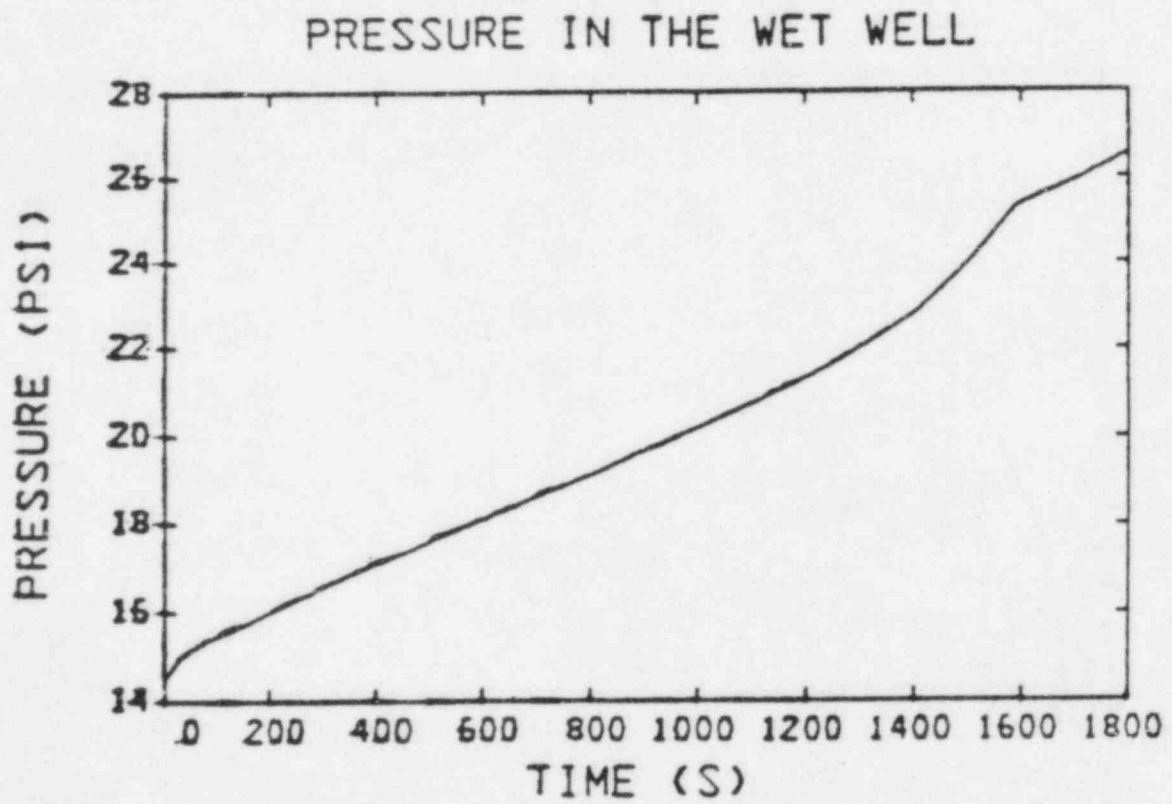


Figure 7.14  
SNL2 Case C: Pressure in the wet well

LANL RESULTS

(HMS)

CASE C

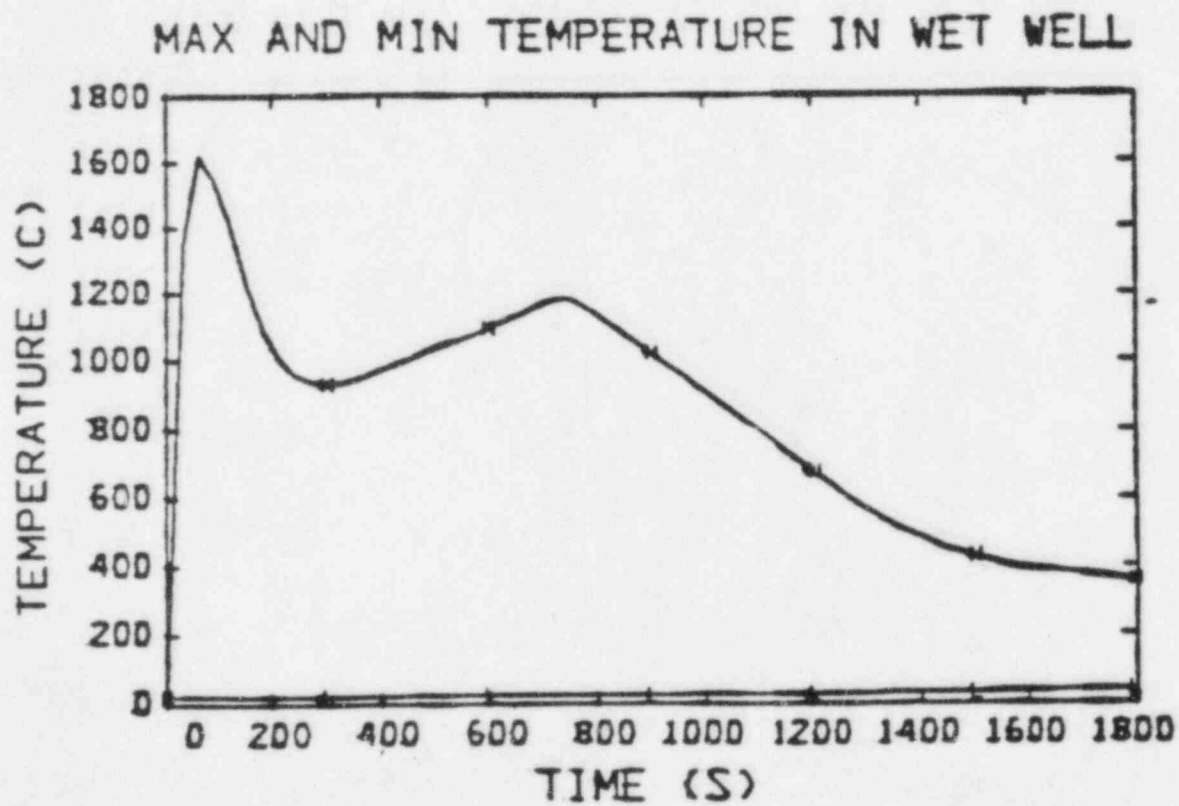
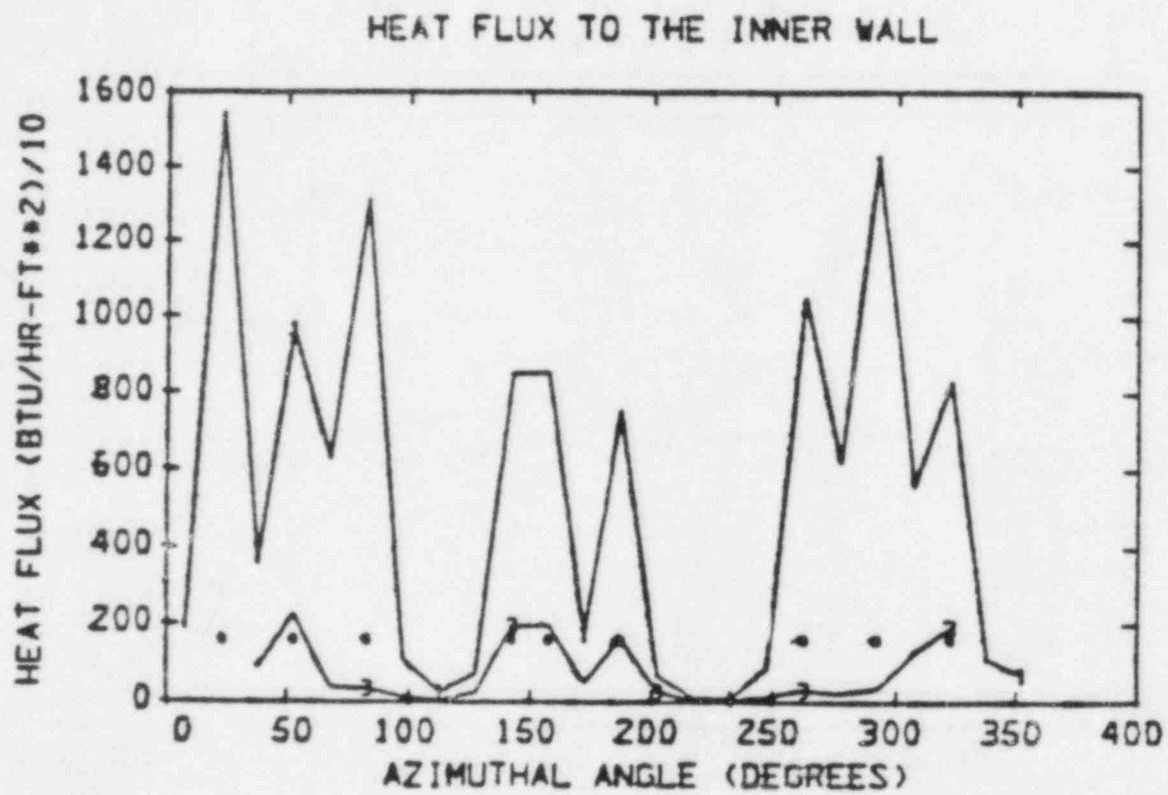


Figure 7.15  
 LANL Max and Min Temperature in Wet Well



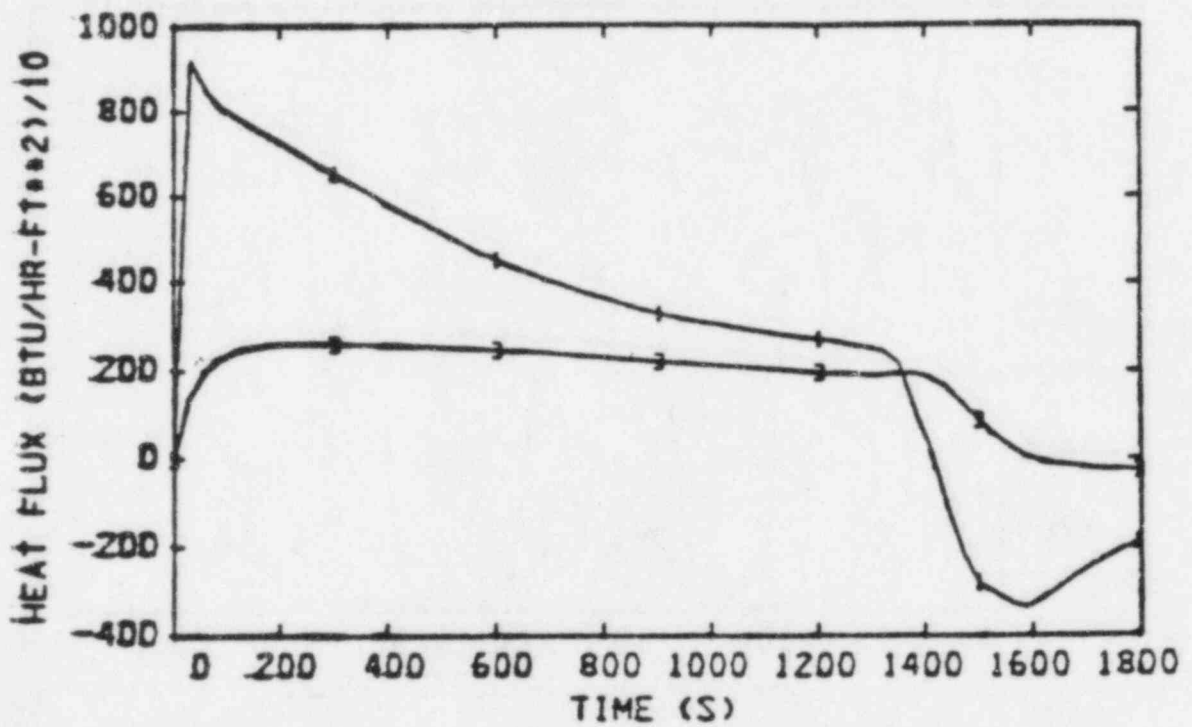


CASE C TIME = 60 1 SECONDS

1 = 10 FEET 3 = 30 FEET \* = SPARGER LOCATIONS

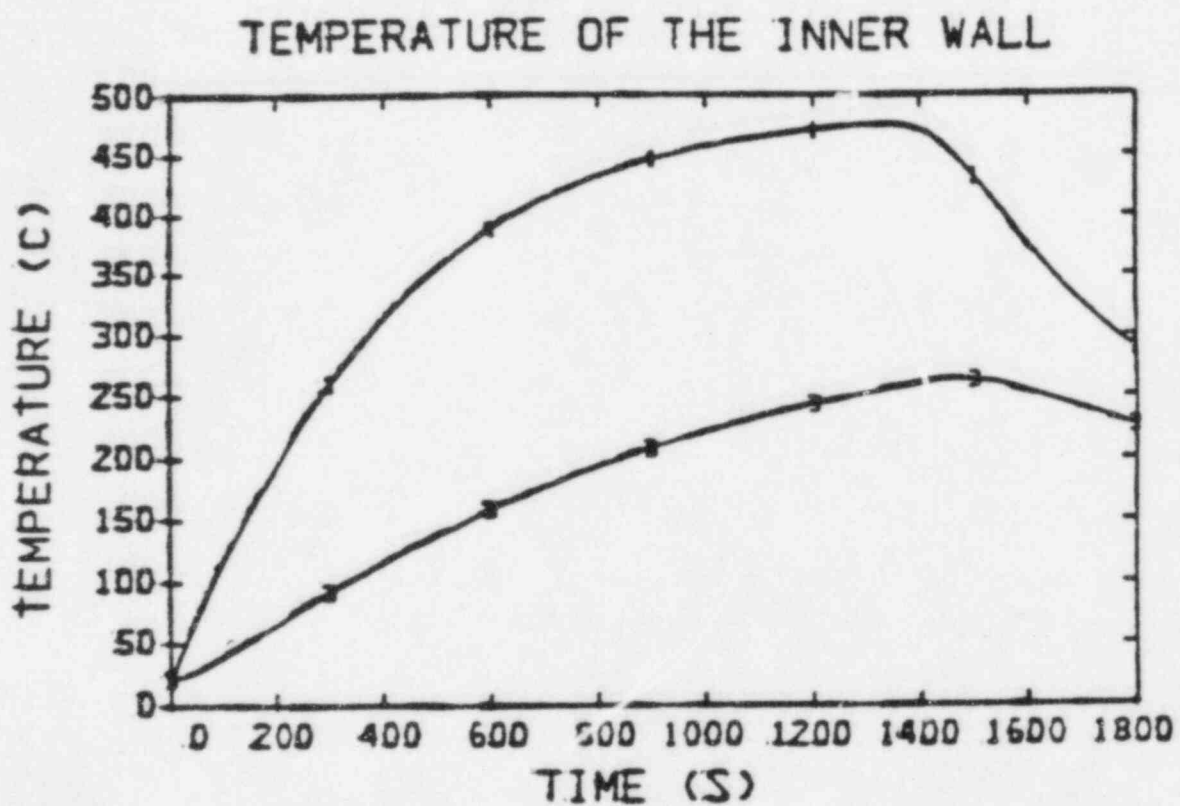
Figure 7.16  
LANL Heat Flux to the Inner Wall

### HEAT FLUX TO THE INNER WALL



CASE I      AZIMUTHAL ANGLE = 157 50 DEGREES  
1 = 10 FEET    3 = 30 FEET

Figure 7.17  
LANL Heat Flux to the Inner Wall vs. Time



CASE C      AZIMUTHAL ANGLE = 157.50 DEGREES  
 1 = 10 FEET    3 = 30 FEET

Figure 7.18  
 LANL Temperature of the Inner Wall

## Chapter 8 DIRECT HEATING EFFECTS (SP-A)\*

### 8.1 Description of Reference Plant Geometry

The potential importance of direct heating effects was illustrated by parametric calculations presented by SNL for the large dry and sub-atmospheric PWRs. The results for the subatmospheric case (SP-2) are presented in this Chapter. The description of this plant and the basic parameters assumed for the analyses can be found in Chapter 3.

### 8.2 Description of the Standard Problem and Objectives

The potential importance of direct heating effects is illustrated by parametric calculations presented by SNL for both SP-1 and SP-2 using parameters recommended by a special subcommittee formed to review this area. It is appropriate to review the finds of the CLWG Direct Heating Subcommittee, as summarized by T. Ginsberg in Appendix A. A consensus of the subcommittee was reached that direct heating effects would not be large if the vessel failed while under low pressure, at least in the case of SP-2. However, no consensus could be reached as to the potential importance of direct heating in high pressure ejection scenarios. Some analysts (designated "Group A" in Appendix A) believed that significant direct heating effects could be ruled out. However, a number of other analysts ("Group B") believed that, at present, "...it is not possible to rule out occurrence of sufficient direct heating to present a severe challenge to PWR large dry containments."

Although no consensus position could be formed that incorporated both groups, it was possible to offer values reasonably reflective of a consensus within each group individually. As a result, the Subcommittee on Direct Heating presented two sets of recommendations on direct heating parameters. Because the direct heating uncertainties dominate any others considered quantitatively by the SP-2 analysts, it was judged that the best single representation of the state of knowledge of the CLWG as a whole would be a set of calculations performed using the various sets of parameters for SP-2 that were presented by the Direct Heating Subcommittee. Hence, a set of calculations, not reported previously by any of the laboratories, was carried out specifically for the SP-2 Summary.

\* CLWG analysts: Bergeron, Williams, Pilch (SNL); Theofanous (University of California). Consensus summary authors: Williams, Bergeron (SNL).

As noted later in this Chapter, there was no standard problem per se established to address this phenomena. The phenomena was analyzed by SNL for SP-1 and SP-2 and by a special Subcommittee. This Chapter is based on excerpts from the summaries produced by those groups. The full report by the special subcommittee is provided in Appendix A.

In Table 8.1, the best-judgment recommendations for SP-2 direct heating parameters are reproduced from Appendix A. Also given are the pressures and temperatures calculated for the present Summary by applying these parameters to the SP-2 base case. In each case, the numbers in the columns headed "thermal" indicate the fraction of the core thermal energy that goes to the indicated process (direct heating or steam quench). For that portion of the core, the fraction of the unoxidized metal therein that releases its chemical oxidation energy to the indicated process is given in the column headed "chemical." The labels "O<sub>2</sub>" and "STM" mean that the metal reaction is with O<sub>2</sub> or steam, respectively; this distinction is important because the reactions of the metals with steam release considerably less energy than the reactions of the same amounts of metal with oxygen. (Hydrogen produced by metal-water reaction is assumed not to react with oxygen in these calculations.) Note that the fractions given under "Chemical" apply only to the fraction of the core material specified under "Thermal", not to the total core inventory. Thus, for the Group B "high" case, the fraction of the total core metallic inventory which reacts with oxygen and contributes to direct heating is 25%, not 50%.

### 8.3 Discussion of Major Phenomenology

The mechanism known as "direct heating" is relevant only to molten corium dispersal to the containment atmosphere following release from a high pressure primary system. It is evaluated here as a special problem (SP-A). There was no standard problem per se defined in connection with the direct heating issue. The concern developed while addressing standard problems SP-1 and SP-2, hence, it was examined in this framework. The relevant phenomenology involves forceful expulsion of the melt from a pressurized reactor vessel and massive dispersion of the molten corium into the containment atmosphere. Under such conditions any metallic component in the melt could be subjected to oxidation and additional direct heating of the containment atmosphere from this source will occur.

### 8.4 Methods of Analysis

The calculational approach employed was that of SNL, i.e., use of the DHEAT code backed by CONTAIN (Ref. 13). However, it should be emphasized that there is every reason to believe that differences in analytical techniques introduce uncertainties that are quite small in comparison with the variations due to differences in the assumed direct heating parameters.

### 8.5 Numerical Results and Sensitivity Studies

#### 8.5.1 Results for SP-2

The SP-2 results are reproduced in Figure 8.1, in which the peak pressures and temperatures are plotted against the fraction of the core which participates in direct heating. For that fraction of the core debris

which participates in direct heating, 100% of the metal (but none of the  $UO_2$ ) was assumed to oxidize and the associated corium was assumed to come into thermal equilibrium with the containment atmosphere. The remainder of the corium was assumed to steam quench without chemical reaction. From these results, it is clear that even moderate amounts of direct heating can have very important effects upon containment loads. Based upon CONTAIN and DHEAT results these are both thermal and chemical contributions to the total direct heating effect in Figure 8.1, with the effect of the chemical energy release being somewhat larger than that of the core thermal energy.

Participants in the direct heating evaluation were asked to provide "high", "low", and "best-estimate" values as to the fractions of the core thermal energy and the metal oxidation energy that might be transferred to the containment atmosphere in the direct heating process. Group A, believing the process to be negligible, provided only a single estimate. The estimates of the Group B analysts themselves spanned a considerable range, but there was consensus among the group that the uncertainties are large and that the differences among the various Group B estimates should not be viewed as being particularly significant. There was also consensus that the "high" estimates, at least, would fall within the range for which Figure 8.1 implies that severe challenges to the containment will arise.

The pressures and temperatures given in the last two columns of Table 8.1 were calculated assuming containment conditions at vessel failure taken from the CONTAIN calculations, rather than those specified in the definition of SP-2. Use of the latter would reduce pressures by about 0.04 MPa (but increase temperatures somewhat, except when direct heating is negligible). Even allowing for this effect of the initial conditions, it is obvious that only the results for the Group A parameters are comparable to those results in Table 3.4 that included no direct heating. For Group B, even the "low" parameters yield significant enhancement of containment pressures and temperatures by direct heating, and the "high" case presents a very severe challenge. Even this case does not represent a consensus as to an absolute upper limit: one analyst estimated "high" parameters which would imply pressures and temperatures of the order of 0.3 MPa and 1500 K, respectively.

Both the SP-2 analysts and the members of the Direct Heating Subcommittee have cautioned that there are many factors not taken into account in the results discussed here. Both conservative and non-conservative factors are involved. Two of the most important factors are:

- (a) The assumption that 100% of the corium is molten and is released coherently when the vessel fails.
- (b) Neglect of possible hydrogen-oxygen recombination in direct heating scenarios. Even when the criteria for self-propagating hydrogen burns, in the usual sense, are not met, high containment temperatures and large surface areas of suspended hot

particulate might promote recombination in direct heating scenarios. This effect could increase containment pressures by up to 0.1-0.3 MPa in typical cases.

Some analysts believed that the net effect of the various factors not treated was to render the "high" calculations, at least, excessively conservative. There was no consensus to this effect, however.

#### 8.5.2 Sensitivity Study with Direct Heating for Figures 8.2 and 8.3

The starting point for this analysis is adaptation of the consensus parameters for the "High" SP-2 base case reported for Group B of the Direct Heating Subcommittee. These parameters include 50% of the total corium thermal energy and 25% of the total corium potential energy from metal oxidation going to direct heating. However, the cases defined for the sensitivity study differ from the base case in up to three important ways that could significantly affect direct heating:

- (a) In all cases, the corium contains much more steel, but less unoxidized zirconium, than does the base case.
- (b) In four of the sensitivity study cases, the primary system pressure is specified to be much lower than for the base case (for present purposes, it was redefined as being fully depressurized in these four cases.)
- (c) In four of the sensitivity study cases, the corium temperatures were defined as being much lower than in the base case, so low that it is likely that steel would be the only corium component actually molten to a large degree.

The SNL analysts were the only team to explicitly confront these differences since only they performed the sensitivity study with direct heating included. They described the prescriptions which they developed for modifying the direct heating parameters to take into account these factors. Though qualitatively reasonable, these prescriptions are rather arbitrary in terms of the actual numbers assumed; nonetheless, better prescriptions are not available. Hence, they will be employed here except for the prescription used for the first of the above items, the difference in composition. The Group B base case parameters are rather different from those used by SNL analysts for SP-1 and SP-2, and applying the prescription used by them to the present case would almost totally eliminate the chemical contribution to direct heating, something that is judged contrary to the spirit of the recommendations of Group B of the Direct Heating Subcommittee. Therefore, no allowances for the difference in composition has been made in the present work.

Major assumptions used for the sensitivity study calculations with direct heating area as follows:

- (a) In the high pressure cases involving the higher temperature (3000K) coriums, the parameters were as in the "high" base case: 50% of the core thermal energy and 25% of the total available metal oxidation energy goes to direct heating; 50% of the corium steam quenches with 30% of the associated zirconium undergoing reaction with water, with the heat produced going to steam generation.
- (b) In the high pressure cases involving the lower temperature (1800K) coriums, only the steel (analyzed as consisting of iron) was assumed to participate in direct heating, with the percentages being as above. The rationale is that sufficient fragmentation for efficient direct heating is judged improbable for constituents that are solid. The remainder of the iron, and all of the other constituents, were assumed to steam quench.
- (c) In the low pressure sequences, the only direct heating allowed for in the higher temperature corium cases was reaction of 25% of the zirconium with steam, with the energy going to direct heating. (The resulting direct heating effects are not large because the amounts of unoxidized zirconium are relatively small in these coriums.) In the low temperature, low pressure cases, no direct heating was allowed for.
- (d) Steam spike calculations for the high temperature coriums included reaction of 30% of the available zirconium with water, but no chemical energy release was assumed for the low temperature corium steam spike calculations. Water available for steam generation was assumed to include both cavity water and accumulator water in high pressure sequences and only cavity water was included in the low pressure sequences. If water was exhausted, energy remaining in unquenched corium was ignored.
- (e) For all sequences, the containment conditions at vessel failure time were assumed to be the same. (This is not realistic; different RCS pressures imply sequences that differ in ways that would affect containment conditions.)

It must be stressed that the Direct Heating Subcommittee has not considered in detail how the direct heating parameters might vary as a function of the accident sequence parameters considered here, and no endorsement by the Subcommittee of the above prescriptions is implied. No clear conflicts between these prescriptions and the recommendations of the Subcommittee are known, however.



Figures 8.2 and 8.3 present, respectively, the pressures and temperatures obtained in the following sets of calculations for the sensitivity study:

- (a) The results labeled "BNL Low" in Figures 8.2 and 8.3, which were obtained by BNL for the complete sensitivity study using the same assumptions they used for their base case "low" steam spike calculations. These assumptions included incomplete corium-water mixing, followed by CORCON calculations with film boiling on the top surface.
- (b) The shaded zone, labeled "High Steam Spike Range," represents the range of results spanned by the calculations summarized in Figures 3.2 and 3.3.
- (c) The results labeled "Nominal Direct Heating" were calculated for the present Summary using the consensus recommendations of the Direct Heating Subcommittee Group B for SP-2 "high" base case direct heating parameters (Table 8.1) as a starting point. Since these recommendations were clearly not intended to be applicable for all the parameter combinations of the sensitivity study, the direct heating parameters were varied as a function of these parameters as discussed above. For the Cases 3, 4, 7, and 8, it was assumed that the primary system was fully depressurized, since the pressure specified in Table 3.2 was incompatible with the specification that accumulator discharge occurred prior to vessel failure.

Obviously, the range spanned by the results given in Figures 8.2 and 8.3 greatly exceeds the range spanned by the results for the more restricted steam spike sensitivity study of Chapter 3. The dominant effect is that of direct heating though the difference between the "BNL Low" results and the other steam spike results is also significant in some cases. The extremely large direct heating effects calculated for some of the high pressure ejection cases arise from the very large corium masses with very high steel content specified in Table 3.2. For the high pressure cases, the thermal energy contributes slightly over 60% of the total direct heating for the higher-temperature coriums (cases 1 and 5), while chemical energy contributes about two thirds of the total for the lower-temperature coriums (cases 2 and 6).

It is noteworthy that the wide spread in the results applies only to the high pressure ejection cases. For the low pressure cases, there was little difference between the "low" and the "high" steam spike calculations of BNL, and the direct heating prescription described above

largely or entirely eliminates direct heating in the low pressure cases. It should be emphasized that this elimination of direct heating is based upon assumptions, not mechanistic calculations. These assumptions are believed to be reasonably consistent with the consensus of the Direct Heating Subcommittee, although the Subcommittee did not explicitly consider the question in detail.

Limitations in the base case calculations noted at the close of Section 8.2 also apply here. These include the highly conservative assumption of coherent release of 100% of the molten corium and the nonconservative neglect of hydrogen-oxygen recombination which may occur under severe direct heating conditions.

#### 8.6 Considerations of Loads and Likelihood of Containment Failure\*

The resulting containment loads will depend principally on the quantities of melt actually dispersed and the amounts of metallic components oxidized. In the bounding case of a whole-core dispersal and 100% oxidation of all cladding, a peak pressure of 12 bars (176 psia) and a peak temperature of 1,000°K (1340°F) can be calculated. In general, rather extreme assumptions had to be utilized to produce loads of sufficient magnitude to challenge a large dry containment. On the other hand the quantification of the dispersal (i.e., distorted pathways)\*\* and oxidation processes, as well as of the availability of metallic components for oxidation, are uncertain. As a result it did not become possible to arrive at a consensus conclusion regarding the relative likelihood of loads for any case of material involvement below the one specified.

Examination of the attainability of the initial condition invoked for direct heating provides an alternative, potentially more promising, approach to this problem. Although the CLWG did not deal, as a whole, with this aspect, calculations were developed which indicated that, due to strong natural circulation currents of the high pressure steam, temperature gradients within the primary system components were rather modest. Since the structural properties of steel and steam generator tube material degrades rapidly above 1300°F, it was concluded that primary system failure and depressurization would occur prior to core melt. Clearly, steam generator tube failures would also imply a path to the outside. If these initial results were to be confirmed it would be possible to conclude that only low pressure scenarios are relevant to containment capability evaluations.

\* Considerations of the likelihood of containment failure from the various load sources described in this report have been provided by the NRR staff and is based on extended discussions with staff consultants and staff members involved in containment loads and performance activities.

\*\* The IDCOR program has initiated a study to examine in detail the geometry of the flow paths to containment for core debris for all plants.

## 8.7 Conclusions and Recommendations

- (a) If direct heating parameters are assumed similar to the "high" values of the Direct Heating Subcommittee Group B consensus, a very severe threat to containment integrity results. No consensus could be reached among SP-2 analysts as to whether these parameter values are credible.
- (b) Of the parameters treated quantitatively and in detail by the SP-2 analysts, the direct heating question is the dominant uncertainty. Other important issues, not analyzed in detail, appear to include the fraction of the core that might actually undergo coherent ejection and the extent of hydrogen-oxygen recombination, especially under strong direct heating conditions.
- (c) It is recommended that the results calculated for SP-2 using the various Group A and Group B consensus parameters of the Direct Heating Subcommittee be taken as providing the best representation of the CLWG position on SP-2. There is a consensus among the SP-2 analysts that results for this Standard Problem should not be interpreted as actual predictions of the containment loads to be expected for any specific accident sequence in any specific plant. Some analysts believe that at least the "high" SP-2 results are unrealistically conservative, but there is no consensus to this effect.

Table 8.1

SP-2 Pressures and Temperatures with Direct Heating

<u>Group and Case</u>	<u>Direct Heating</u>		<u>Water Quench</u>		<u>Pressure (MPa)</u>	<u>Temp. (K)</u>
	<u>Thermal</u>	<u>Chemical</u>	<u>Thermal</u>	<u>Chemical</u>		
A: All	2%	--	80%	--	0.53	431
B: "High"	50%	50% O <sub>2</sub>	50%	30% STM	1.08	944
B: "Central"	25%	50% STM	75%	25% STM	0.78	611
B: "Low"	15%	50% STM	85%	0	0.68	539

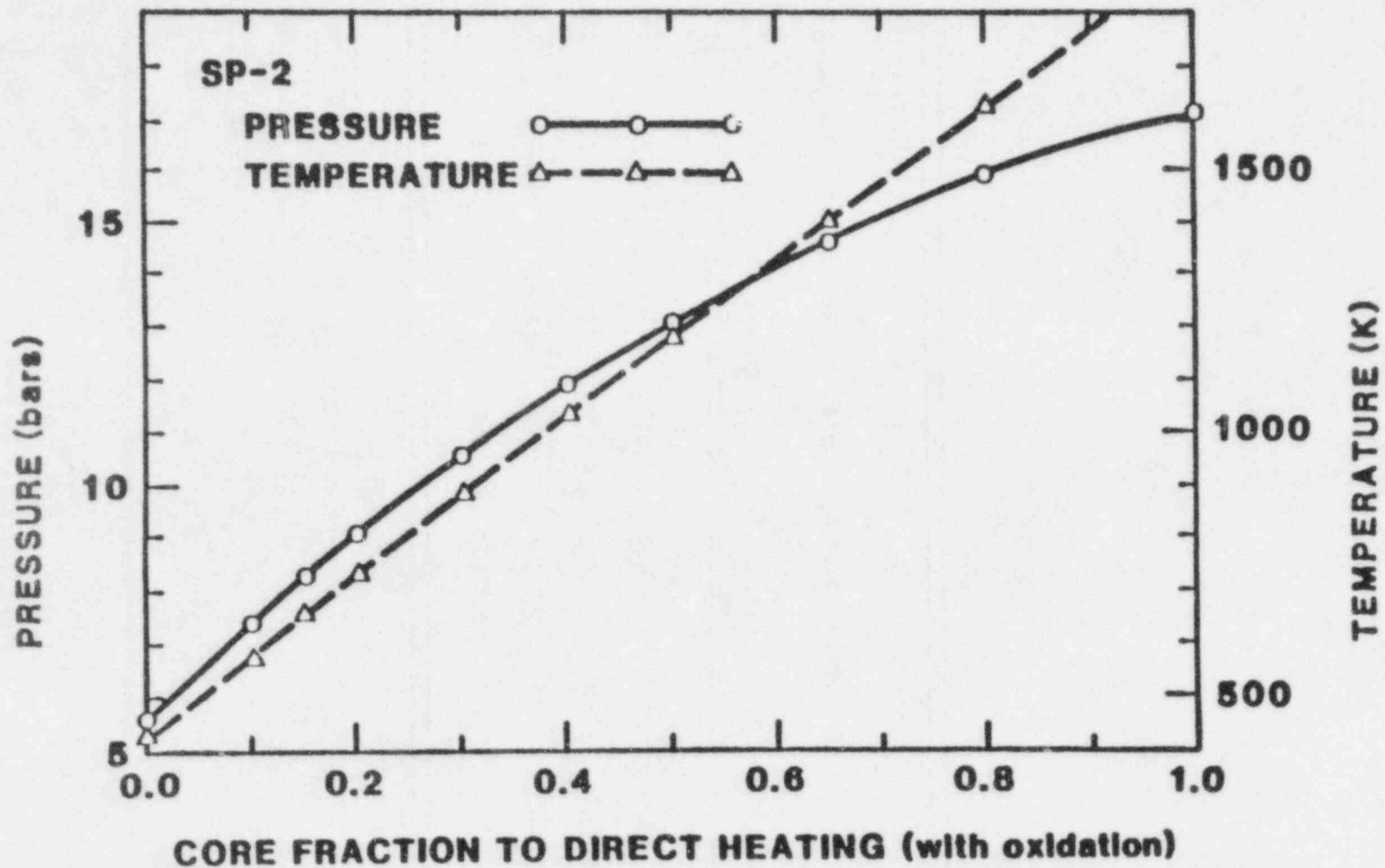


Figure 8.1 SP-2 pressure and temperature as a function of core fraction involved in direct heating (with metal oxidation)

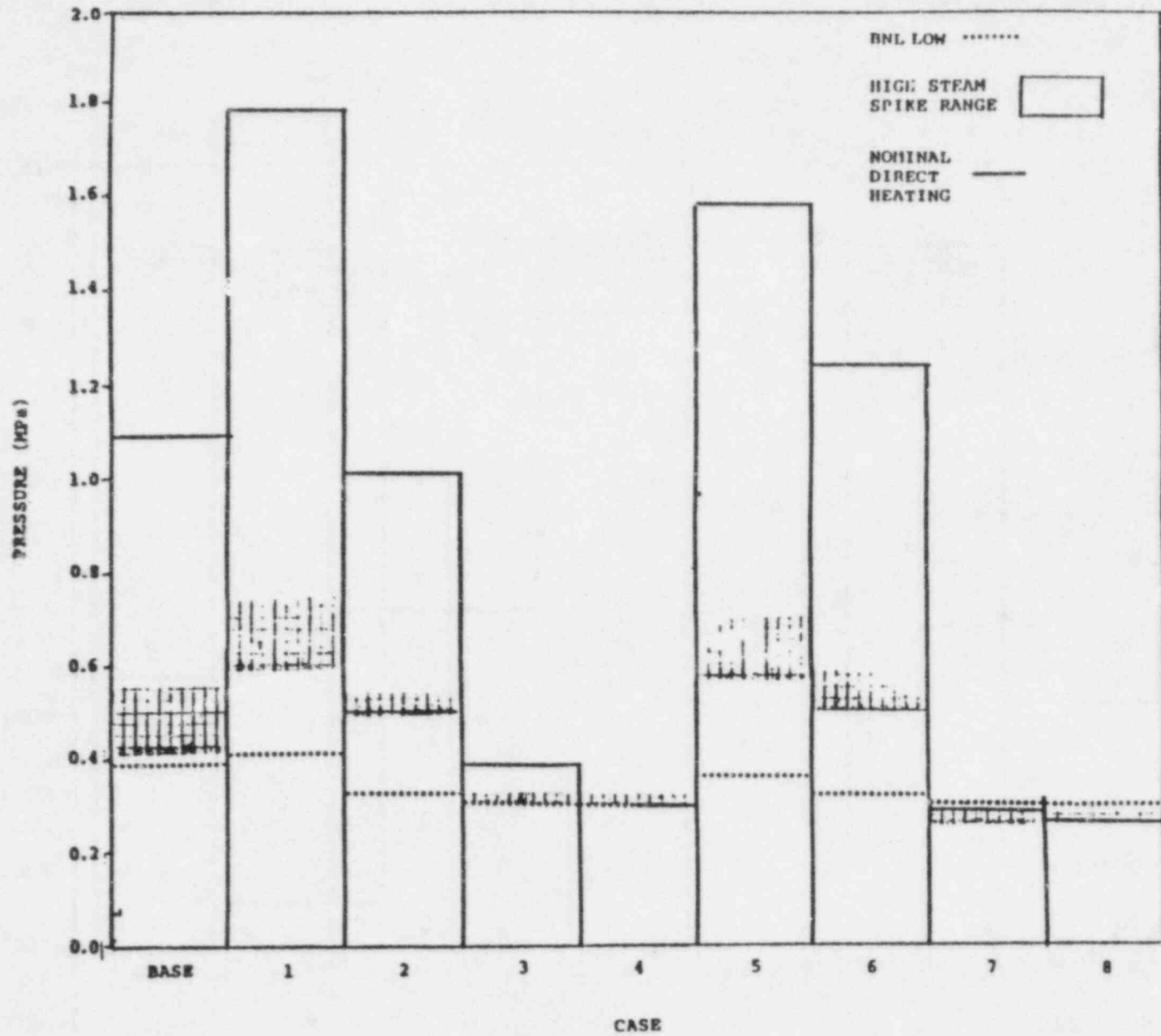


Figure 8.2 Calculated SP-2 pressures for the "low" and "high" steam spikes and for the nominal direct heating scenario

8-12

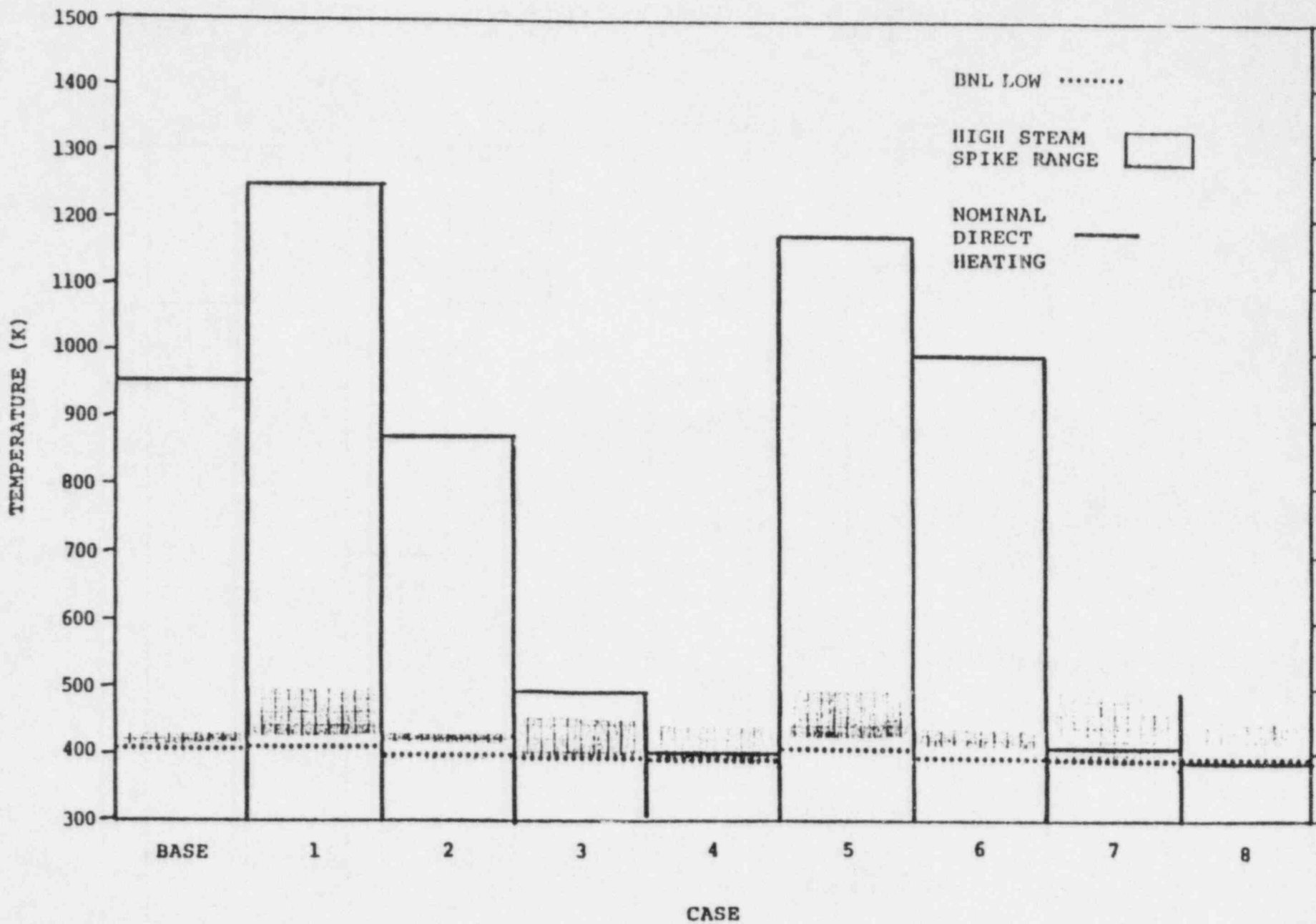


Figure 8.3 Calculated SP-2 temperatures for the "low" and "high" steam spikes and for the nominal direct heating scenario

## 9.1 IDCOR/NRC Comparisons

The Industry Degraded Core Rulemaking Program (IDCOR) is an effort on the part of the nuclear utilities to develop the technical basis for determining whether changes in regulatory requirements are needed to reflect severe accident considerations. The NRC has recognized the potential benefit of factoring the IDCOR methods and results into the agency's decision process on severe accidents. In an ongoing series of meetings, NRC is evaluating IDCOR's methods, assumptions and results. The purpose of this interaction is to improve NRC and IDCOR understanding of severe accidents, to identify areas of agreement, disagreement or misunderstanding, and to define a course of action for resolving uncertainties.

Several of the meetings have had a direct bearing on the question being addressed by the CLWG; namely, the likelihood and mode of early containment failures. The first meeting, held in Harpers Ferry, West Virginia on November 29 to December 1, 1983, focussed on models for the physical phenomena and chemical processes which govern accident progression from accident initiation to the point of the containment failure. The third meeting, held in Rockville, Maryland, on May 15-17, 1984, concentrated on selecting important accident sequences and on calculated containment loads (pressures and temperatures) for representative BWR and PWR containment designs.

Discussions at those meetings revealed numerous areas in which the IDCOR representatives and NRC contractors disagreed about fundamental phenomenology, modeling assumptions and calculational methods. Efforts are under way to resolve those differences, where possible, to the satisfaction of both parties. Of the many issues raised, a few stand out as having a direct and substantive impact on the likelihood and mode of early containment failure. The discussion below concentrates on those issues and their impact on specific containment types.

### 9.1.1 Large Dry Containments

Both IDCOR and CLWG examined the TMLB' sequence for Zion. In the IDCOR calculation, about half the core is assumed to be expelled from the reactor cavity at vessel failure and spread out in a thin layer on the steam generator room floor. The remaining core debris gradually falls under gravity to the cavity floor, and gradually pressurizes containment due to steam production. After dryout at about 10 hours, the containment pressurization proceeds more slowly due to core-concrete interaction in the cavity, and reaches the failure pressure at about 24 hours. A total of 555 lbm of hydrogen was assumed to be produced, and no global burns were calculated to occur.



The CLWG results were based on two assumptions which differed markedly from those used by IDCOR; (1) essentially the entire core directly entered the cavity and participated in production of a steam spike at the time of vessel failure, and (2) about 2000 lbm of hydrogen were produced. Major steam partial pressures occur within an hour of vessel failure. Despite these differences, the CLWG conclusion, that early overpressure failure of large dry containments under steam spike loads alone is physically unreasonable, is in essential agreement with the IDCOR results.

This conclusion, however, is still open to question for sequences, such as TMLB', in which the reactor vessel might fail at high pressure. There is experimental evidence\* which indicates that such a high pressure blowdown would disperse a significant fraction of the core debris through the cavity and keyway into the upper regions of containment in the form of aerosols. This could result in significant direct heat transfer to, and chemical reactions with, the containment atmosphere, with the potential for early overpressure failure. As described in Chapter 8 and Appendix A the NRC staff and consultants are currently unable to reach consensus on the likelihood of such a scenario. IDCOR representatives contend that a high pressure ejection would not result in significant dispersal of core debris in aerosol form. Their view is that the core debris would be flooded in the reactor cavity rather than entrained in the flashing liquid during a high pressure melt-through. Without the intimate mixing of corium and steam, IDCOR believes the core debris does not form aerosols, but moves up the keyway as a liquid. IDCOR postulates that a film forms on the forward wall as the corium makes the upward turn at the far end of the keyway. The type of dispersal mechanism envisioned by IDCOR is consistent with the Zion TMLB' results described above. IDCOR is currently reviewing all domestic PWR containment designs to assess the flow paths for dispersal.

#### 9.1.2 Ice Condenser and Mark III

Differences between CLWG and IDCOR results for the PWR Ice Condenser and BWR Mark III containments relate to hydrogen production and combustion. The IDCOR MAAP code embodies two assumptions which tend to suppress in-vessel hydrogen production; (1) all Zr-water reactions are turned off when the clad temperature reaches a user-specified value (usually 2300°K), and (2) following the onset of fuel relocation, blockages are assumed to form at the grid plates and block the further flow of steam in the channel.

The NRC MARCH code, on the other hand, includes a "regionalized slumping" model in which molten fuel from the hottest core regions slumps into the water in the lower plenum and produces steam for further interaction with the intact fuel rods in colder regions.

\* At small scale and with only limited simulation of cavity/keyway geometries and of the characteristics of core debris.

The differences in hydrogen production in-vessel is illustrated by comparing results for the TMLB' sequence for Sequoyah (Table 9.1). Calculations with MARCH predicted considerably more hydrogen, with most of the difference coming after the onset of core slump. During that period the MAAP code suppresses hydrogen production due to the 2300°K temperature cutoff while the MARCH "regionalized slumping" model continues to produce steam for the Zr-water reaction.

Differences also show up in hydrogen production for the Mark III. Based on Oak Ridge National Laboratory SASA calculations, the CLWG Standard Problem 6 assumes total hydrogen production ranging from 1000-3000 lb. as input to the diffusion flame calculations. Table 9.2 compares this assumption with IDCOR calculations of in-vessel hydrogen production for various sequences.

IDCOR has performed sensitivity analyses with various input parameters and modeling assumptions, including the channel blockage model and the 2300°K cutoff temperature. Partial results shown in Table 9.3 show a strong sensitivity to channel blockage but relatively little effect of a higher cutoff temperature. Both NRC and IDCOR recognize that sensitivity analyses have to be extended to include the effect of uncertainties in accident sequence and core melt phenomena.

Neither the MARCH nor the MAAP calculations predict significant hydrogen production during energetic fuel/coolant interactions in the lower plenum.

For the ice condenser and Mark III systems the combustion of hydrogen in containment is also handled quite differently by NRC and IDCOR. As the accident progresses, the IDCOR MAAP code calculates a theoretical flame temperature based on the concentrations of hydrogen and steam in containment. If the flame temperature criterion of 1310°F is exceeded, a global burn is assumed to occur, regardless of whether an identifiable ignition source is present. NRC sponsored MARCH calculations can allow (via user input) higher concentrations of hydrogen to accumulate before ignition, and thus predict higher peak pressures due to deflagrations. Furthermore, IDCOR calculations of dry cavity sequences sometimes show continuous burning of combustible gas in the hot regions above the core-concrete pool. Oxygen for these reactions is transported to the cavity region by natural convection currents. Continuous burns in the reactor cavity can not be predicted in NRC sponsored calculations, since the codes used for these calculations do not yet model natural convection processes.

The combination of differences in hydrogen production and combustion models between MAAP and MARCH is seen in the containment pressure calculations for TMLB' (Figure 9.1) for Sequoyah. The MARCH results show three distinct large hydrogen deflagrations (which were assumed to be initiated at 8v/o hydrogen), two of which exceed the nominal failure pressure for Sequoyah (65 psi) within about three hours after vessel failure. The MAAP results, based on lower in-vessel hydrogen production and on continuous burning in the reactor cavity, show no distinct hydrogen deflagrations.

### 9.1.3 BWR Mark I

Hydrogen ignition in the BWR Mark I containment is precluded by nitrogen inerting. As discussed in Chapter 5, the dominant threats to this containment arise from temperature and/or pressure caused by the core-concrete interactions. For similar transient-induced accidents with comparable initial conditions, large differences are observed between calculations by CLWG and IDCOR in the temperatures and pressures generated in the drywell. As illustrated in Figure 9.2, the CLWG calculations predict substantially higher pressures and lower temperatures than IDCOR.

The apparent reason for this discrepancy is the way in which the melt energy is partitioned between downward erosion of the concrete and upward radiation to the drywell atmosphere. The IDCOR model calculates that the core debris falls below the ablation temperature shortly after vessel failure and penetration stops at a depth of 0.06 ft. Heat transfer to the concrete is then limited to conduction, while radiation heats the atmosphere above.

The NRC CORCON code incorporates additional detail which tends to extend the concrete ablation process and produce more non-condensable gases. This leads to more pressurization of containment and to lower temperatures. The differences shown in Figure 9.2 are exaggerated because this particular CLWG standard problem calculation (SP-4) did not account for any thermal radiation from the top surface of the melt. However, separate calculations with the coupled MARCH-CORCON code, in which radiative heat transfer to the containment atmosphere was included, exhibited the same qualitative behavior. The calculated drywell temperatures were still lower than those calculated by IDCOR and the pressures were higher, although the discrepancies with IDCOR in the predicted temperatures were not as large as in Figure 9.2. As shown in the Figure, the magnitude of the discrepancies between CLWG and IDCOR depends somewhat on the assumed spread of corium debris, but the differences remain substantial.

In general, IDCOR postulates that containment failure consists of a break size sufficient to prevent full pressurization, while NRC considers the possibility of prompt catastrophic containment failure. The IDCOR model leads to long release durations for fission products and consequently to greater reduced predictions of early fatalities.

### 9.1.4 Containment Response

The significance of the disparities outlined above will depend on our perception of how containment fails. Heretofore, both NRC and IDCOR have utilized relatively simple criteria of pressure and temperature for containment failure. NRC, through the Containment Performance Working Group, has launched an effort to better specify the modes and magnitudes of containment leakage and other failures under various conditions. No similar effort is planned at this time by IDCOR.

### 9.1.5 Recommendations for Further Analysis or Tests

The following recommendations for further study have emerged from CLWG analyses and interactions with IDCOR.

- (a) Direct heating is a potentially dominant contributor to early possibilities of major containment overpressure failure and may also increase the effects of high temperature attack or local environmental attack with implications for possible increases in likelihood of local failures. Additional tests, with better simulation of containment geometries, corium characteristics, and the effects air/water as oxidizers and heat sinks are needed. Some additional tests are already being planned by industry. CLWG should increase participation in such efforts. Without new test information, the issues and uncertainties of direct heating effects cannot be resolved by further analysis.
- (b) Possible temperature stratification in the containment during severe accidents has not yet been fully evaluated. This could influence possibilities of local containment failure and CLWG's definition of the most appropriate load estimates and related uncertainty levels.
- (c) The possible existence, stability, and magnitude of standing hydrogen diffusion flames in Mark III needs additional testing; such tests are already being planned by industry and CLWG should participate in developing test parameters. This could include additional analysis of: the likely access rates of hydrogen to the wetwell; present assumptions of the effects of multiple access points and the interactions of flames from multiple points; actual flame heights; mechanistic evaluation of upper limit assumptions of hydrogen flow through any one access point; existence of ignition sources, etc.
- (d) The possibility of local detonation in ice condenser containment has been suggested. Additional analysis of the potential likelihood and load levels may be appropriate to help define the possibilities of local containment failure.
- (e) It has been suggested that lower (dead end) compartments of ice condenser have generally non-flammable conditions, and that, since most penetrations are believed to be in the lower walls, the ice condenser containment is relatively unsusceptible to local failure due to hydrogen burn. The assumption could be reevaluated.

- (f) A comparison calculation by IDCOR and NRC of a single standard problem has been suggested as a means of further resolving differences on issues. CLWG should evaluate the usefulness of this approach and the specific issues most capable of being resolved (for example, are core melting, deformation, and hydrogen generation susceptible to improved definition by more analyses and sensitivity studies).
- (g) The possible existence of flammable conditions has been noted in SP-2 for some cases of RPV failure at low pressure, but the contributions of such loads have not been calculated. CLWG should evaluate the need for further study.
- (h) It would be desirable to conduct an additional study for Mark I (Appendix G.iv) to determine whether assumption of slightly lower ablation temperature for limestone concrete (e.g. 1725K) would sufficiently increase the efficiency of this concrete as a heat sink to cause low assumed initial corium temperatures (e.g. 1775K) to quickly fall below the melting point of steel (1750K) and thereby prevent the melt-through of the drywell steel wall which has been calculated to occur if the concrete ablation temperature is assumed to be the same as steel melting temperature.
- (i) It has been noted that, as steam inerting disappears in sub-atmospheric PWR containment (particularly for cases of limited cavity water which tends to limit steam inerting) there is a possibility of substantial hydrogen burning which might produce loads equaling or exceeding those of the steam spike. This may deserve further study.
- (j) Other items should be added by analysis; for example, is more work required to establish consensus best estimates of loads, to prepare graphs of P/T/t envelopes to translate load estimates to probability density functions with appropriate treatment of uncertainty, is additional work needed to deal with any IDCOR/NRC issues directly related to source term development, etc.

## 9.2 International Comparison Calculations

NRC is participating in the CSNI PWG2 Task Group on ex-vessel severe accident thermal hydraulics. This effort involves the analysis and evaluation of two standard problems involving the pressure and temperature loads in a PWR with a large dry containment. These problems will be analyzed by the member nations using their own techniques. Results of CLWG analyses, when complete will be provided to the Task Group for comparison and development of additional insights relative to the likelihood type, and severity of any early containment failure.

### 9.3 NRC Source Term Reassessment

To provide more coherent technical support to deal with regulatory issues involving severe accident considerations, both the NRC and the U.S. nuclear industry have developed special source term programs. A "Nuclear Power Plant Severe Accident Research Plan" was formulated by the NRC and published as NUREG-0900 in January 1983. A considerable amount of NRC staff effort is directed at two technical issues that currently seem to stand out as having particular significance to source term questions and to the resolution of regulatory policy matters. These are (a) the sequences and phenomena that can lead to early gross failure of the containment and (b) the potential for substantial increases in containment leakage under severe accident loads prior to (or even preventing) major structural failure, called "leak before break."

#### 9.3.1 Containment Analyses

The importance of the mode, timing, and leak rate of the reactor containment to postulated severe accident sequence was recognized during early source term reassessments. Two working groups (comprised of NRC staff and contractors) were formed to develop and analyze problems concerning containment response to severe accident sequences. The Containment Loads Working Group (CLWG) was set up to develop and analyze standard problems for estimating containment pressures and temperatures (the containment "loads") for important accident sequences and for unique plant types. The Containment Performance Working Group (CPWG) was charged with developing and analyzing models for containment performance when increased leakage from the plant is sufficient to reduce the pressure and prevent catastrophic failure. Results from the CLWG work is the subject of this report. The CPWG work is reported in NUREG-1037. Summaries of the work performed by both groups are provided in appendices to the NRC's source term reassessment program reported in NUREG-0956.

TABLE 9.1

PERCENT OF ZIRCALOY REACTED IN TMLB' SEQUENCE

<u>Timing</u>	<u>% of Zircaloy Reacted</u>	
	<u>IDCOR-MAPP</u>	<u>NRC-MARCH *</u>
Prior to onset of core slump into lower plenum:	23%	25%
During core slump:	7%	24%
Total In-Vessel	<u>30%</u>	<u>49%</u>

- \* CLWG Standard Problem 3 for Sequoyah the ice-condenser reference plant parametrically assumes that 30-60% of Zr will oxidize in-vessel. The Mark III Standard Problem 6 parametrically assumes that approximately 68% of Zr (except channel boxes) will be oxidized within 30-75 minutes (3000 lb. total) from combined in-vessel and ex-vessel reaction.

TABLE 9.2

COMPARISON OF HYDROGEN PRODUCTION IN CLWG STANDARD PROBLEM  
SP-6 (MARK III) CALCULATIONS VS. IDCOR CALCULATIONS

<u>Case</u>	<u>In-vessel Hydrogen (lbm)</u>	
	<u>IDCOR</u>	<u>NRC</u>
T1QV	10	--
AE	4	--
T23C	460	--
CLWG Assumption	---	1000-3000



TABLE 9.3

IDCOR Sensitivity Results for Mark III T1QUV

<u>Case</u>	<u>In-vessel Hydrogen Production</u>
Modified Base Case *	417 lbm.
No Channel Blockage	1443
Higher Cutoff Temperature (2500°K)	449

- \* The base case value of 200 lbm. hydrogen was for the case of late actuation of the ADS, causing a rapid loss of steam. The modified base case involves a slower core uncover with no ADS actuation.

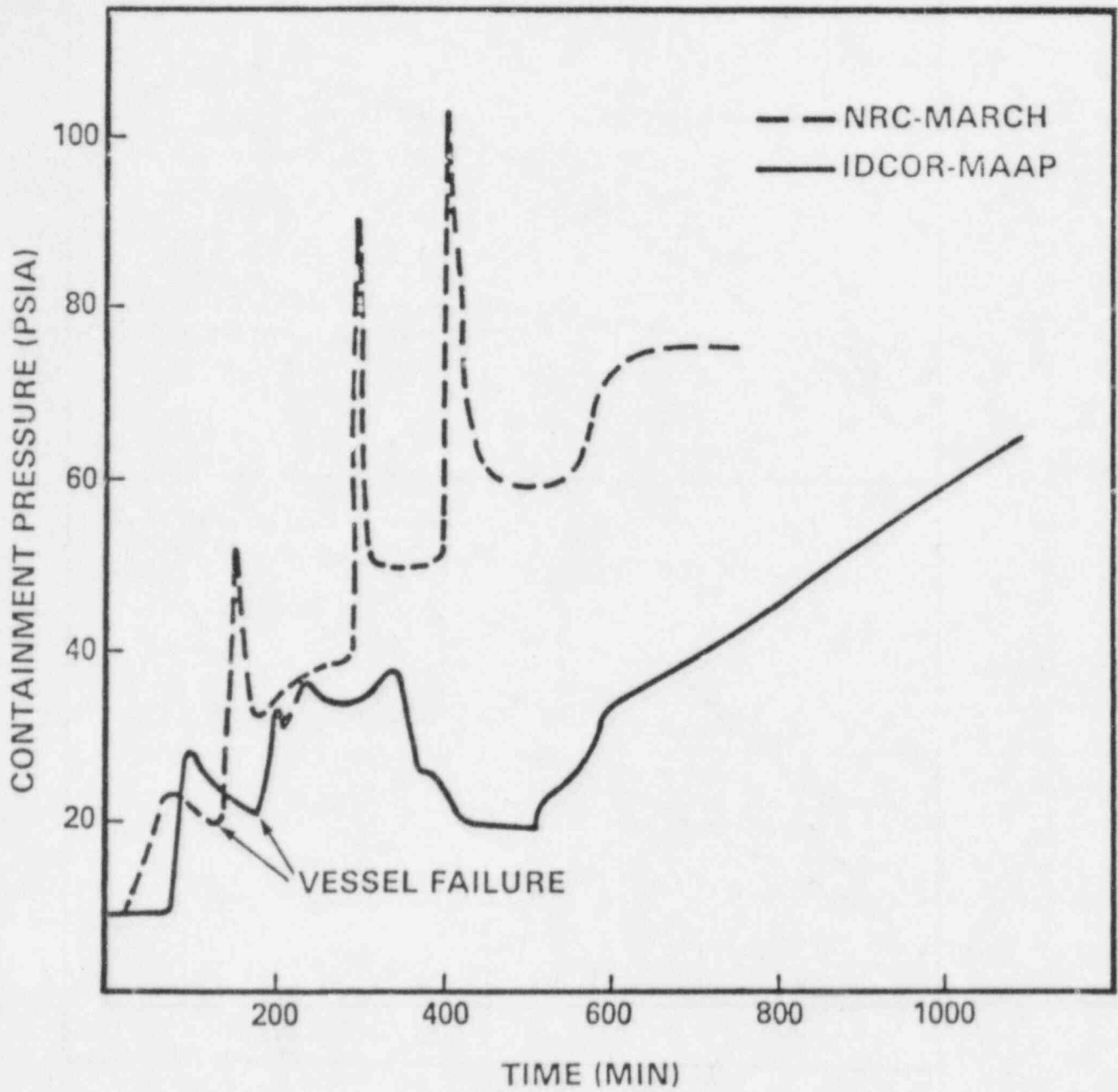


Figure 9.1

CONTAINMENT PRESSURE VS. TIME  
 FOR TMLB' WITH A DRY REACTOR CAVITY  
 FOR AN ICE CONDENSER PLANT

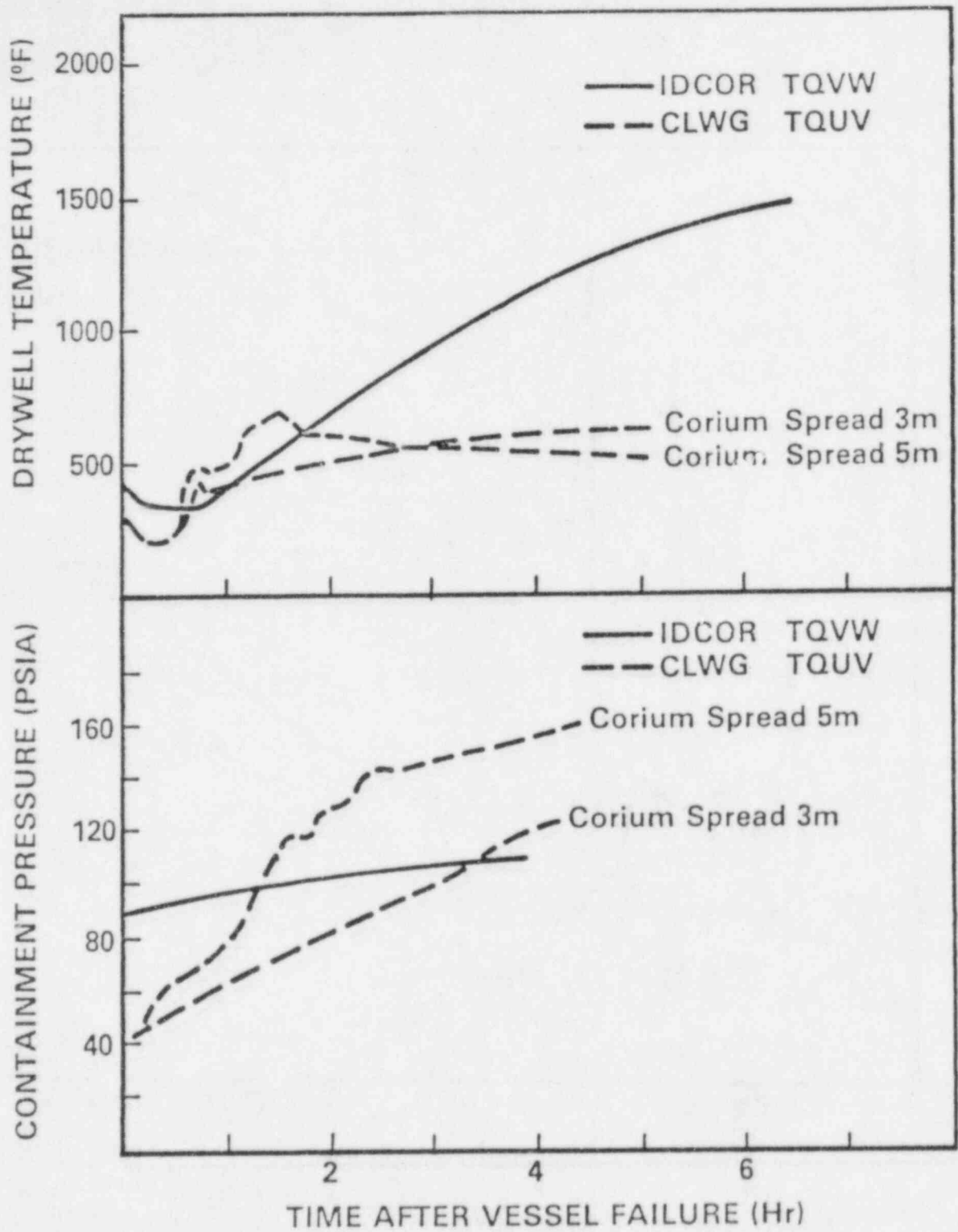


Figure 9.2

**DRYWELL PRESSURE AND TEMPERATURE  
VS. TIME FOR MARK I SEQUENCES  
DOMINATED BY CORE-CONCRETE  
INTERACTIONS; CLWG VS. IDCOR**

## 10.1 Conclusions

Based on the CLWG results described in the proceeding chapters the staff has concluded that, in general early containment failure as a result of overpressurization due to steam-spikes alone is not likely. On the other hand the studies also identify several areas in which reduction of uncertainties would appear beneficial. Perhaps the most important one, as it may affect all reactor types and containments, is that associated with melt release at high pressure (direct heating problems). Since initial evaluations indicate that primary system failure, and hence depressurization, could be possible prior to core melt, a high priority in this area is to address whether a high pressure scenario persisting to core melt is physically realizable. Also important are studies on the potential flow paths for corium dispersal from the reactor cavity to the containment atmosphere. The second major topic area, affecting principally the ice-condenser plants, is hydrogen combustion. This is a rather complex topic and it may be resolved in a number of contributing subproblems including: hydrogen generation, release, ignition, burning, and possibly transition to detonation. Finally, some residual uncertainties in corium-concrete interactions should be mentioned. They concern the long-term temperature evolution of the melt and affect not so much the development of pressure loads as they do the so-called "vaporization release" (source term) and the containment temperature (seal integrity). This problem is of principal interest to Mark I containments. Other areas include extension of studies of ex-vessel corium-water interactions in specific BWR geometries and integration of the individual load processes calculated by the CLWG.

## 10.2 Specific Recommendations for Further Study

The results from the CLWG studies indicate the following items are appropriate for additional study:

- (a) Examination of additional issues related to direct heating:
- evaluate the potential for local primary system over-temperature failures leading to depressurization before catastrophic failure of the lower vessel which can result in rapid expulsion of corium from the reactor cavity to containment atmosphere.
  - evaluate IDCOR's studies on the effect of geometric configurations on the flow paths for corium dispersal from the reactor cavity to the containment atmosphere in existing designs.
  - evaluate experimental results and requirements as needed to resolve the direct heating issue.

(b) Examination of additional issues related to hydrogen burning:

- possibility of detonation in ice-condenser containments
- effect of (and potential for) various ignition modes (mainly timing of ignition)
- effect of (and potential for) various hydrogen generation and release rates
- possible unconventional recombination modes of H<sub>2</sub>O (even in steam-inerted conditions) as a source of additional chemical energy leading to more severe early pressure and temperature loads
- possible steam de-inerting (condensation) leading to potential additional early hydrogen burning loads in containment; similar behavior in lower ice-condenser compartments which might lead to hydrogen burning and to potential over-temperature loading of penetrations
- participation in ongoing industry model studies related to stable hydrogen diffusion flames in Mark III wetwells.

(c) Evaluation of processes in corium-concrete reactions and heat transfer that:

- affect calculated pressures and temperatures in Mark I containments and consequent uncertainties concerning early over pressures and timing of potential penetration failure
- affect long-term temperature behavior of the melt in Mark I and the so-called "vaporization release" contributions to source terms.

(d) Extension of the study of ex-vessel corium-water interactions to include the effects of Mark II downcomer and suppression pool configurations in non-reference (i.e., non-standard problem) plants.

(e) Integration of the various containment loading mechanisms that can result from various core melt accident scenarios.

The nature of these future studies will be defined more precisely in conjunction with activities related to implementation of the Commission's severe accident policy statement.

CHAPTER 11 REFERENCES

1. R. O. Wooten and P. Cybulskis, "MARCH 2 (Meltdown Accident Response Characteristics) Code Description and User's Manual," Battelle Columbus Laboratories, October 1983 DRAFT.
2. R.O. Wooten and H. I. Avci, "MARCH (Meltdown Accident Response Characteristics) Code Description and User's Manual," NUREG/CR-1711, U.S. Nuclear Regulatory Commission, Washington, D.C., October 1980.
3. R. K. Cole, D. P. Kelley, and M. A. Ellis, CORCON-MOD2: "A Computer Program for Analysis of Molten Core Concrete Interactions," NUREG/CR-3920, August 1984.
4. A. L. Camp, M. J. Wester, and S. E. Dingman, "HECTR: A Computer Program for Modeling the Response to Hydrogen Burns in Containments," "Proceedings of the Second International Workshop on the Impact of Hydrogen on Water Reactor Safety," NUREG/CP-0038, (p. 827), U.S. Nuclear Regulatory Commission, October 1982.
5. A. L. Camp, V. L. Behr, and F. E. Haskin, "MARCH-HECTR Analysis of Selected Accidents in an Ice-Condenser Containment," Sandia National Laboratories, in preparation.
6. "Safety Evaluation Report Related to the Operation of Sequoyah Nuclear Plant, Units 1 and 2," NUREG-0011, Supplement No. 6, U.S. Nuclear Regulatory Commission, December 1982.
7. F. E. Haskin, V. L. Behr, and J. Jung, "Containment Management Study for Severe PWR Accidents," "Proceedings of Tenth Water Reactor Safety Research Information Meeting," NUREG/CP-0041, Vol. 2, (p. 480), January 1983.
8. R. M. Harrington and L. J. Ott, "MARCH 1.1 Code Improvements for BWR Degraded Core Studies," Appendix B of NUREG/CR-3179 (October 1983).
9. D. D. Yue and T. E. Cole, "BWR4/MARK I Accident Sequence Assessment," NUREG/CR-2825 (December 1982).
10. W. B. Murfin, "A Preliminary Model for Core/Concrete Interactions," SAND77/0370 (August 1977).
11. A. L. Camp, *et. al.*, "HECTR Version 1.0 User's Manual," Sandia National Laboratories, in preparation.

12. J. F. Muir, et. al., "CORCON-MOD1: An Improved Model for Molten-Core/Concrete Interactions," NUREG/CR-2142, September 1981.
13. M. E. Senglaub, et. al., "CONTAIN, A Computer Code for the Analysis of Containment Response to Reactor Accidents Version 1A Draft," NUREG/CR-2224, June 1984.

APPENDIX A

CONSENSUS SUMMARY ON DIRECT HEATING

Prepared by:

T. Ginsberg  
Brookhaven National Laboratory  
Department of Nuclear Energy  
Upton, New York 11973

June 1984

Subcommittee on Direct Heating: Members

K. Bergeron, SNL  
W. Bohl, LASL  
D. Cho, ANL  
M. Corradini, U. of Wisconsin  
T. Ginsberg, BNL  
M. Pilch, SNL  
D. Powers, SNL

B. R. Seghal, EPRI  
J. Sienicki, ANL  
B. Spencer, ANL  
D. Squarer, EPRI  
T. G. Theofanis, Purdue University  
D. Williams, SNL  
R. Wright, NRC (Chairman)



## Appendix A - Consensus Summary on Direct Heating

### 1. Definition of Subcommittee Task

The objectives of the direct-heating subcommittee were:

- (i) to evaluate the various approaches to dealing with the high-pressure melt ejection direct heating problem offered by the various members,
- (ii) to make recommendations, based upon as broad a consensus as possible, for calculation of the containment loading due to the combined effects of water quench (steam spike), direct heating of the containment atmosphere and chemical energy release, as appropriate to Standard Problems (SP) 1 (Zion) and 2 (Surry).

The recommendations are based upon experimental data and models available as of April 1984.

### 2. Constraints

The subcommittee, with broad consensus, felt that the analysis of the direct-heating problem in its broad context was being constrained by the initial conditions as posed in the definition of SP-1 and SP-2. It was felt that a broader approach to the problem is required which considers (i) the melt mass available for discharge from the vessel upon failure, (ii) the temperature of the melt upon ejection and, (iii) the mass of unreacted metals available for ejection from the vessel. All of these issues call for methods of treating in-vessel core degradation events.

It was broadly recognized that analytical treatment of the direct-heating problem is currently constrained by the lack of an adequate experimental data base to support development of appropriate calculational models required for objective, mechanistic assessment of the transport processes. This constraint is aggravated by the recognition that "generic" solutions are not possible and that each containment system must be dealt with individually.

### 3. Mitigating Mechanisms

The subcommittee heard many plausible arguments relating to physical mechanisms which would mitigate the effects of direct heating and chemical reactions. These include:

- (i) incoherent core melting and melt injection from the reactor vessel,
- (ii) plausibility of lower melt temperatures,

- (iii) two-phase melt injection dynamics,
- (iv) melt freezing to structures in cavity,
- (v) melt flow across obstructions above cavity,
- (vi) melt droplet fallout in containment,
- (vii) melt deposition on structures,
- (viii) water-melt mixing and heat transfer in containment atmosphere.

The subcommittee recognizes that these mechanisms may indeed be mitigative. It was generally accepted, however, that the relevant mechanisms are not understood and that objective, mechanistic methods to treat most of these processes are not in place at the present time. It was also observed that augmenting mechanisms also exist, e.g.,  $H_2$  recombination with oxygen in containment on the surface of hot suspended debris.

As a result of the lack of an adequate data base, an inability to reliably extrapolate the available data to full-scale, prototypic accident conditions, and the lack of appropriate modeling, it was generally recognized that the individual subcommittee quantitative recommendations would be subjective in nature.

#### 4. Prior Approach to High-Pressure Melt Ejection Sequence: SP-1

At prior CLWG meetings an approach was taken which neglected the question of direct heating of the containment atmosphere by core melt and chemical energy release.

For SP-1, in which adequate water was assumed to be present in containment prior to melt ejection, it was recommended that the containment loading be computed assuming that within a 1-hour time frame:

- (i) 100% of the available core melt would be quenched by heat transfer to water,
- (ii) 30% of the zirconium would react with steam, with the liberated chemical energy also transferred to the water to produce steam.

This recommendation was adopted for the "high, best estimate and low" calculations.

## 5. Recommendations

### 5.1 Approach

Despite the lack of an adequate technological base, the subcommittee was charged with prescribing a method for computation of containment loading, based upon the judgment of its members, which includes the effects of core melt water quench, direct melt heating of the atmosphere and chemical energy release.

The parametric approach adopted is an extension of the approach described in Section 4 above. It was assumed that the entire core melt inventory specified in the standard problem is available for ejection from the vessel. In the context of a global containment energy balance calculation, subcommittee members were asked to specify, on a best judgment basis:

- (i) The fraction of the core melt stored energy which is transferred to water,  $f_w$ ,
- (ii) The extent of metallic chemical reaction energy release of the melt which is quenched in water. This is specified as extent of reaction with steam.
- (iii) The fraction of core melt stored energy which is transferred directly to atmospheric heating.
- (iv) The extent of metallic chemical reaction energy release of the fraction of core melt which transfers energy directly to the atmosphere. This is specified as the extent of reaction with either steam or with oxygen.

It is recognized that large uncertainties exist in specification of the parameters characterized above. The subcommittee members were therefore asked to specify the above parameters for three calculational estimates of containment loading: "high, best judgment, low." The "high" represents a subjective judgment that the numbers would give an estimate of containment pressure and temperature, when used in a containment calculation, that is at the high end of the uncertainty band. The "low" estimate would correspond to an estimate at the low end of the uncertainty band. All of the estimates are based upon the subjective assessment of the individual of the various mechanisms involved in the interaction process, the available experimental evidence and analytical model. The estimates apply only to the stated initial conditions of SP-1 and SP-2, and should not be applied to any other set of initial conditions.

### 5.2 Differing Points of View

After some discussion, the subcommittee members generally agreed that the available experimental data (ANL/SNL) suggested that some quantitative modification of the prior recommendations (Section 4) was required in order to

reflect the possible effects of chemical energy release to, and direct heating of, the containment atmosphere in the high-pressure melt ejection accident sequence. There was, however, a major difference of opinion in the proposed recommendations of the extent of direct heating and chemical reaction to be accounted for in containment load calculations. This difference in opinion was greatest for the "high"-prediction, and was irreconcilable. It was agreed that only additional experimentation could lead to resolution.

The opinions of the subcommittee members (those that participated in the estimation process) split along two lines. The opinions of the two groups can be represented as follows:

Group A: Small Direct Heating Effect on Basis of Present Data<sup>(1)</sup>

This group strongly argued that:

- (i) The initial conditions, principally the quantity of molten fuel available for ejection from the vessel, was preventing realistic assessment of the direct heating process,
- (ii) The EPRI-ANL experiments clearly demonstrated the effectiveness of water as the heat transfer medium in the simulated Zion containment atmosphere,
- (iii) The above-cavity structures, as simulated in the EPRI-ANL experiments, are significant in removal of dispersed core melt material from the containment atmosphere,
- (iv) The SNL experiments provide evidence only for the mass of material ejected from the reactor cavity.
- (v) The available experimental evidence supports the conclusion that thermal energy no greater than 2% of the initial melt simulant stored energy entered into direct atmospheric heating.

The group concluded that the available experimental data base supports direct heating effects of masses of core melt no greater than 2% of both SP-1 and SP-2.

Group B: Significant Direct Heating Effects Cannot be Ruled Out<sup>(2)</sup>

The arguments supporting the group's opinion were:

- 
- (1) Group A: Seghal, Sienicki, Spencer, Squarer, Corradini (SP-1).
  - (2) Group B: Bergeron, Ginsberg, Pilch, Powers, Theofanus, Williams, Wright, Corradini (SP-2).

- (i) The ANL and SNL experiments (Zion simulations) both suggest nearly complete melt entrainment from the reactor cavity under prototypic conditions,
- (ii) The effectiveness of water as the quenching medium has not been conclusively demonstrated by experiment. The ANL experiments, which included water, cannot be reliably scaled to prototype conditions.
- (iii) Based upon their expected size (<1 mm), the core debris can release its thermal and chemical energy on a time scale of just a few seconds.
- (iv) The ANL experiments did not contain an air atmosphere and, hence, conclusions with respect to chemical reaction effects cannot be drawn from these experiments.
- (v) Hydrogen recombination with oxygen following metallic reaction with steam cannot be precluded.

The group concluded that large uncertainties exist in specification of the key parameters involved in the perceived major direct heating mechanisms. As a result, major uncertainties exist in prediction of the containment loading resulting from the combination of direct heating, chemical reaction and water quench. The group concluded that, at present, "...it is not possible to rule out occurrence of sufficient direct heating to present a severe challenge to PWR large dry containments."

### 5.3 Recommendations

The individual estimates of the direct heating parameters defined in Section 5.1 were received and sorted out. The estimates were divided into Group A and Group B responses. The estimates are presented in Tables 2-5. As shown in Table 1, each respondent proposed a "High," "Low" and a "Best Estimate" judgment. For each of these categories the respondent gave an estimate of the percentage of melt thermal energy (assumed proportional to the equivalent melt mass) transferred directly to the atmosphere. This is presented as the "Thermal"- "Direct Heat" contribution. The respondent also presented an estimate of the percentage of melt thermal energy transferred to available water to produce steam. This is presented as the "Thermal"- "Water Quench" contribution. For each of the "Direct Heat" and "Water Quench" contribution estimates, the individuals provided an estimate of the associated chemical reaction energetics. These estimates are presented in Tables 2-5, under the "Chemical" heading, in terms of the percentage of available metallic phase which enters a chemical reaction, either in a steam, or in an air, environment.

Consider the sample table, Table 1. Under "Best Estimate" column,  $x\%$  of the available corium thermal energy is transferred directly to the atmosphere. In addition,  $y\%$  of the metallic content of material ejected to the atmosphere is assumed to react with oxygen. The associated chemical energy is transferred directly to the atmosphere. Looking again at Table 1,  $w\%$  of the available corium thermal energy is assumed quenched in water. Of the corium mass which is quenched,  $z\%$  of its metallic phase chemically reacts with steam with no hydrogen recombination. The chemical energy is transferred to the water.

### 5.3.1 Group A Response

Table 2 presents the Group A response for both Standard Problems 1 and 2. The table reflects the opinion of Group A that currently available data support direct heating effects involving no more than 2% of the ejected core material stored thermal energy. The 80% water quench estimates are based upon the expected loss of melt to locations where water might not be available for quenching.

### 5.3.2 Group B Response

Table 3 presents the range of responses from those individuals who support the Group B position of Section 5.2. Note that in Table 3 the top-line parameters under "Direct Heat" is associated with the top-line parameters of "Water Quench" (and similarly for the bottom line parameters). Thus, under the "Best Estimate" parameters of Table 3-1, one respondent proposed that 25% of the core melt transferred its thermal energy directly to the atmosphere, while 75% was presumed quenched in water. A second respondent proposed a 50%-50% split between energy transfer via direct heating and water quench. Similarly, individual differences in judgment pertinent to chemical reaction are also shown.

It is noted that there was a spread in the quantitative estimates of the parameters even within Group B. This should not be surprising, considering the subjective nature of the estimation process. This group believes, however, that the differences observed in Table 3 lie within, and are representative of, the uncertainties in the physical parameters which govern the direct heating and chemical energy release phenomena.

As far as Group B is concerned, the figures shown in Table 3 are meant to imply that the uncertainty in the range of expected physical behavior is large. Therefore, it is not possible to rule out direct heating effects of such a magnitude that would present a severe challenge to large dry PWR containments. The Group stresses that the absolute values of the numbers presented were arrived at subjectively and are quite uncertain. The numbers pertain only to the initial conditions of Standard Problems 1 and 2, and should not be scaled in any way for a change in initial conditions.

6. Summary: Recommendation to CLWG

The differences in technical judgment between Group A and Group B could not be resolved. As a result the Subcommittee on Direct Heating presents two sets of best-judgment recommendations on direct-heating parameters.

Tables 4 and 5 are presented as consensus of Group A and Group B, respectively.

Table 1  
Sample Parameter Table

	Low		Best Estimate		High	
	Thermal	Chemical	Thermal	Chemical	Thermal	Chemical
Direct Heat			x%	y% O <sub>2</sub>		
Water Quench			w%	z% STM		



Table 2

Group A: Parameters for SP-1 and SP-2

	Low		Best Estimate		High	
	Thermal	Chemical	Thermal	Chemical	Thermal	Chemical
Direct Heat	<2%*	---	<2%	---	<2%	---
Water Quench	~80%	---	~80%	---	~80%	---

\*The 2% estimate was derived from the available ANL experiments. Corradini analyzed the ANL results, applied them to prototypic conditions, and obtained 5%. The 2% figure is presented as the best judgment of most of Group A. The difference, as far as impact on containment loading, is small.

Table 3-1

Group B: Range of Parameters for SP-1

	Low		Best Estimate		High	
	Thermal	Chemical	Thermal	Chemical	Thermal	Chemical
Direct			25%	50% STM*	50%	50% O <sub>2</sub>
Heat	0	0	50%	50% O <sub>2</sub> **	55%	100% O <sub>2</sub>
Water	50%	30% STM	75%	30% STM	50%	30% STM
Quench	100%	0	50%	0	45%	30% STM

\*STM refers to metal-steam reaction. Because of the small heat of reaction of iron-steam, this is nearly equivalent to zirconium reaction only.

\*\*O<sub>2</sub> refers to oxidation of both iron and zirconium in an atmosphere which allows for hydrogen recombination with oxygen.

Table 3-2

Group B: Range of Parameters for SP-2

	Low		Best Estimate		High	
	Thermal	Chemical	Thermal	Chemical	Thermal	Chemical
Direct	0	0	16.5%	50% STM	33%	100% O <sub>2</sub>
Heat	50%	10% O <sub>2</sub>	50%	50% O <sub>2</sub>	100%	50% O <sub>2</sub>
Water	50%	30% STM	83.5%	30% STM	67%	30% STM
Quench	85%	0	50%	0	0	0

Table 4

Group A: Parameters for SP-1 and SP-2

	Low		Best Estimate		High	
	Thermal	Chemical	Thermal	Chemical	Thermal	Chemical
Direct Heat	<2%	---	<2%	---	<2%	---
Water Quench	~80%	---	~80%	---	~80%	---

Table 5-1

Group B: Representative Parameters for SP-1

	Low		Best Estimate		High	
	Thermal	Chemical	Thermal	Chemical	Thermal	Chemical
Direct Heat	0	0	27.5%	50% STM	50%	50% O <sub>2</sub>
Water Quench	100%	0	72.5%	30% STM	50%	30% STM

Table 5-2

Group B: Representative Parameters for SP-2

	Low		Best Estimate		High	
	Thermal	Chemical	Thermal	Chemical	Thermal	Chemical
Direct Heat	15%	50% STM	25%	50% STM	50%	50% O <sub>2</sub>
Water Quench	85%		75%	30% STM	50%	30% STM

APPENDIX B

CORIUM/CONCRETE INTERACTION IN THE MARK I CONTAINMENT DRYWELL  
AND LOCAL LINER FAILURE

Prepared by

G. A. Greene  
Experimental Modeling Group  
Department of Nuclear Energy  
Brookhaven National Laboratory  
Upton, New York 11973

CORIUM/CONCRETE INTERACTION  
IN THE MARK I CONTAINMENT DRYWELL AND LOCAL LINER FAILURE

1. INTRODUCTION

The Containment Loads Working Group (CLWG) Standard Problem 4 is a TQUV-type accident sequence in a Mark I BWR containment in which all coolant injection fails at the time of reactor SCRAM from 100% power. Without coolant injection, the core uncovers within 30 minutes and since the ADS is assumed not activated, the primary system remains at high pressure. Shortly, the uncovered core of the reactor begins to melt, slumps into the RPV lower plenum, and eventually causes the reactor lower head to fail approximately three hours after accident initiation. The molten corium is assumed to be displaced onto the reactor containment drywell floor immediately and to begin to attack the concrete.

The Mark I containment consists of the drywell, pressure suppression pool, downcomer vents connecting the drywell and suppression pool, a containment cooling system, isolation valves, etc. The drywell is a steel pressure vessel, cylindrical at the top and spherical at the bottom. The vent system to the wetwell has eight circular downcomer pipes which penetrate the steel drywell liner, terminating in the pressure suppression pool. The suppression pool is a toroidal steel pressure vessel which contains subcooled water for condensing primary system steam during normal transients.

The particular containment design for Standard Problem 4 was Brown's Ferry Nuclear Power Station. A drawing of the Brown's Ferry Containment Building is shown in Figure 1. In this containment, the molten core debris, consisting of approximately 80% of the core inventory, is assumed to fall downward into the reactor pedestal region into a deep pool, filling the two containment sumps, and then flowing outward through the doorways over the entire annular drywell floor area. The sump volumes are approximately  $7.2 \text{ m}^3$ . Subtracting this from the initial corium inventory of  $32.3 \text{ m}^3$  leaves  $25.1 \text{ m}^3$  to be spread over a total of  $110 \text{ m}^2$  of floor area. Assuming an even spread of all the debris over all the floor results in a corium pool depth of 22 cm. Although this spreading is not mechanistically calculated, it is considered reasonable for the limiting high temperature debris case since pathways through the many obstructions are available, and there is empirical evidence that corium will flow at depths characteristic of this calculation [1]. For the high temperature limiting case, it is assumed that the debris will spread up to the steel containment liner itself.

Previous containment analyses of the Mark I BWR [2] have considered the  $\gamma$ -mode of containment failure as the dominant mode. The  $\gamma$ -mode is over-pressure failure of the drywell liner resulting in release of fission products and aerosols directly into the reactor building. The failure pressure for this event has been estimated at 132 psia [3].

However, recent results from the SASA program analyses of the Mark I BWR have indicated that high temperatures in the drywell during ex-vessel core/concrete interactions may result in containment failure due to seal

degradation prior to gross failure due to over-pressurization [4,5,6]. Recent efforts by the Containment Performance Working Group (CPWG) have concentrated on determining the probability and timing of over-temperature failure of these penetrations, and the rate of leakage into the reactor building [7].

It has become evident that a third mode of drywell failure must be considered under these specified accident conditions in addition to the gross over-pressure failure and the leak-before-failure modes. This third mode of failure is local ablation of the steel drywell liner due to contact with the molten corium. Since pathways through the obstructions on the drywell floor are available, molten core debris can be assumed to flow outward from the pedestal region and contact the drywell liner. As long as the corium is at a temperature greater than the steel melting temperature, it will present a threat to the containment integrity due to local melt-through. Should this occur, a large flow path to the reactor building and standby gas treatment system, bypassing the wetwell, will be available for blowdown of the high temperature concrete decomposition gases from the ex-vessel core/concrete interaction, aerosols, and volatile fission products. Although the gap between the drywell liner and the concrete is filled with fiberglass and polyester foam (see Figure 2), it is doubtful that they will present any significant resistance to the flow of these high temperature gases from the drywell.

The objectives of this study are to:

- (1) Develop a methodology to calculate the attack of molten core debris on the drywell liner,



- (2) Parametrically study the impact of corium temperature, concrete composition, and fraction of core in corium on liner melt-through, and
- (3) Compare the results to over-pressure and over-temperature failure times for a Mark I BWR.

## 2. PROBLEM SPECIFICATIONS FOR SENSITIVITY STUDIES

The CLWG Standard Problem 4 addresses the issue of the timing of the failure of the drywell due to over-temperature soaking of penetration seals (leak-before-fail) versus gross over-pressure failure of the steel liner ( $\gamma$ -mode failure). For the SP-4, the core debris temperature and composition, the concrete composition, and the fraction of the core released were specified [8,9]. The specifications of the corium and concrete compositions as well as a summary of the sensitivity calculation specifications for SP-4 are listed in Tables 1 and 2, respectively.

The approach taken in the local liner failure calculations was somewhat different than for the SP-4 calculations reported in Appendix D of this report. For SP-4, radiative heat transfer from the surface of the corium debris to the drywell containment structures and atmosphere was eliminated. All the sensible energy in the debris was thus forced into ablation of concrete, maximizing the concrete erosion rate and the generation of concrete decomposition gases. For the local liner failure calculations, however, radiative heat transfer from the corium debris surface was modeled. This enabled a more accurate calculation of the transient corium temperature, the most important variable in the calculation of the liner ablation rate.

The concrete types that were used in the calculations were a basalt-type and a limestone-type concrete, identical in composition to those specified for SP-4 (see Table 1). Three core debris temperatures were assumed: 2550 K, 1900 K, 1775 K. Mechanistically, the low temperature debris case is

inappropriate since the debris probably would not be able to flow to the liner prior to solidifying. The radius of spreading of the debris on the drywell floor was assumed to be 6 meters and the depth of the debris was held uniform. The debris required to fill the drywell sumps was subtracted from the debris inventory in order to calculate the corium depth. The radiative emissivity of the corium was given a constant value of 0.5. The fraction of the core that was allowed to participate in the core/concrete interaction was assumed to be 80% or 60%.

Although the TQUV accident sequence is a high pressure sequence with failure of the ADS, this was assumed to have no impact on the disposition of the corium in the drywell upon failure of the RPV. In other words, the debris was allowed to spread uniformly and homogeneously across the floor; high pressure jetting, impaction on the steel liner, and direct atmospheric heating were neglected. Although modeling of these phenomena may be desirable, they were neglected since they were beyond the scope of this study.

A complete list of the parametric calculations chosen for the local liner melt-through evaluations is shown in Table 3.

### 3. CALCULATIONAL MODEL

In order to assess the drywell liner response to heat transfer from a pool of molten core debris during a core/concrete interaction, a calculational procedure consisting of both code calculations and hand calculations was developed. The general methodology was to calculate the melting attack on the steel liner by molten core debris that is simultaneously attacking the drywell concrete floor. The calculational tool that was used to analyze the attack of molten core debris on the drywell concrete floor was the CORCON-MOD1 computer code [10], as modified at BNL [11-13].

CORCON-MOD1 is a general model describing the thermal and chemical interactions between molten core debris and structural concrete. The major components of the system are the concrete cavity, the molten debris pool, and the gas atmosphere and surroundings above the pool. The geometry of the system is formulated as a two-dimensional, axisymmetrical cavity, although specific geometries not available as code-supplied options may be user-input.

The code offers three default concrete compositions or the user may input a specific concrete composition. The core debris is assumed to be molten and consist of metallic and oxidic phases, primarily  $UO_2$ ,  $FeO$ ,  $ZrO_2$ , steel, and Zr. The metallic and oxidic phases are assumed to separate into unmixed overlying layers. Mixture layers and an overlying water layer are not available in CORCON-MOD1. A gas atmosphere exists above the pool as well as structural surroundings, with which mass and energy exchange with the molten pool may occur.

Thermodynamic and transport properties as well as phase transition criteria for the molten debris pool are internally calculated at each time step. Mass and energy transfer between the various layers of core debris, as well as between the debris and the surroundings, occur instantaneously and are assumed to be in equilibrium. Models are included for heat transfer across the melt-concrete interface, between pool layers, and from the pool to the atmosphere and surroundings. The interaction between the pool and concrete is driven by the local temperature difference between the two and varies around the periphery of the pool. The pool-concrete interface is treated as an incompressible gas film composed of concrete decomposition gases. Heat transfer across this film is calculated by appropriate convective heat transfer models.

The erosion of concrete is modeled as one-dimensional, steady-state ablation. As the concrete is heated it decomposes, releasing  $H_2O$  and  $CO_2$  into the pool or gas film and molten concrete slag into the pool. The molten oxide slag is transported to the oxide layer, diluting the layer density and eventually resulting in an inversion of the oxide and metallic pool layers. The concrete decomposition gases that bubble through the pool,  $H_2O$  and  $CO_2$ , oxidize the metallic layer, resulting in the release of chemical energy and production of  $H_2$  and  $CO$ .

Convective heat transfer within the pool is enhanced by the bubbling of concrete decomposition gases. Internal heat transfer is modeled by either gas injection across liquid-liquid interfaces or gas agitation along liquid-liquid interfaces. Energy sources in the pool consist of chemical reactions and decay heat generation.

The form of the code used in the local liner failure mode calculations was identical to the BNL version of CORCON-MOD1 used for the CLWG Standard Problems 4 and 5.

From the results of the CORCON code calculations, the maximum sideways heat transfer coefficient across the gas film to the ablating concrete,  $h_i$ , was calculated at each time step as

$$h_i = \frac{q''_{\text{conv}} + q''_{\text{rad}}}{T_{\text{interface}} - T_{\text{abl,concrete}}}$$

where  $q''_{\text{conv}}$  and  $q''_{\text{rad}}$  are the convective and radiative components of heat transfer per unit area across the gas film, and  $T_{\text{interface}}$  and  $T_{\text{abl,concrete}}$  are the melt-gas film interfacial temperature and the concrete ablation temperature, respectively.

This heat transfer coefficient was then input into the calculational procedures for the transient heat-up of the steel liner and the steel liner ablation calculations. The heat transfer from the molten corium to the steel liner was modeled as one-dimensional transient convective heat transfer with sensible and latent heat transfer. The transient heat-up of the liner from its initial temperature to the steel melting temperature was calculated as

$$(\rho c)_{\text{steel}} V \frac{dT_{\text{steel}}}{dt} = h_i (T_i - T_{\text{steel}}) A$$

subject to the initial condition

$$T_{\text{steel}}(t=0) = T_0 = 300 \text{ K}$$

where  $\rho$  is the steel density,  $c$  is the specific heat,  $V$  is the liner volume, and  $A$  is the contact area of the liner with the molten core debris. Note that  $V/A$  is the liner thickness,  $\delta$ .

Once the liner is calculated to have heated to its melting temperature of 1750 K, the rate of melting of the steel liner is calculated until the calculational procedure is terminated. The melt rate of the liner is calculated as follows:

$$\rho_{\text{steel}} h_{fs,\text{steel}} \frac{d\delta}{dt} = h_i (T_i - T_{\text{ablate}})$$

subject to the initial condition

$$\delta(t = t_0) = 3 \text{ cm}$$

where  $h_{fs}$  is the latent heat of the steel,  $T_{\text{ablate}}$  is the steel ablation temperature, and  $t_0$  is the time at the start of the ablation calculation.

The calculation proceeds until one of three criteria are satisfied. First, the calculation is terminated when the thickness of steel ablated exceeds the initial liner thickness. This time,  $t_{\text{ablate}}$ , indicates the

containment failure time at which point fission products and aerosols would flow into the gap between the liner and shield wall, eventually finding their way into the reactor building. The second criterion which will terminate the calculation is if the downward erosion depth into the concrete exceeds the bubbled-up depth of the corium against the steel liner. Once the erosion depth exceeds the corium pool depth, it is assumed that contact of the corium with the steel is ended and the threat to the liner is over. If the liner is not penetrated at this time, it is not estimated to fail by melt-through. The third criterion for termination of the calculation is if the calculated corium-steel interfacial temperature falls below the steel melting temperature. Once this occurs, melting of the liner ends and failure by melt-through is avoided.

Some of the physical properties and physical constants used in the calculations to be discussed are listed below:

$$\begin{aligned}\rho_{\text{steel}} &= 8000 \text{ kg/m}^3, \\ h_{\text{fs,steel}} &= 2.7 \times 10^5 \text{ J/kg}, \\ c_{\text{psteel}} &= 500 \text{ J/kg K}, \\ \delta_{\text{wall}} &= 3 \text{ cm} .\end{aligned}$$

The specific results of the parametric sensitivity calculations performed in this study are discussed in the next section.



#### 4. RESULTS OF PARAMETRIC CALCULATIONS

The results of the calculations that were performed for the local liner failure problem are indicated in Table 4. Indicated on the table are the concrete type, corium temperature, percent of core participating in the interaction, total time to fail liner, total downward erosion at end of calculation, and thickness of liner ablated.

It is clear from the table that in most cases studied, the steel liner was calculated to fail by ablation very rapidly, in one case as rapidly as 3-1/2 minutes after contact with the molten core debris. In two of the eight cases studied, it was calculated that the liner would not fail by local melt-through at all. This occurred for the 1775 K and 1900 K corium temperature cases on the basaltic-type concrete. Due to the low ablation temperature assumed for the basaltic concrete cases ( $\approx 1450\text{K}$ ), the corium temperature dropped very rapidly upon contact with the concrete since the basaltic concrete acts as a rapidly ablating, low temperature heat sink. As a result, the corium debris fell very rapidly below the steel ablation temperature, 1775 K, ending the ablation of the liner early. If at this time the liner had not been calculated to have been penetrated, it was assumed that no further threat by local melt-through will occur and the calculation was terminated. The only basalt concrete cases in which the drywell liner failed by melt-through were for the high corium temperature cases of 2550 K. For these two cases, it took only 5-1/2 minutes to ablate the liner and fail the drywell.

For all the limestone concrete cases studied, the steel drywell liner was calculated to melt through rapidly. The time to melt through varied from 3-1/2 minutes for the 2550 K corium cases to 45 minutes for the 1775 K corium case. Once again as for the 2550 K basalt cases, varying the percent of the core from 80% to 60% had little impact on the failure times. Since the ablation temperature of the limestone-type concrete was assumed to be 1750 K, the same as the melting temperature of the steel liner, the debris remained slightly above this temperature long enough to insure the eventual melt-through failure of the drywell liner, even for the case that the debris initial temperature was 1775 K.

It is apparent from these results that variation of the fraction of core in the core/concrete interaction had no impact on the ablation rate for both the high debris temperature, limestone and basalt concrete cases. In none of the calculations did the corium debris penetrate deep enough into the concrete to terminate the calculations.

It is not clear if assigning the same ablation temperature to both the limestone concrete and the steel liner had any impact on the results of the low temperature limestone concrete-liner failure calculations. It would be desirable to lower the concrete ablation temperature by 25 K to see if it would lower the debris temperature below the steel ablation temperature in time to prevent failure of the drywell by melt-through, in much the same way the basalt concrete calculations behaved.

It is clear, however, that the only cases that liner failure by melt-through was avoided were those for which the corium debris temperature fell below 1750 K prior to liner melt-through.

## 5. DISCUSSION OF RESULTS

Until recently, the most likely mode of containment failure in a Mark I BWR was considered to be over-pressurization of the drywell and structural failure of the drywell liner with blowdown into the reactor building. This failure mode has been calculated to occur when the drywell pressure exceeds 132 psia [3].

Motivated in part by some recent results from the SASA program at ORNL, recent work by the Containment Performance Working Group (CPWG) has indicated that in a wide spectrum of accident conditions, failure of sealing materials due to degradation at elevated temperatures may occur prior to exceeding the ultimate capacity of the containment by over-pressure, and that leakage through these degraded seals may in some cases relieve the drywell pressurization and prevent structural failure entirely. This second mode of drywell failure would lead to an earlier transport of airborne aerosols and fission products into the reactor building, although probably at a lower flow rate than the  $\gamma$ -mode failure. This would allow less time for natural processes to attenuate the aerosol concentration; however, specific conclusions concerning the ultimate risk to the public have not been reported.

It is now apparent that if the Mark I containment is going to fail under the stress presented by an ex-vessel core/concrete interaction, it is likely to do so extremely early in the ex-vessel stage of the interaction due to melt-through of the steel drywell liner if the core debris is able to flow to

and ablate the liner. In many cases, the drywell liner was calculated to fail within five minutes of contact with molten core debris, taking as long as 45 minutes in one case. In only two cases, with relatively low temperature debris interacting with a highly basaltic concrete, was the liner calculated to survive.

A comparison of calculated or estimated drywell failure times (time after RPV failure) for these three failure modes discussed is presented in Table 5. The calculations are for a TQUV accident sequence in a Brown's Ferry-type Mark I containment with no CRD flow. In these calculations, the containment response calculations were performed with the MARCH 1.1B computer code [14] developed at ORNL, which contains some modeling changes specific to the Mark I not available in MARCH 1.1 [15]. The containment failure results which are presented employed CORCON-MOD1 calculations which were input to MARCH 1.1B in tabular form, bypassing the INTER model [16] in MARCH, which has been shown to overpredict concrete erosion rates and gas generation rates during core/concrete interactions.

The containment leakage times quoted in Table 5 are estimated from Reference 7 using the pressure-temperature histories from Appendix D of this report. Using the medium pre-existing leak area results for ethylene propylene seal material at 500 F, the seal soak time to initiate leakage is 18 minutes and the ramp time to totally degrade the seal material is 16 minutes. The over-temperature failure times listed indicate the sum of the times to achieve 500 F in the drywell atmosphere plus an additional 34 minutes. All times listed in Table 5 are "time after RPV failure."

Note that the over-pressurization failure times vary from over two hours for CLWG Case 1 to over eight hours for Cases 2 and 3. Case 4, with an extrapolated over-pressure failure time of 16 hours, is considered highly unlikely to actually fail the containment at all on pressure.

The over-temperature failure times from the CPWG criteria are significantly shorter, varying from one hour for Case 1 to 3-1/2 hours for Case 2. Cases 3 and 4 are not calculated to fail at all on over-temperature.

However, the local liner melt-through calculations indicate that failure may be expected as early as 3-1/2 to 5-1/2 minutes after the initiation of ex-vessel core/concrete interactions for Cases 1 and 3, to as much as 45 minutes for Case 2. These times are much less than the failure times for either of the other two failure modes. Case 4 was not calculated to melt through the liner.

What is evident from this comparison is that all three containment failure modes need to be considered simultaneously in order to accurately predict the pressure-temperature history in a Mark I BWR drywell. Leakage through drywell seals as well as through local breaches in the liner due to melting must be considered when estimating the structural response of the drywell. The transport of fission products and aerosols, as calculated by the methodology developed for the Accident Source Term Project Office (ASTPO) by Battelle Columbus Laboratories [17], will also be affected by the location and timing of containment failure, as well as mode of failure, leakage area, and flow rate through the leakage area.

## REFERENCES

1. Powers, D., Personal Communication, April 1984.
2. Reactor Safety Study, "An Assessment of Accident Risks in U.S. Commercial Nuclear Power Plants," WASH-1400, 1975.
3. Griemann, L.G., Famous, P., Wold-Tinsai, A., Ketalaar, D., Lin, T. and Bluhm, D., "Reliability Analysis of Steel Containment Strength," NUREG/CR-2442, 1984.
4. Yue, D.D. and Cole, T.E., "BWR 4/MARK I Accident Sequence Assessment," NUREG/CR-2825, November 1982.
5. Cook, D.H. et al., "Station Blackout at Brown's Ferry Unit One - Accident Sequence Analysis," NUREG/CR-2182, November 1981.
6. Cook, D.H. et al., "Loss of DHR Sequence at Brown's Ferry Unit One - Accident Sequence Analysis," NUREG/CR-2973, May 1983.
7. Containment Performance Working Group, "Containment Leak Rate Estimates," NUREG-1037 (for comments), Draft 4, April 4, 1984.
8. Silberberg, M., "Phenomenological Standard Problems for BWRs," NRC Memorandum, Dated November 3, 1983.
9. Silberberg, M., "Completion of BWR MARK I, MARK II Standard Problems," NRC Memorandum, Dated January 20, 1984.
10. Muir, J.F., Cole, R.K., Corradini, M.L. and Ellis, M.A., "CORCON-MOD1: An Improved Model for Molten Core-Concrete Interactions," SAND 80-2415, 1981.
11. Greene, G.A., "Status of Validation of the CORCON Computer Code," BNL-NUREG-33375, July 1983.
12. Letter from G. A. Greene to R. K. Cole, Dated January 31, 1984, Regarding "Interfacial Liquid-Liquid Heat Transfer."
13. Letter from G. A. Greene to R. K. Cole, Dated February 10, 1984, Regarding "Void Fraction in Bubbling Pools and Surface Heat Flux Model."
14. Harrington, R.M. and Ott, L.J., "MARCH 1.1 Code Improvements for BWR Degraded Core Studies," Appendix B of NUREG/CR-3179, September 1983.
15. Wooton, R.O. and Avci, H.I., "MARCH (Meltdown Accident Response Characteristics) Code Description and User's Manual," NUREG/CR-1711, BMI-2064, October 1980.

REFERENCES (Cont.)

16. Murfin, W.B., "A Preliminary Model for Core/Concrete Interactions," SAND-77/0370, August 1977.
17. Gieseke, J.A., Cybulskis, P., Denning, R.S., Kuhlman, M.R. and Lee, K.W., "Radionuclide Release Under Specific LWR Accident Conditions: Volume II - BWR MARK I Design," BMI-2104, May 1983.



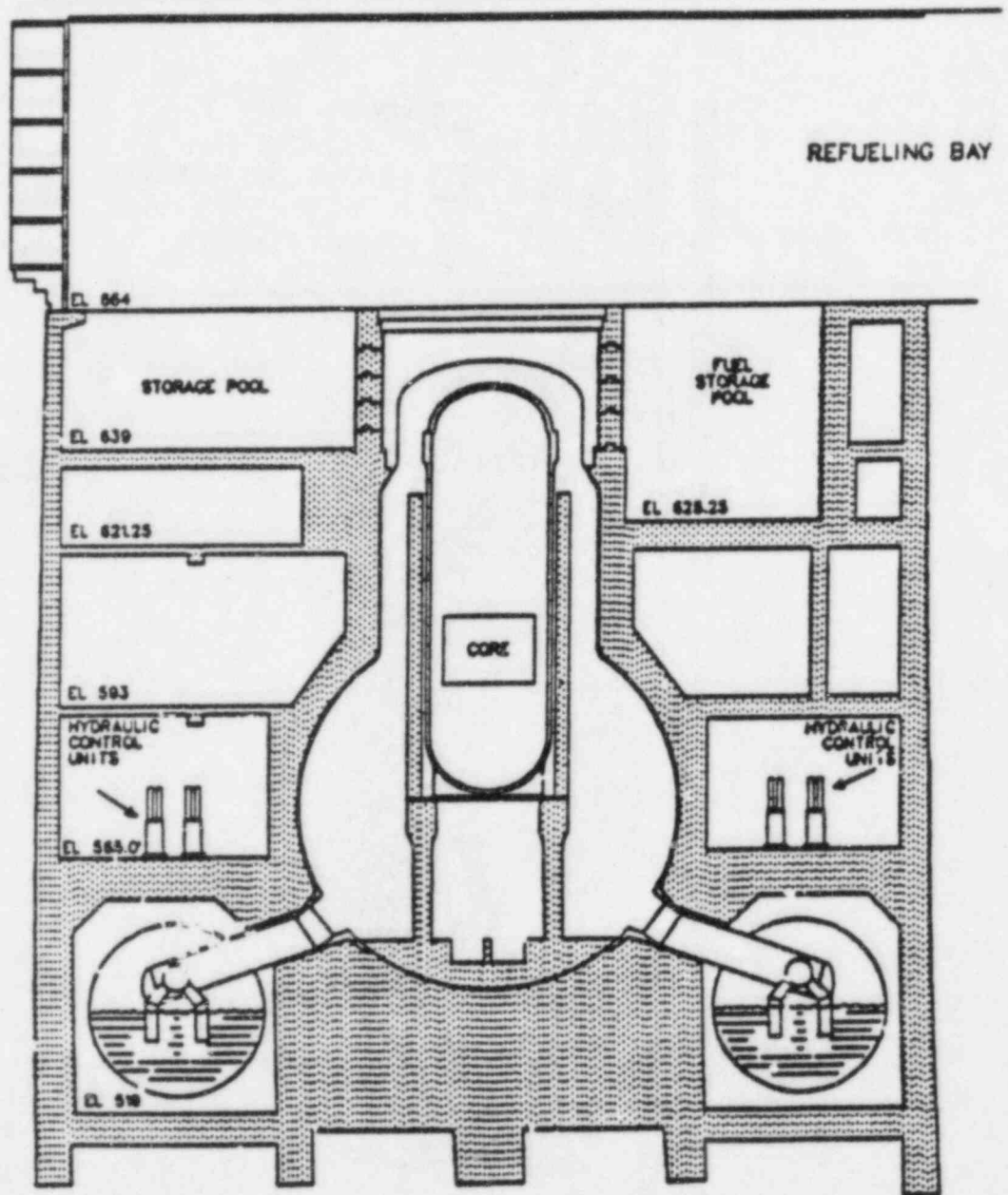


Figure 1 Longitudinal Section of BFNP Reactor Building  
(ORNL-DWG 82-6007 ETD)

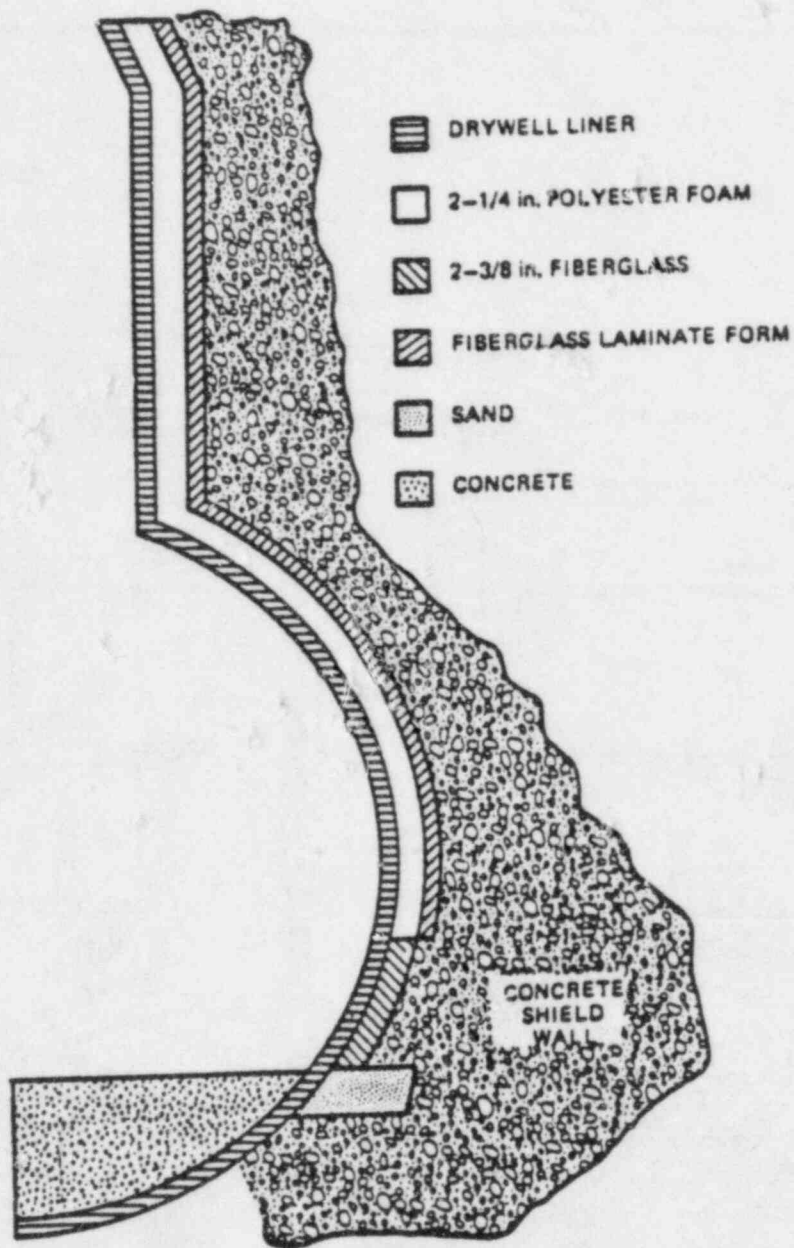


Figure 2 Drywell Liner - Concrete Shield Wall Gap Geometry  
(ORNL-DWG 83-4244 ETD)

TABLE 1

SPECIFICATION OF CORIUM AND CONCRETE  
COMPOSITIONS FOR SP-4

CONCRETE	LIMESTONE	BASALT
WEIGHT FRACTIONS:		
CaCO <sub>3</sub>	0.80	0.01
Ca(OH) <sub>2</sub>	0.15	0.18
SiO <sub>2</sub>	0.01	0.57
Free H <sub>2</sub> O	0.03	0.04
Al <sub>2</sub> O <sub>3</sub>	0.01	0.20
CORIUM		
UO <sub>2</sub>	127000 kg	
ZrO <sub>2</sub>	9160 kg	
FeO	12250 kg	
Fe	41920 kg	
Zr	45380 kg	
Ni	4450 kg	
Cr	8000 kg	

TABLE 2

SUMMARY OF SENSITIVITY CALCULATION  
SPECIFICATIONS FOR SP-4

Case Number	1	1a	2	3	3a	4
Corium Spread (m)	5	5	3	5	5	3
Debris Temperature (K)	2550	2550	1755	2550	2550	1755
Concrete Type	L	L	L	B	B	B
Free H <sub>2</sub> O (%)	3	6	3	4	8	4
Steel in Corium (lb)	140K	140K	140K	140K	140K	140K

TABLE 3

MATRIX OF BWR MARK I LOCAL FAILURE CALCULATIONS

CASE NUMBER	1	2	3	4	5	6	7	8
Corium Spread (m)	6	6	6	6	6	6	6	6
Debris Temperature (K)	1775	1775	1900	1900	2550	2550	2550	2550
Concrete Type	B	L	B	L	B	L	B	L
Corium Fraction (%)	80	80	80	80	80	80	60	60
Corium Composition	----- See Table 1 -----							

TABLE 4

SUMMARY OF BWR MARK I LOCAL FAILURE  
CALCULATION RESULTS

RUN	CONCRETE*	CORIUM TEMPERATURE (K)	% OF CORE	TIME TO FAIL LINER(S)	AXIAL <sup>+</sup> CONCRETE EROSION (cm)	THICKNESS <sup>+</sup> OF LINER ABLATED (cm)
1	B	1775	80	NO MELT-THROUGH	3.3	0.1
2	L	1775	80	2842	1.2	3.0
3	B	1900	80	NO MELT-THROUGH	7.4	0.3
4	L	1900	80	895	1.5	3.0
5	B	2550	80	328	4.0	3.0
6	L	2550	80	208	1.6	3.0
7	B	2550	60	325	3.6	3.0
8	L	2550	50	226	1.6	3.0

\* B = Basalt, L = Limestone

+ At liner melt-through time.

TABLE 5

COMPARISON OF APPROXIMATE DRYWELL FAILURE TIMES  
BY OVER-PRESSURE, OVER-TEMPERATURE, AND LINER MELT-THROUGH

CLWG CASE	DEBRIS TEMPERATURE CONCRETE COMPOSITION	MAXIMUM DRYWELL <sup>+</sup> P AND T	CLWG OVER-PRESSURE FAILURE(MIN)	CPWG OVER-TEMPERATURE FAILURE (MIN)	LINER MELT-THROUGH FAILURE(MIN)
1	2550 K, Limestone	145 psia 622K(660F)	133	62	3.5
2	1755 K, Limestone	88 psia 533K(500F)	500*	329	45
3	2550 K, Basalt	108 psia 477K(400F)	460*	No Leakage Calculated	5.5
4	1755 K, Basalt	65 psia 411K(280F)	950* Failure Unlikely	No Leakage Calculated	No Melt-Through Calculated

\* Extrapolated value.

<sup>+</sup> Maximum during five hours of core/concrete interaction.

APPENDIX C

EX-VESSEL STEAM EXPLOSIONS IN THE MARK II CONTAINMENT

Based on Excerpts from

"Analysis of Ex-vessel Fuel-Coolant Interactions in an LWR"

by

M. L. Corradini  
C. C. Chu  
K. Y. Huh  
G. A. Moses  
J. Norkus  
M. D. Oh  
T. Welzbacker

Published as UWRSR (University of Wisconsin Research Staff Report)  
May 18, 1984



In current analyses of severe core melt accidents in light water reactors the NRC is reassessing the radioactive source term that could be released to the environment. As part of this effort we have performed analyses for a group of containment standard problems, investigating the effect of ex-vessel fuel-coolant interactions. In particular, we performed an analysis of a steam explosion in a Mark II suppression pool; the results indicate that the dynamic pressure from the explosion might be of concern if the explosion occurs outside the downcomer tubes.

Steam explosions can occur in the wetwell suppression pool of a Mark II boiling water reactor, and involve a large fuel mass (specifically SP-5). However, our parametric calculations suggest that, based on current fuel-coolant mixing estimates, the dynamic pressure-time impulse from a steam explosion may not threaten the concrete supporting wall for the vessel pedestal or the outer containment wall. Further analysis is required to verify that this conclusion is valid over a wide range of fuel-coolant mixing conditions.

#### Ex-Vessel Fuel-Coolant Interactions in a BWR Mark II Suppression Pool

In Standard Problem 5 (SP-5) [1] two accident sequences were identified as potentially important for a BWR-Mark II plant; these were a high pressure meltdown sequence (TQUV) and a low pressure meltdown sequence (TQUX), both resulting from an unanticipated transient followed by reactor scram with a loss of emergency coolant injection capability. This combination of events allows the reactor core to overheat and melt. In the absence of successful operator intervention the molten core is considered to fail the reactor pressure vessel lower plenum wall and pour into the drywell pedestal region (see Figure III.1 - specific to SP-5 problem). For this specific Mark II geometry the downcomer tubes to the wetwell and into the suppression pool are outside the pedestal region on the annular drywell floor. The dimensions of the downcomer and the wetwell region are given in Table III.1.

When the molten corium fuel is ejected from the RPV and begins to flow into the downcomer tubes, the major issue we are concerned with is the potential for steam

explosions in the suppression pool. The reason for concern is that if an explosion occurs and involves enough fuel mass the dynamic pressure pulse from the explosion in the water phase could be large enough to damage the concrete pedestal wall or wetwell containment wall. This in turn may threaten containment integrity early in the accident.

The method one would use to determine if the steam explosion dynamic pressure could damage the structural walls would be to construct a pressure-time failure limit line; this identifies the pressure-time combination which would cause failure. This has been done for the SP-5 Mark II wetwell and pedestal walls (see Figures III.2 and III.3). The assumptions that were used to calculate these values were:

- (1) The walls' thicknesses were considered to be thin compared to the wetwell diameter;
- (2) The pressure loading was uniform both spatially and temporally (average uniform square wave);
- (3) Failure was defined based on a ductile strain criteria  $\epsilon_f/\epsilon_y = 10$ [16];
- (4) The walls were considered to be free standing, i.e. the containment wetwell wall calculation neglected the structural support of soil outside the containment.

The first three assumptions are reasonable given the approximate nature of the calculations. The ratio of the wall thickness to the pedestal diameter is small ( $\sim 0.14$ ). The pressure loading used in the calculation was a square wave; one would use these results by computing the average pressure by

$$F_1 = \frac{1}{t_d} \int_0^{t_d} p(t) dt \quad (22)$$

where  $t_d$  is the characteristic time of the pressure pulse.

$F_1$  is the average applied pressure over  $t_d$

This failure limit estimate is based on a simple elastic-plastic calculation (see Figure III.4) where one calculates the resistance to deformation of the structure,  $R_m$ [16],

$$R_m = \frac{\rho_y \Delta_w}{R_w} \quad (23)$$

where  $\rho_y$  is the yield stress of the wall material

$w$  is the supporting wall thickness

$R_w$  is the radius of curvature of the wall;

and then calculates the natural frequency of the structure,  $T$ [16],

$$T = 2\pi \sqrt{\frac{m_s}{K_s}} = 2\pi \sqrt{\frac{\rho_w R^2 w}{E_w}} \quad (24)$$

where  $\rho_w$  is the wall density

$E_w$  is its Young's Modulus.

Knowing  $R_m$  and  $T$ , one forms the ratio of  $R_m/F_1$  and  $t_d/T$ ; with a definition of failure based on a strain criteria,  $\mu$ , then Figure III.4 can be used to determine if the structural wall would fail. The final assumption is known to be an underestimate of the strength of the wetwell wall if it is supported by soil outside the containment. This is likely to be the case for the wetwell which is below grade and therefore this failure criteria should be considered quite conservative. The surrounding earth would have two effects. First it would decrease the natural frequency substantially (~factor of 3), and second it increases the allowable pressure,  $R_m$ , because the earth overburden pressure acts as a compressive stress counteracting some of the tensile load from the explosion (analogous to prestressing the wall). A crude estimate of these two effects is presented in

Figure III.3 where we have increased T by a factor of 3 and considered an earth overburden existing from the drywell floor to the wetwell floor (~16 m). Knowing the steam explosion dynamic pressure history in the water phase will provide us with  $F_1$  and  $t_d$  and use these failure curves to estimate if there is a potential problem.

### General Description of the Physical Phenomena

When the fuel begins to pour out of the reactor vessel it will begin to spread over the reactor drywell floor. As the molten fuel pools up on the pedestal base it will flow out the personnel doorways and spread out across the annular drywell floor, where the downcomer tubes are located. (In problem SP-5 the downcomer tubes are outside the pedestal region, however, in other Mark II designs there are downcomers within the pedestal region). The fuel flowrate out of the RPV would be in the range of 560-5600 kg/s, depending on the RPV driving pressure (0.1 to 7 MPa). As the fuel flows from the RPV into the downcomer tubes a quasi-steady state situation would occur where the RPV inflow into the drywell matches the drainage down the tubes. The molten corium fuel thickness,  $t$ , on the drywell floor would be approximately given by

$$t_f = \left( \frac{\dot{m}_f}{\rho_f N \pi D_d g^{1/2}} \right)^{2/3} \quad (25)$$

where  $m_f$  is the fuel flowrate,  
 $D_d$  is the downcomer diameter,  
 $g$  is the gravitational acceleration,  
 $N$  is the number of tubes that drain.

For these flowrates the thickness is approximately 20-100 mm ( $N=10$ ). Since this film thickness is so thin and the drywell area is large (~32m<sup>2</sup> in the pedestal and ~500 m<sup>2</sup> in the outer drywell annulus) the fuel will rapidly cool due to radiation heat transfer (upward heat flux ~3MW/m<sup>2</sup>) and decomposition of the concrete (downward heat flux ~1 MW/m<sup>2</sup>). As it cools it will solidify and form

an insulating debris layer on the concrete base. The actual mass frozen on the drywell floor is a function of time; but a simple estimate shows that one requires about 10-30 mm of fuel debris to reduce the downward heat loss substantially and this corresponds to 40-120 mtons of fuel held up on the drywell floor as a solid. Based on the Mark II SP-5 conditions this leaves about 25-50% of the fuel mass available to drain into the downcomer tubes. There are approximately 85 tubes through which the fuel can drain; however because the flow is relatively slow it seems reasonable that only the first row of tubes (~10) would actually have significant drainage. As the corium fuel flows down the steel tubes it will quickly freeze due to the cold steel wall with cold water surrounding it. As the fuel pour continues it will advance down the tube insulating it from further freezing by a corium fuel crust. The steady flow film thickness is approximately given by

$$\epsilon_f = \left( \frac{3\mu_f \dot{m}_f}{N\pi D_{p_f} \Delta\rho g} \right)^{1/3} \quad (26)$$

where the fuel viscosity and other terms have been previously defined. This results in a fuel film thickness of 1.5-3 mm for these conditions, and this is the probable initial crust thickness and corresponds to a freezing rate of about 3100 kg/s initially. This suggests that at most the initial corium fuel flowrate into the suppression pool downcomers is 2500 kg/s; this would increase with time as the fuel crust insulates the tube wall from further fuel cooling and solidification.

The final question that one must answer is what is the character of mixing before the steam explosion in the tube or below it as the fuel enters the water. Consider first the condition of fuel-coolant mixing in the downcomer tube itself. There have been no experiments of fuel flow down a tube in the presence of coolant to determine the mixing phenomena; therefore the following comments are based on physical intuition. The fuel as it flows as a film will only mix with the water

in the tube if the vapor production rates and flowrates up out of the tube are large enough to create sufficient steam forces and fuel entrainment mixing (see Figure III.5). This mixing would be greatest at the top of the mixture when all the steam flow would have to exit at its highest velocities. Therefore, if mixing occurs it would best be at the surface of the downcomer. The total time to flow down the submerged tube is a couple of seconds; therefore the largest mass of corium fuel that could mix in the tubes is less than 3500 kg before some of the fuel would reach the suppression pool base (based on the total fuel inventory in the tubes) and some trigger occurs or some of the fuel mass settles out as a pool or quenched debris. We have no good estimate of the fuel mixing size; although since the fuel entrainment would be caused by a vapor-flooding phenomena one would expect the size to be of the order of a Taylor critical wavelength (~10 mm). For the second situation of mixing below the tube the same arguments apply here except that now no pipe wall restrains the mixing (Figure III.5). In this case droplets would be formed as the fuel drops off the tube end. The triggering timing is again the same as discussed before because the tube submerged depth is about half the total water depth; therefore a couple seconds are only available for fuel mixing outside the tube. An upper limit on the fuel mass that could mix is about 3500 kg. In this case though the mixture size would be strictly controlled by Taylor instabilities and the estimate of ~10 mm seems quite reasonable. Better estimates of the fuel mass that could mix should be done, but must await further analysis of FITS experiments and detailed mixing calculations.

#### 1-D Parametric Steam Explosion Model Results

To investigate the effect of a steam explosion in the wetwell region we performed a series of four preliminary calculations for the conditions as specified in the previous section; i.e., a corium fuel mass of 3500 kg at 2700K, a coolant mass equal to the fuel at 300K, and a fuel mixing diameter of approximately 10 mm. We employed a one-dimensional parametric explosion model we are currently developing to analyze the FITS experiments. The key unknowns in performing these calculations are the fuel fragmentation size after the explosion and the

time required for this fragmentation. Because we do not know the mechanisms for fuel fragmentation in steam explosions it is difficult to predict what would occur here at these large scales. Therefore, our approach here is to take the one-dimensional parametric model results which match the integral pressure and velocity results and FITS debris data and perform dimensionless scaling to predict what the fuel fragmentation behavior would be in this case. Our starting point was to successfully model the pressure history and conversion ratio of the FITS tests. In doing this we found that the fuel fragmentation diameter,  $D_{frag}$ , required to match the data was in the range of  $100\ \mu\text{m}$ , the local fragmentation time,  $\tau_{frag}$ , on the order of  $100\ \mu\text{s}$ , and to match the range of pressure data an initial steam void fraction in the range of 10-50%. On this last value let us point out that in most of the FITS experiments the measured integral void fraction in the fuel-coolant mixture was always large, 40-50%. However, because we do not know how this overall steam volume is distributed in the mixture, we considered that the fuel and coolant near the bottom and side of the mixture boundaries might have a much smaller void since steam flow would be up and out of the region leaving only the vapor film around the fuel. Hence, the value of 10% which seems to match the base pressure measurements in the FITS tests.

Now the actual physical values used in the Mark II calculations are not necessarily equal to these values used in FITS. What remains constant are the dimensionless initial conditions and governing equations used to model the phenomena. For example, Table III presents the initial conditions for the base case and other calculations performed. The base case represents a dimensionless scaling of the FITS initial conditions (see Table III.2) so that all the governing equations dimensionless groups and initial conditions are properly matched. Notice that because of property differences (iron-alumina vs corium) and scale differences (two orders of magnitude) the initial conditions are not the same; most notably the fuel fragmentation diameter and time. To observe the effect of the slug mass and the void fraction we performed sensitivity calculations in Cases 1 and 2. The actual slug mass is probably less than an order of magnitude greater than

the fuel and coolant mass but greater than their sum; likewise the actual void fraction is probably larger than 5% at the mixture periphery but smaller than 50%. Therefore, Cases 1 and 2 are reasonable variations to account for a range of initial conditions, assuming our dimensionless scaling of  $D_{frag}$  is correct. If this is not the case, we also performed a final calculation, Case 3 where we used the exact values of  $D_{frag}$  and  $T_{frag}$  from FITS calculations; our opinion is that this calculation would represent an energetic explosion and rapid energy transfer rate to the coolant.

The results are given in Figures III.6 and III.7. Notice that the range of the peak pressures in the explosion interaction zone varies from about 11 MPa for the base case down to 0.2 MPa for Case 2; while the pulse half width duration is about 5-20 msec. In the prolem SP-5 the downcomer tubes are located in the annulus region where one must consider compression loads on the pedestal region (Figure III.2) and tension loads on the containment wetwell wall with soil support (Figure III.3). Now comparing the pressure histories in Figure III.6 and III.7 directly to Figure III.2 and III.3 is not really proper because of these effects. First, the wall is some distance away from the explosion zone therefore the pressure will decay as  $1/r^2$  away from the source which will decrease the pressure at the wall by at most an order of magnitude. Second, since the wall is approximately rigid and the wave impact on the wall will cause a pressure increase. Finally if the explosion occurs in the downcomer pipe, the pipe wall will partially reflect the shock and decrease the loading. The cumulative affect of the first two geometrical effects would be to slightly lower the pressure at the wall. Based on Figures III.2 and III.3 the loadings indicate that the pedestal or wetwell wall survives. This conclusion is even more certain if the steam explosion occurs within the downcomer tubes, due to shock wave reflection which reduces the wall pressure. The major uncertainties have to do with the structural modeling of the wetwell wall supported by soil and the initial conditions for the fuel-coolant mixing in the wetwell. The values for  $D_{frag}$  and  $T_{frag}$  in the parametric are also uncertain, however it is our feeling that it is initially reasonable to use the scaling analysis employed in the base case and Cases 1 to 3.



The final point that should be made is that this conclusion is very geometry specific; i.e. the geometry of another Mark II containment wetwell design may completely change the results. The reason for this is the location of the downcomer tubes within the pedestal region and the existence of a freestanding containment wetwell wall could alter the conclusion. In the first case the melt could pour directly into the pedestal wetwell water and stress the pedestal wall in tension; a situation where the wall is much weaker. Given the current initial conditions the wall would be predicted to fail. In the second case the lack of soil support makes the freestanding wetwell wall much weaker and given current conditions it too would be predicted to fail. A survey of plant designs might be called for to identify these two design differences (e.g. Shoreham).

#### CSQ Empirical Explosion Results (Contributed work by M. Berman, SNL)

As part of the effort to understand the wave propagation effects of the steam explosion in the wetwell, calculations were done using the CSQ-II 2D hydrodynamics wave code for simulation of shock wave propagation from an energetic steam explosion. This has been done in the past to empirically analyze FITS tests [17] where one inputs three empirical constants to match pressure data; the macroscopic propagation velocity,  $V_e$ , the fuel energy deposited in the coolant,  $E_E$ , and the time over which this energy is deposited in the coolant,  $\tau_E$ , the values for these parameters were chosen based on matching the FITS-9B test [18] i.e.  $V_e = 300$  m/s,  $\tau_E = 1.6$  msec, and  $E_E = 0.7$  MJ/kg (this energy corresponds to about 40% of the total fuel energy for the corium in the Mark II). No specific scaling laws were used to rationalize using these values; one should then regard these values as very rough approximations to the proper empirical constants to be used. The wetwell geometry was simplified to two-dimensional axisymmetric-concentric cylinders (Figure III.8); the inner cylinder represents the fuel-coolant explosion mixture with or without the downcomer pipe present and the outer cylinder represents the rigid wall (the wetwell pedestal wall). The lower and upper boundaries are represented as a rigid wall and free surface respectively. The results of the preliminary calculations are given in Table III.3 and associated figures. The two variables in these calculations are the steam void fraction and the presence of the downcomer tube. In all cases when one compares the

pressures and time durations from these calculations to the pedestal failure calculation (Figure III.2), one finds that the wall does not fail; although the failure limit line is approached in the absence of the downcomer tube as the steam void fraction decreases.

Once again, it should be pointed out that our present results could change based on the geometry of the Mark II wetwell and on the fuel-coolant initial conditions. For example, if the downcomer tubes exist inside the pedestal region, then similar steam explosions could fail the pedestal wall because it is much weaker in tension. Therefore, it seems prudent that one surveys current Mark II wetwell designs to verify that unusual structural weaknesses do not exist, and that the fuel-coolant mixture initial conditions are better known.

Steam explosions can occur in the suppression pool on a Mark II BWR and may involve a large fuel mass. Our current parametric calculations suggest that, based on current fuel-coolant mixing estimates, the dynamic pressure-time impulse from a steam explosion may not threaten the pedestal wall and the wetwell wall in problem SP-5. We specifically emphasize the SP-5 design because we have found the failure criteria for the concrete wall to be design specific. The two important factors structurally appear to be if the downcomer tubes are inside or outside the pedestal wall and if the containment wetwell wall is a free-standing structure or supported by the surrounding soil overburden (see Figures III.2 and III.3 and compare to Figures III.6-III.7 and Table III.3). If the former case is true for either factor the support walls are much more susceptible to damage from a steam explosion. We would recommend that Mark II designs be examined to determine their design specific features. Additionally, we assumed a number of initial conditions for fuel-coolant mixing at large scales to do these calculations; we would further recommend continued analysis of the FITS experiments and of the scaling of the phenomena to determine the range of conditions where the Mark II designs are threatened, if any.

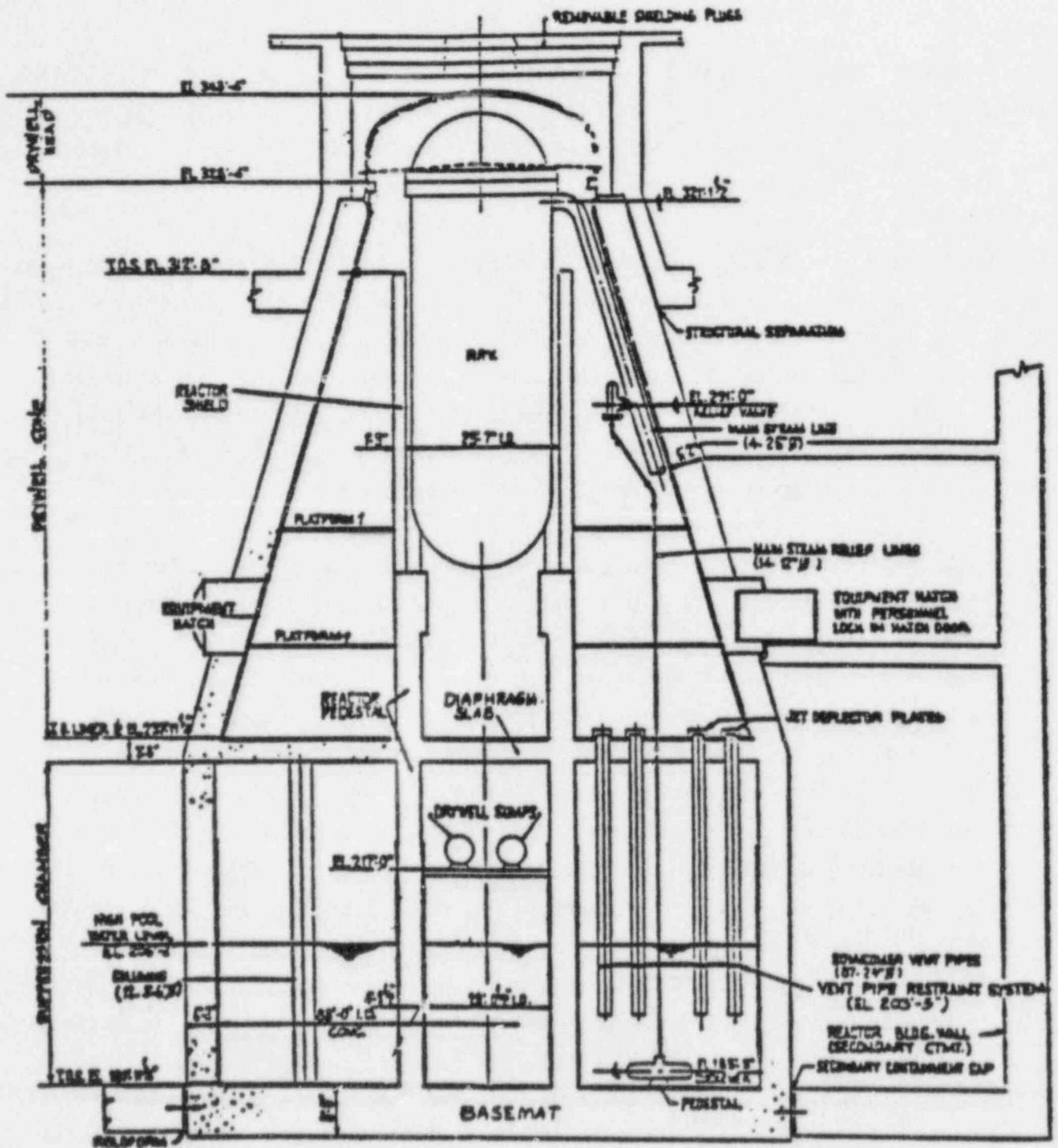


Figure III.1  
 BWR Mark II Containment Geometry for SP-5

APPROXIMATE FAILURE LIMIT LINE FOR UNIFORM

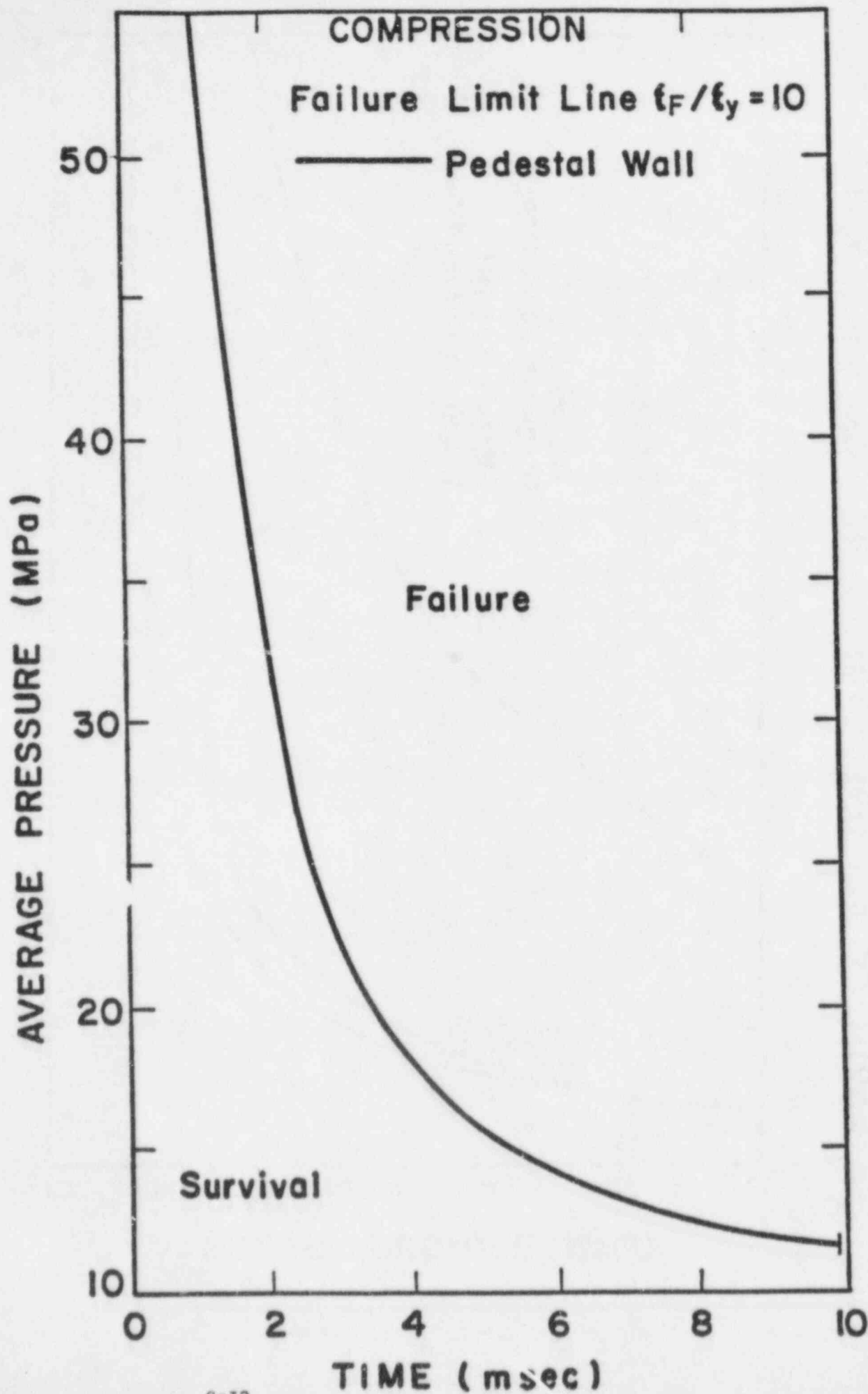
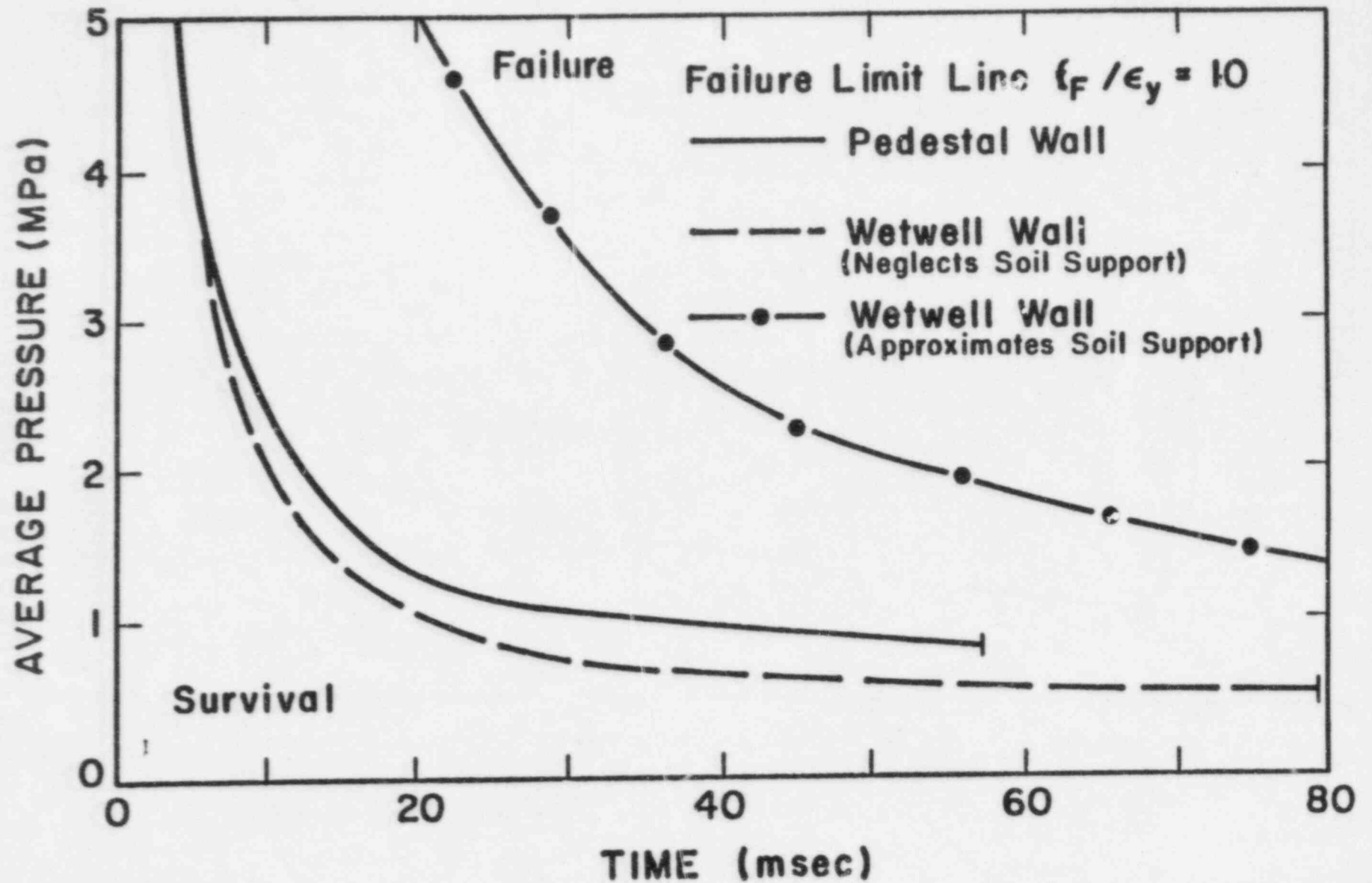


Figure III.2

Figure III.3

### APPROXIMATE FAILURE LIMIT LINE FOR UNIFORM TENSION



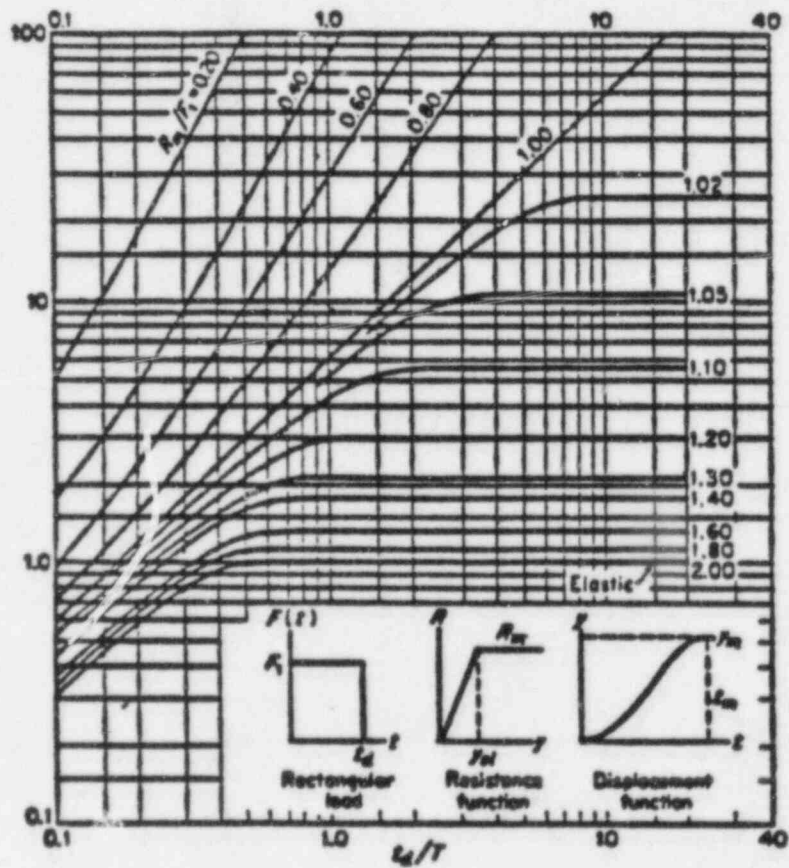
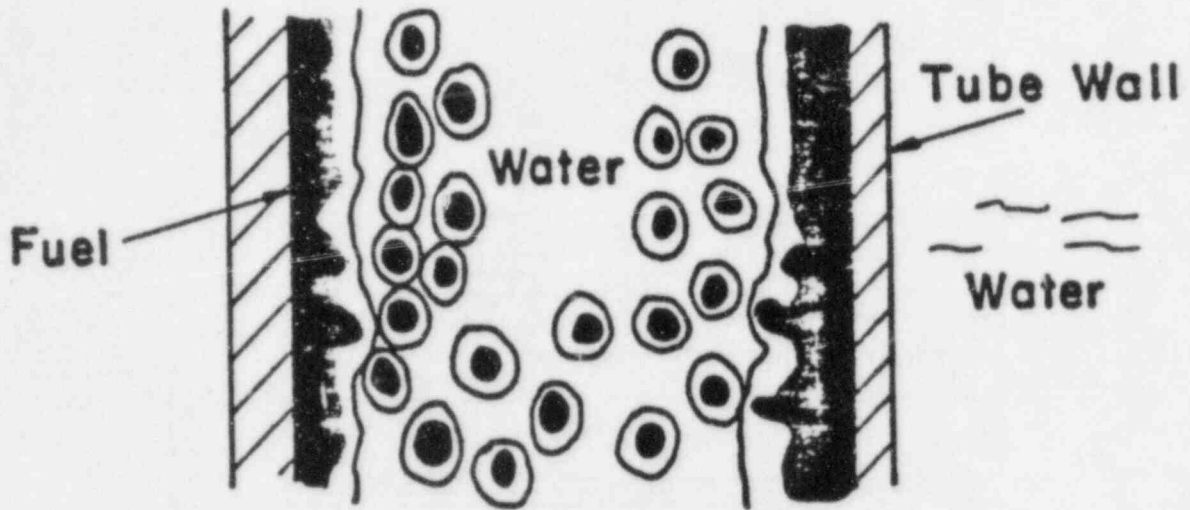


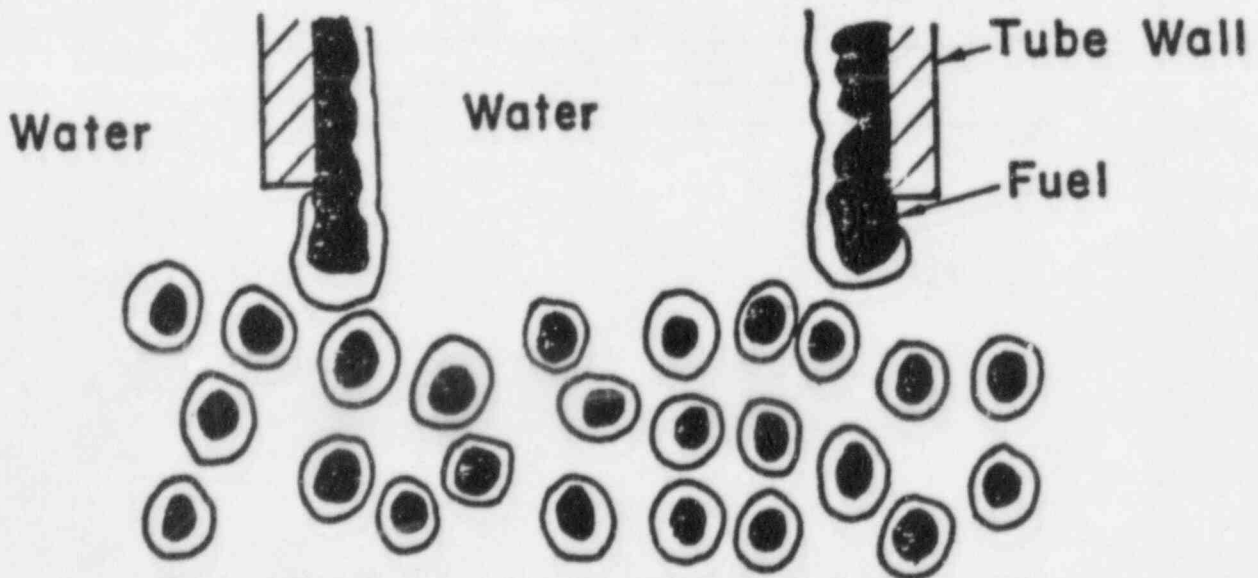
Figure III.4

Maximum Response of Elastic-Plastic One Degree Systems  
 (undamped) due to Rectangular Load Pulses  
 (US Army Corps of Eng. [16])

CONCEPTUAL PICTURE OF SUPPRESSION POOL  
FUEL - COOLANT MIXING

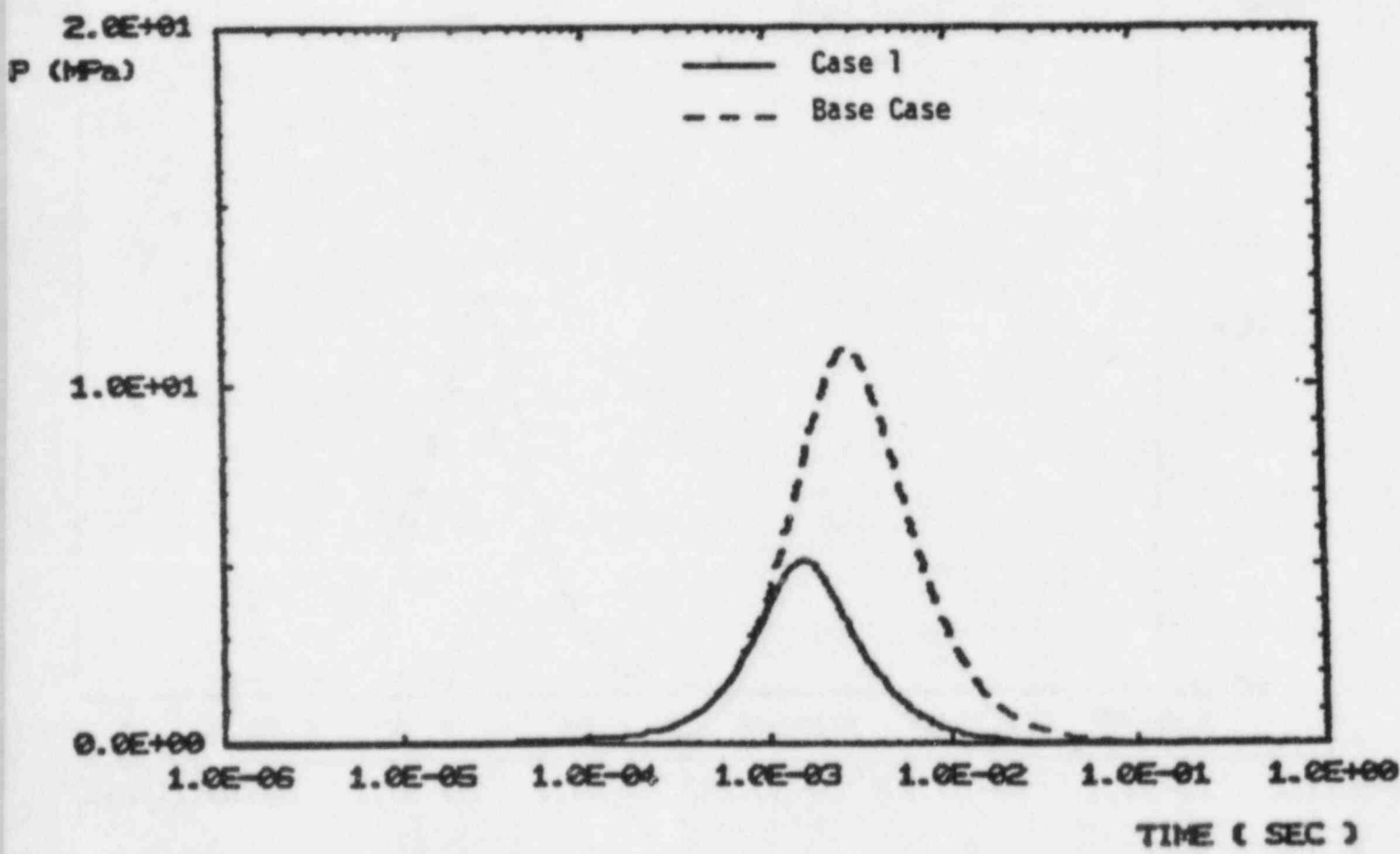


WITHIN DOWNCOMER TUBE



BELOW DOWNCOMER TUBE

r\_1

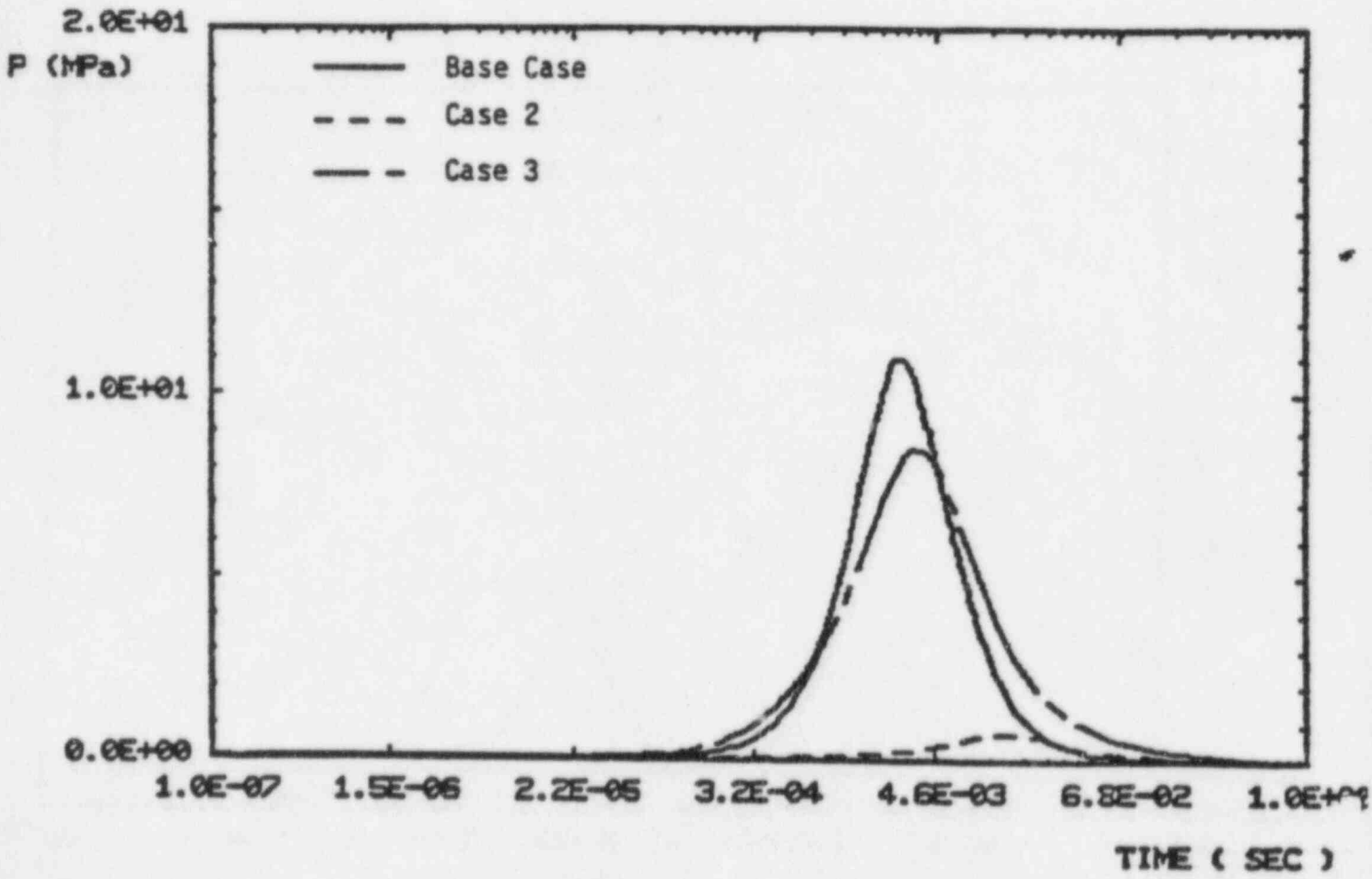


**Pressure vs. Time**

Figure III.6 Liquid Phase Coolant Pressure History for Base Case and Case 1



2\_1



**Pressure vs. Time**

Figure III.7 Liquid Phase Coolant Pressure History for Base Case and Case 2 and 3

Figure III.8

# CSQ STEAM EXPLOSION CALCULATIONS BWR MARK II WETWELL

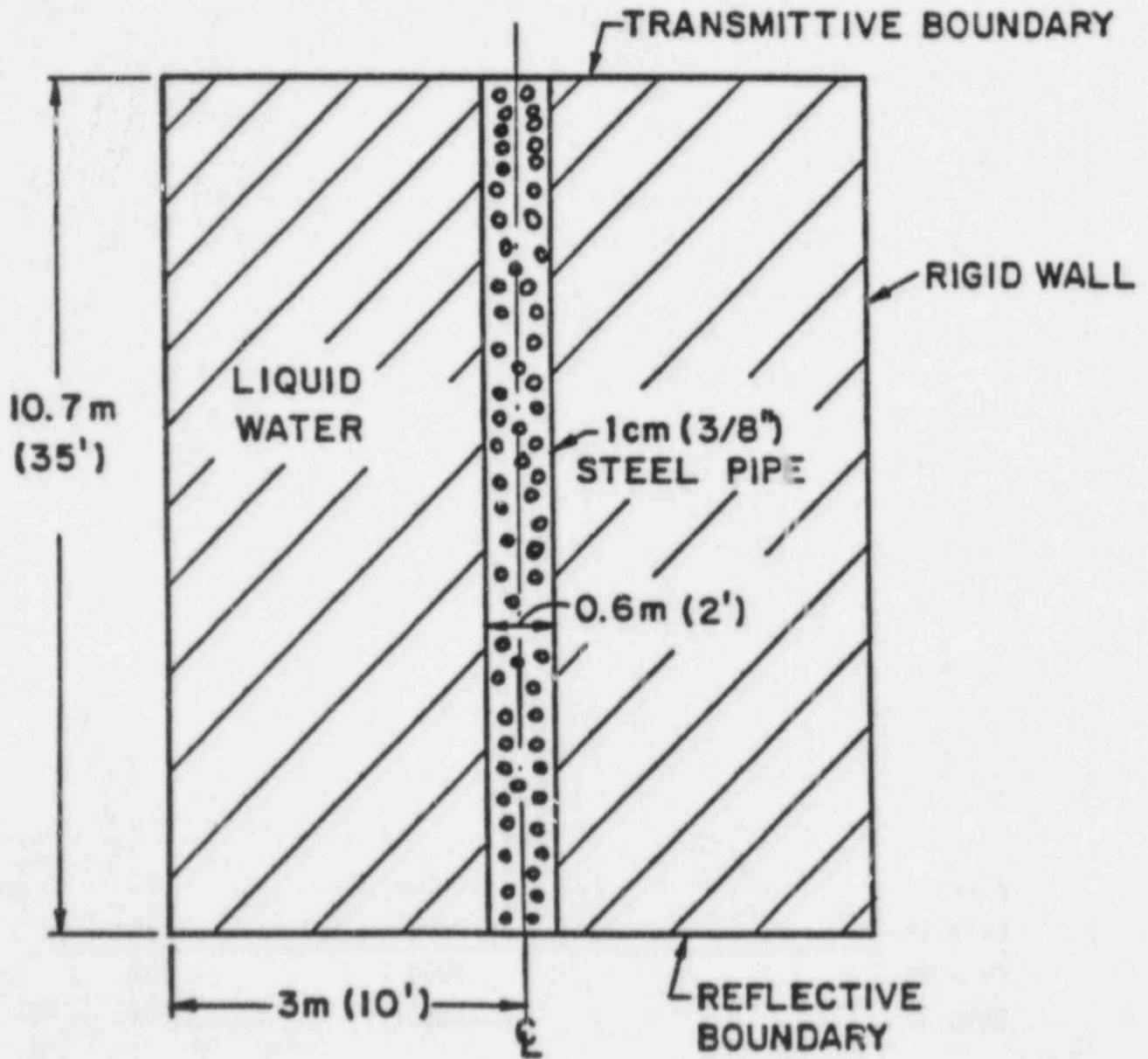


TABLE III.1

Major Parameters for Test Cases  
of Standard Problem 5 Steam Explosion Calculations

I. Geometry		
Number of Downcomers		87
Average Separation Distance		1.35 m
Nominal Diameter		0.61 m
Nominal Thickness		0.0127 m
Nominal Length		12.8 m
Suppression Pool Air Volume		4440 m <sup>3</sup>
Suppression Pool Water Volume		3450 m <sup>3</sup>
Assumed Water Temperature		300 K
Suppression Pool Water Depth		7 m
Downcomer Submergence Depth		3.35 m
Wetwell Diameter		26.8 m
Pedestal Outer Diameter		11.47 m
Pedestal Wall Thickness		1.46 m
Wetwell Wall Thickness		1.88 m
II. Reactor Pressure Vessel		
RPV Pressure		6.9 MPa/0.241 MPa
Hole Diameter		0.15 m
III. Cases		
	<u>Slug Mass (kg)</u>	<u>Steam Void Fraction</u>
Base Case*	70000	5%
Case 1*	7000	5%
Case 2*	7000	50%
Case 3 <sup>†</sup>	7000	50%

\* Based on Scaling of FITSB Tests for  $m_f \sim 3500$  kg and  $m_f/m_c = 1$

<sup>†</sup> Based on FITSB Debris Sizes - No scaling for  $m_f \sim 3500$  kg and  $m_f/m_c = 1$

TABLE III.2

Comparison of FITS Conditions to Mark II Conditions  
for Base Case Calculations

	<u>FITS*</u>	<u>MARK II</u>
	<u>Iron-Alumina</u>	<u>Corium</u>
<u>Fuel</u>		
Fuel Mass (kg)	5	3500
Fuel Temperature (K)	2700	2700
Fuel Frag. Diameter ( $\mu\text{m}$ )	100	750
Fuel Frag. Time ( $\mu\text{s}$ )	100	1000
	<u>Water</u>	<u>Water</u>
<u>Coolant</u>		
Coolant Mass (kg)	5	3500
Coolant Temperature (K)	300	300
Overall Slug Mass (kg)	100	70000
Overall Void Fraction (%)	10	5

\* These values are representative of FITS conditions; they do not match any one experiment but rather a group of tests (FITSA).

TABLE III.3

CSQ Rigid Wall Load Calculations<sup>+</sup>

Case	Energy Deposited (MJ/kg <sub>c</sub> )	Coolant Density (kg/m <sup>3</sup> )	Void Fraction	Pressure (MPa) [Ø 1 m]	Time (ms) ]	Pressure (MPa) [Ø 3 m]	Time (ms) ]
1	0.7	660	0.34	3	10	9	8
				7.5	6	8	6
1P*	0.7	660	0.34	1.1	0.2	0	-
2	0.7	830	0.17	40	0.2	1.7	0.6
				20	1.0	10	7
				10	3		
2P*	0.7	830	0.17	23	0.2	10	1
				10	1	2.5	4
3	0.7	880	0.12	50	0.3	32	0.6
				35	1	20	4
3P*	0.7	880	0.12	30	0.3		
				20	1.0	21	1
				10	2	8	4

<sup>+</sup> Based on the interaction of 3500 kg of fuel transferring 40% of its thermal energy to 3500 kg of coolant in an axisymmetric cylinder geometry (see Figure 24)

\* With downcomer pipe present at 0.3 m radius (see Figure 24)

## References

- (1) T. Spies, M. Silberberg et al., "Draft Report on Containment Loads during a Severe Core-Melt Accident," NUREG-0956.
- (2) T. Ginsberg, "Draft Report on Direct Containment Atmospheric Heating," Brookhaven National Laboratory (April 1984).
- (3) P. Cybulskis et al., "Reactor Cavity Debris Interaction Models (HOTDROP)," Battelle Columbus Laboratory, Draft Report (transmitted for CLWG Mtg. of July 19, 1983).
- (4) G. Moses and M. Corradini, "Documentation for the M1 Module of MEDICI," University of Wisconsin Report, UWRSR-14 (April 1984).
- (5) R.E. Henry et al., "Establishment of a Permanently Coolable State," Trans. Am. Nucl. Soc., 39, 368 (1981).
- (6) H.K. Fauske, "Some Aspects of Liquid-Liquid Heat Transfer and Explosive Boiling," Proc. Fast React. Safety Mtg., Beverly Hills, CA (1974).
- (7) R.E. Henry and H.K. Fauske, "Nucleation Characteristics in Physical Explosions," Proc. of Third Spec. Mtg. on Sod. Fuel Int. in Fast React., Tokyo, Japan (1976).
- (8) D.H. Cho et al., "Mixing Considerations for Large-Mass, Energetic Fuel-Coolant Interactions," Proc. ANS/ENS Fast React. Safety Mtg., Chicago, IL (1976) CONF-761001.
- (9) R.E. Henry and H.K. Fauske, "Core Melt Progression and the Attainment of a Permanently Coolable State," Proc. of Ther. React. Fuels Mtg., Sun Valley, ID (1981).
- (10) R.E. Henry and H.K. Fauske, "Required Initial Conditions for Energetic Steam Explosions," Fuel-Coolant Interactions, ASME HTD-V19, Wash. DC (1981).
- (11) M.L. Corradini, "Proposed Model for Fuel-Coolant Mixing During a Core Melt Accident," Proc. Int'l Mtg. on Thermal Reactor Safety, NUREG/CP-0027 (August 1982).
- (12) L. Baker and L.C. Just, "Studies of Metal-Water Reactions at High Temperatures, III Experimental and Theoretical Studies of Zr-H<sub>2</sub>O Reactions," ANL-6548, Argonne (May 1982).
- (13) M. Berman, Light Water Reactor Safety Quarterly, Sandia National Laboratories, SAND80-1304; Jan.-March, 1 of 4 (1980), April-June, 2 of 4 (1980), July-Sept., 3 of 4 (1980), Oct.-Dec., 4 of 4 (1980); SAND81-1216, Jan.-March (1981); SAND82-0006, April-Sept. (1981); SAND82-1572, Oct. 1981-March 1982 (1982), April-Dec. 1982 to be published.

References (cont'd)

- (14) D.J. Buchanan and T.A. Dullforce, "Fuel-Coolant Interactions," CLM-P362, Culham Laboratory Report (1973).
- (15) M.L. Corradini, "Hydrogen Generation During Fuel-Coolant Mixing," Proc. ANS/ENS 2nd Int'l Mtg. on Nuclear Reactor Thermalhydraulics, Santa Barbara, CA (1983).
- (16) J. Jung, Sandia National Laboratories, Private Communication (April 1984).
- (17) D.E. Mitchell et al., "Intermediate Scale Steam Explosion Phenomena: Experiments and Analysis," SAND81-0124, NUREG/CR-2415 (Sept. 1981).
- (18) M. Berman et al., "Core Melt/Coolant Interactions: Modelling," 10th Water Reactor Information Mtg., Gaithersburg, MD (October 1983).
- (19) T.G. Theofanous, Purdue University, Private Communication (August 1983).

**BIBLIOGRAPHIC DATA SHEET**

NUREG-1079 DRAFT

SEE INSTRUCTIONS ON THE REVERSE

2 TITLE AND SUBTITLE

Estimates of Early Containment Loads From Core  
Melt Accidents  
Draft Report for Comment

3 LEAVE BLANK

4 DATE REPORT COMPLETED

MONTH

YEAR

November

1985

5 DATE REPORT ISSUED

MONTH

YEAR

December

1985

5 AUTHOR(S)

Containment Loads Working Group (CLWG)

7 PERFORMING ORGANIZATION NAME AND MAILING ADDRESS (Include Zip Code)

Office of Nuclear Reactor Regulation  
U.S. Nuclear Regulatory Commission  
Washington, D.C. 20555

8 PROJECT/TASK/WORK UNIT NUMBER

9 PIN OR GRANT NUMBER

10 SPONSORING ORGANIZATION NAME AND MAILING ADDRESS (Include Zip Code)

Same as Item 7, above.

11a TYPE OF REPORT

Technical (Draft)

b PERIOD COVERED (Inclusive dates)

12 SUPPLEMENTARY NOTES

13 ABSTRACT (200 words or less)

The thermal-hydraulic processes and corium debris-material interactions that can result from core melting in a severe accident have been studied to evaluate the potential effect of such phenomena on containment integrity. Pressure and temperature loads associated with representative accident sequences have been estimated for the six various LWR containment types used within the United States. Summaries distilling the analyses are presented and an interpretation of the results provided.

14 DOCUMENT ANALYSIS - a KEYWORDS/DESCRIPTORS

core melting  
severe accident  
containment integrity

15 AVAILABILITY STATEMENT

Unlimited

16 SECURITY CLASSIFICATION

(This page)

Unclassified

(This report)

Unclassified

17 NUMBER OF PAGES

18 PRICE

b IDENTIFIERS/OPEN ENDED TERMS



UNITED STATES  
NUCLEAR REGULATORY COMMISSION  
WASHINGTON, D.C. 20555

FOURTH CLASS MAIL  
POSTAGE & FEES PAID  
USNRC  
WASH D C  
PERMIT No G 87

OFFICIAL BUSINESS  
PENALTY FOR PRIVATE USE, \$300

120555076877 1 1AN1F119A19E1  
US NRC  
ADM-DIV OF TIDC  
POLICY & PUB MGT RA-PDR NUREG  
#501  
WASHINGTON DC 20555